MISSOURI CLIMATIC ATLAS FOR DESIGN OF LAND APPLICATION SYSTEMS (MDNR WP-1400)

Revised, 2004

Q. Steven Hu

Participating Organizations:
Missouri Department of Natural Resources
Missouri Climate Center, University of Missouri-Columbia
Department of Biological and Agricultural Resources, University of Missouri-Columbia
Food and Agricultural Policy Research Institution, University of Missouri-Columbia
USDA Natural Resources Conservation Services, Missouri Office
School of Natural Resources, University of Nebraska-Lincoln
U.S. Environmental Protection Agency, Region 7

Working Group:
Sherry Chen, Song Feng, Charles Fulhage, Tod Hudson, Steve McIntosh, Claudia Scheer, and Donald Schuster

ACKNOWLEDGEMENTS

This Atlas, essential to design of land application systems in Missouri, was made possible by funding from the Missouri Department of Natural Resources through a grant from the U.S. Environmental Protection Agency, Region 7 over a two-year period, 1999-2000.

In addition to the scientists and engineers in the Working Group of this project, many individuals, including Mr. Ken Arnold, Mr. Troy Chockley, and Mr. Frank Miller of the Water Pollution Control Program in the Missouri Department of Natural Resources, participated in initiating and supporting this project. During the project, several others also devoted their talent to analyses and contributed to the completion of this Atlas. Special thanks are due to Dr. Song Feng of the School of Natural Resources at the University of Nebraska-Lincoln (UNL), who completed most of the calculations in this project; to Mr. Patrick Guinan of the School of Natural Resources at University of Missouri-Columbia, who provided the climate data from Missouri Automated Weather Stations Network; to Ms. Qiwen Huang, a graduate student at the UNL Department of Computer Sciences for her work in turning the calculation results into graphics; and to Dr. Sunil Narumalani for sharing his computer resources and helping develop the graphics.

Finally, questions regarding to the products in this Atlas should be directed to Mr. Tod Hudson at the Missouri Department of Natural Resources and to Dr. Q. Steve Hu at the UNL.

TABLE OF CONTENTS

Acknowledgements …… 1
1. Introduction ...……...…….. 4
2. Precipitation .....……..……..... 6
2.1. Norms of annual and monthly precipitation ……..…. 6
2.2. Probability of various precipitation events …….……. 19
a. 1 in 10-year maximum and minimum annual precipitation …..... 19
b. 1 in 10-year 2-day precipitation ……... 21
c. 1 in 10-year 10-day precipitation ……. 22
d. 1 in 25-year 1-day precipitation ……... 23
e. 1 in 25-year 10-day precipitation ……. 24
f. Maximum and minimum number of days with precipitation at 1 in 10-year 25
2.3. Monthly and annual precipitation for specific wet and dry years ……... 27
a. 1973 …….. 27
b. 1982 …….. 40
c. 1988 …….. 53
d. 1993 …….. 66
e. 1995 …….. 79
3. Surface Air Temperature ……... 92
3.1. Norms ……... 92
a. Annual minimum, mean, and maximum temperatures ……. 92
b. Monthly minimum, mean, and maximum temperatures ……... 95
3.2. Cold temperature statistics – latest ending date and earliest beginning date of frost ... 131
3.3. Probability of extremely cold temperatures ……. 133
a. Average and 1 in 10-year number of days in a year with daily minimum temperature at or below 32ºF ……. 133
b. 1 in 10-year coldest mean and minimum temperatures in the months of autumn, winter, and spring ……... 135
4. Surface Runoff ...…….. 150
a. Annual mean surface runoff …….. 150
b. 1 in 5-year surface runoff for dry and wet years ……... 151
c. 1 in 10-year surface runoff for dry and wet years ……. 153
d. 1 in 25-year surface runoff for dry and wet years ……. 155
e. 1 in 50-year surface runoff for dry and wet years ……. 157
5. Surface Evaporation …….. 159
a. Average annual free water surface evaporation …… 159
b. Average annual potential surface evaporation …….. 160
c. Free water surface evaporation, May – October ……... 161
6. Rainfall minus evaporation …… 162
7. Seasonal soil temperature at 2 inches …… 163
a. Spring …… 163
b. Summer ……. 164
c. Autumn …….. 165
d. Winter …… 166

8. Prevailing wind direction and average wind speed …….. 167
a. Spring wind speed ……. 167
Spring prevailing wind direction ……..……. 168
b. Summer wind speed …….. 169
Summer prevailing wind direction ……..… 170
c. Autumn wind speed ……... 171
Autumn prevailing wind direction ……. 172
d. Winter wind speed …… 173
Winter prevailing wind direction ……... 174
9. Solar radiation at the surface …… 175
a. Spring …… 175
b. Summer ……. 176
c. Autumn …….. 177
d. Winter …… 178
Appendix A: Climate data used in the Atlas …… 179
Appendix B: Methods used in developing the Atlas …… 186
References …… 194

MISSOURI CLIMATIC ATLAS FOR DESIGN OF LAND APPLICATION SYSTEMS (MDNR WP-1400)

1. Introduction

As a result of changing climate conditions, a concern has emerged as to the accuracy of indicators of local and regional climatic conditions and extremes for use in design of land application systems, including lagoons for waste water treatment and dams for managing water resources. Evidence warranting this concern is illustrated by the differences which can be observed between the two panels of Fig. 1 showing annual precipitation averaged first over the period of 1941-80 and then over the period of 1961-90. A contrast of these differences indicates that in most of southern Missouri the annual precipitation increased by nearly 2 inches from the early to the latter period.

While illustrating substantial changes in precipitation, the differences between the two panels in Fig. 1 show a need to reevaluate climate parameters and provide an accurate description of the climate environment in Missouri for use in engineering and planning purposes. This need is fulfilled by this revised Missouri Climatic Atlas, which describes and documents the recent climatic conditions, their norm and probability distributions, based on observed precipitation, temperature, soil temperature and moisture, wind and solar radiation, and observed and calculated evaporation in the recent 30 years from 1971 to 2000.

The climate norms of the most recent 30 years (average condition over those years) and probability distributions (variation ranges) of climate variables also have useful implications for the climate conditions of the next 10 years because of the large inertial in climate variations and the small trends in changes of the climatic parameters. Thus, the information provided in this Atlas can be used as the climatic guidance in design of future land application systems in Missouri.

In addition to the 30-year climate norms and variations, this Atlas is expanded to include descriptions of monthly average temperature and total precipitation for some years of severe droughts and floods in recent Missouri climate history. Those years include 1973, 1982, 1988, 1993, and 1995. Their climate conditions describe specific and extreme situations in the context of the norm and probability distribution of the 30-year period.

From Chapters 2 to 8, major climate parameters and their statistical properties are presented. Data and details of the methods used in deriving these norms and properties are saved in the Appendices for those who may be interested in the details involved in developing this Atlas.

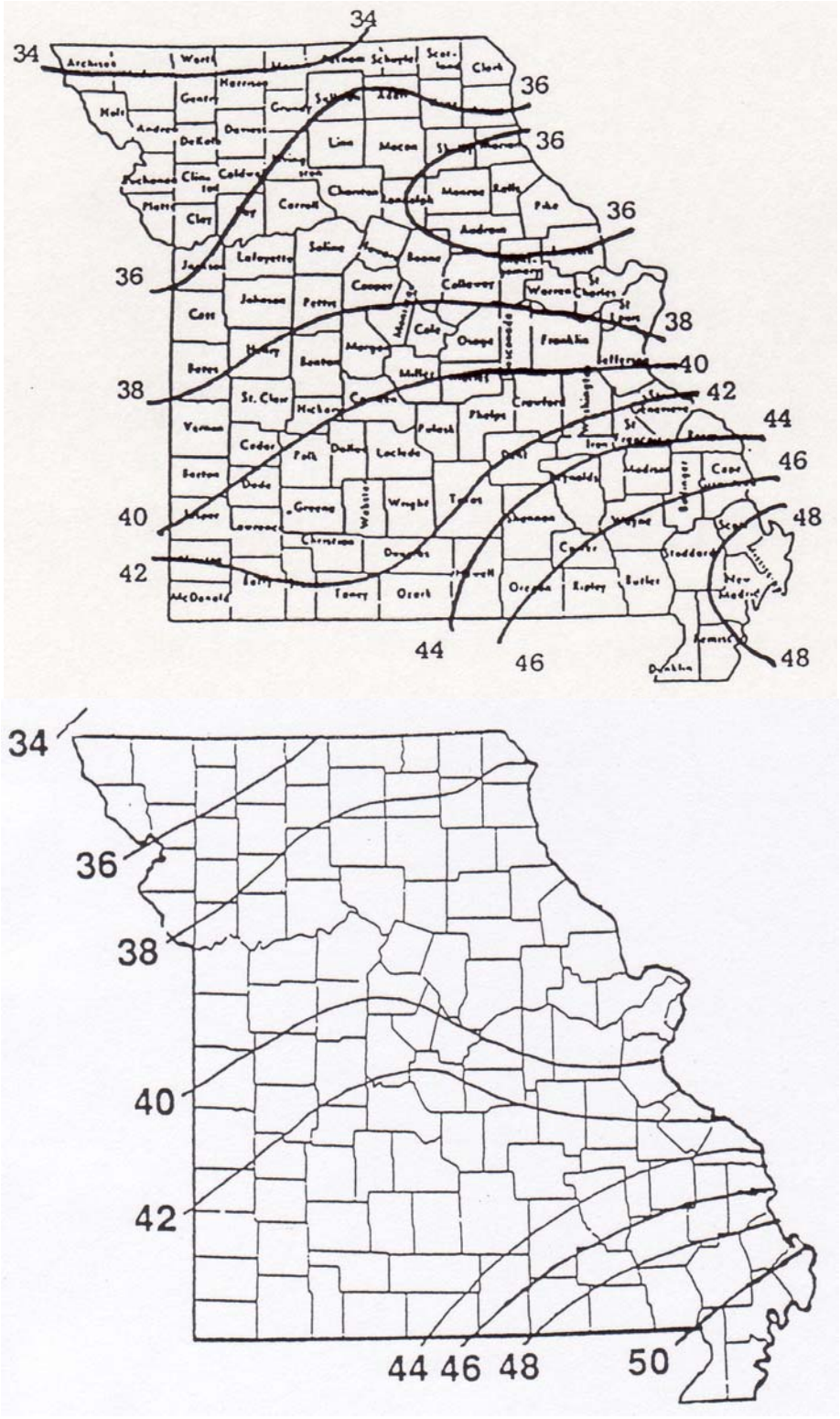

Figure 1: A comparison of average annual precipitation for 1941-80 (upper penal) and for 1961-90 (lower penal) (unit: inches).

2. Precipitation

2.1: Norms

The annual total precipitation and its spatial variation in Missouri for the 30-year period from 1971-2000 is shown in Fig. 2. Annual precipitation varies from 51.0 inches in the southern tier of the bootheel to 33.6 inches in the northwest corner of the state.

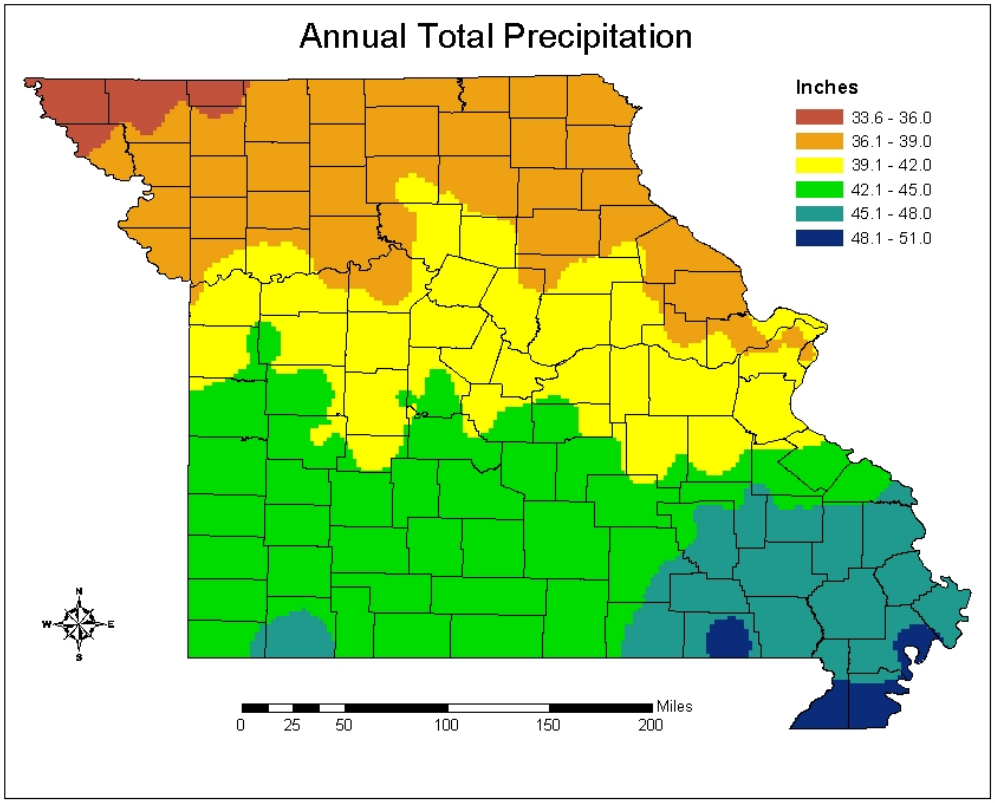

Figure 2: Annual precipitation.

Average monthly precipitation for 1971-2000 is shown in the next 12 figures. Precipitation amounts increase from the south to the north in the cold/cool season from November through April. This precipitation pattern changes in May when rainfall in the western one third of the state increases. In the summer season from June through August, the pattern shows higher amounts of rainfall in the western half of the state than in the eastern half. The bootheel is the driest area in the state in August. This east-west gradient of rainfall changes again in September when rainfall increases in the southeast section of the state during the transition from the warm to cold season. The wettest months of the year are May, June, and September.

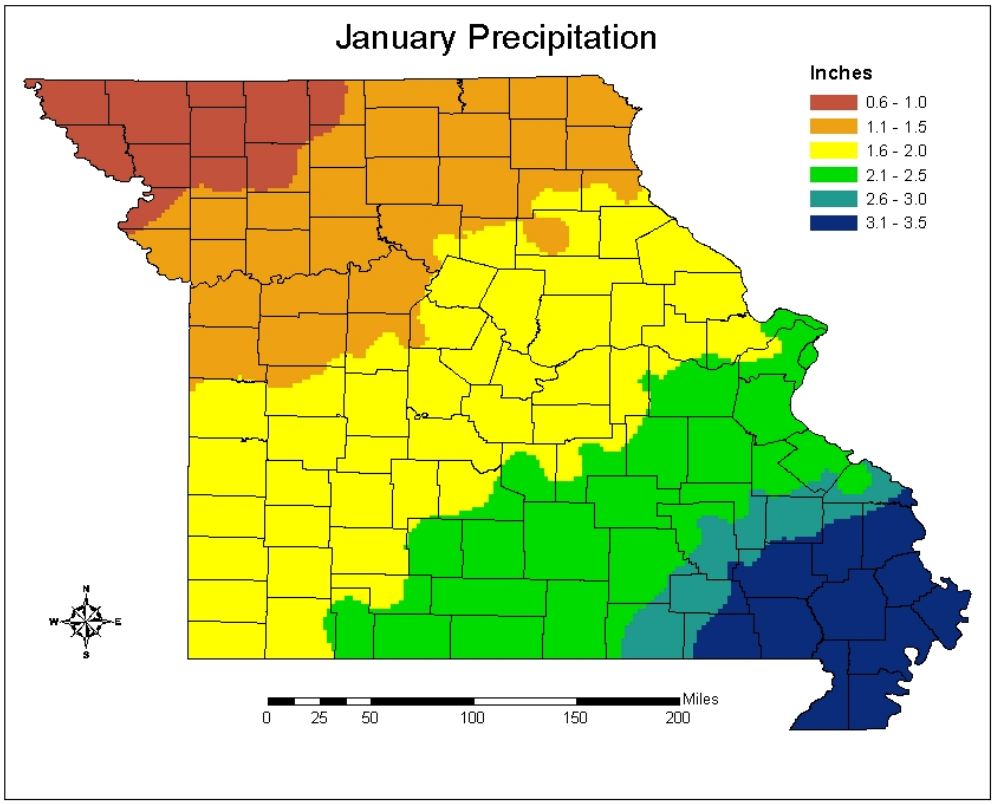

Figure 3: Total precipitation for January.

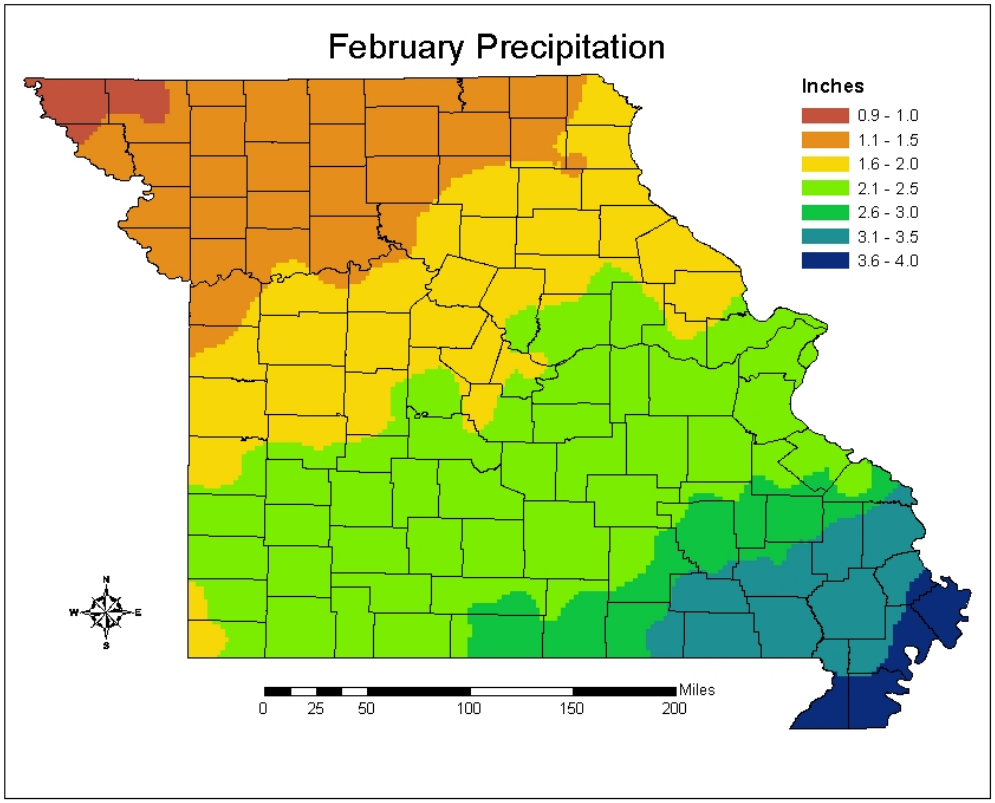

Figure 4: Total precipitation for February.

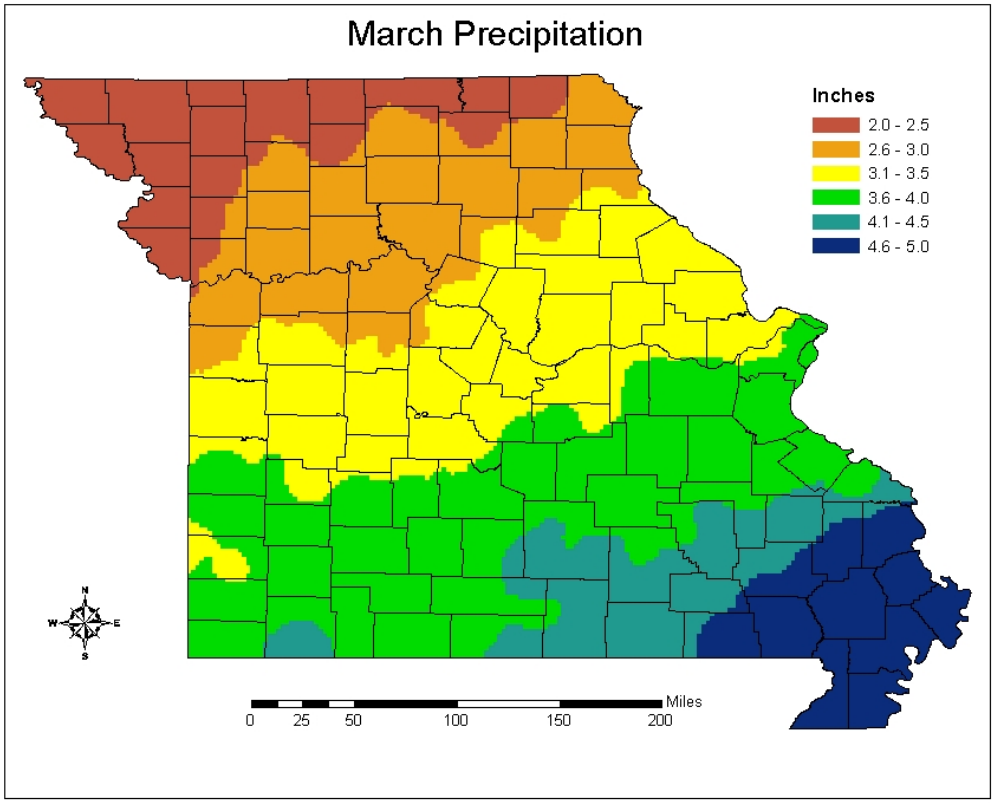

Figure 5: Total precipitation for March.

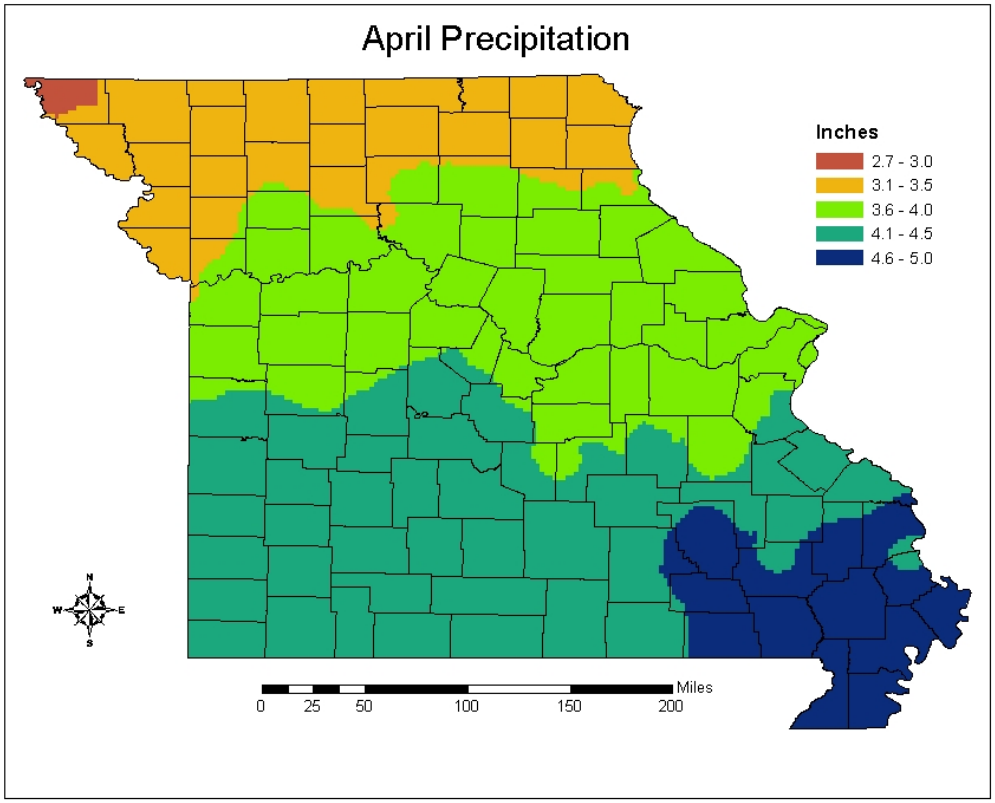

Figure 6: Total precipitation for April.

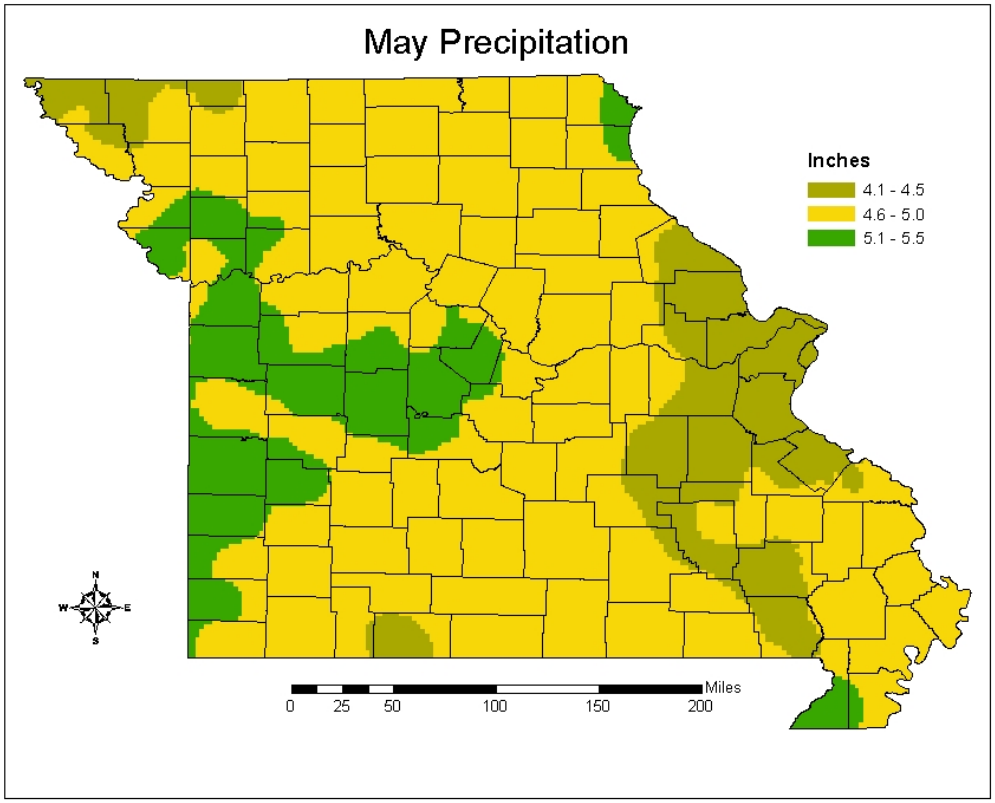

Figure 7: Total precipitation for May.

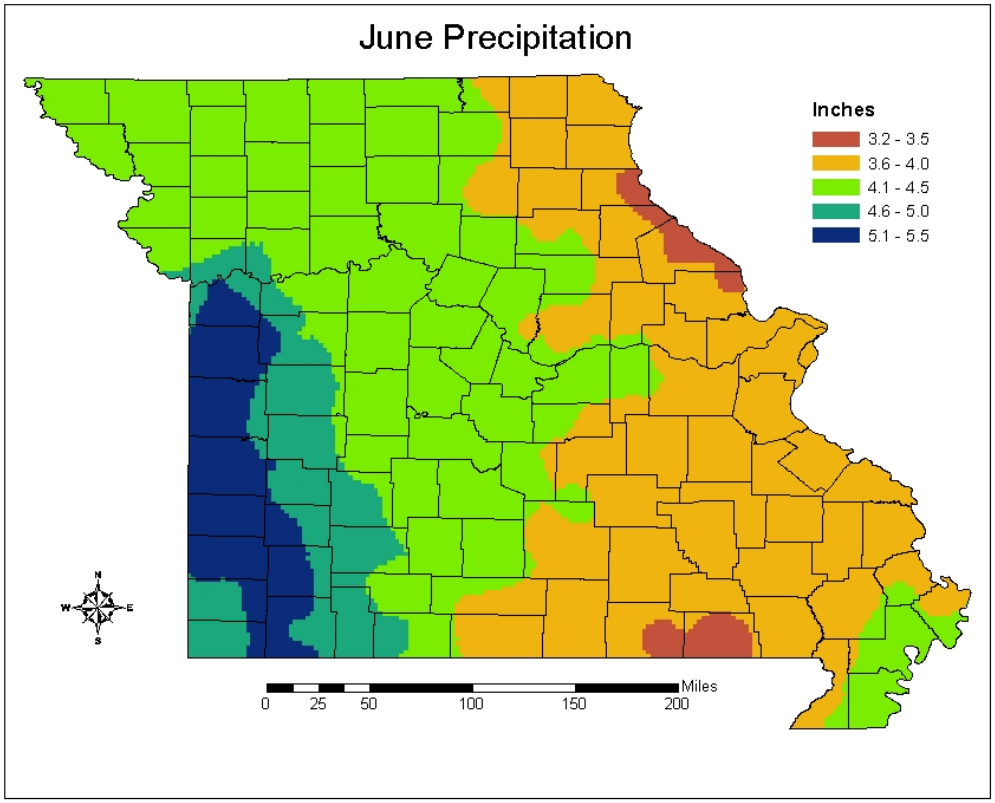

Figure 8: Total precipitation for June.

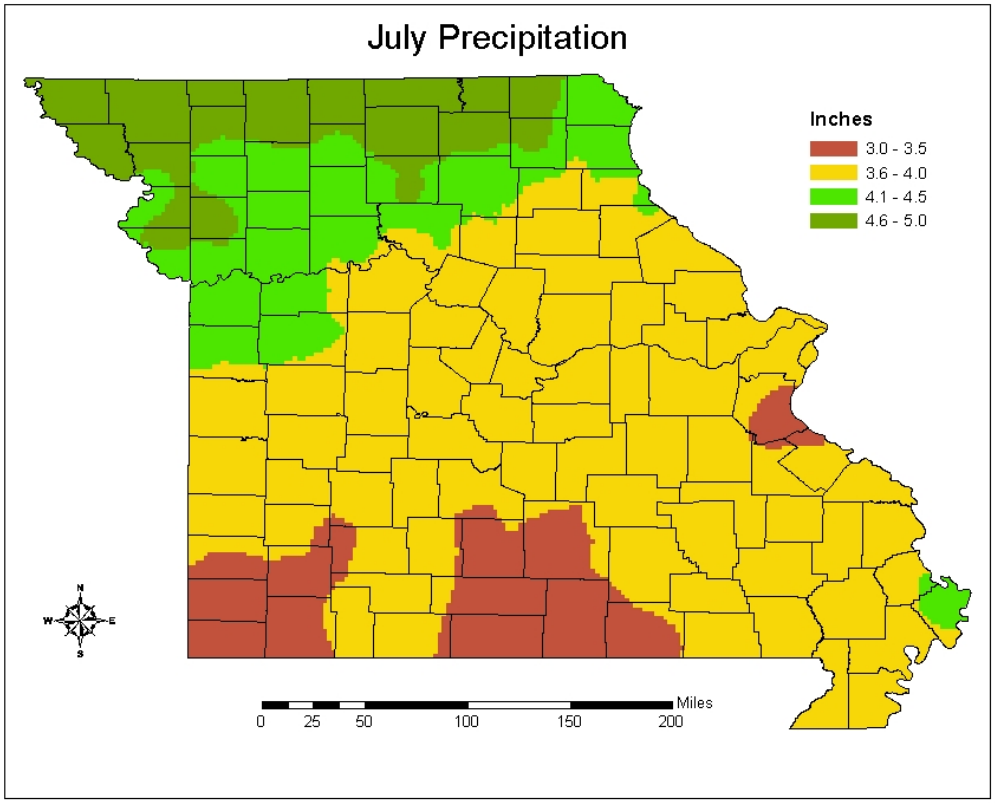

Figure 9: Total precipitation for July.

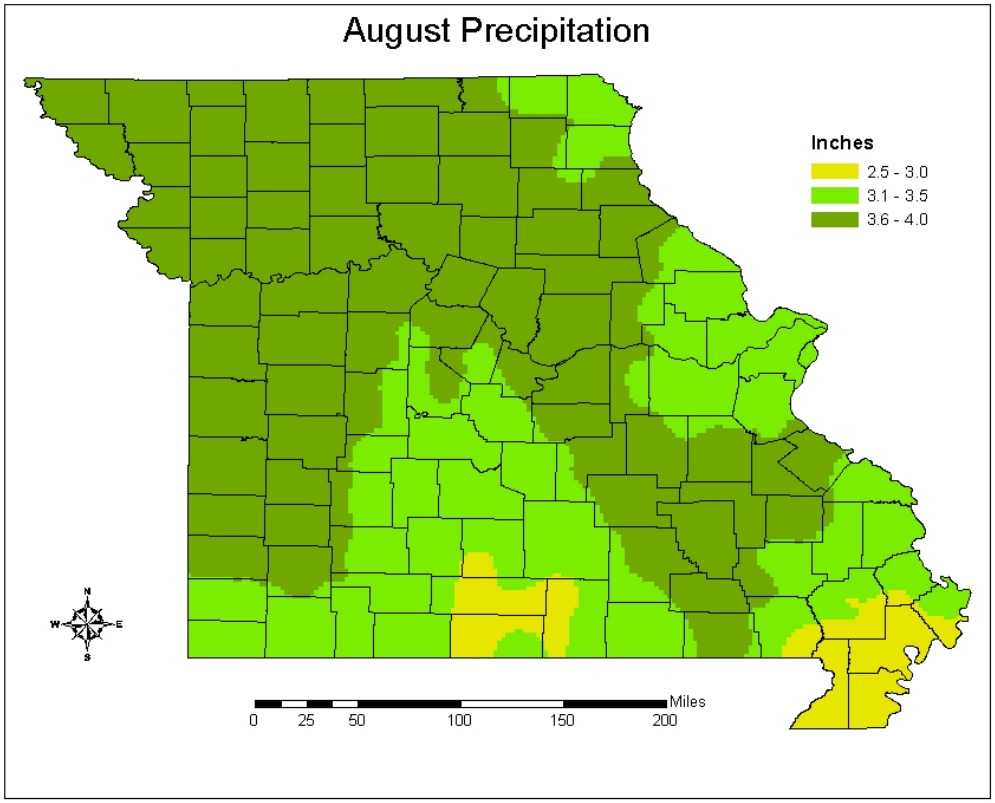

Figure 10: Total Precipitation for August.

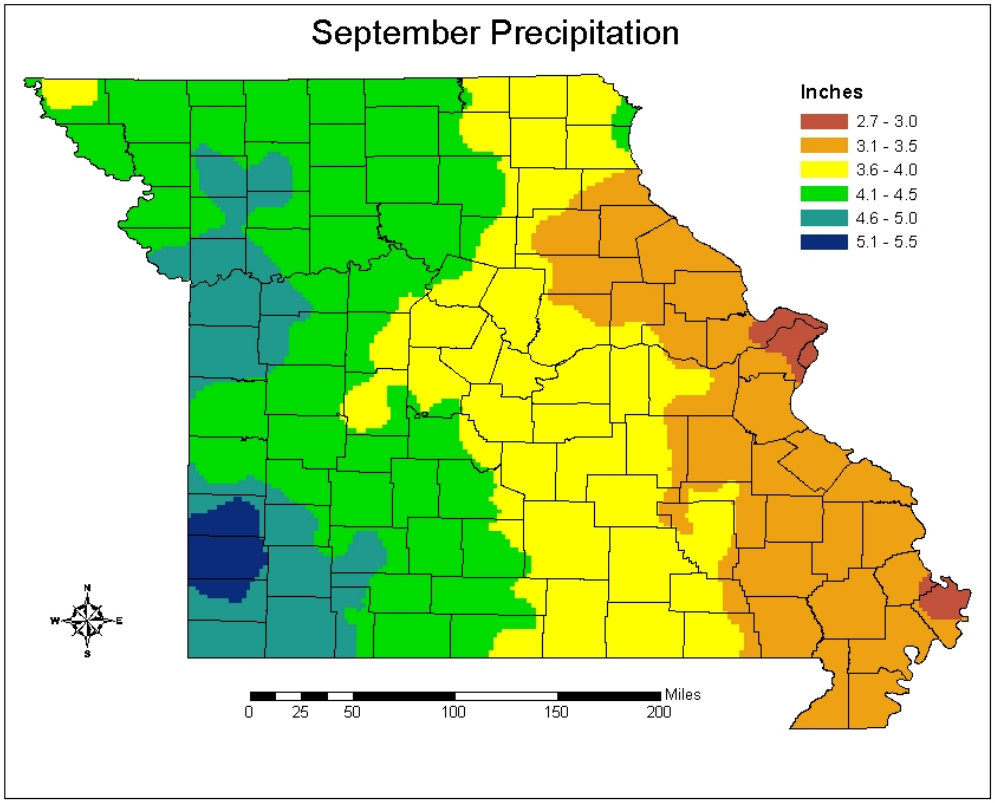

Figure 11: Total precipitation for September.

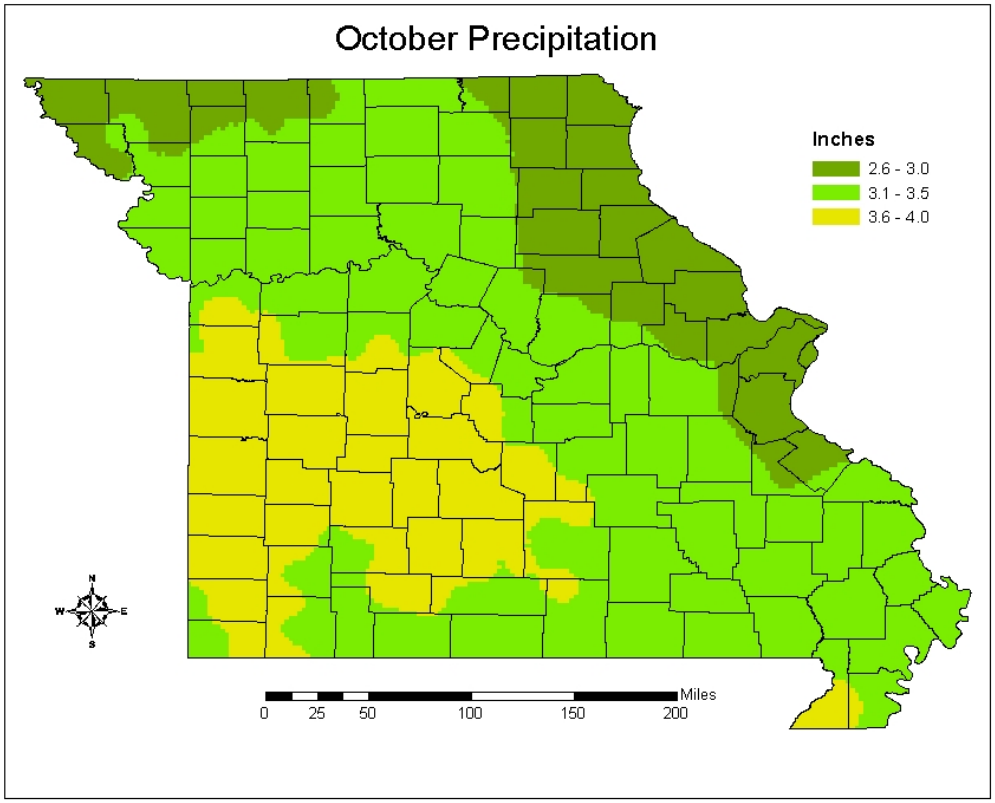

Figure 12: Total precipitation for October.

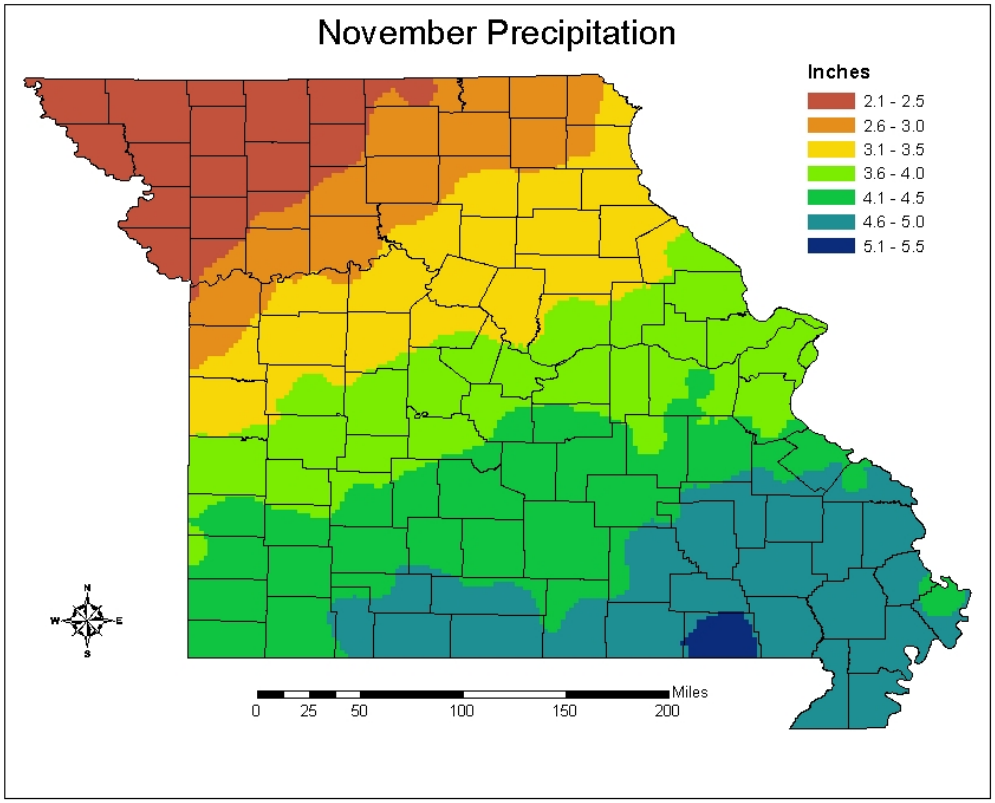

Figure 13: Total precipitation for November.

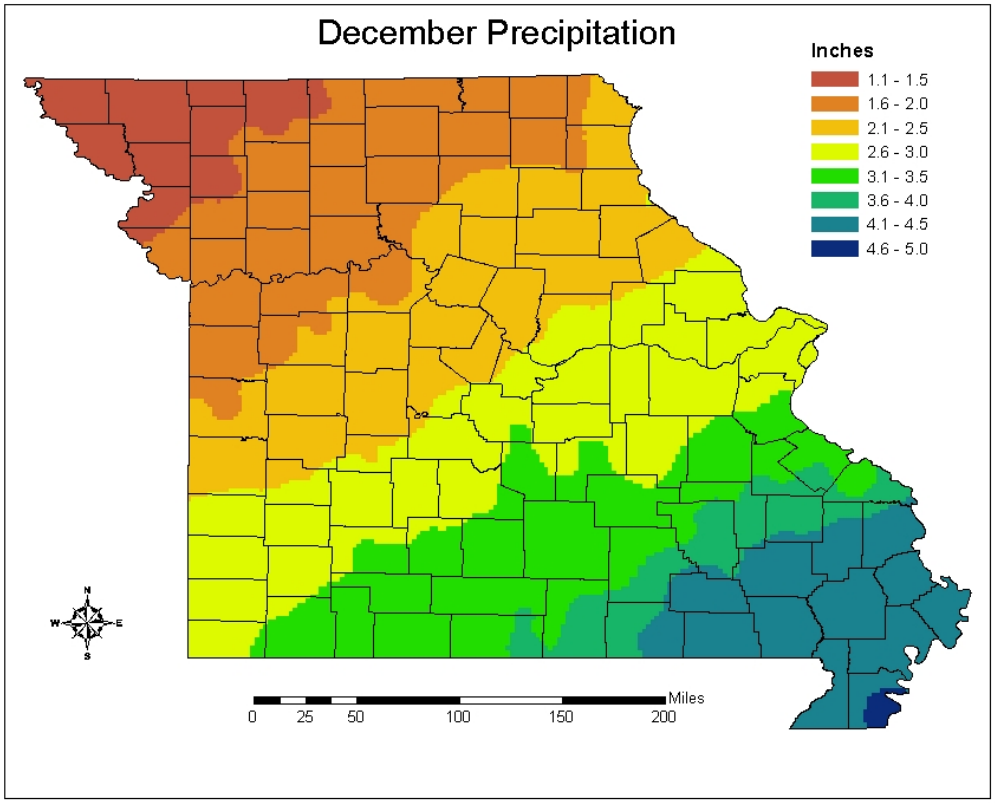

Figure 14: Total precipitation for December.

2.2: Probabilities of various precipitation events

a) 1 in 10-year annual precipitation

Two extremes of 1-in-10-year annual precipitation, the driest and wettest, are shown in Figs. 15 and 16. It is worthy of noticing that both the patterns show precipitation increasing from the north to the south. The amount of precipitation in wet cases is nearly double the amount of precipitation in dry cases at given locations.

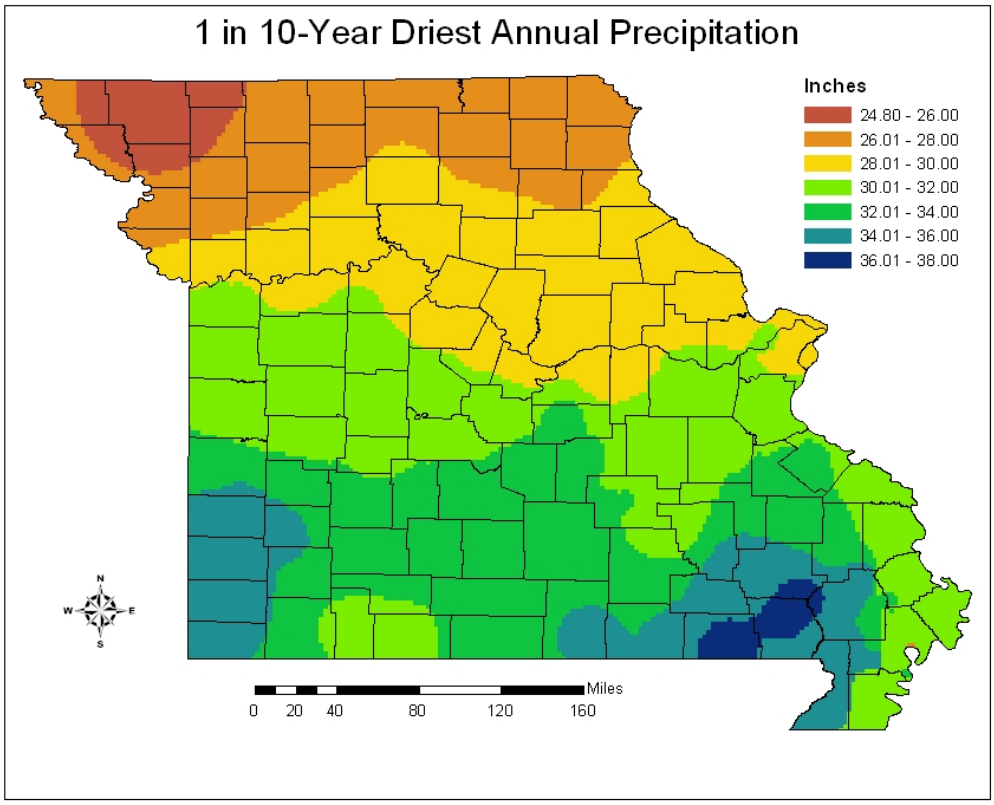

Figure 15: 1 in 10-year dry extreme of annual precipitation.

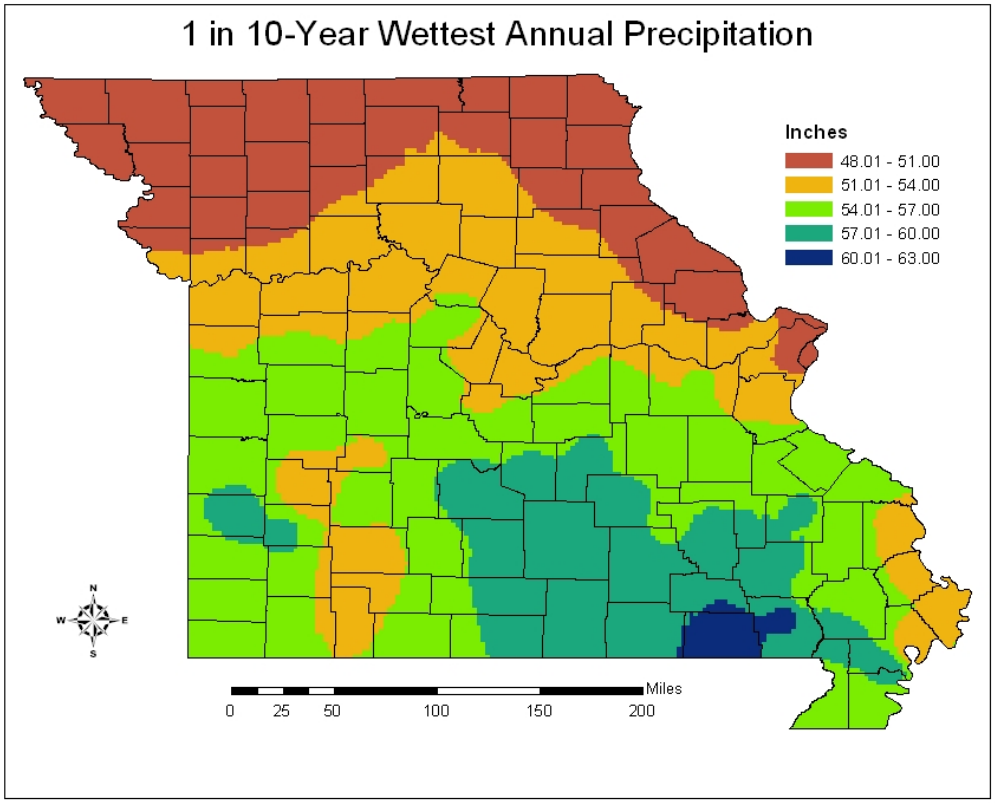

Figure 16: 1 in 10-year wet extreme of annual precipitation.

b) 1 in 10-year 2-day precipitation

Figure 17 shows the 1 in 10-year 2-day precipitation (wettest). This distribution shows a high amount of precipitation in the western central portion of the state and low amount near the eastern boundary of the state, a pattern similar to the warmer season precipitation. This similarity suggests that the heavy 2-day rainfall events occur during the warm season.

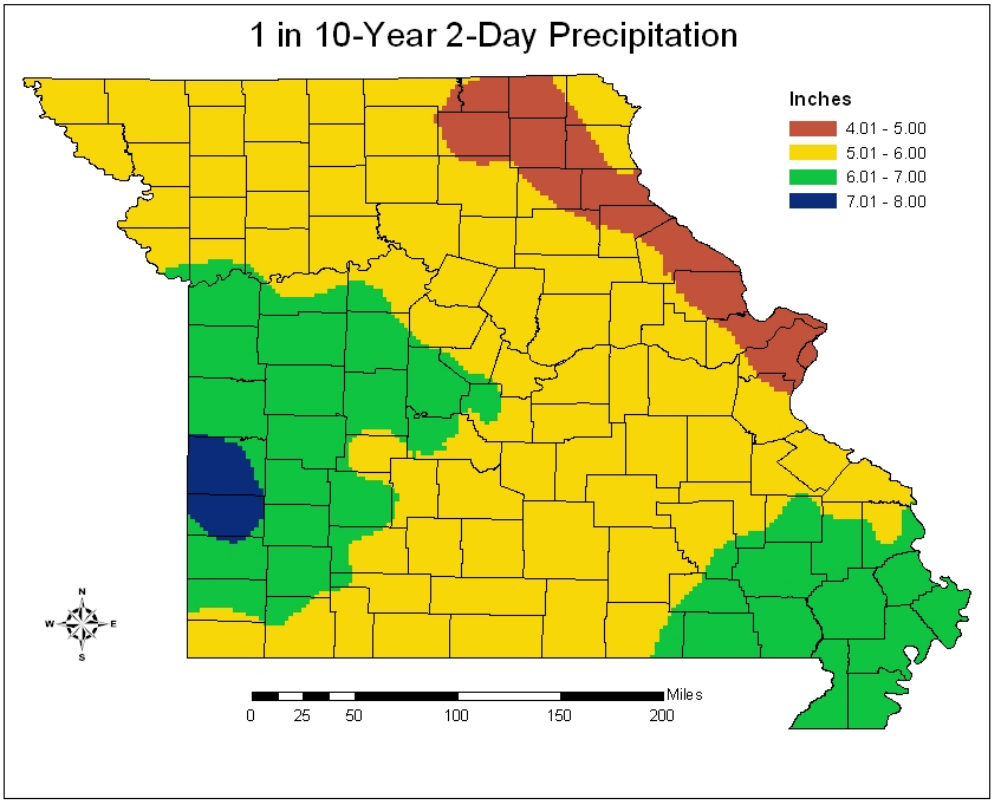

Figure 17: 1 in 10-year 2-day precipitation.

c) 1 in 10-year 10-day precipitation

Figure 18 shows the amount of precipitation during the wettest 10-day period for the occurrence frequency of 1 in 10 years (the driest 10-day precipitation is zero of course). This distribution shows a high amount of precipitation in the western central portion of the state and low amount near the eastern boundary of the state, a pattern similar to the warmer season precipitation. This similarity suggests that the wettest cases occur during the warm season.

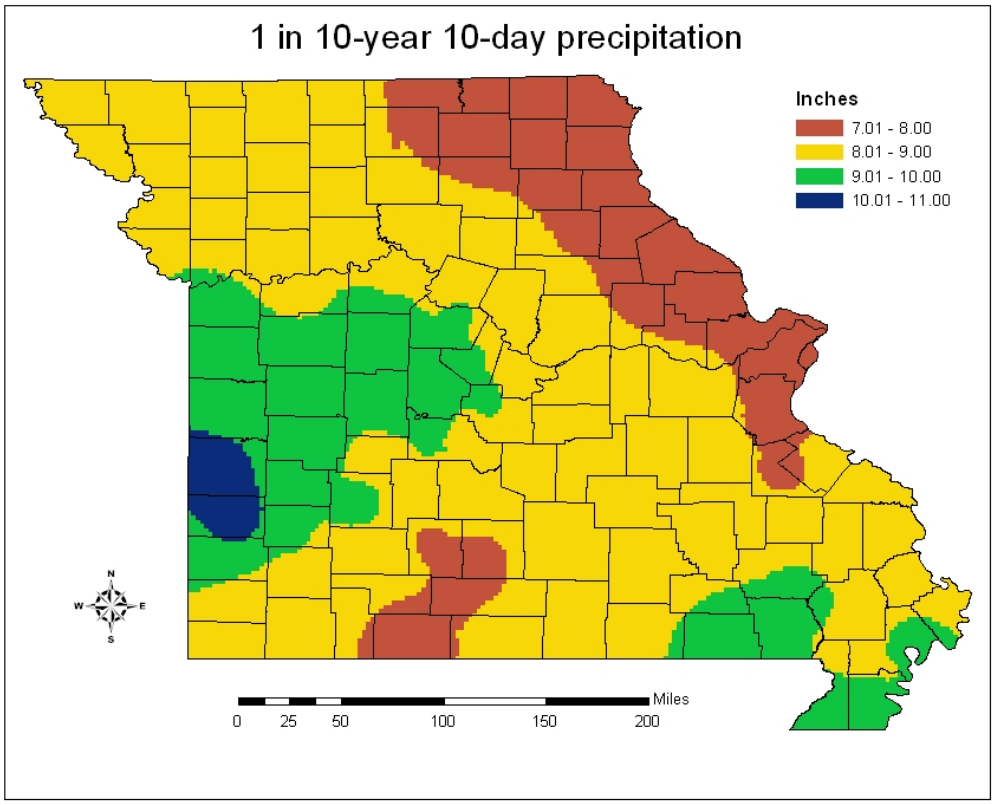

Figure 18: 1 in 10-year 10-day precipitation.

d) 1 in 25-year 1-day precipitation

Figure 19 shows the 1 in 25-year 1-day precipitation, a pattern similar to that in the previous two figures. The center of the largest 1-day precipitation is in the southwestern Missouri around Lamar, and a belt of small 1-day precipitation stretches from the northeast to the St. Louis area.

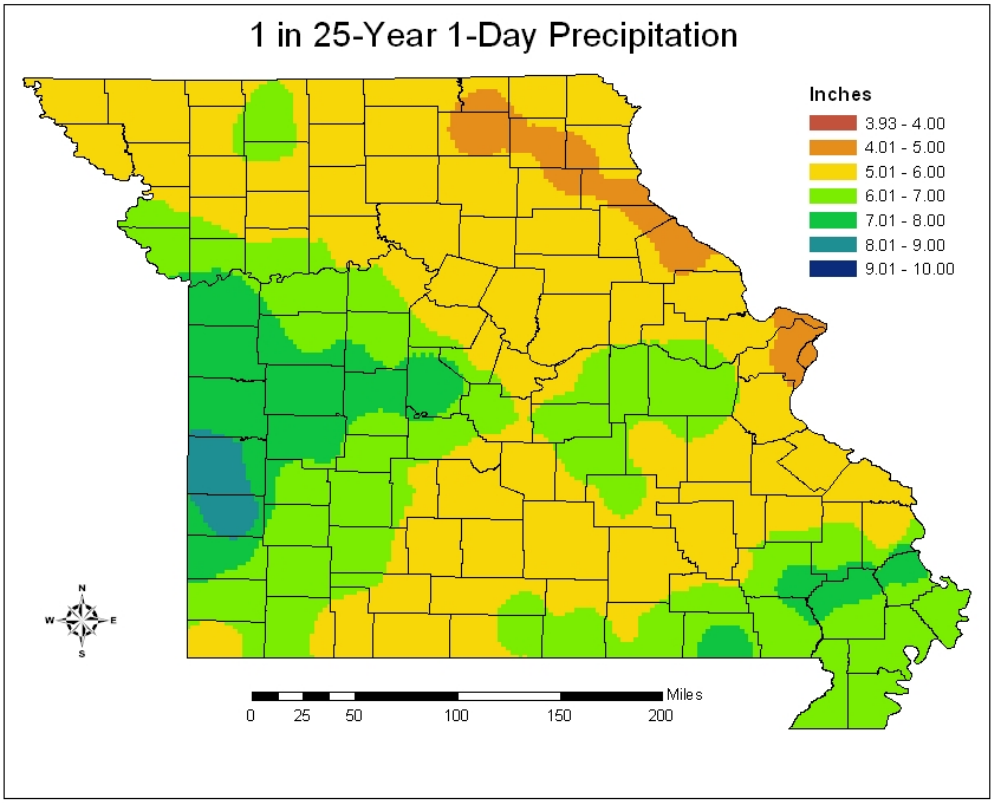

Figure 19: 1 in 25-year 1-day precipitation.

e) 1 in 25-year 10-day precipitation

The 1 in 25-year 10-day precipitation shown below is similar in pattern to the previous three figures. A major point suggested by this similarity is that the warm season precipitation has contributed to the heaviest rain events in the state.

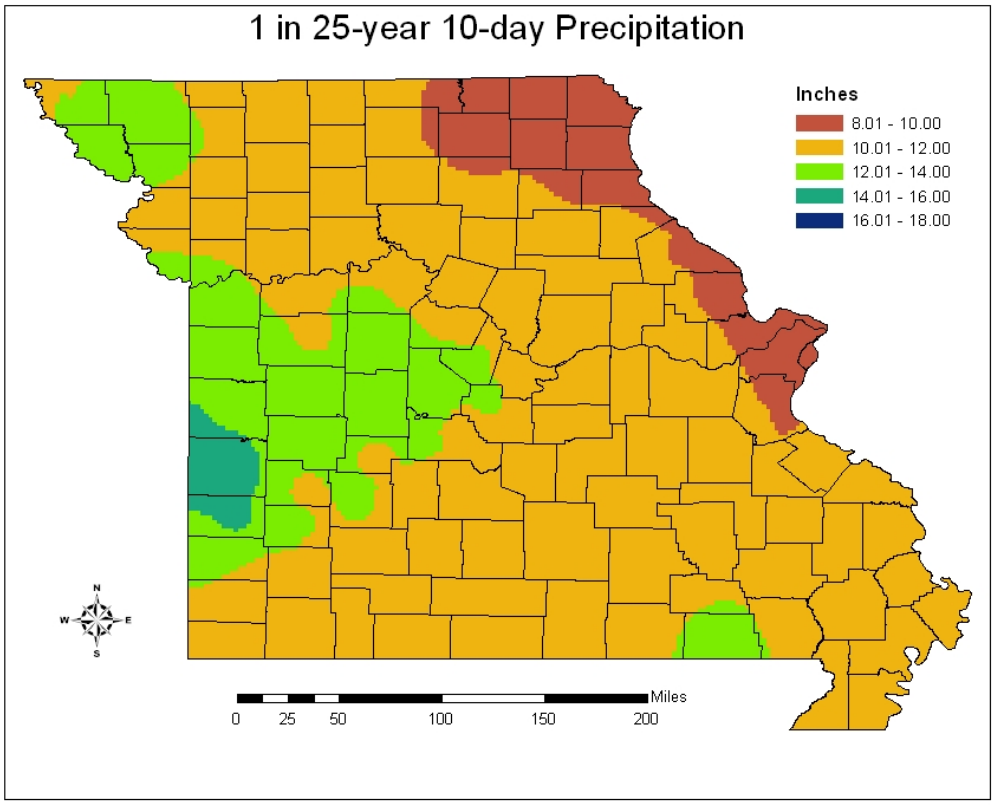

Figure 20: 1 in 25-year 10-day precipitation.

f) Number of days of precipitation occurring once in 10 years

The least number of precipitation days occurring once in 10-years is shown in Fig. 20. Although the pattern shows variations in the number of days from west to east the average number of precipitation days over the state is about 70, that is, only 70 of the 365 days during a year have some observed amount of precipitation (rain or snow).

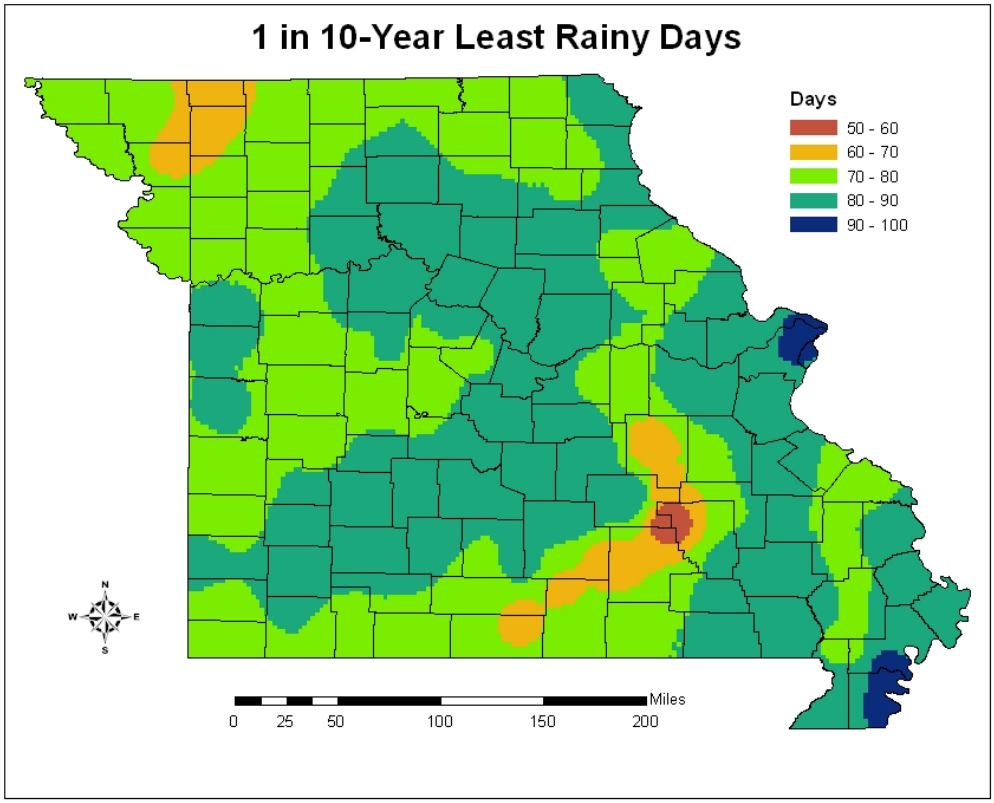

Figure 21: 1 in 10-year fewest number of days with precipitation.

Figure 22 shows the greatest number of precipitation days occurring at a probability of once in 10 years. Although a weak north-south gradient is apparent, suggesting winter precipitation contributes to the total number of precipitation days, the variation across difference regions is small. The average number of days with observed precipitation in the state is 120, that is, 120 of the 365 days in a year have some amount of observed precipitation (rain or snow).

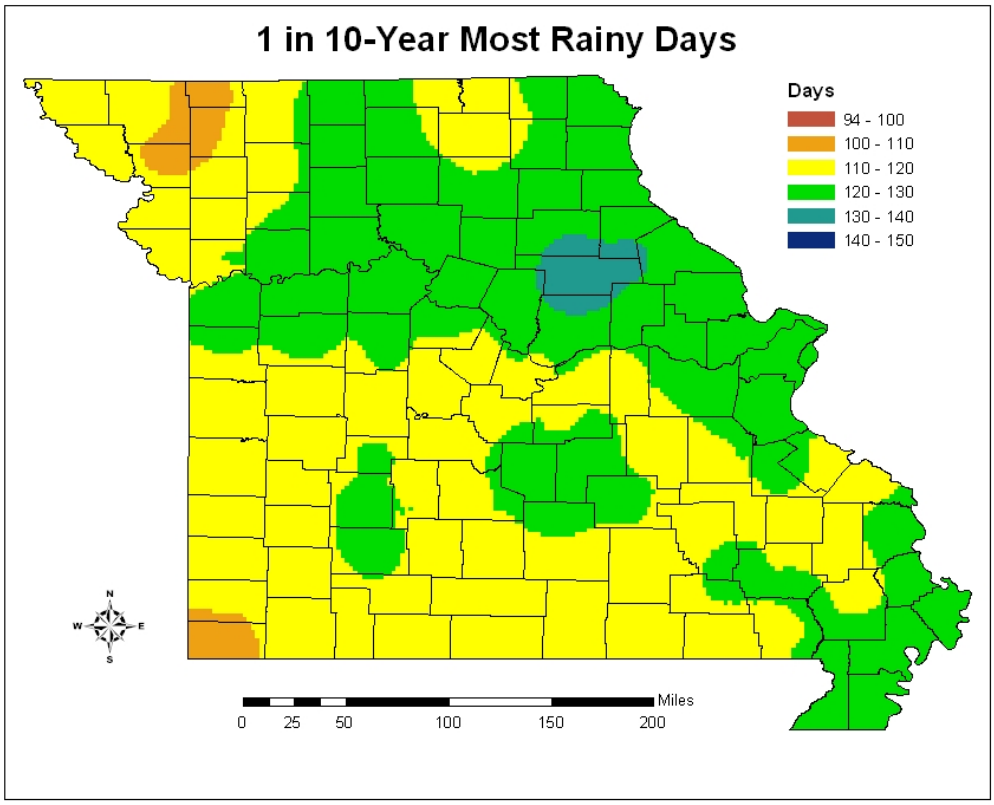

Figure 22: 1 in 10-year largest number of precipitation days.

2.3: Monthly and annual precipitation for specific wet and dry years

a) 1973

The year 1973 was a very wet year. The excessive amount of annual precipitation ranges from 10 inches above normal in northern and east central region to 30 inches above normal in the southeast corner (Fig. 2).

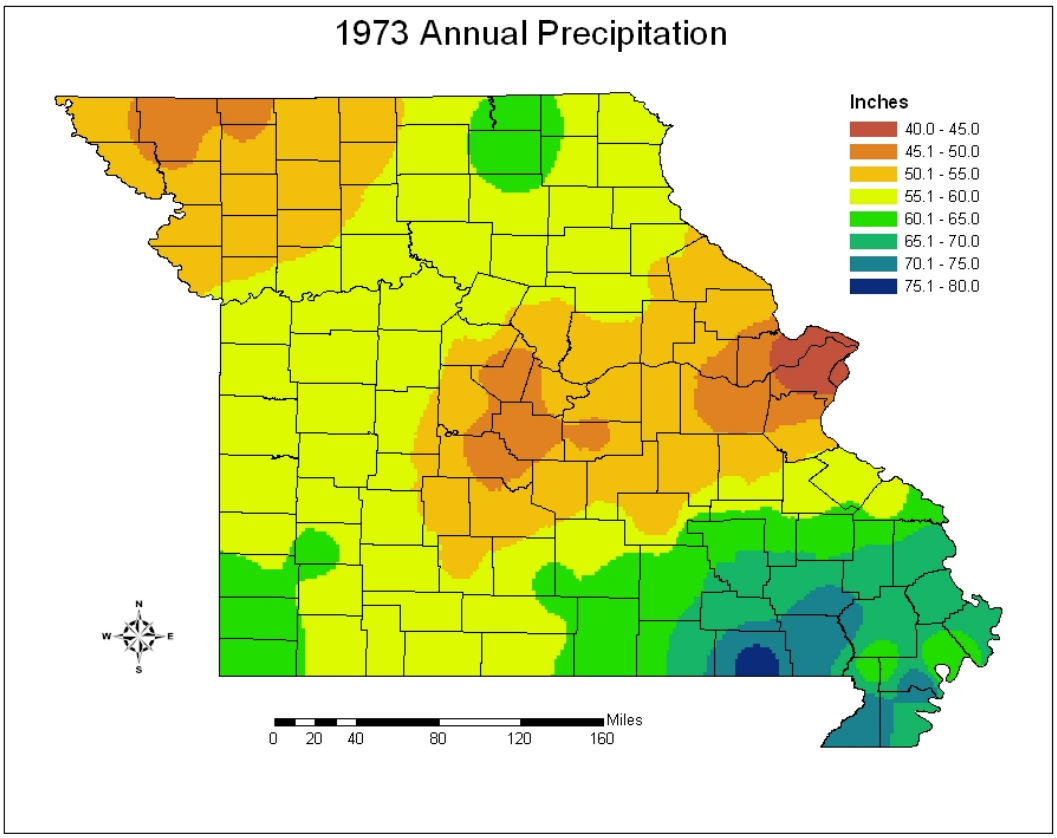

Figure 23: Annual precipitation for 1973.

The next 12 figures show the monthly precipitation in 1973.

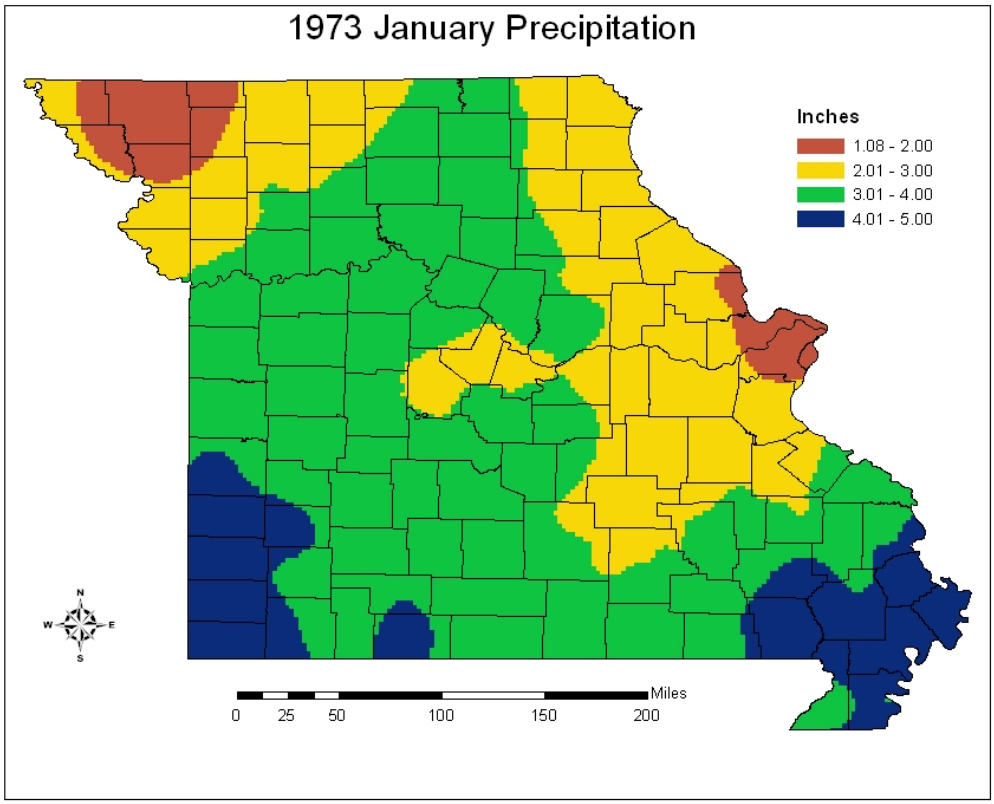

Figure 24: January precipitation, 1973.

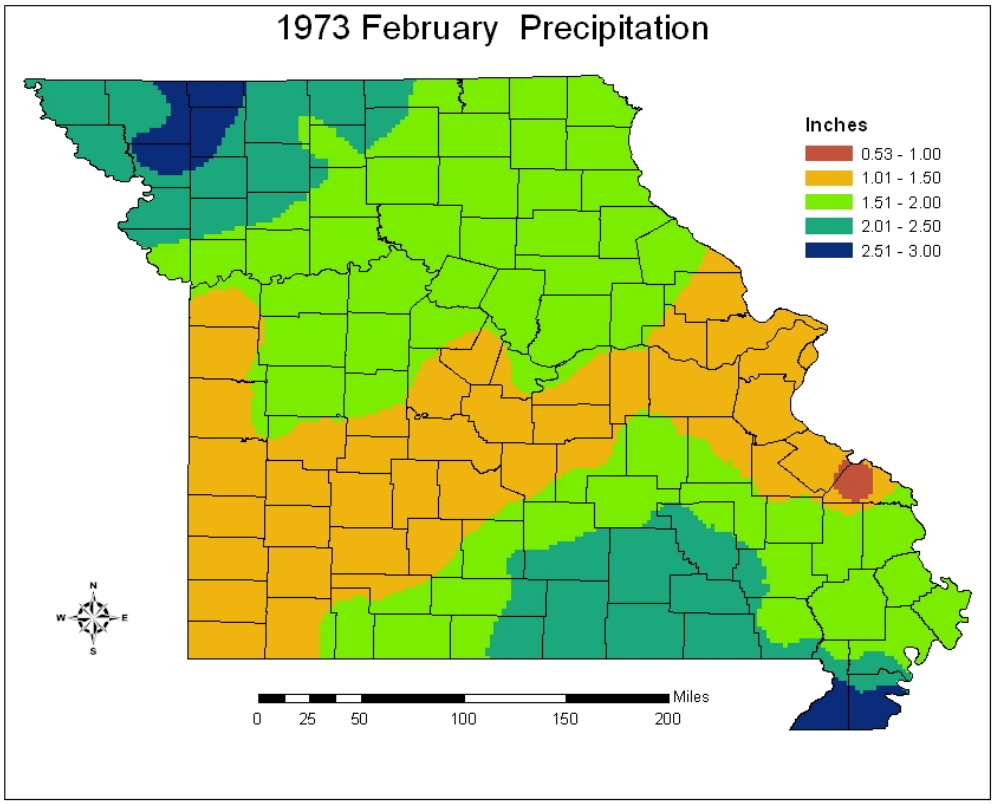

Figure 25: February precipitation, 1973.

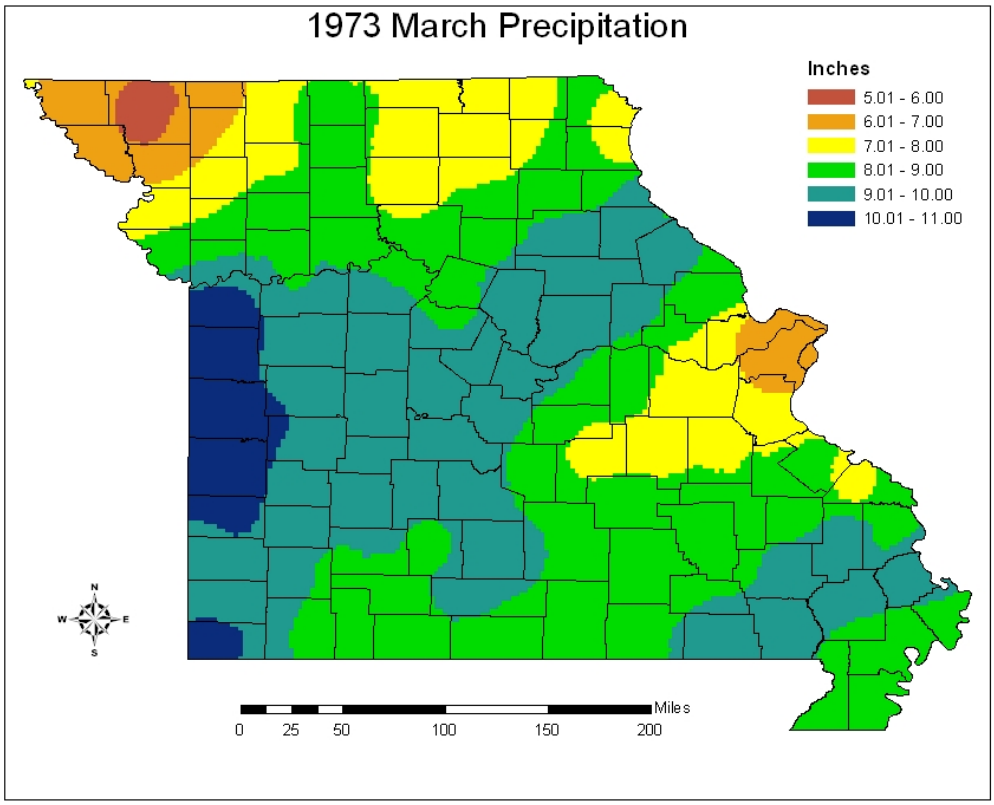

Figure 26: March precipitation, 1973.

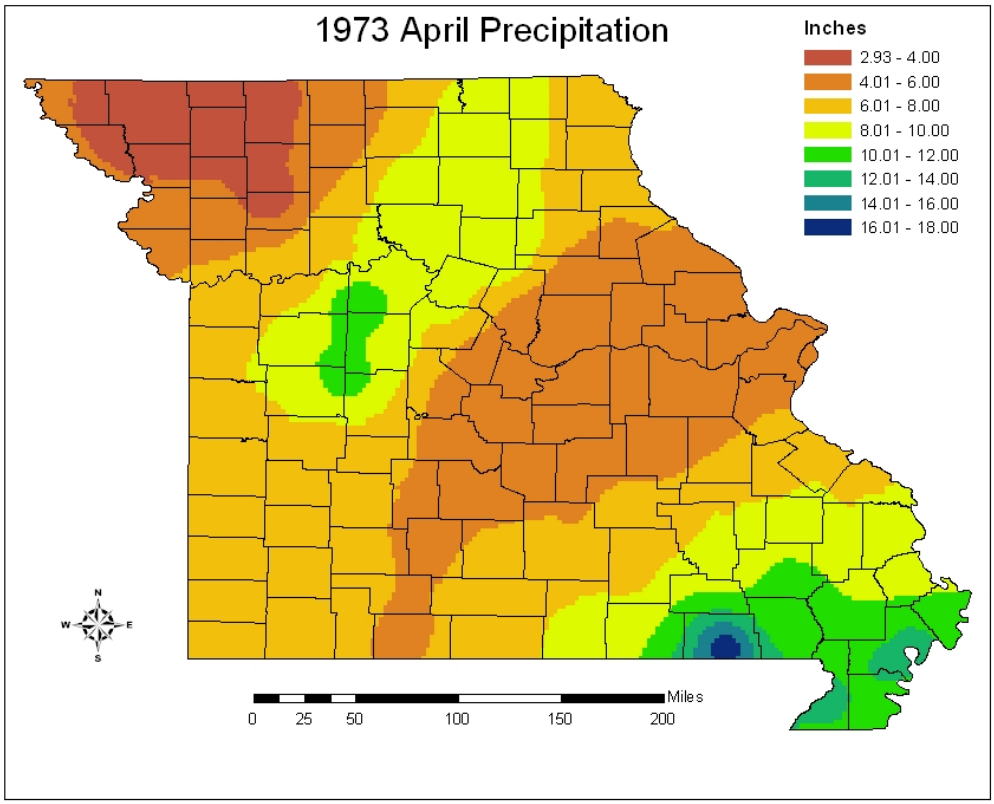

Figure 27: April precipitation, 1973.

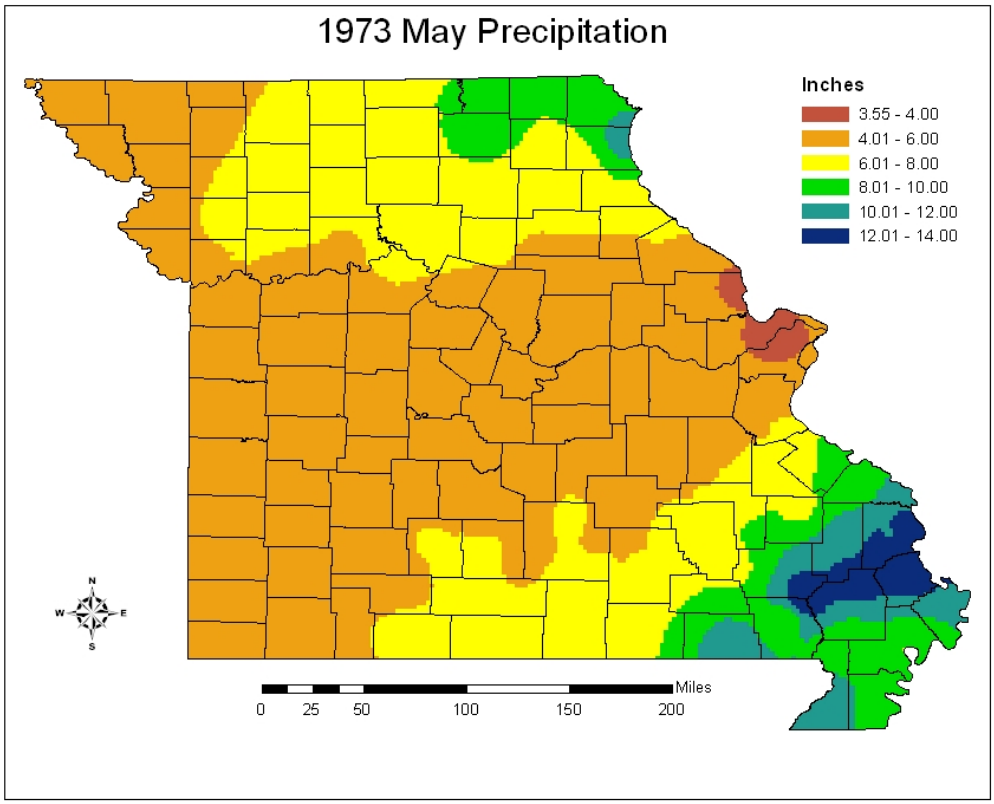

Figure 28: May precipitation, 1973.

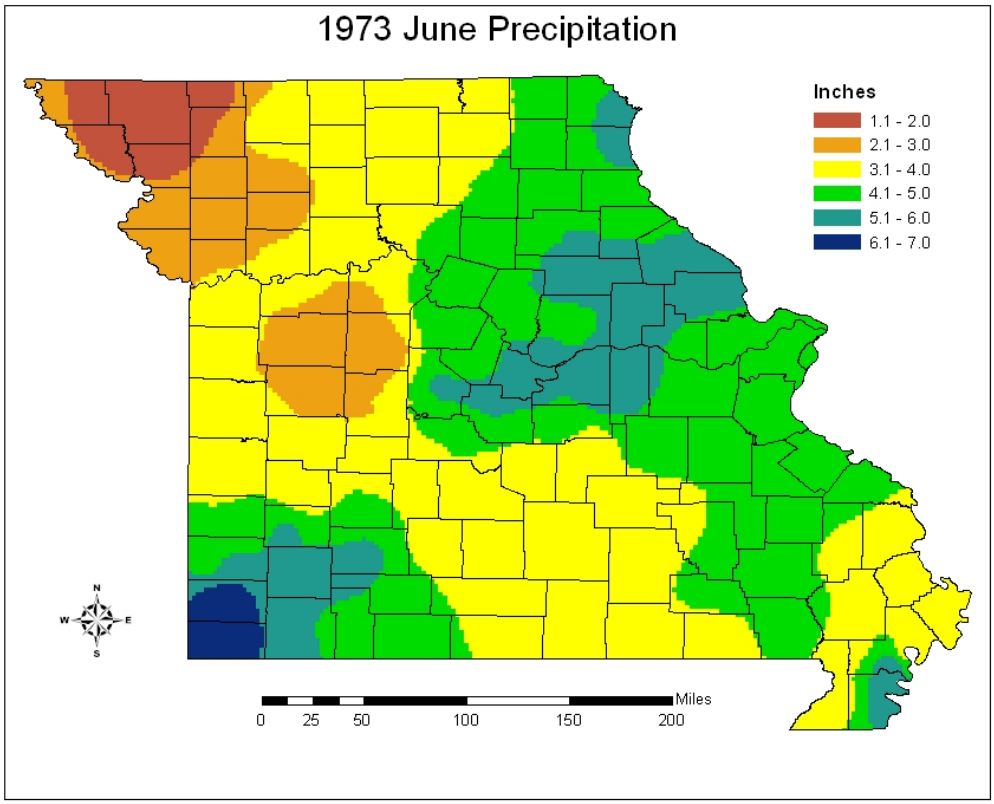

Figure 29: June precipitation, 1973.

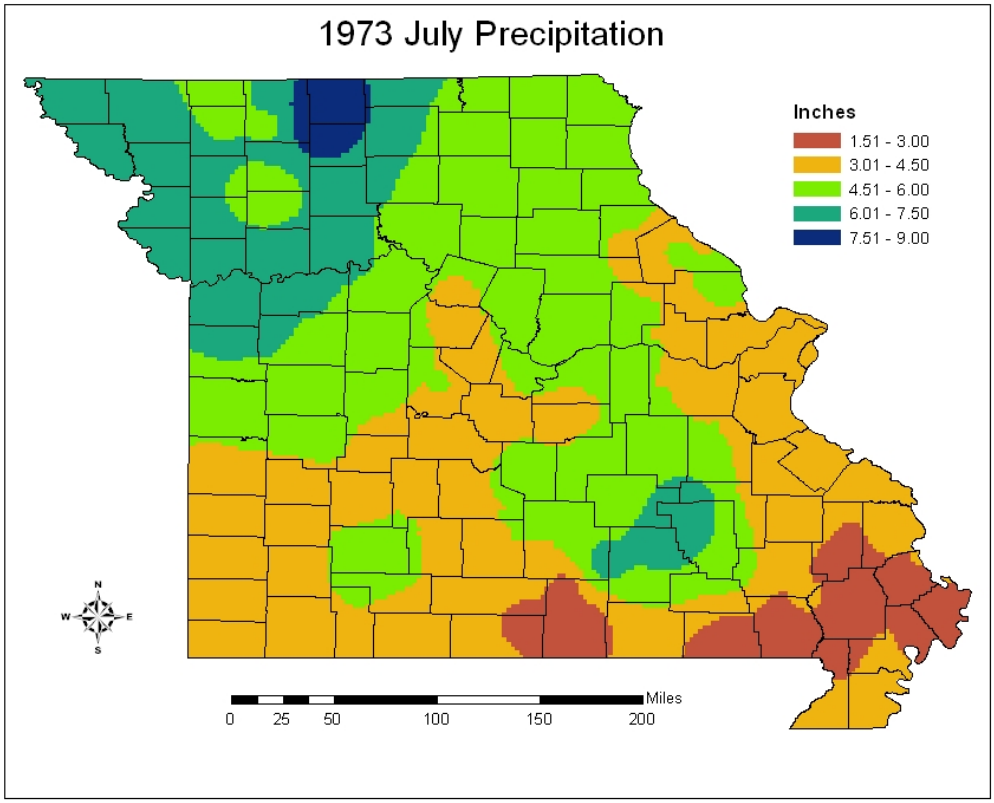

Figure 30: July precipitation, 1973.

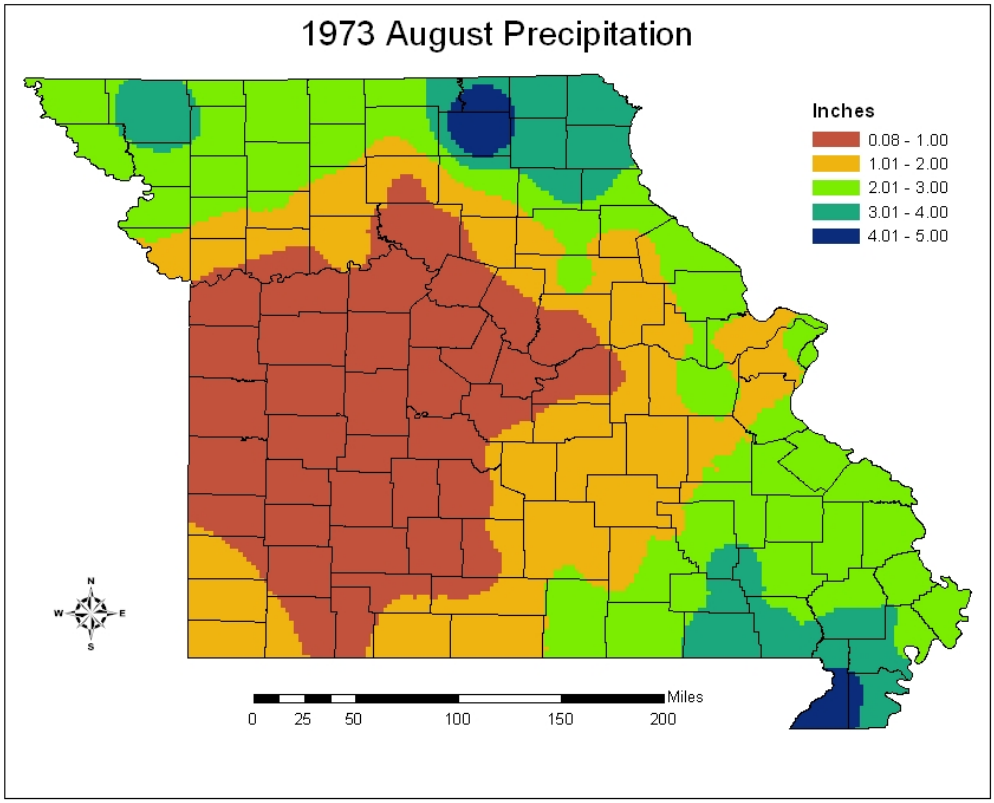

Figure 31: August precipitation, 1973.

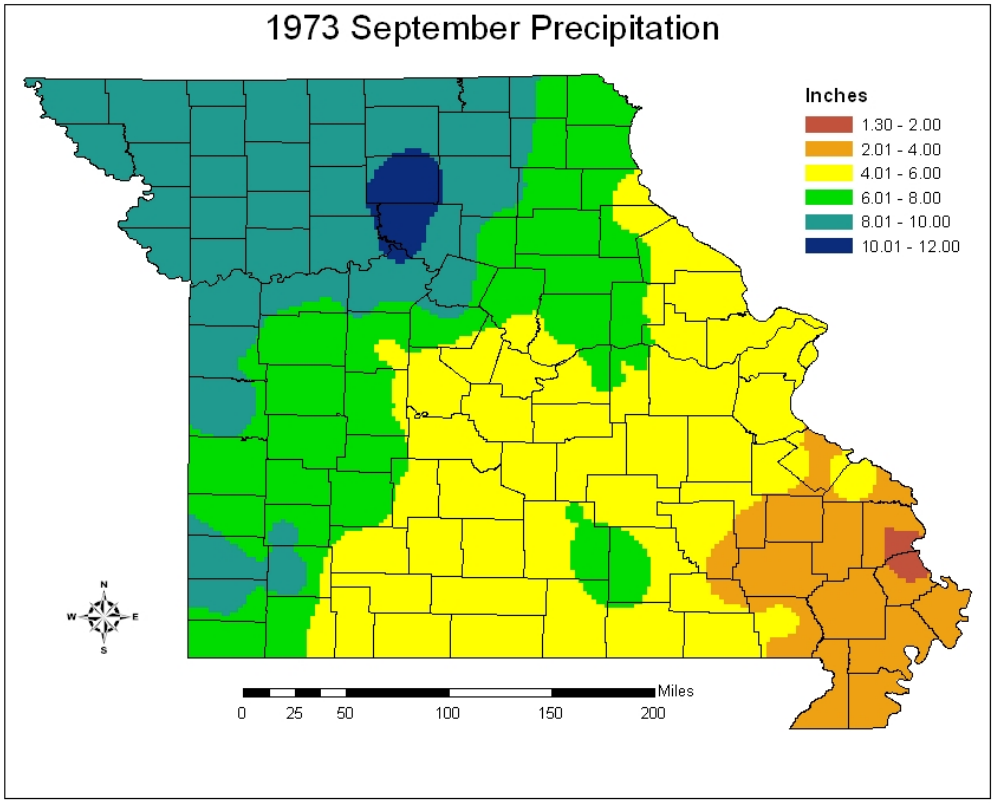

Figure 32: September precipitation, 1973.

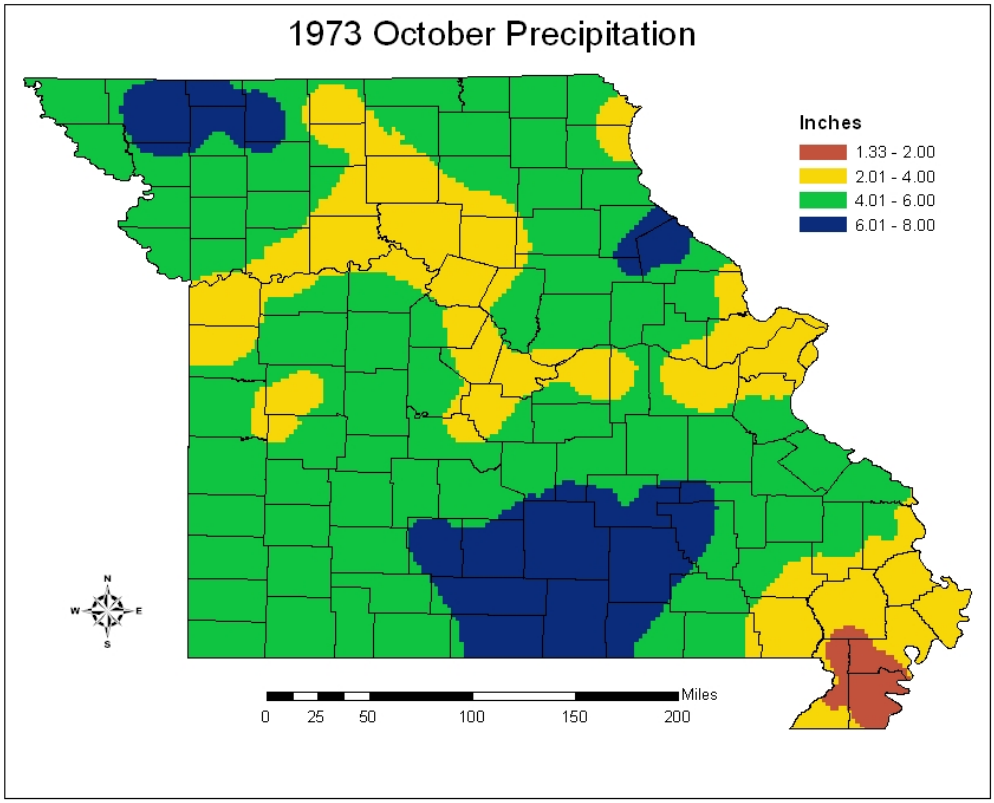

Figure 33: October precipitation, 1973.

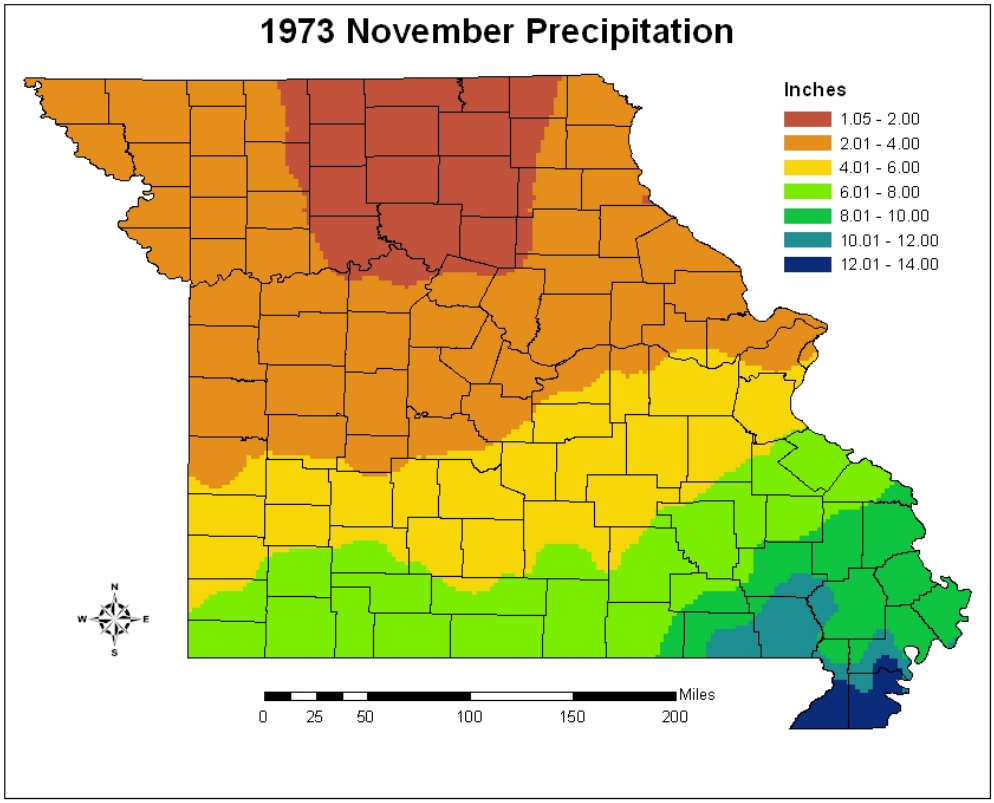

Figure 34: November precipitation, 1973.

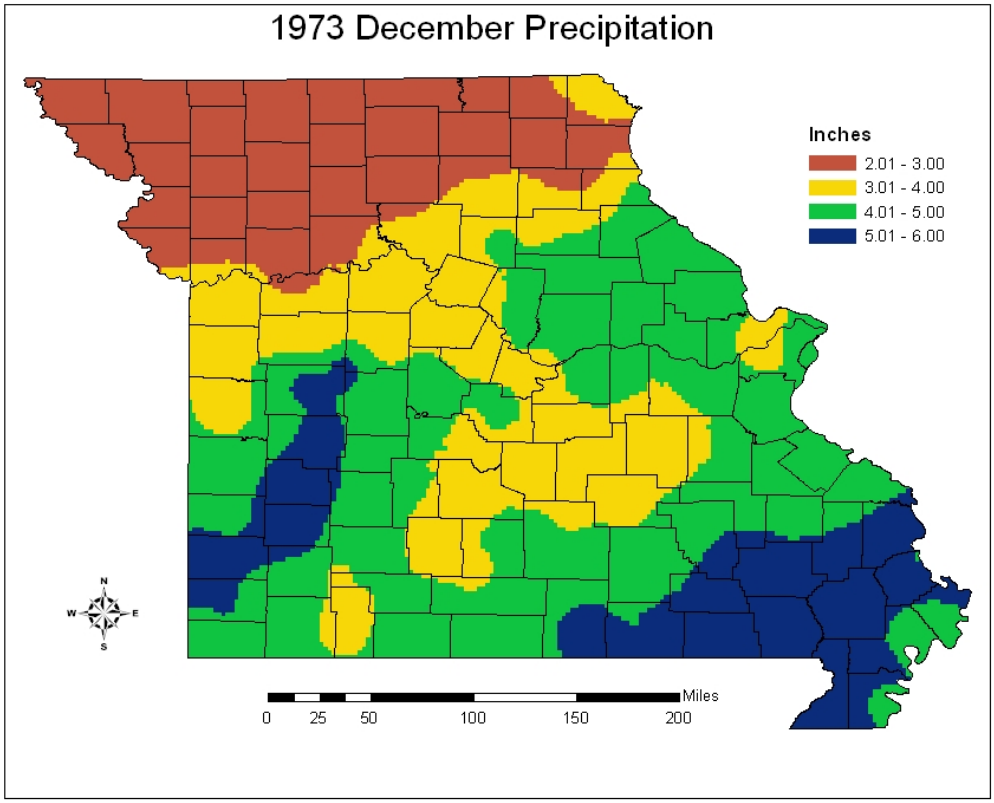

Figure 35: December precipitation, 1973.

b) 1982

The year of 1982 was a wet year, but not as wet as in 1973. During the year the monthly precipitation evolved in a similar way as the average year. Two very wet months in January (Fig. 37) and August (Fig. 43) contributed substantially to the wet anomaly for the year.

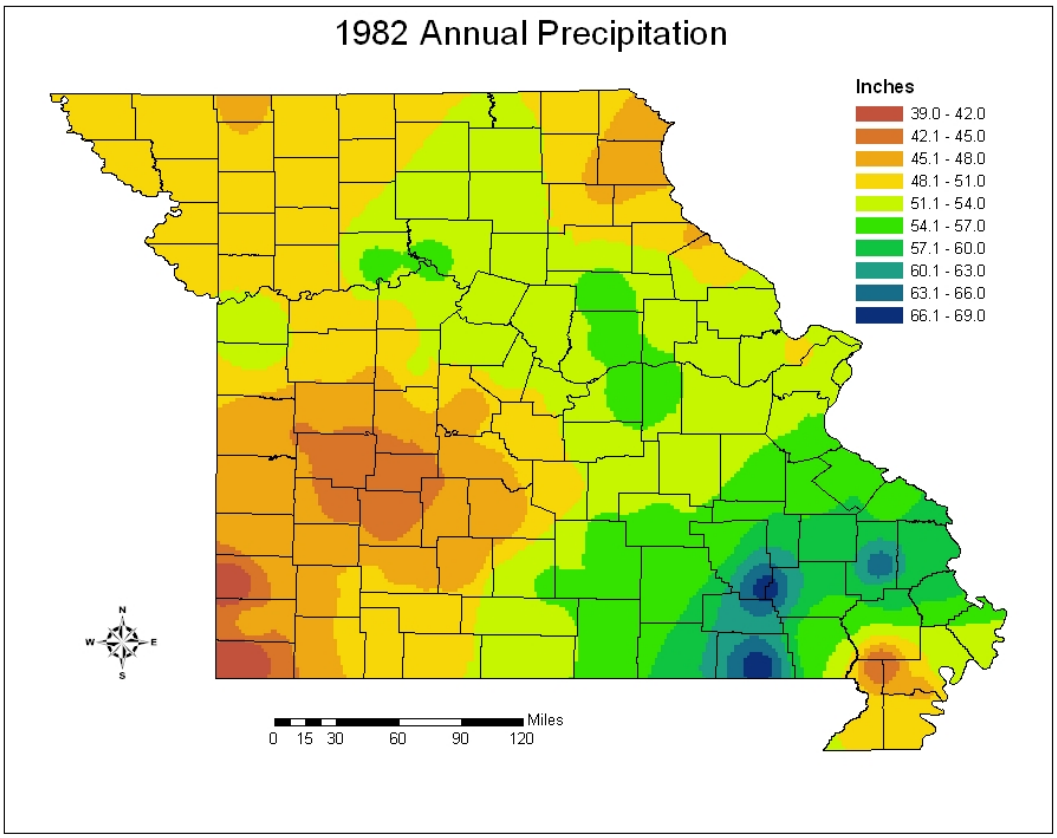

Figure 36: Annual precipitation for 1982.

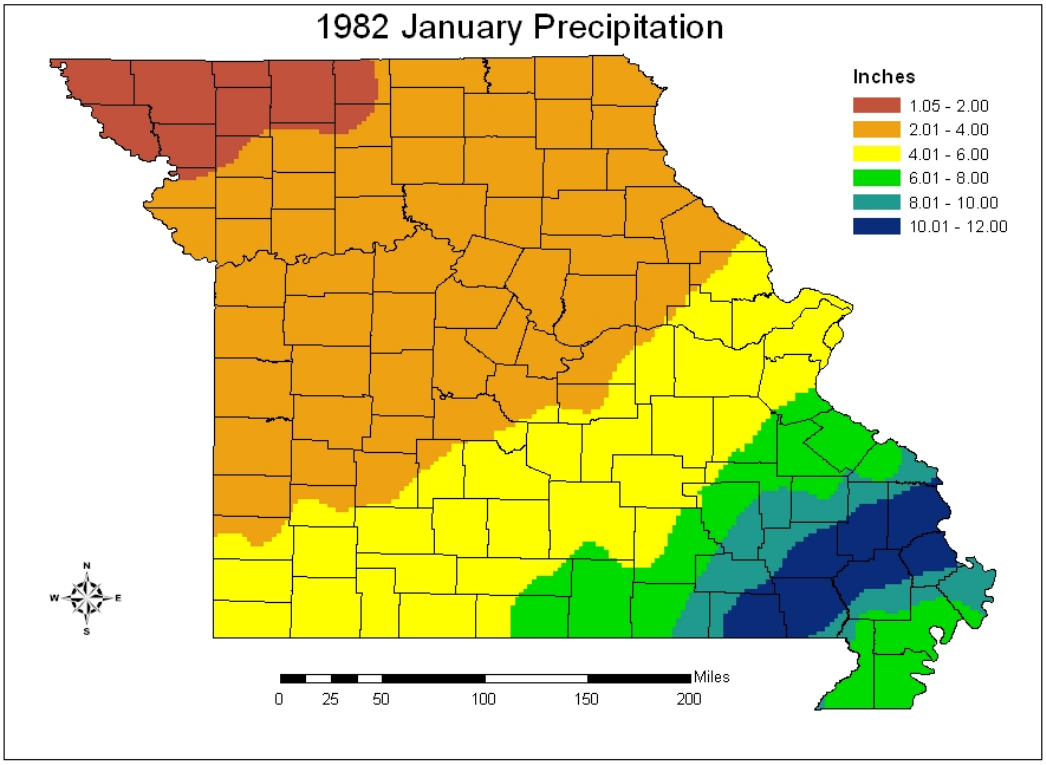

Figure 37: January precipitation, 1982.

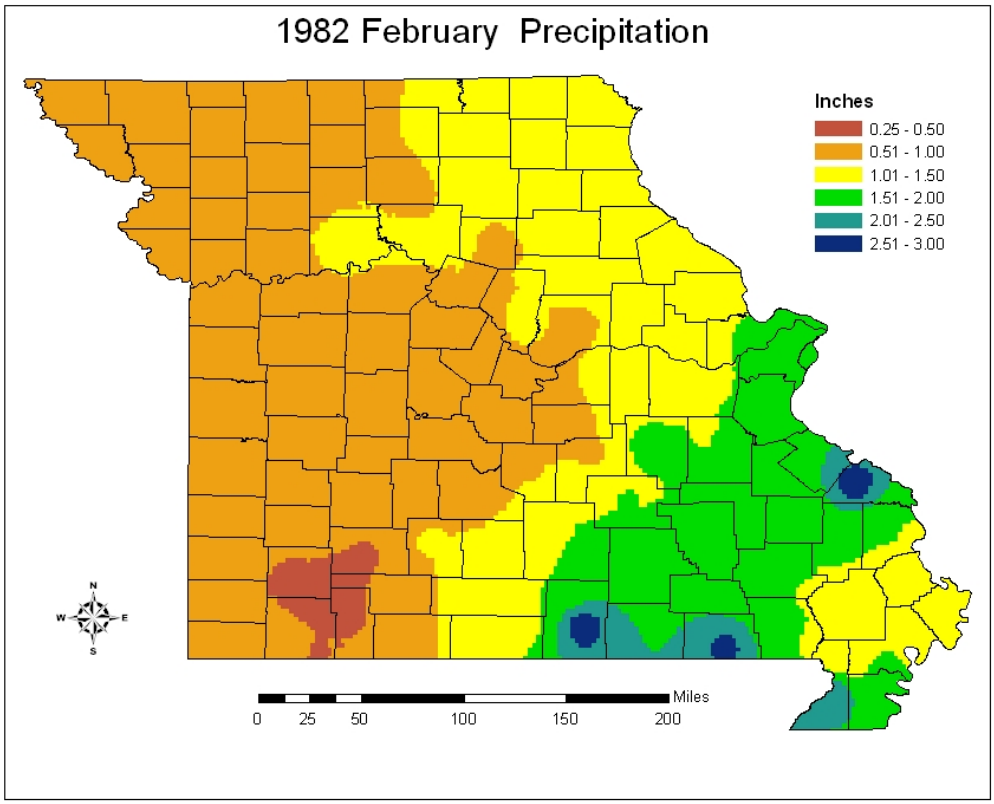

Figure 37: February precipitation, 1982.

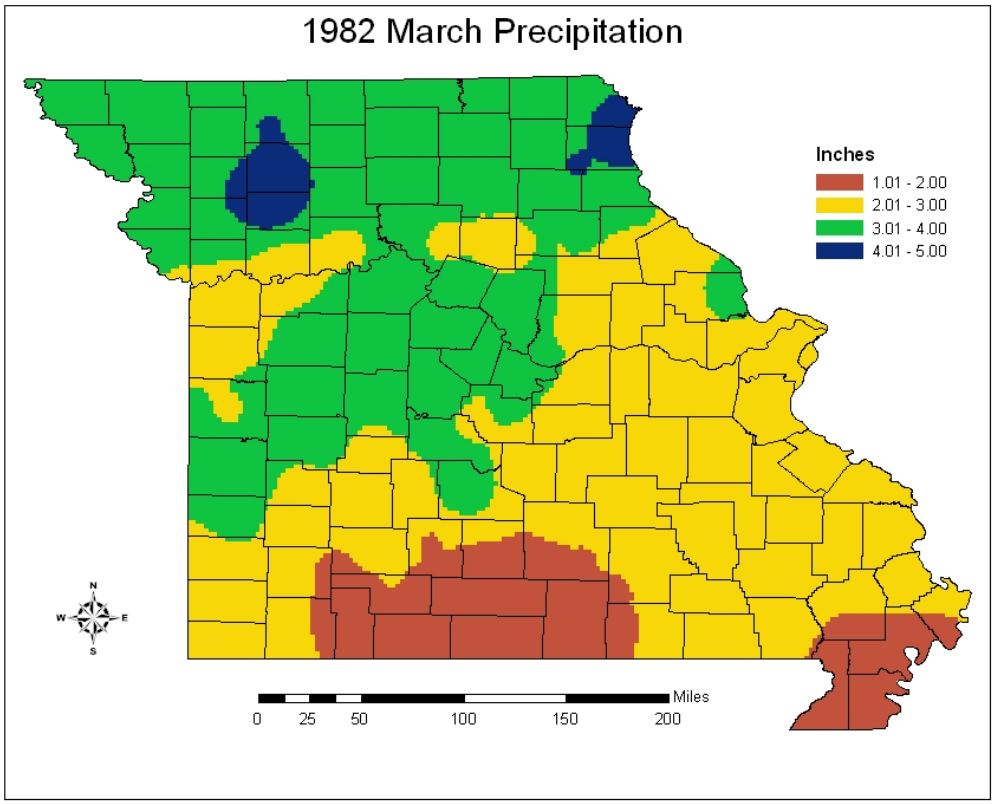

Figure 38: March precipitation, 1982.

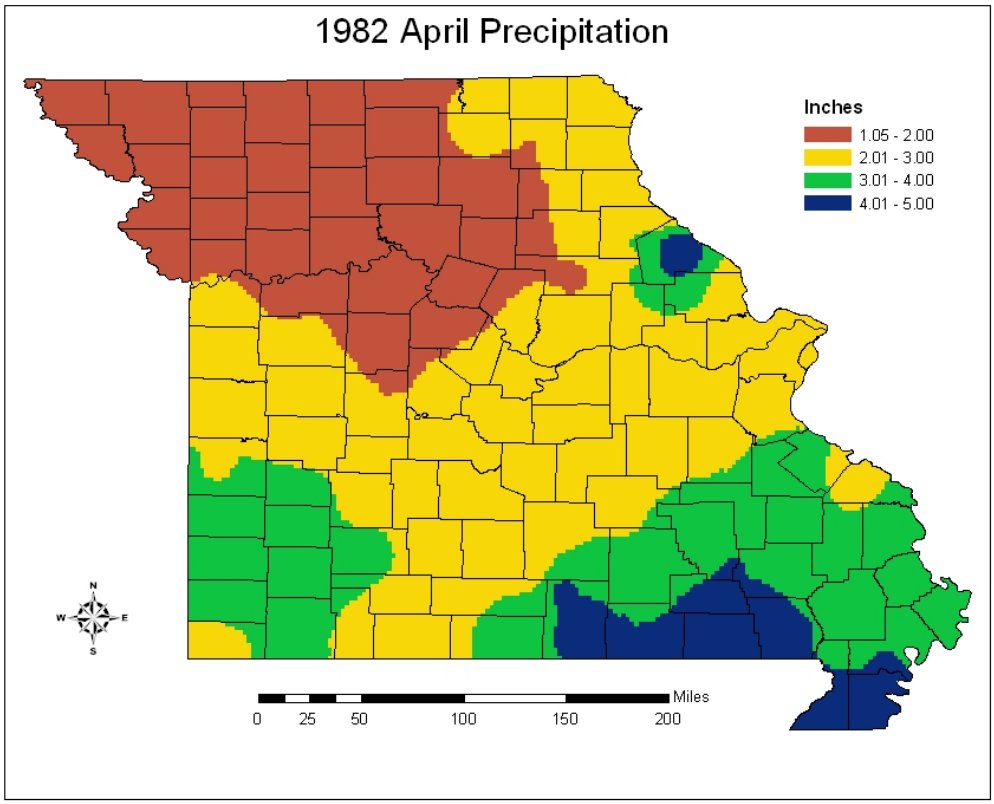

Figure 39: April precipitation, 1982.

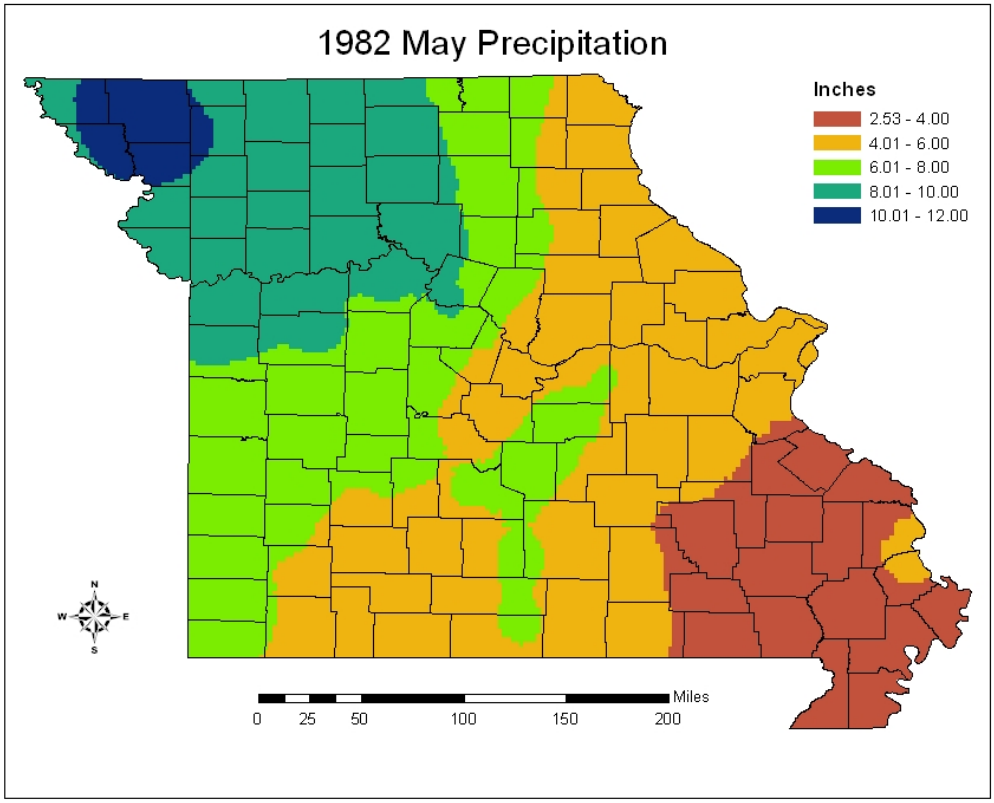

Figure 40: May precipitation, 1982.

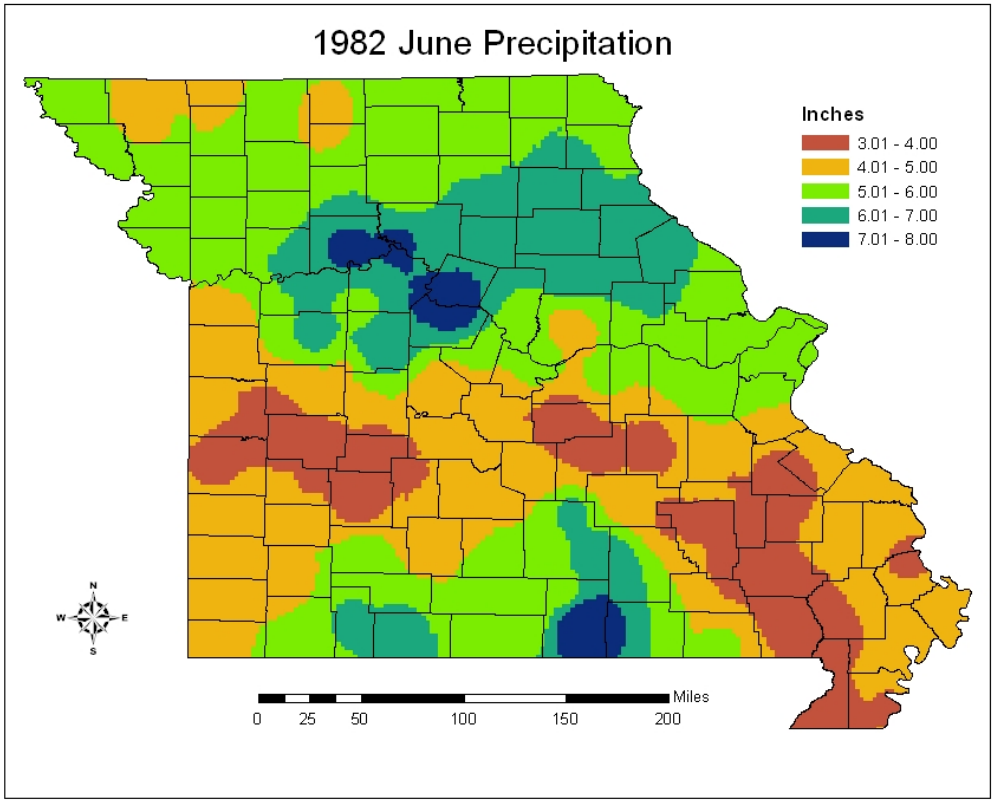

Figure 41: June precipitation, 1982.

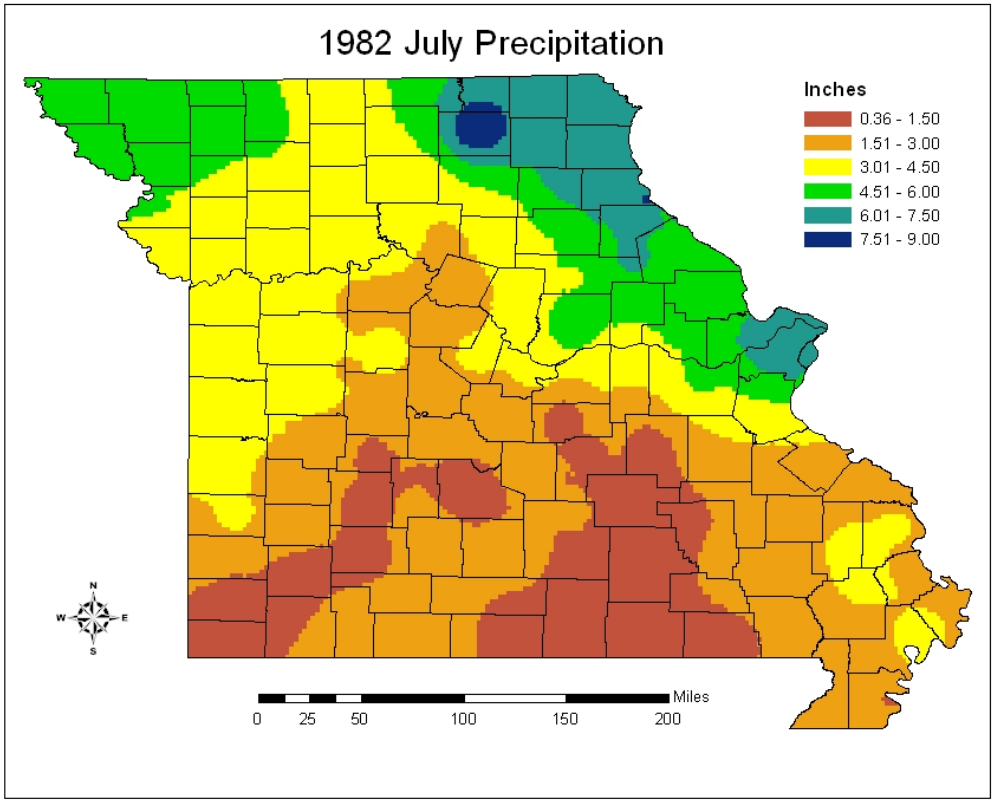

Figure 42: July precipitation, 1982.

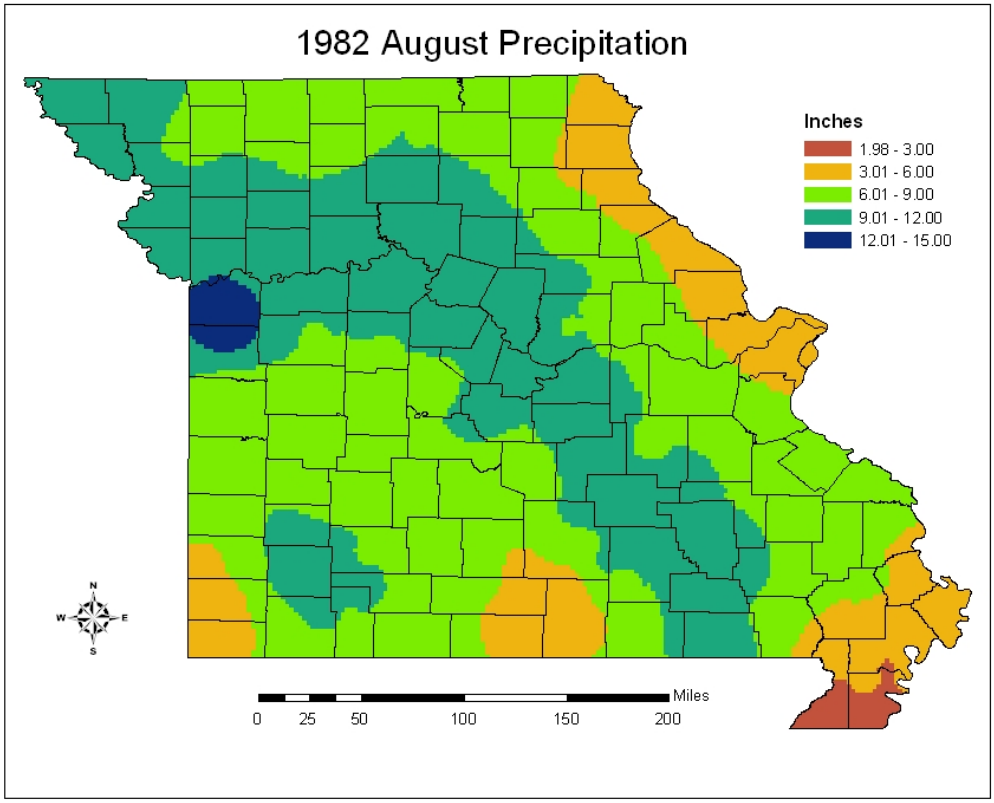

Figure 43: August precipitation, 1982.

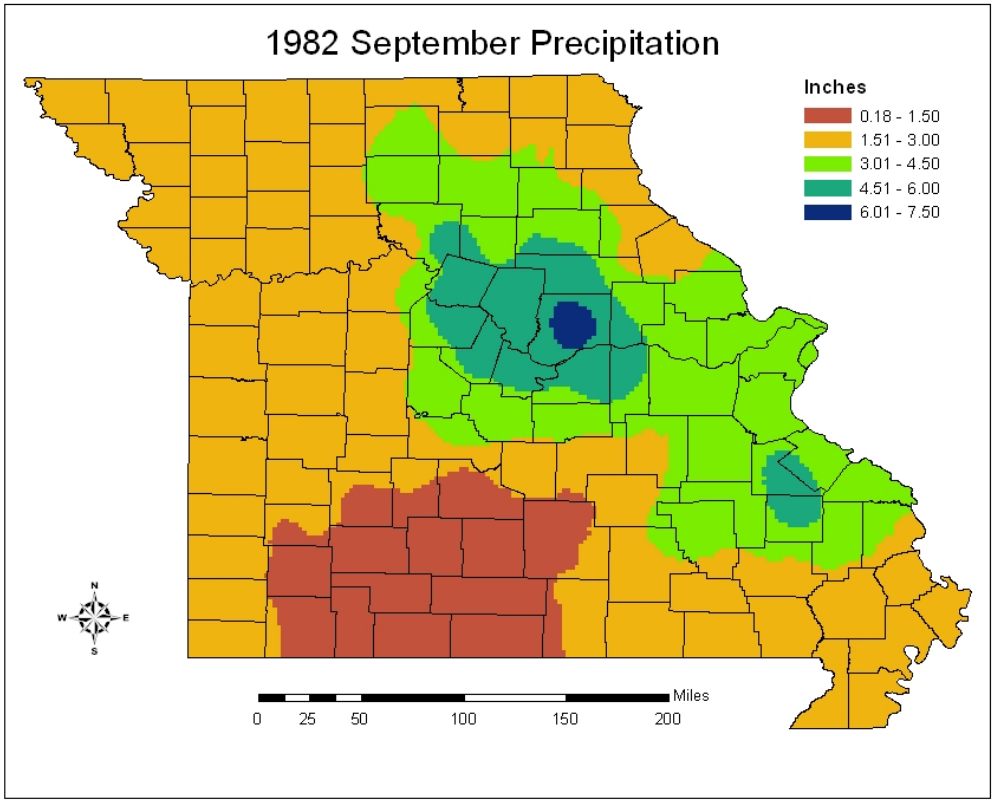

Figure 44: September precipitation, 1982.

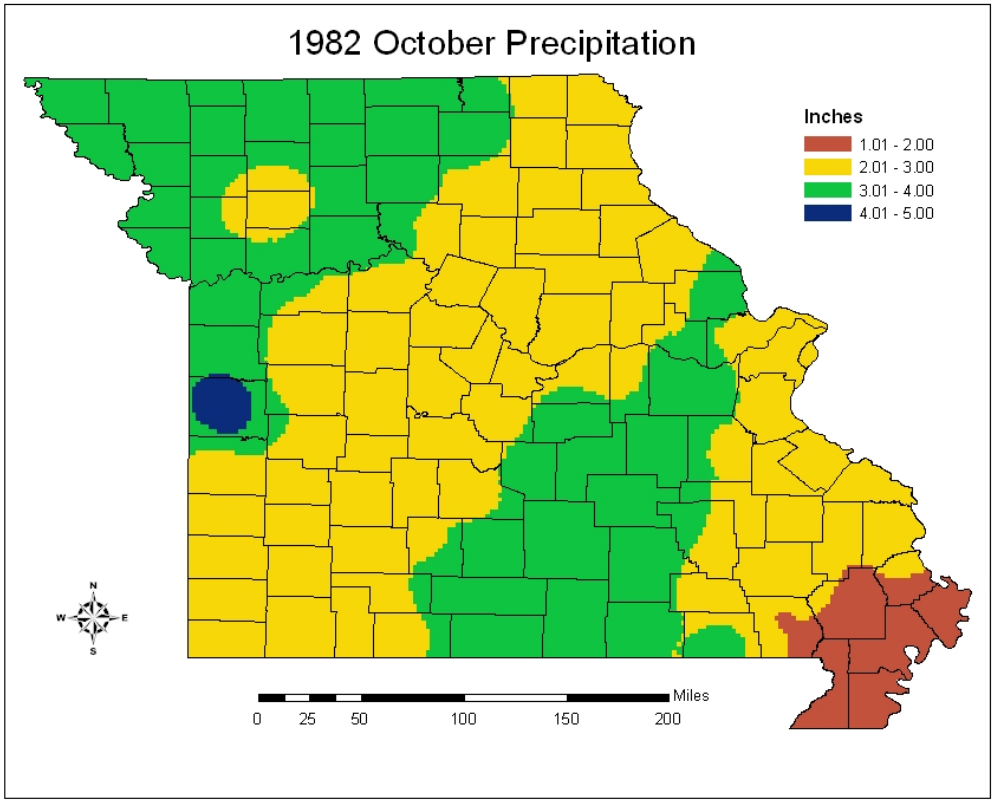

Figure 45: October precipitation, 1982.

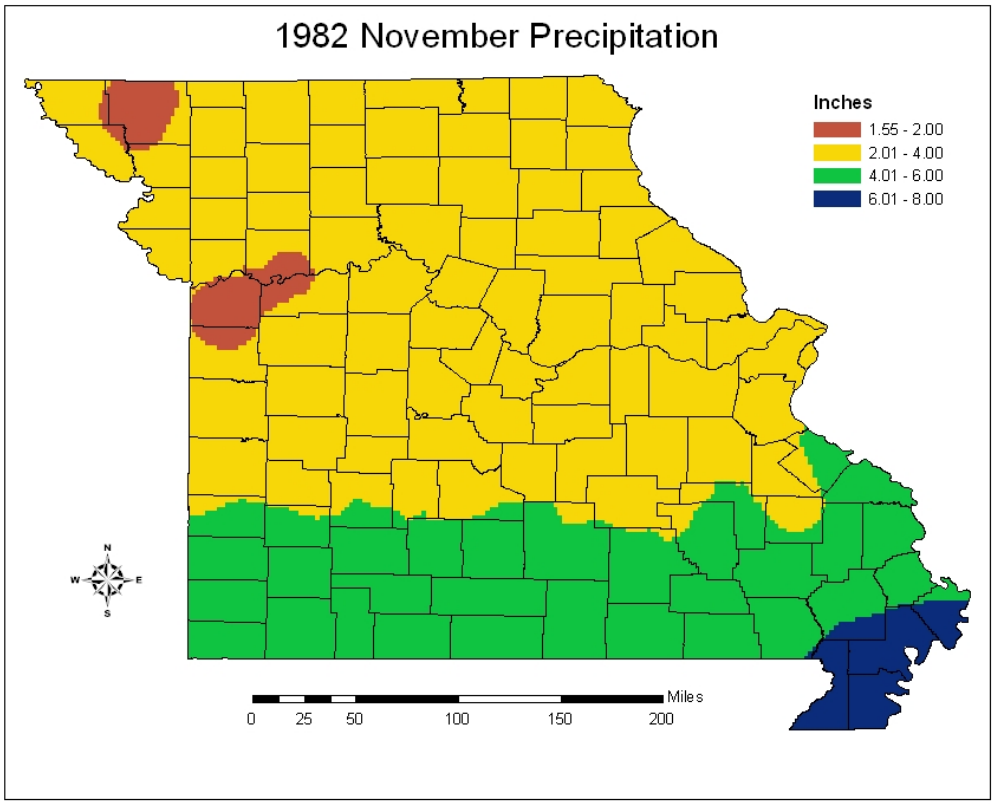

Figure 45: November precipitation, 1982.

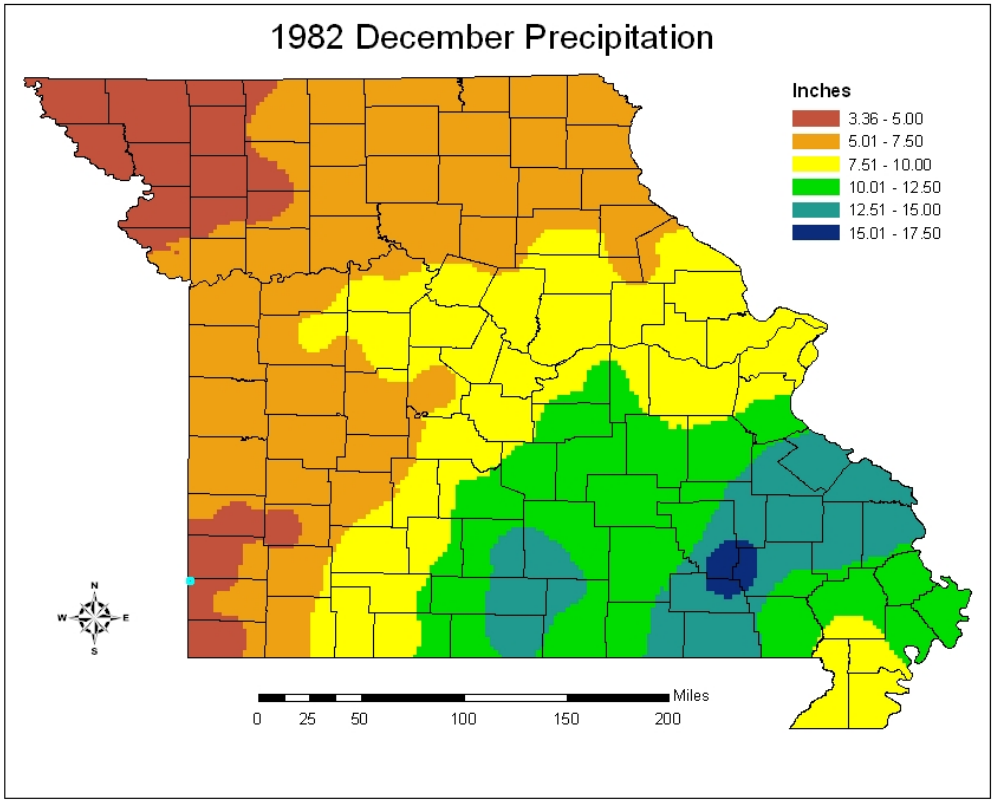

Figure 46: December precipitation, 1982.

c) 1988

A drought developed in 1988. The drought was severe in the northern half of the state and the precipitation deficit decreased toward the south. In the southern tier of the state the annual precipitation was at its climate normal. Several major features in variations of the monthly precipitation in the year could have attributed to the drought. The drought emerged in the north during the winter months; precipitation in March was more than one inch below normal. In April, the precipitation pattern changed when more precipitation was received in the western central Missouri, a pattern usually seen in late summer. This anomaly pattern interrupted the normal wet months from April to June when northern half of Missouri receives most of its annual precipitation. For example, from June to September, the rainfall pattern remained to have more rainfall in the south than in the north, reversing from the normal pattern for the summer months. Missing the entire wet period caused the severe drought in northern Missouri.

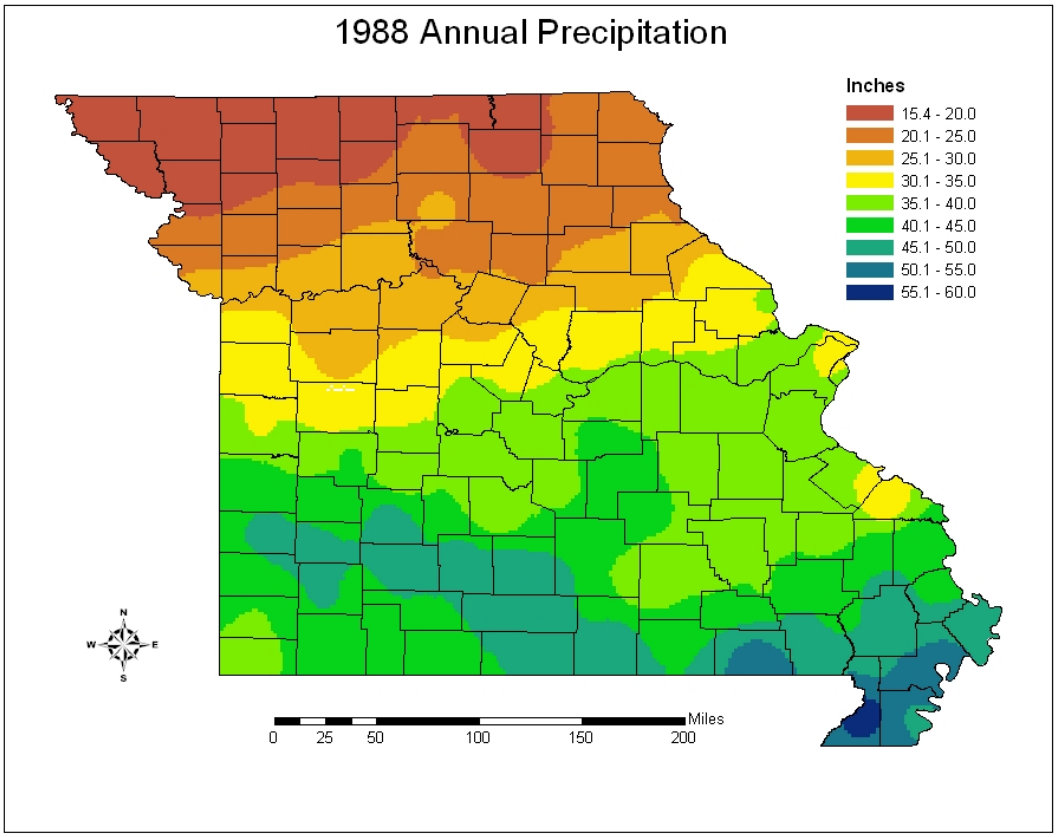

Figure 47: Annual precipitation for 1988.

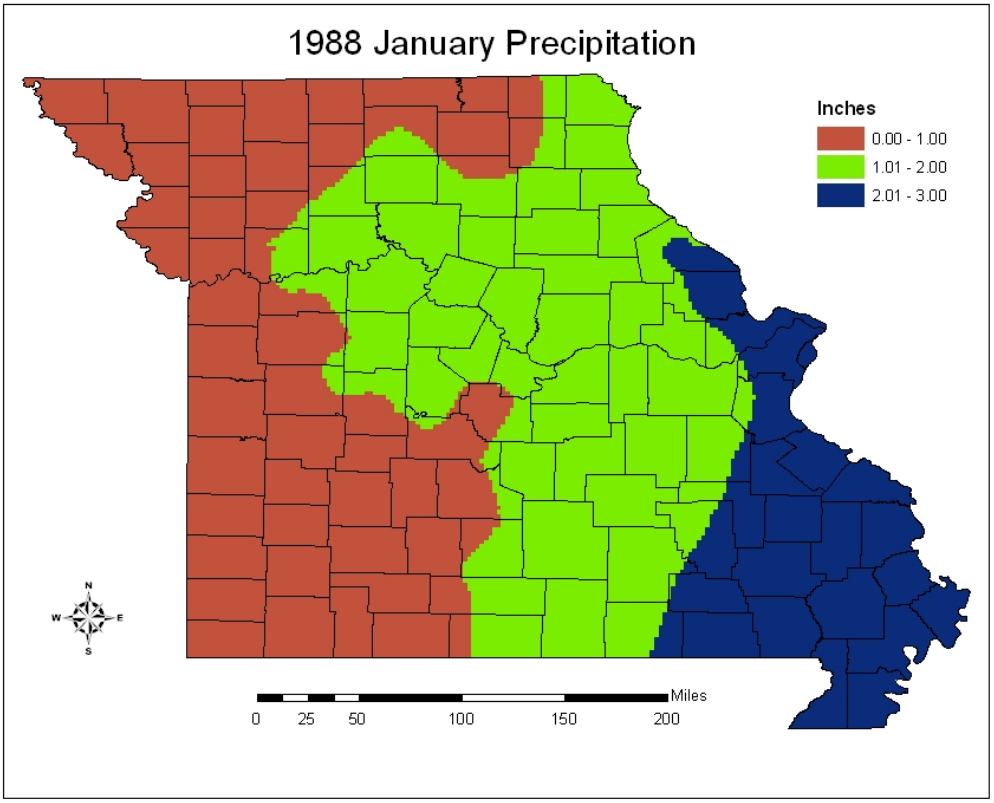

Figure 48: January precipitation, 1988.

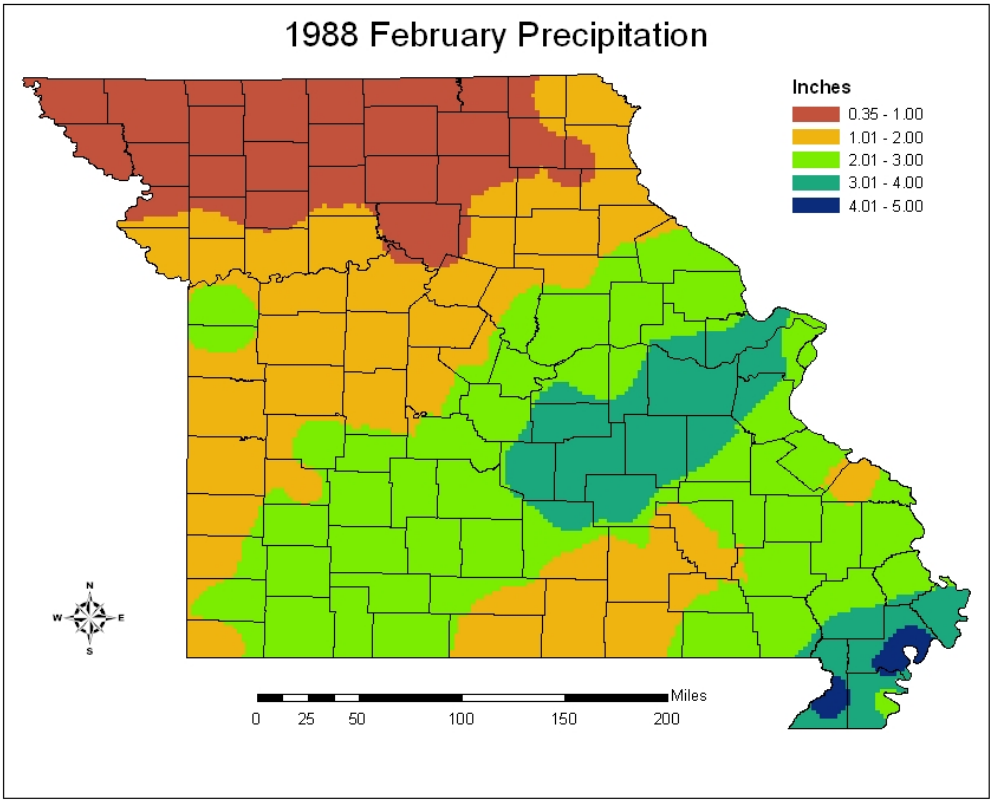

Figure 49: February precipitation, 1988.

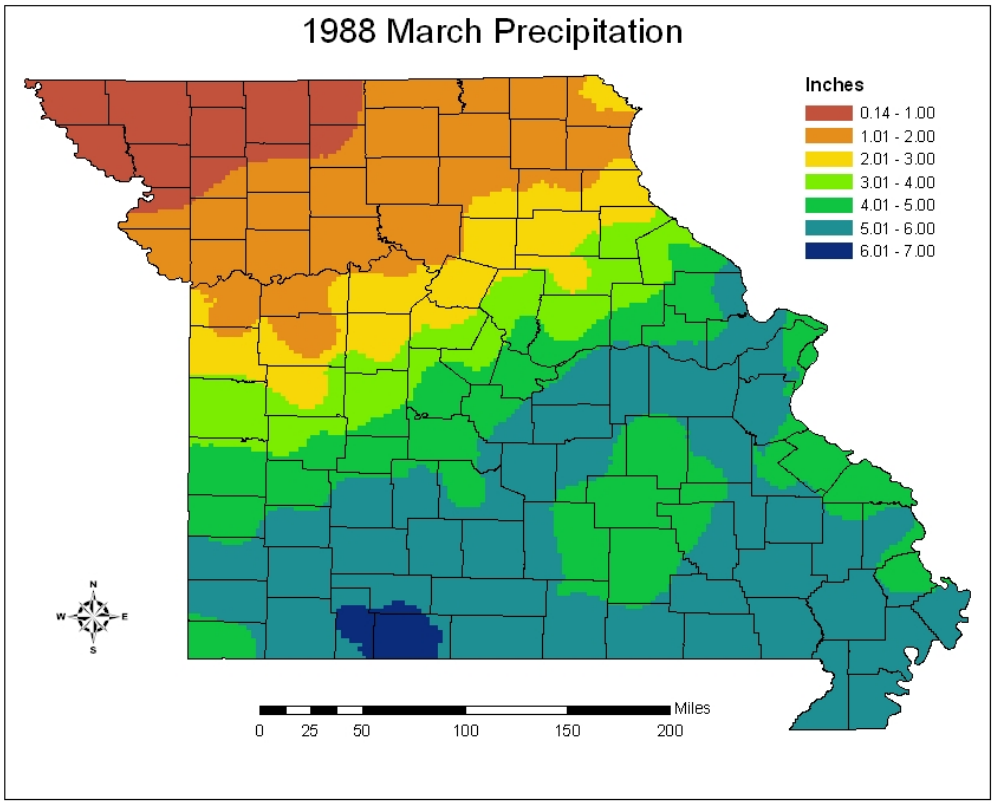

Figure 50: March precipitation, 1988.

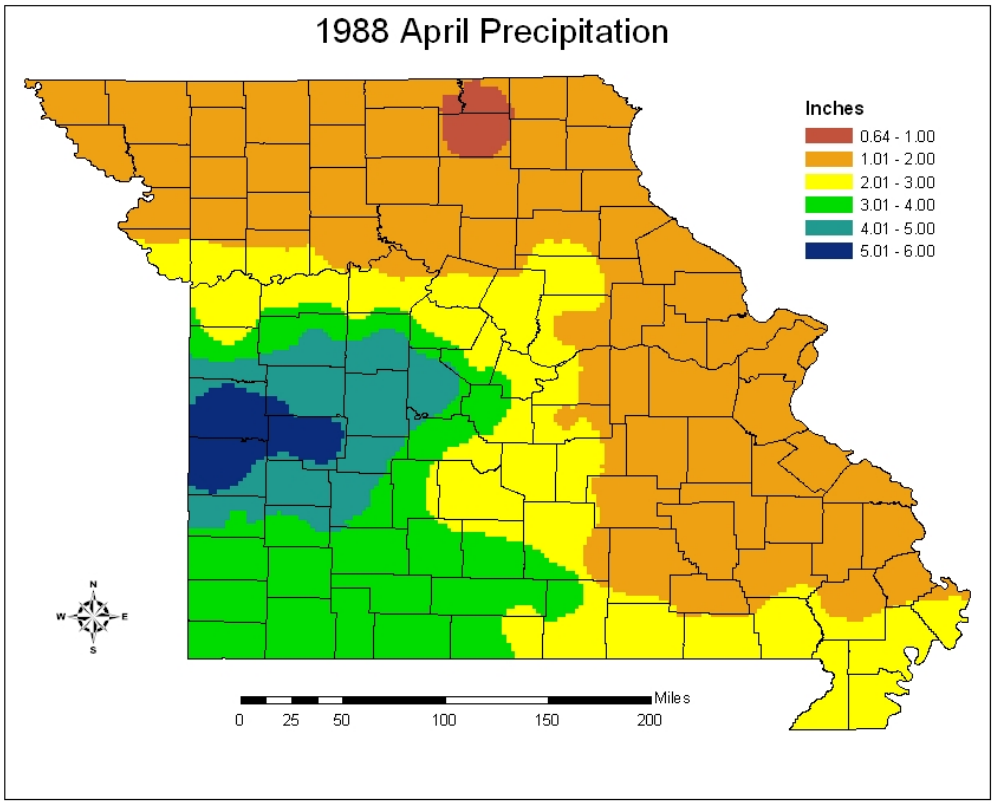

Figure 51: April precipitation, 1988.

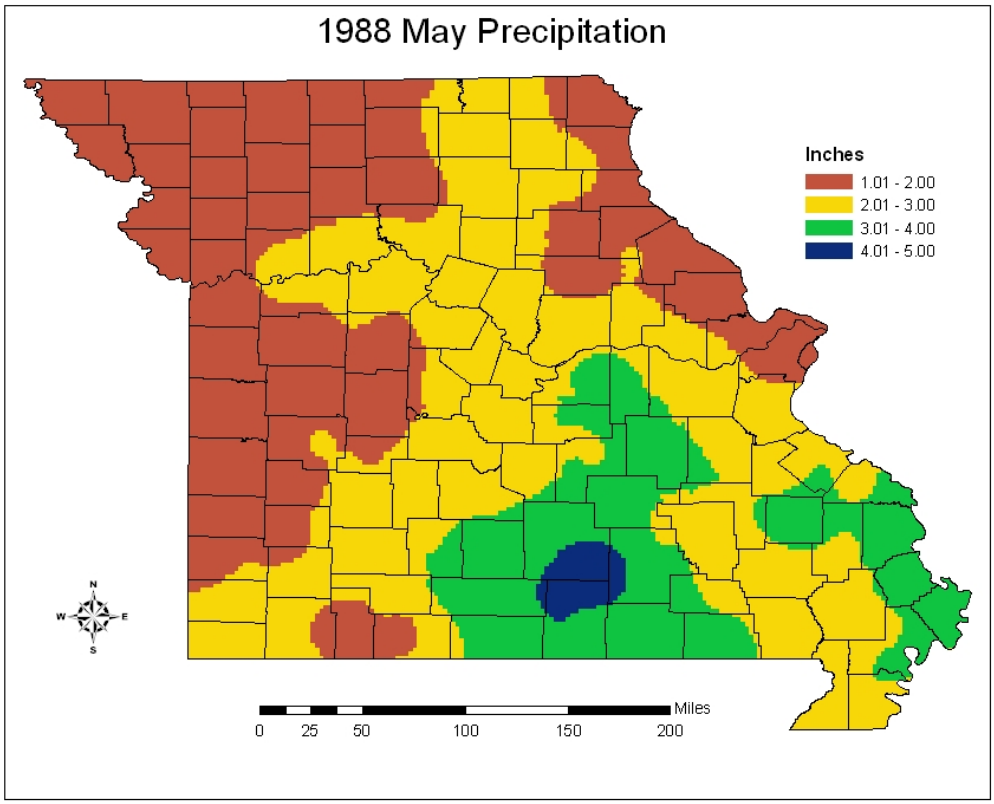

Figure 52: May precipitation, 1988.

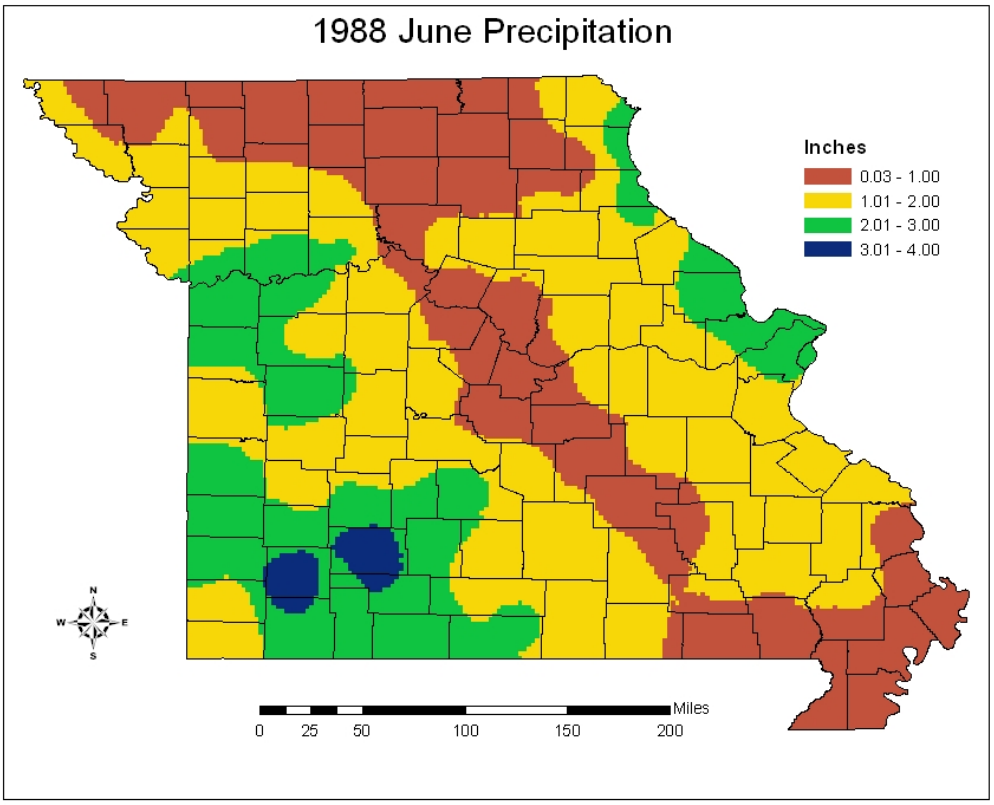

Figure 53: June precipitation, 1988.

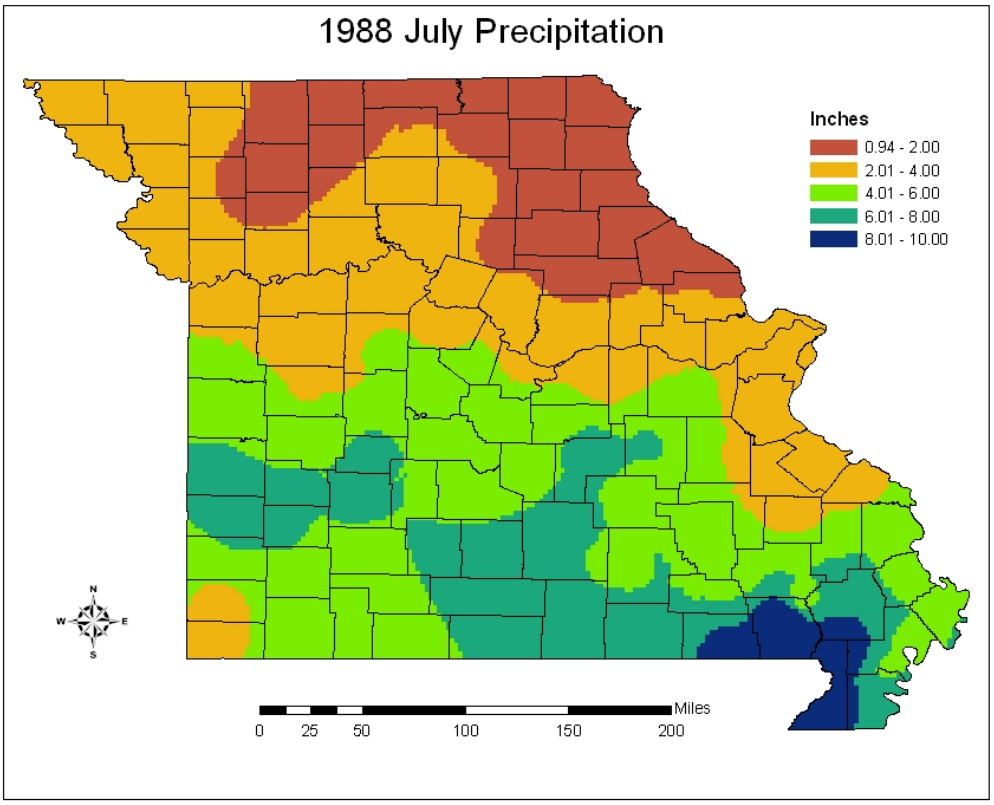

Figure 54: July precipitation, 1988.

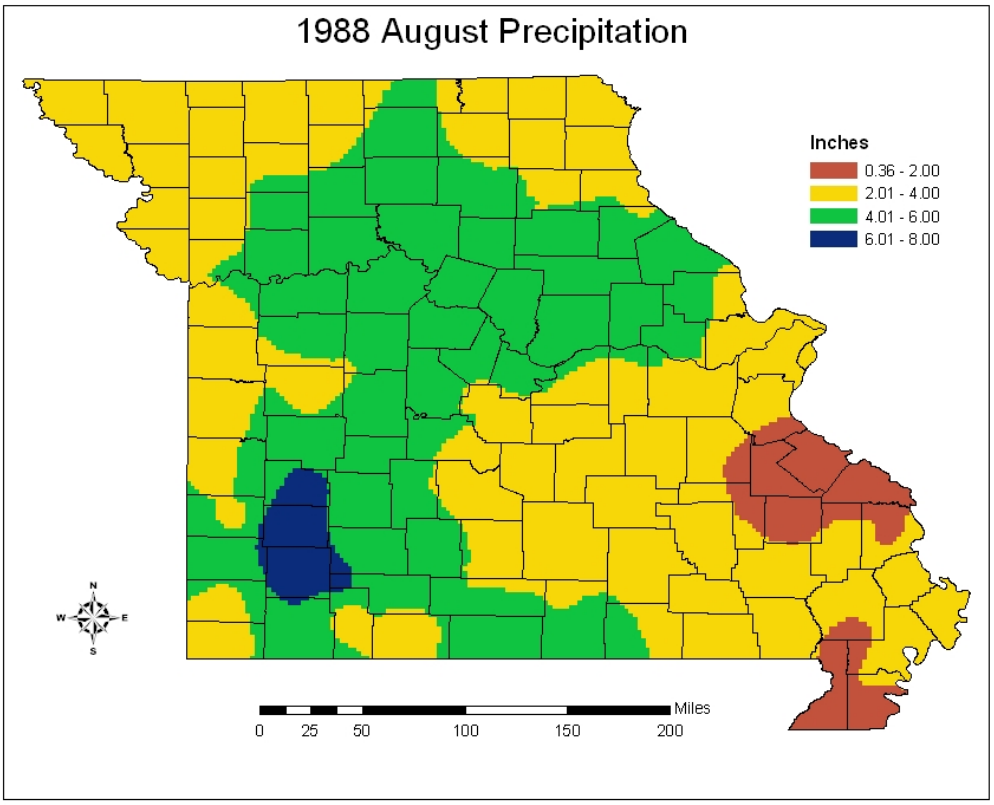

Figure 55: August precipitation, 1988.

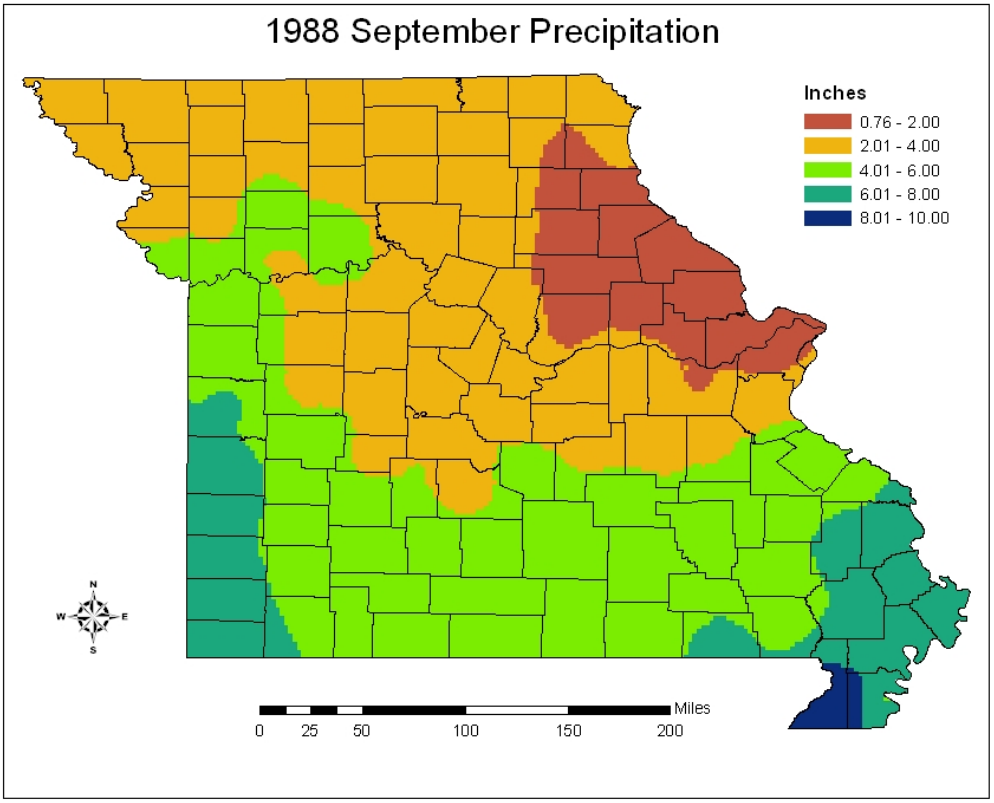

Figure 56: September precipitation, 1988.

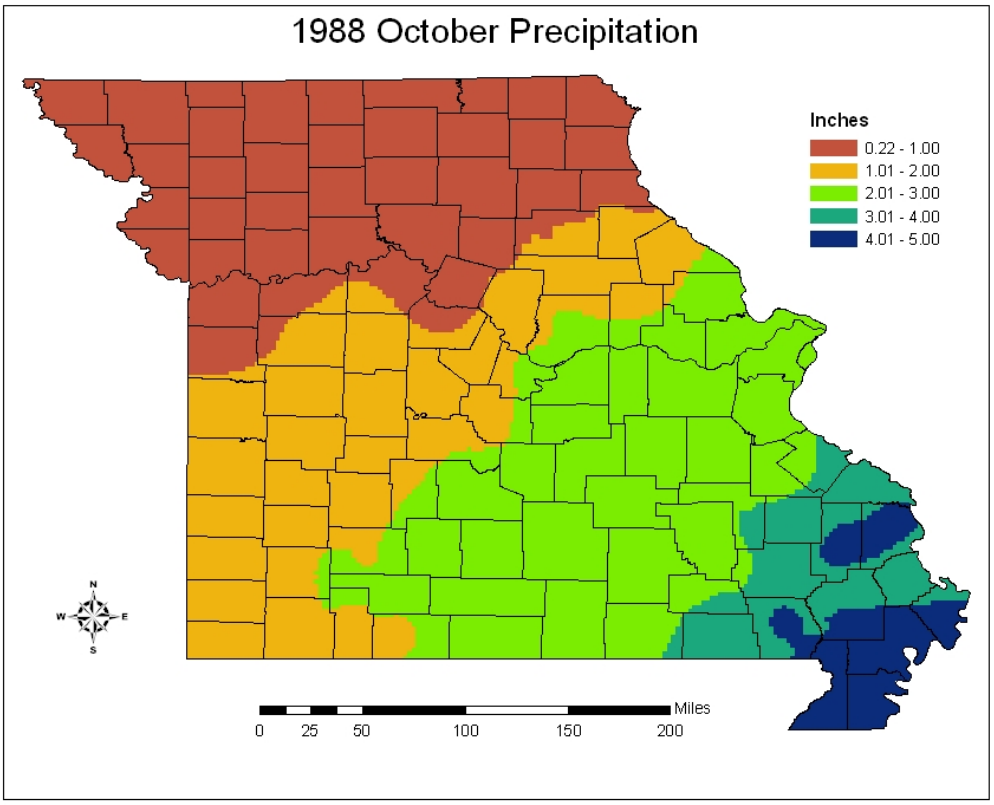

Figure 57: October precipitation, 1988.

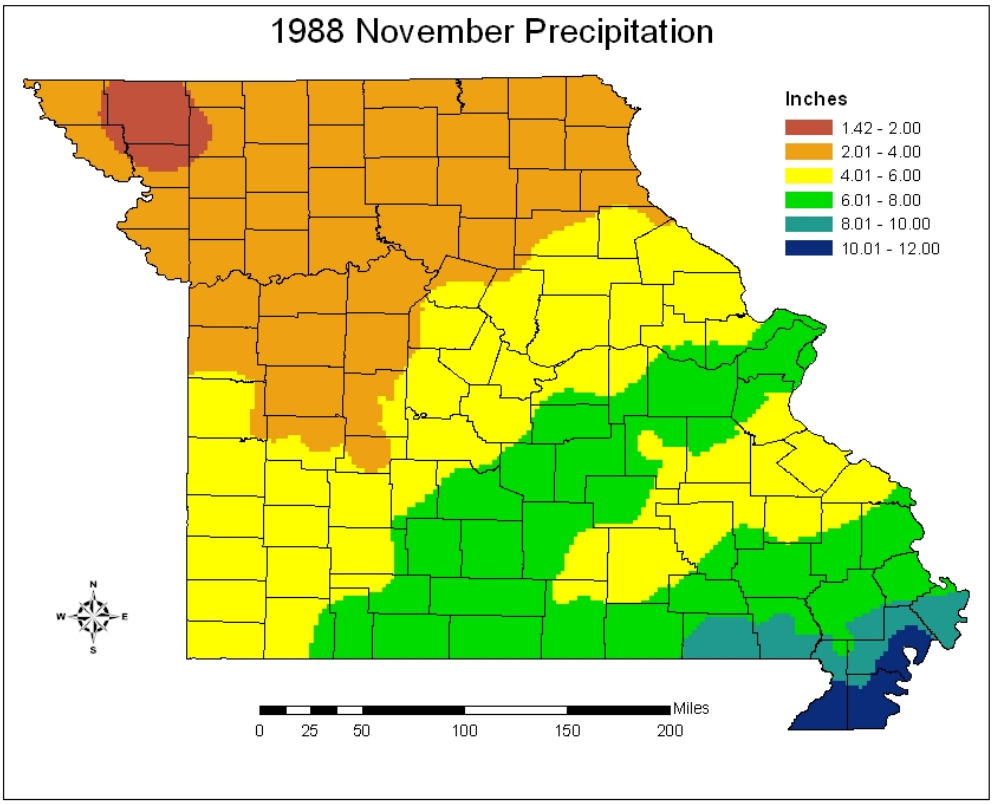

Figure 58: November precipitation, 1988.

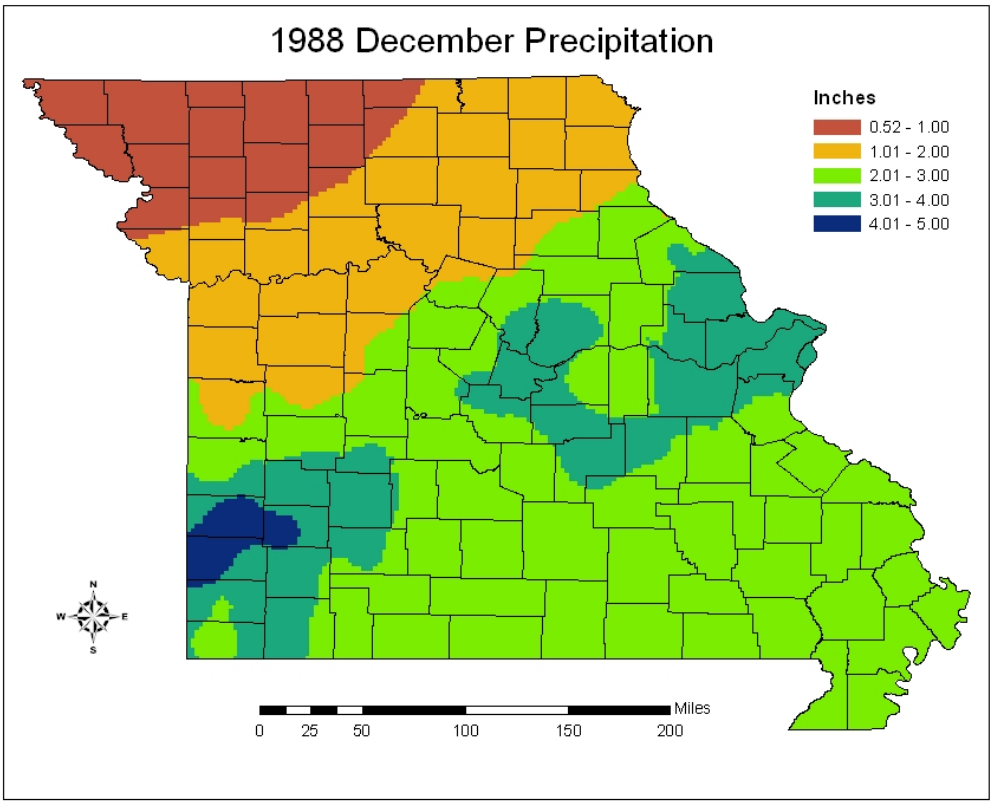

Figure 59: December precipitation, 1988.

d) 1993

A devastating flood struck the central United States in the summer of 1993 as a result of massive rainfall in southern Iowa, northern Missouri and western Illinois. In Missouri, an increase of rainfall in northern regions occurred in April. In June new high total rainfall amounts were recorded in northern Missouri when the rainfall pattern changed to favor more rainfall in the north. June rainfall was more than double its normal amount, and July rainfall was more than quadruple of the normal July rainfall. With the previous wet months the "clay-pan" soils in the region were saturated and the massive rainfall in June and July resulted in wide spread and damaging floods.

The anomalously high amount of precipitation continued through the month of November.

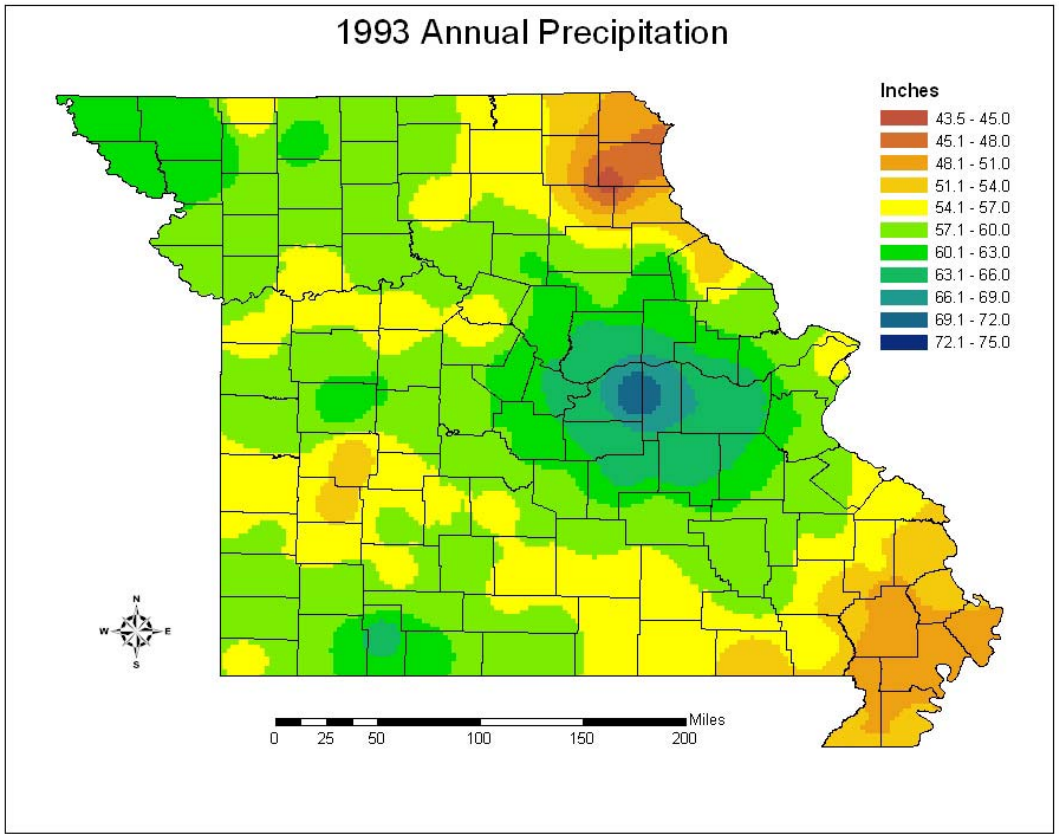

Figure 60: Annual precipitation for 1993.

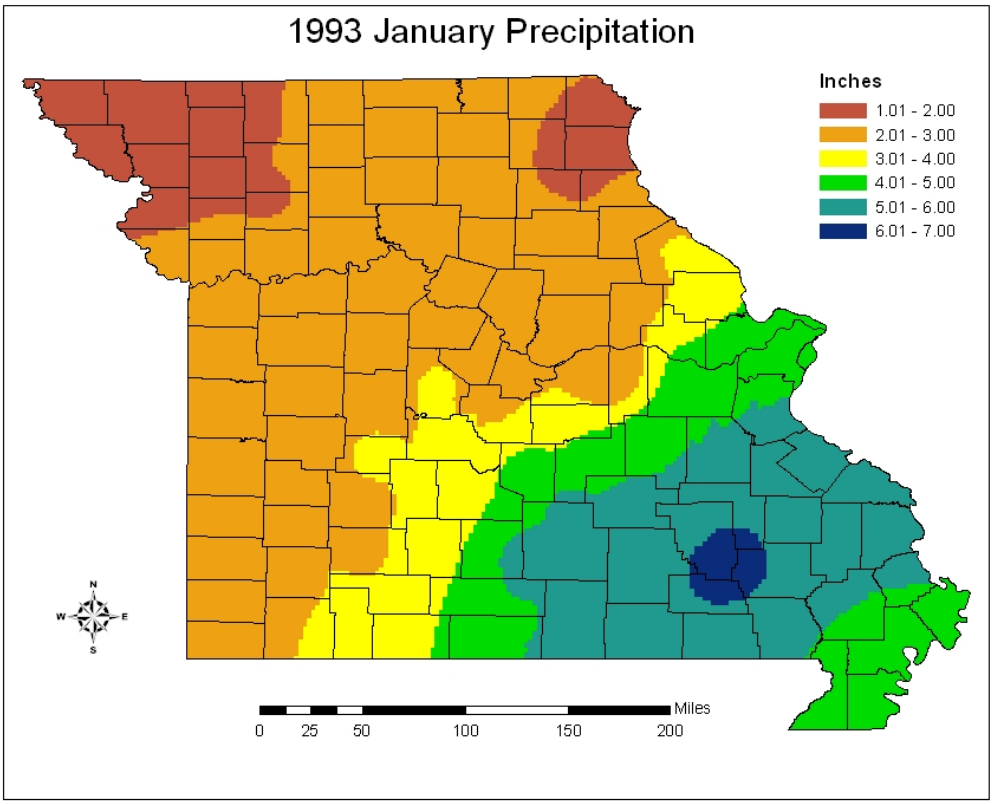

Figure 61: January precipitation, 1993.

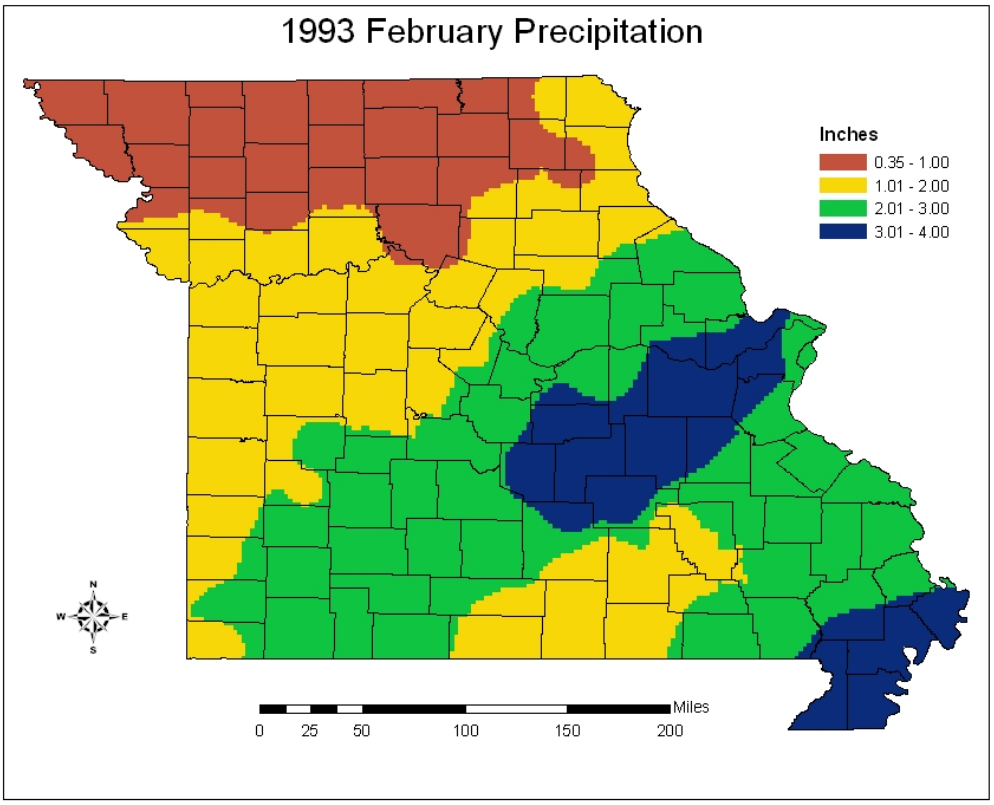

Figure 62: February precipitation, 1993.

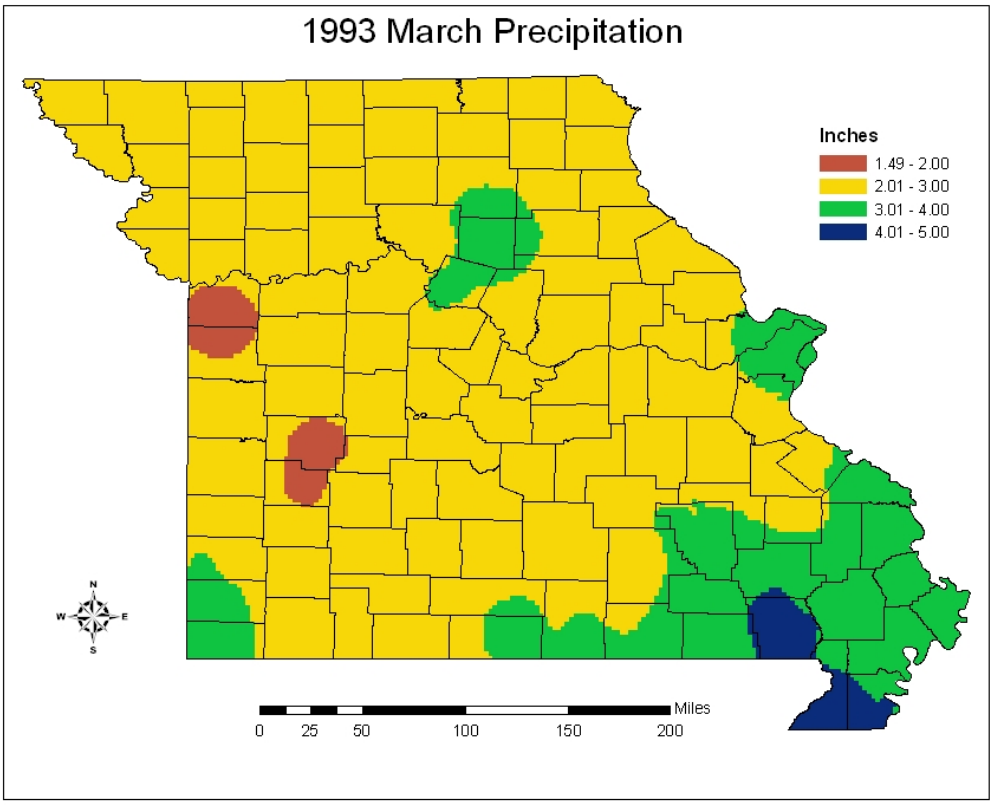

Figure 63: March precipitation, 1993.

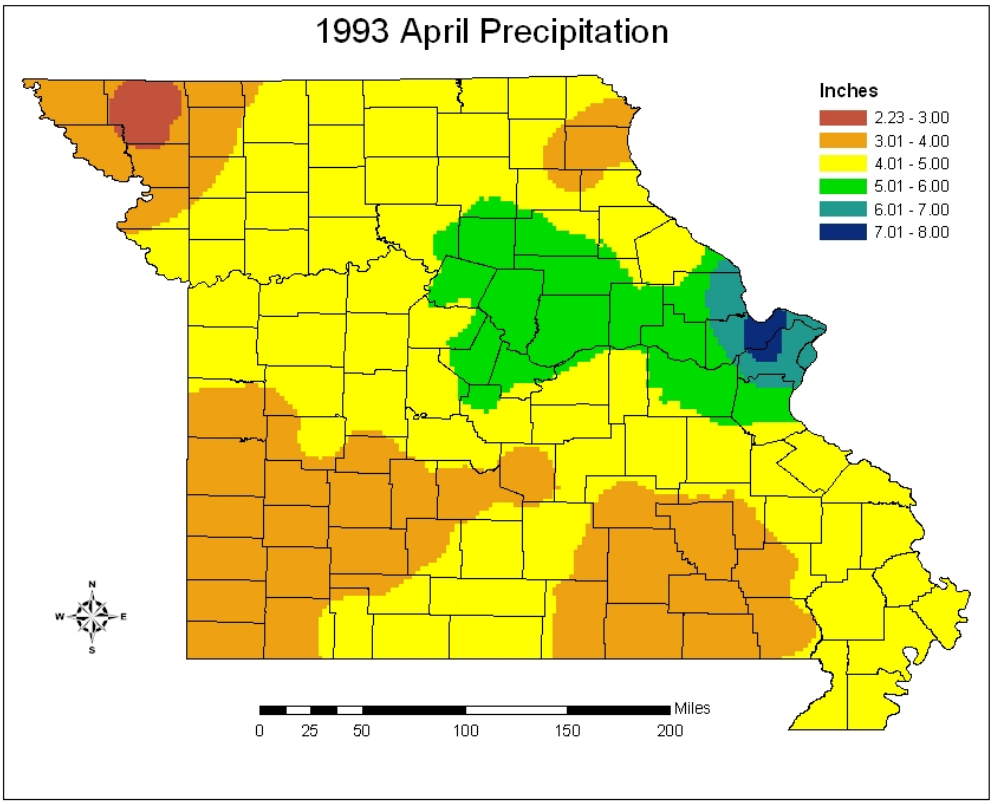

Figure 64: April precipitation, 1993.

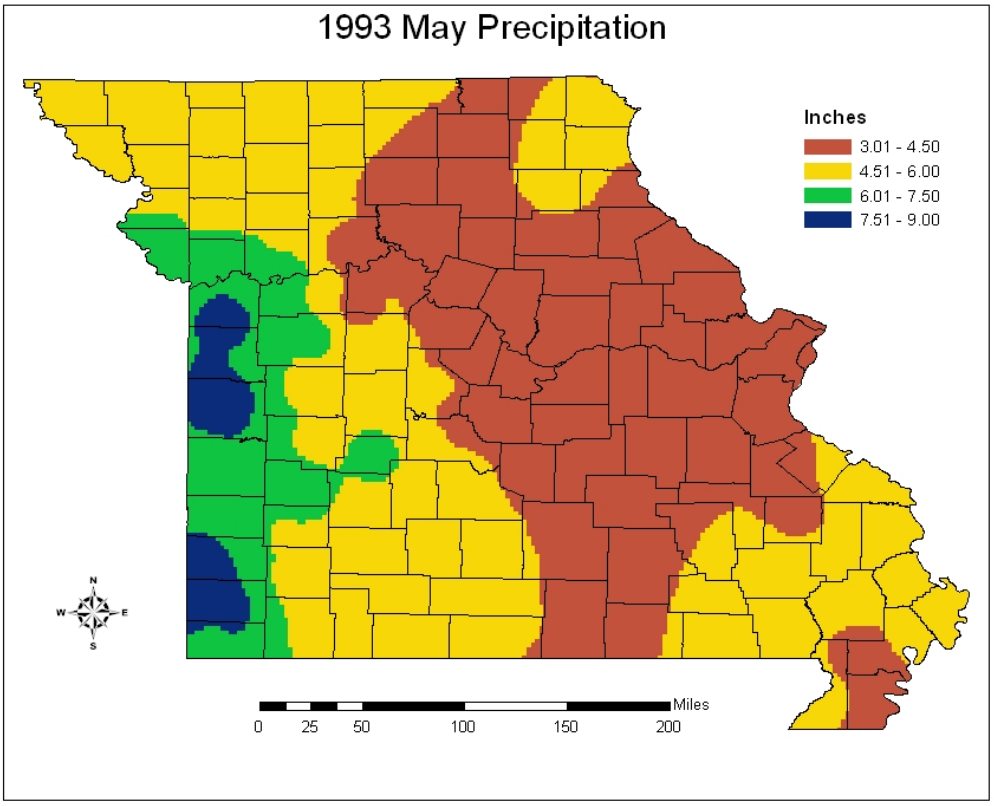

Figure 65: May precipitation, 1993.

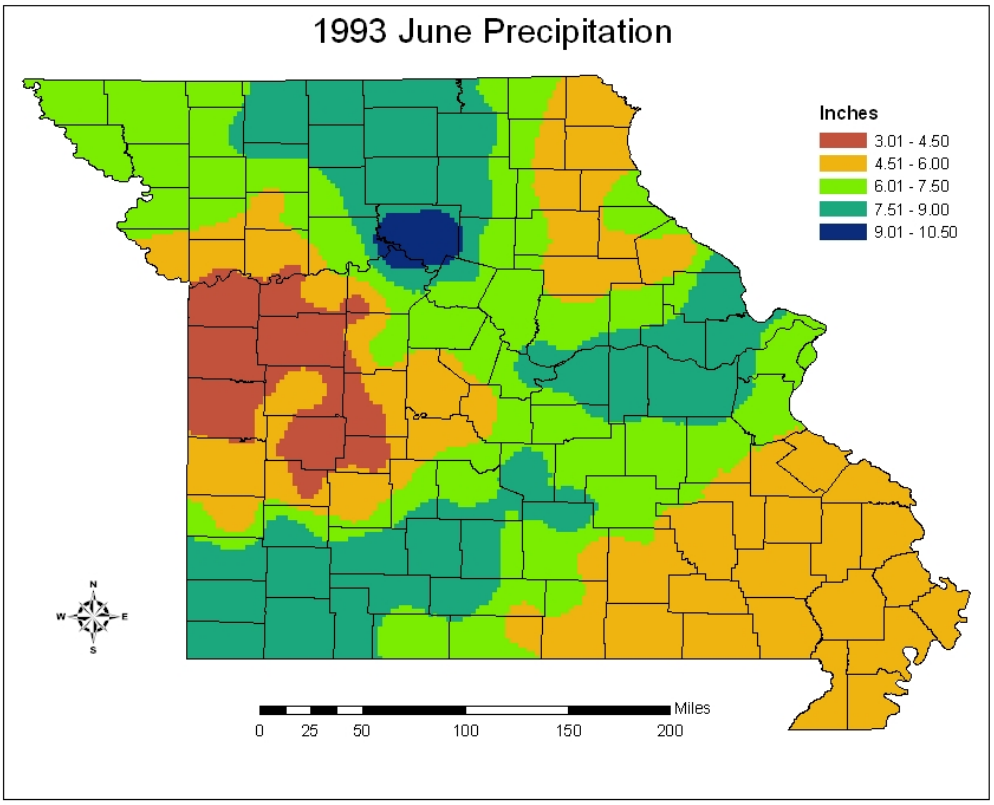

Figure 66: June precipitation, 1993.

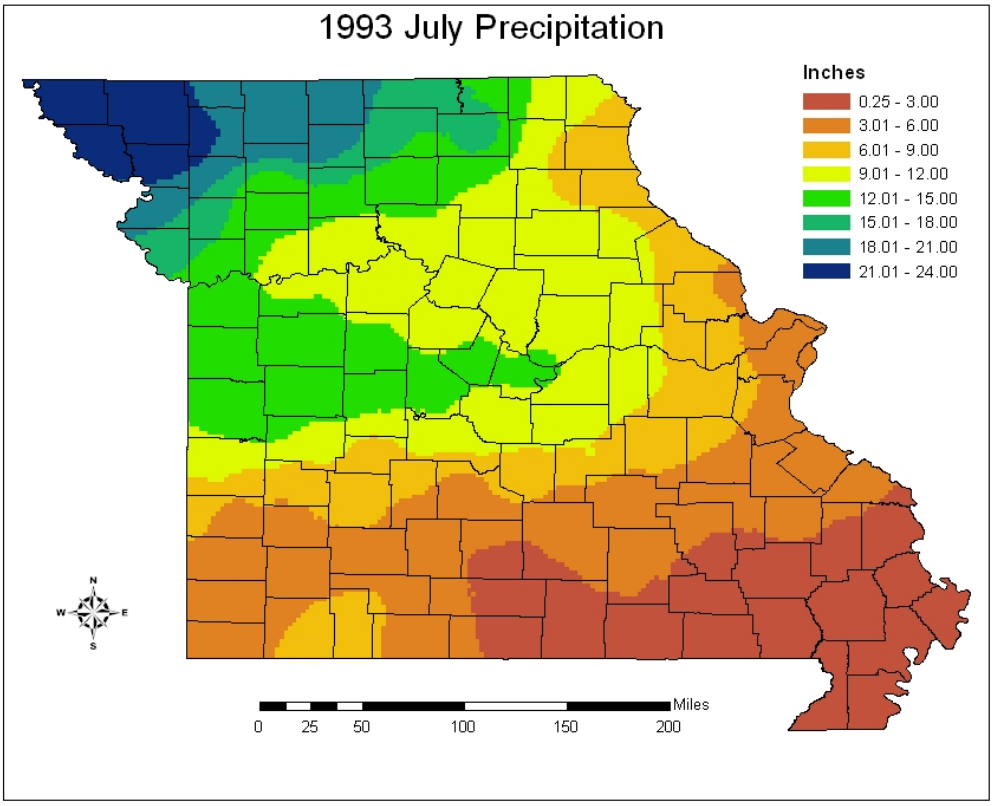

Figure 67: July precipitation, 1993.

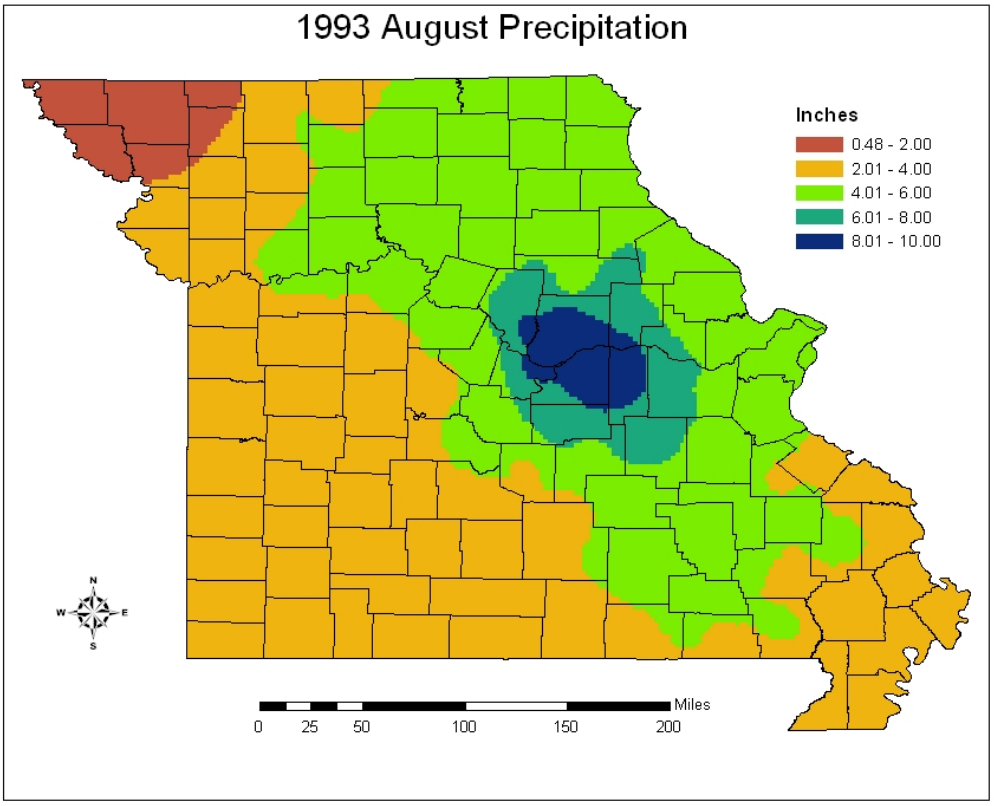

Figure 68: August precipitation, 1993.

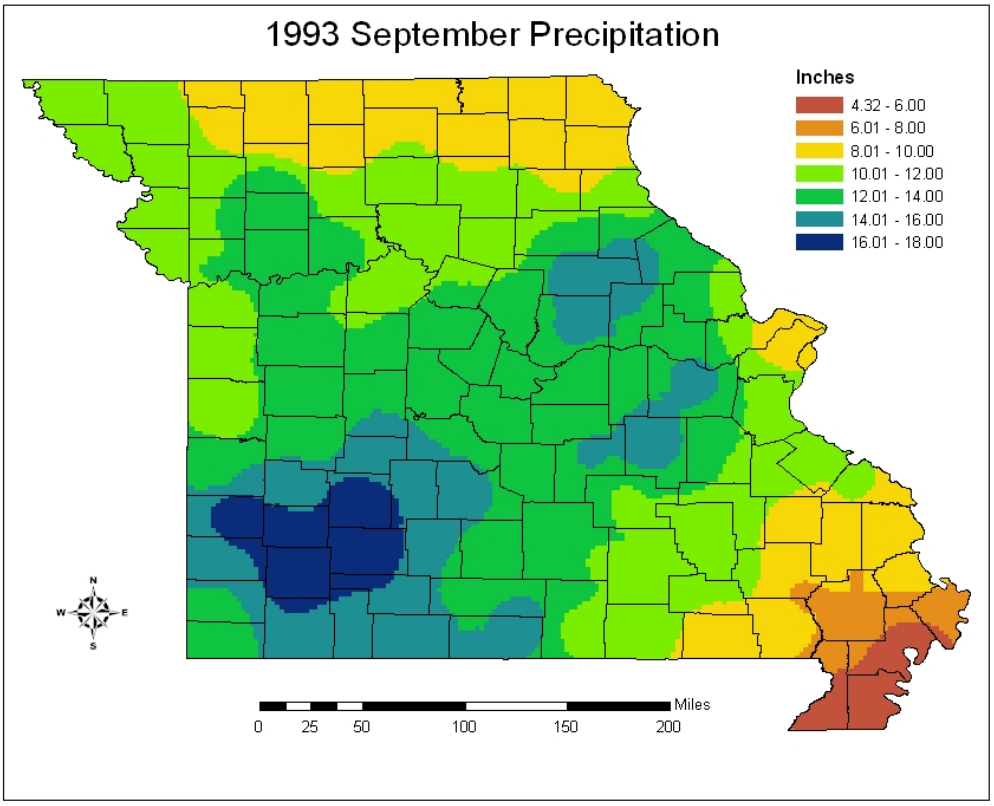

Figure 69: September precipitation, 1993.

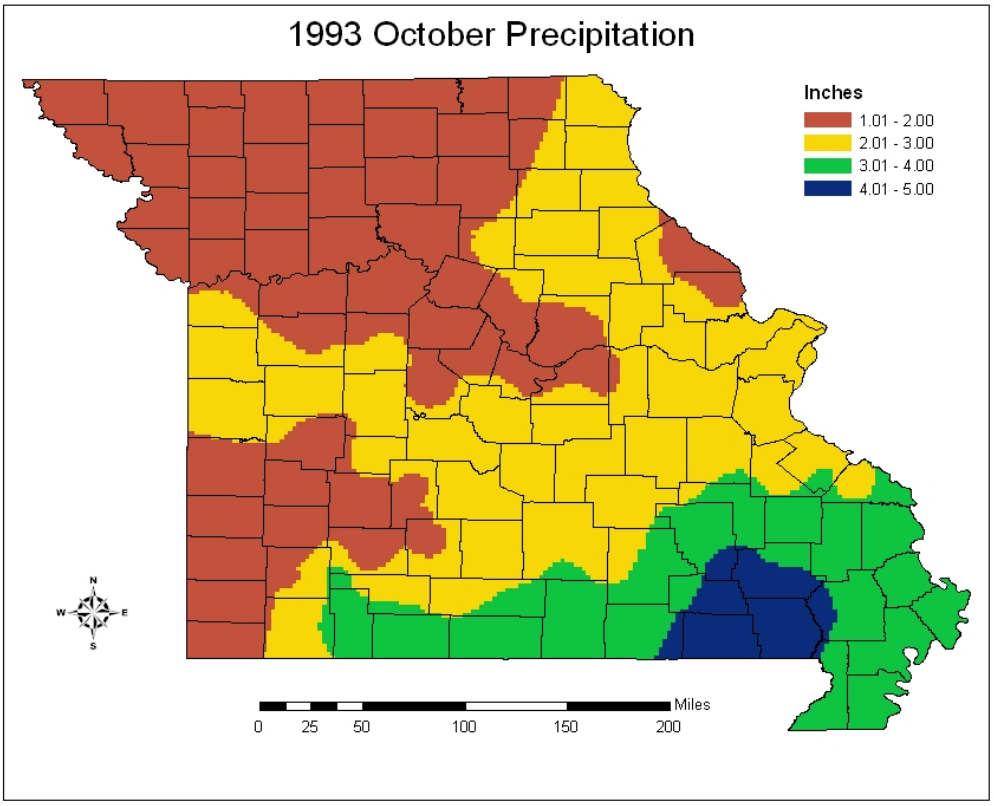

Figure 70: October precipitation, 1993.

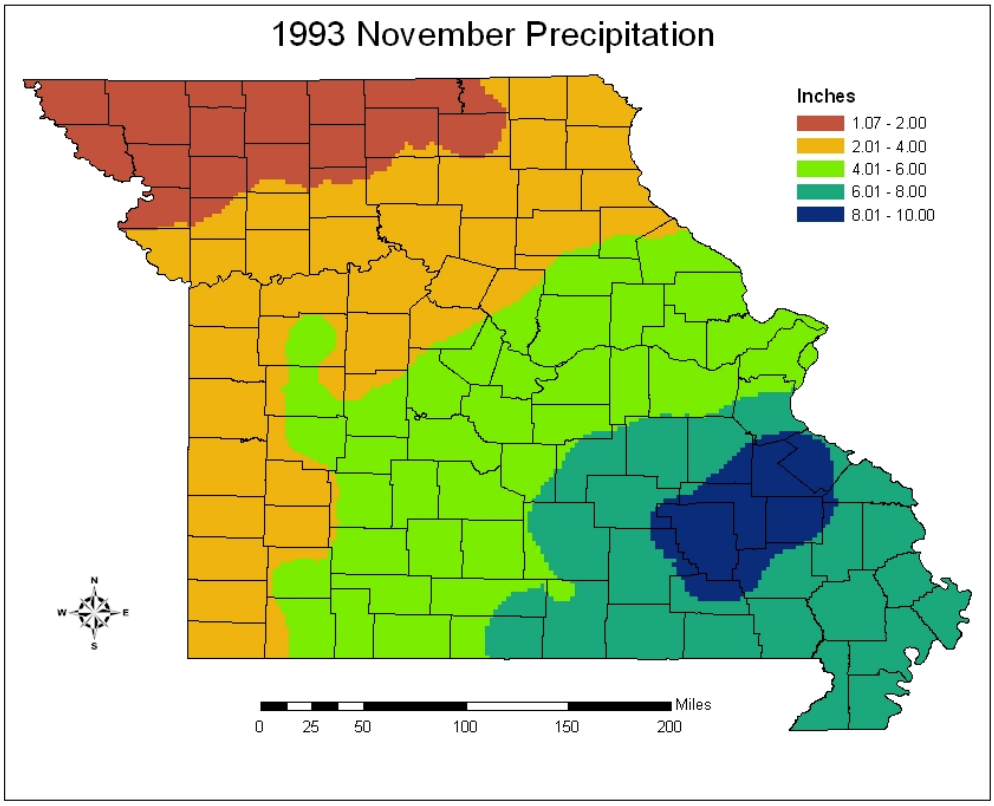

Figure 71: November precipitation, 1993.

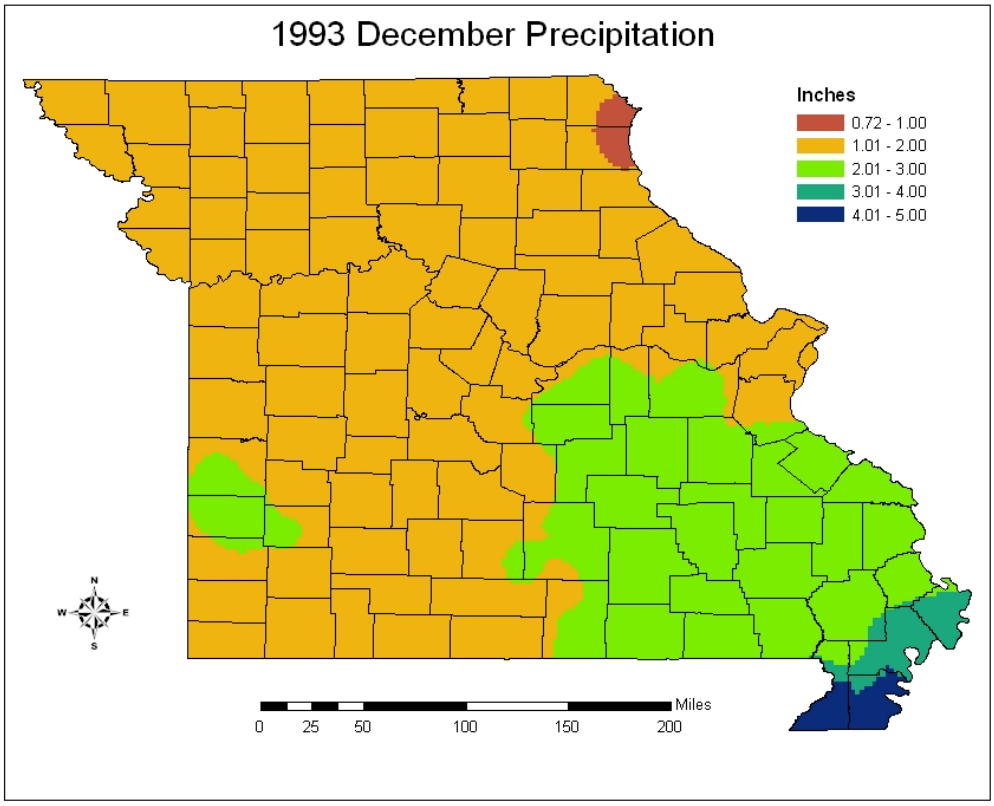

Figure 72: December precipitation, 1993.

e) 1995

An interesting feature of precipitation in 1995 is that the annual precipitation amount is in the range of the normal annual precipitation. However, the spatial distribution of the precipitation amount differs quite dramatically from the normal distribution (Fig. 3). As shown in Fig. 73, the center of large precipitation locates in the central Missouri and south Missouri is nearly 10 inches drier than its normal amount. The above normal annual precipitation in central and northern Missouri in the year resulted from very wet months from April through July, particularly in May and July. Total rainfall in May in central and northern is as high as three times the normal rainfall. A similar situation occurred in July. After the west spring and summer precipitation decreased in fall and winter, yielding the close to normal annual precipitation for the year.

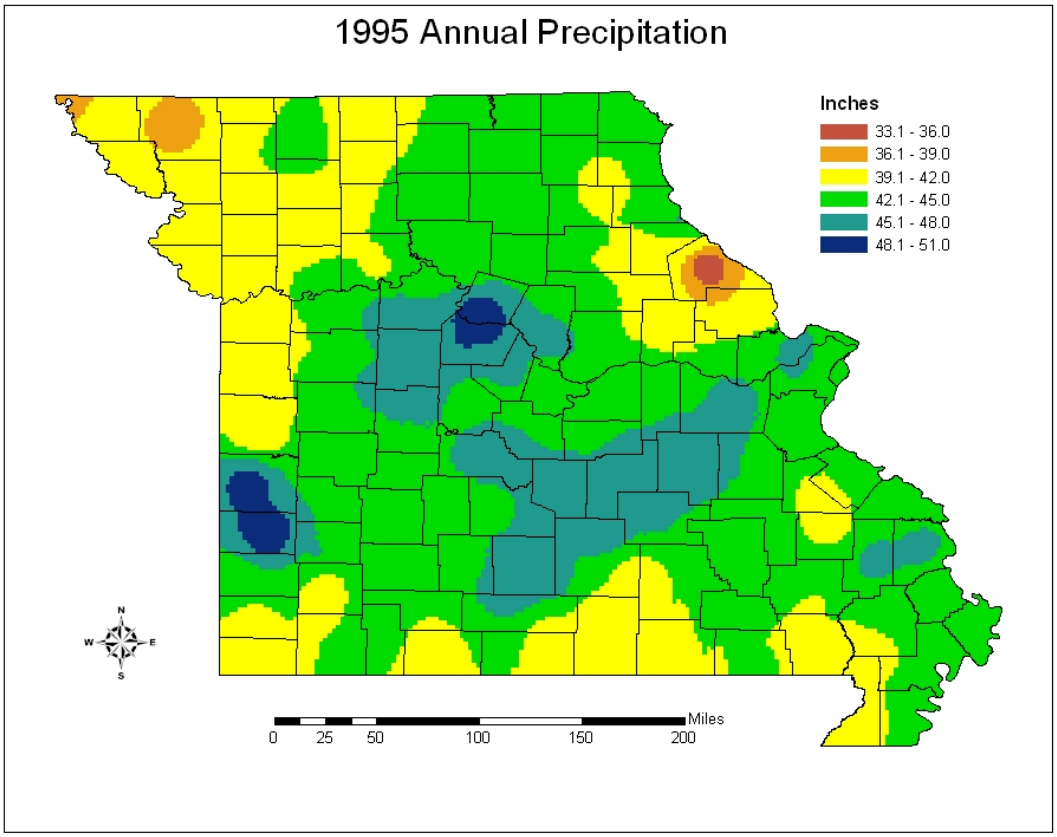

Figure 73: Annual precipitation for 1995.

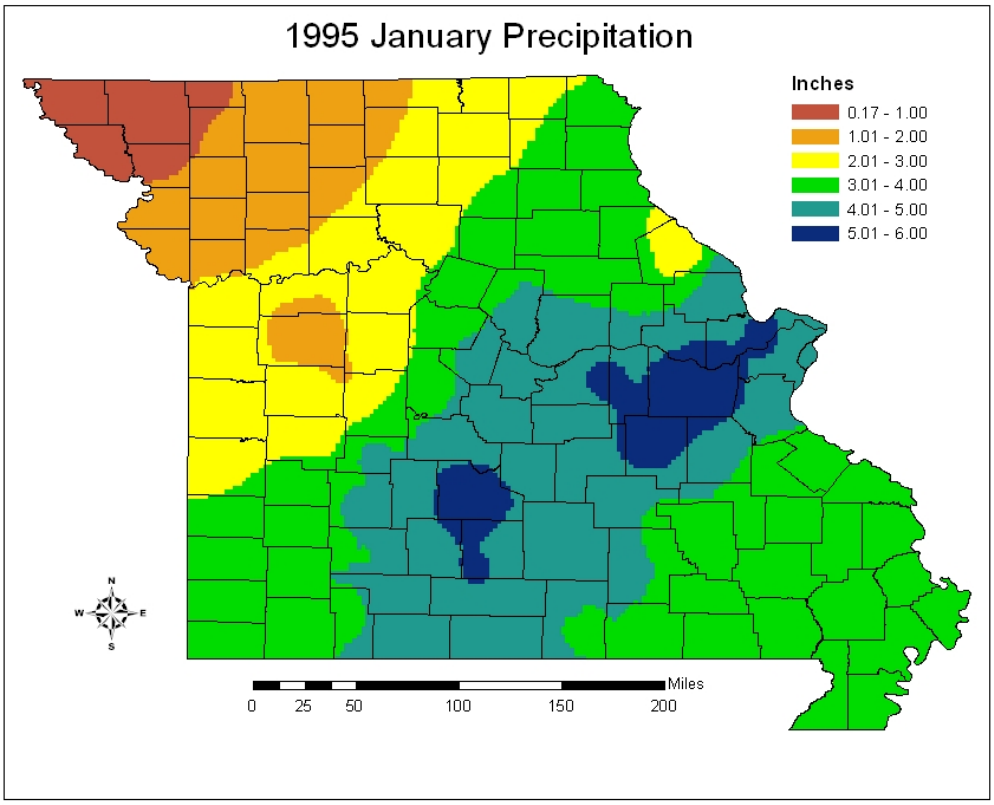

Figure 74: January precipitation, 1995.

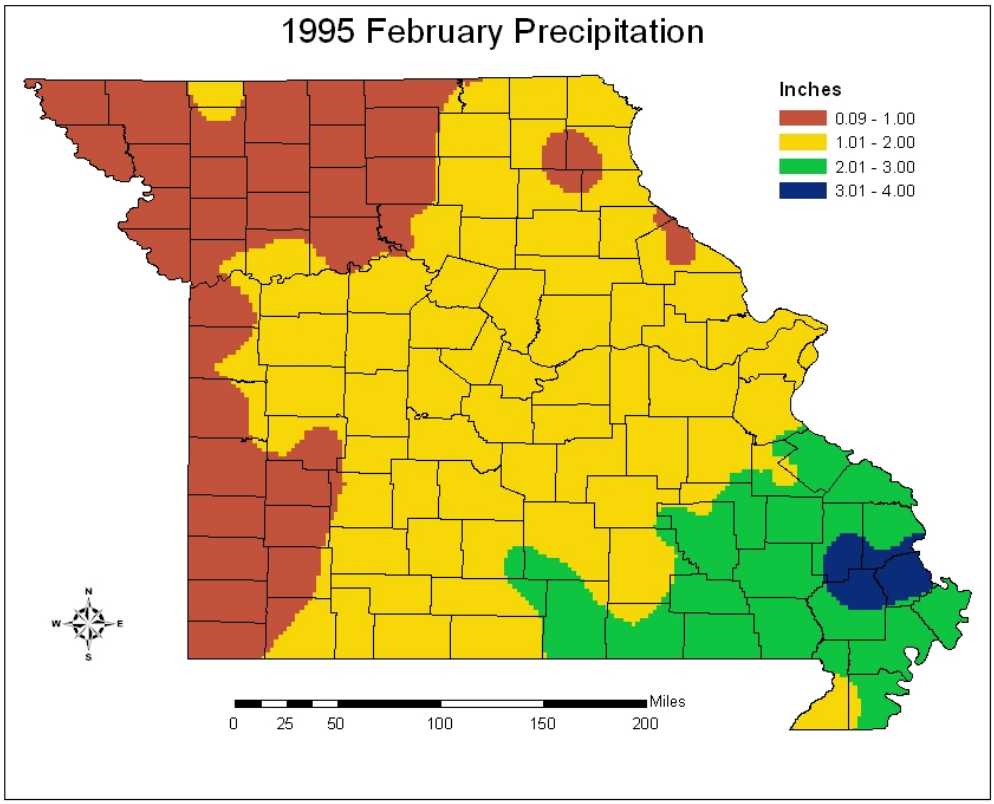

Figure 74: February precipitation, 1995.

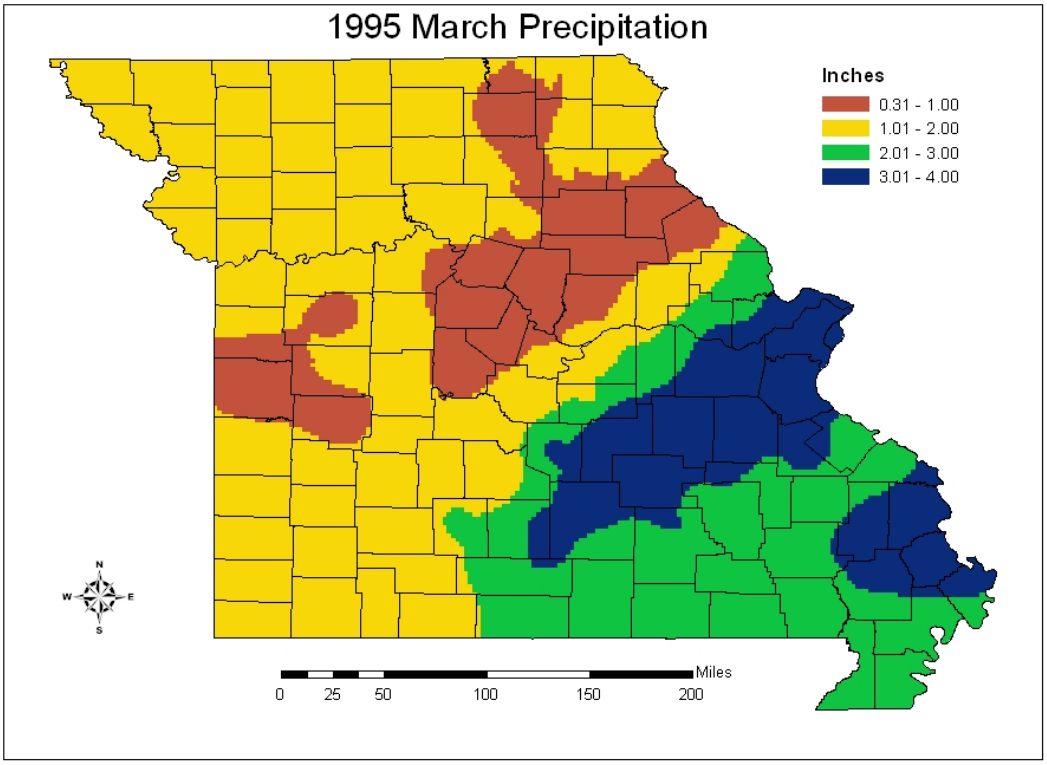

Figure 75: March precipitation, 1995.

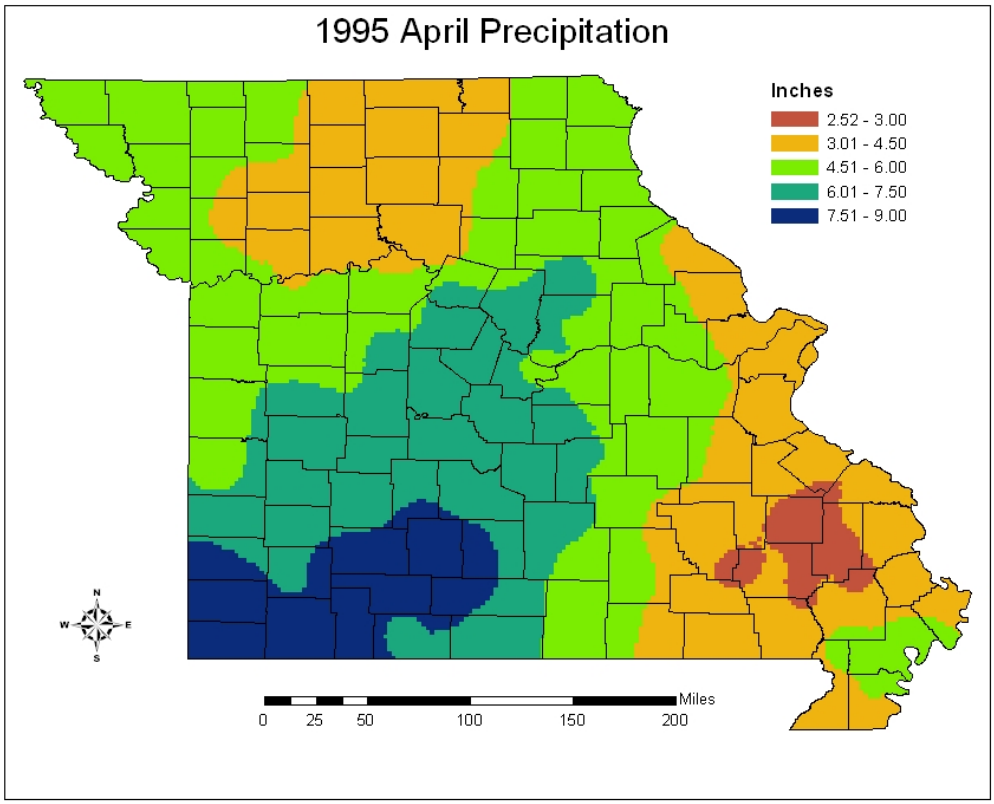

Figure 76: April precipitation, 1995.

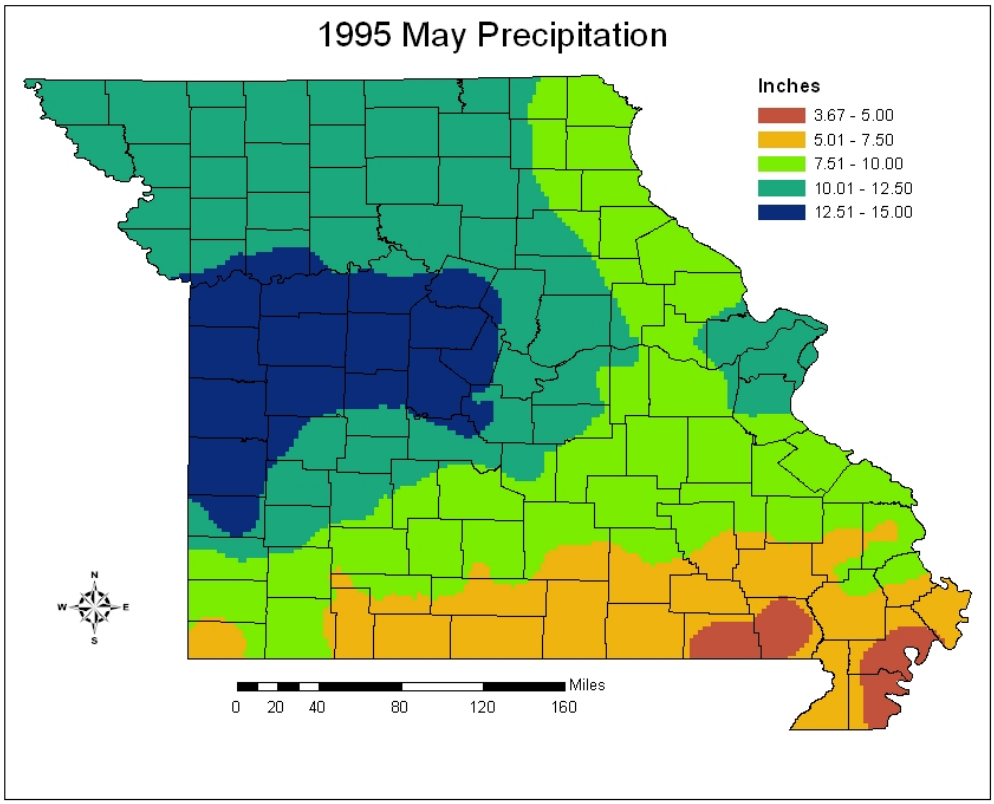

Figure 77: May precipitation, 1995.

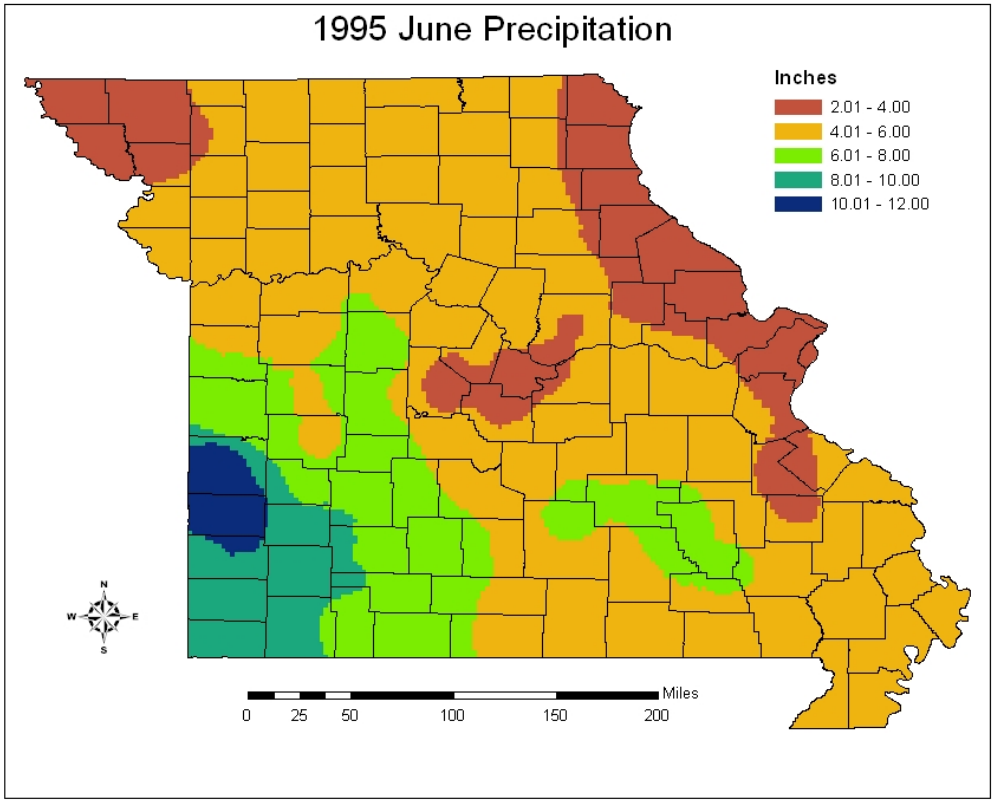

Figure 78: June precipitation, 1995.

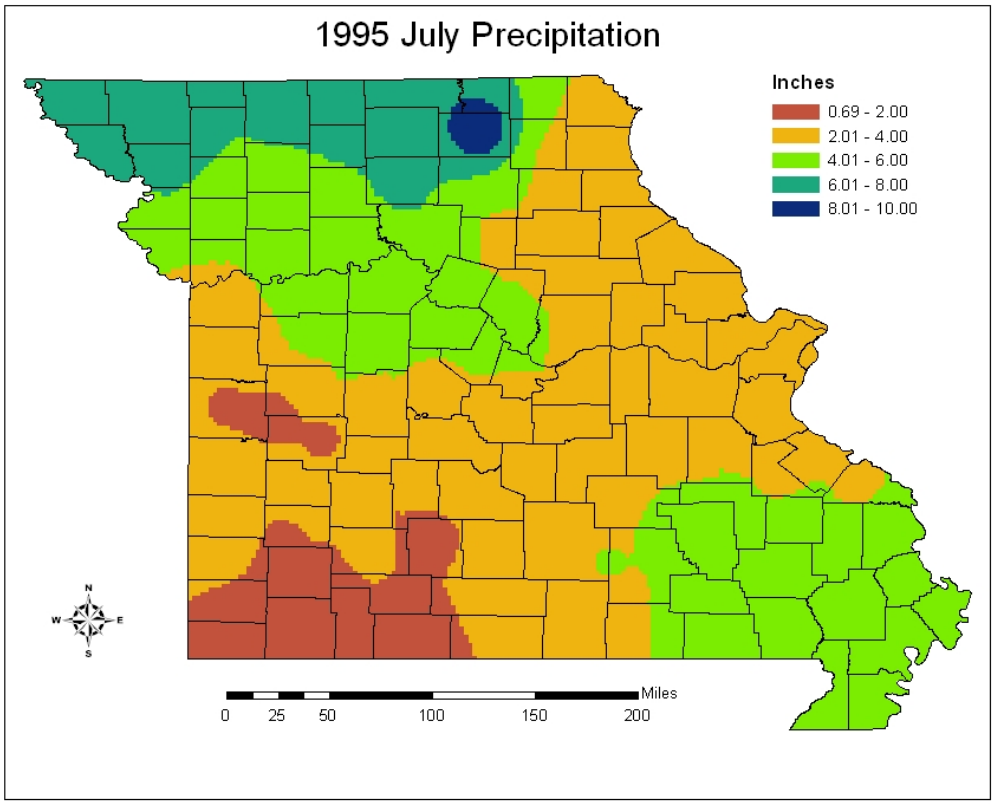

Figure 79: July precipitation, 1995.

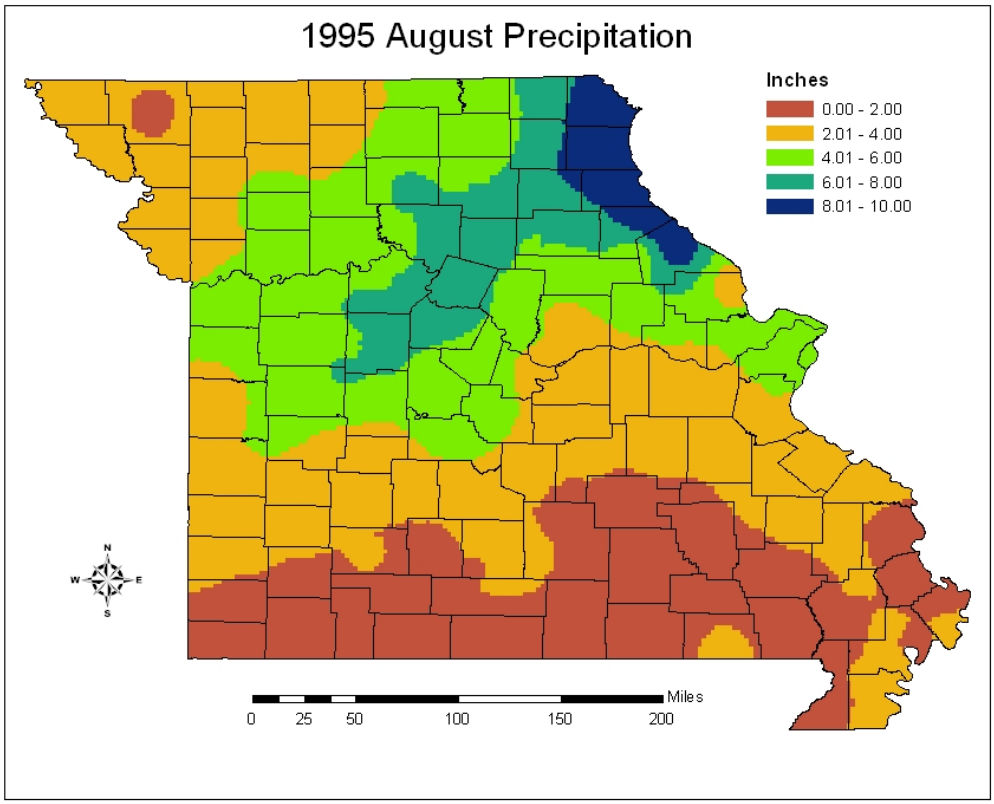

Figure 80: August precipitation, 1995.

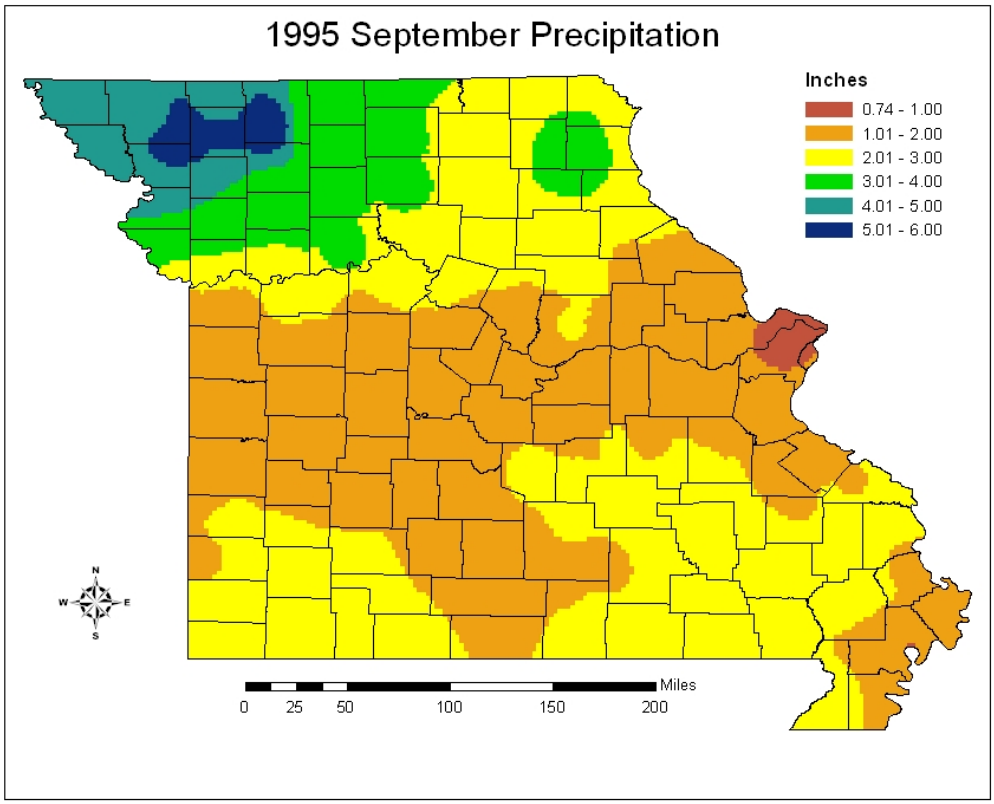

Figure 81: September precipitation, 1995.

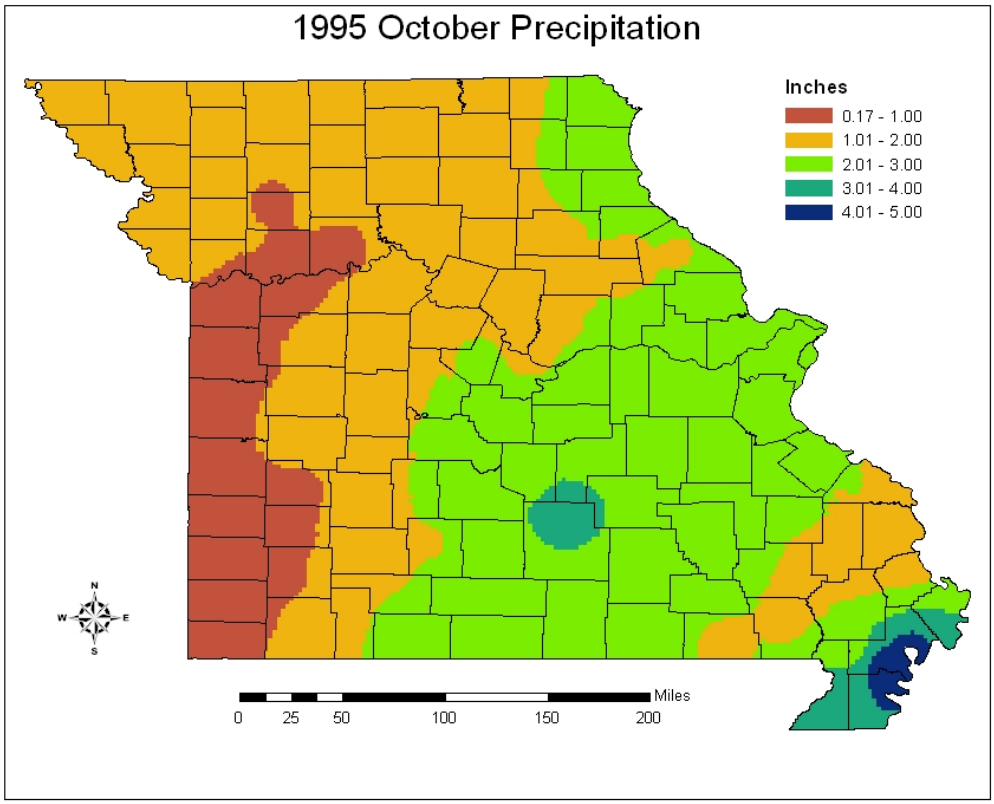

Figure 82: October precipitation, 1995.

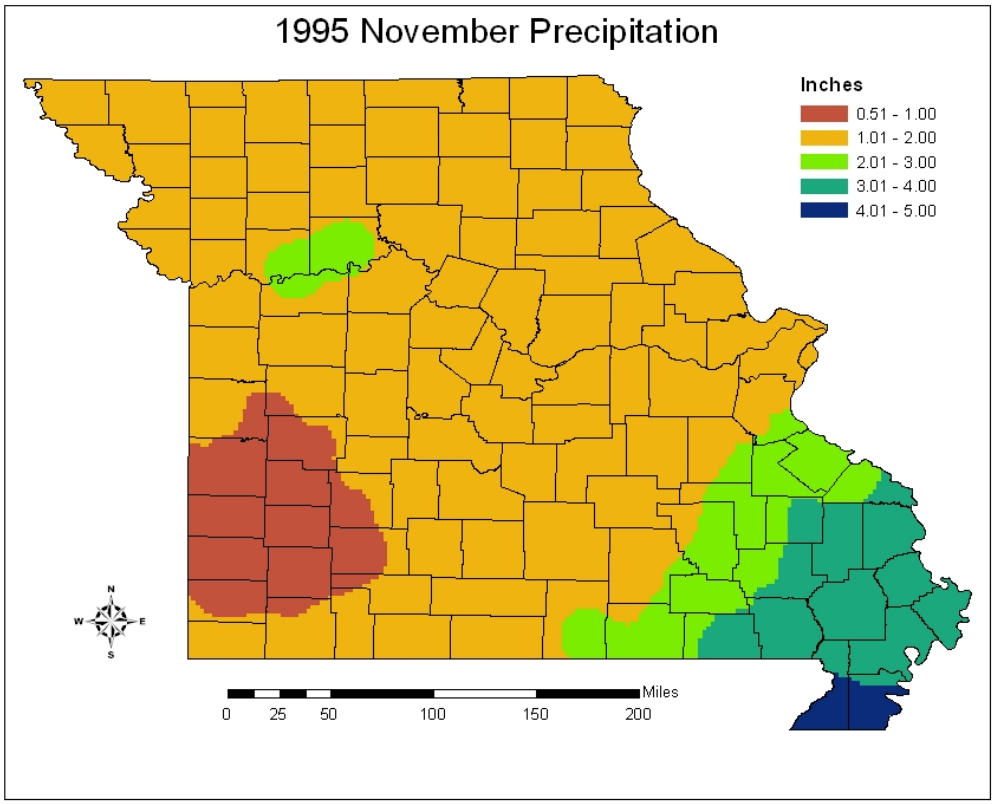

Figure 83: November precipitation, 1995.

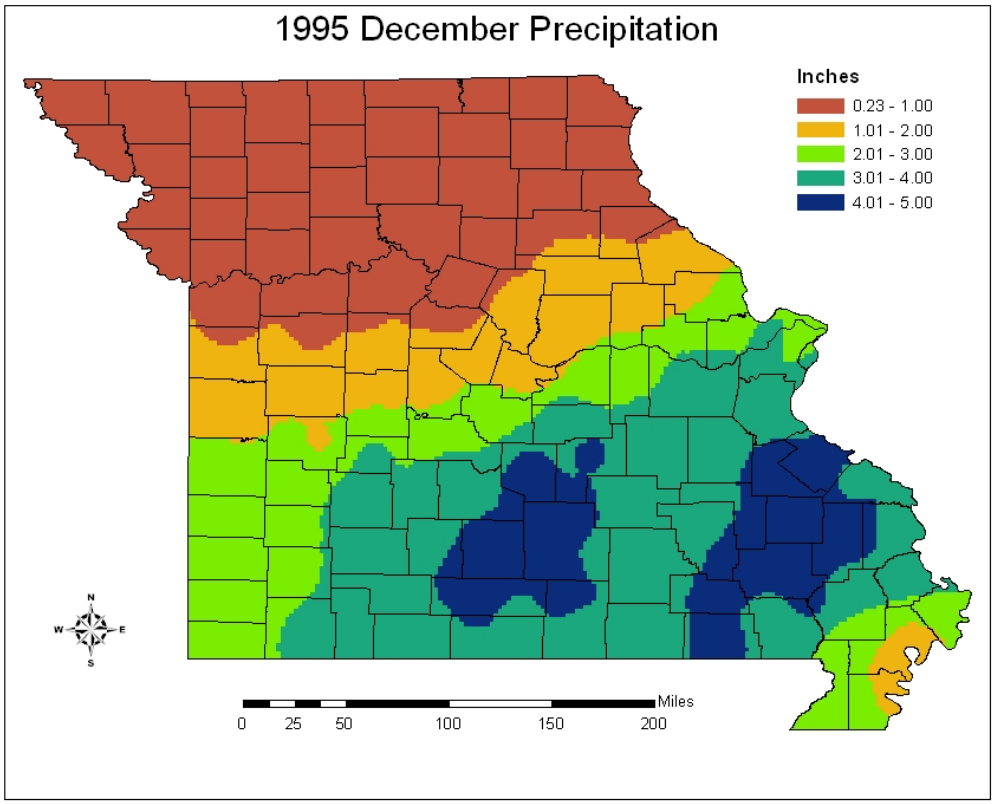

Figure 84: December precipitation, 1995.

3. Temperature

3.1: Norms

Temperature is measured and described by "mean," "maximum," and "minimum" temperatures any specified periods, such as day, month, and year. The maximum and minimum temperatures define the range of temperature variation in the period and the mean temperature is specified as the arithmetic average of the maximum and minimum temperatures. In the following, the 30-year (1971-2000) normal annual and monthly temperatures are presented. For convenience of comparisons, the norms of minimum, mean, and maximum temperatures are put together for the same month and year.

a) Annual temperatures

The normal annual minimum, mean, and maximum temperatures are shown in Figs. 85-87.

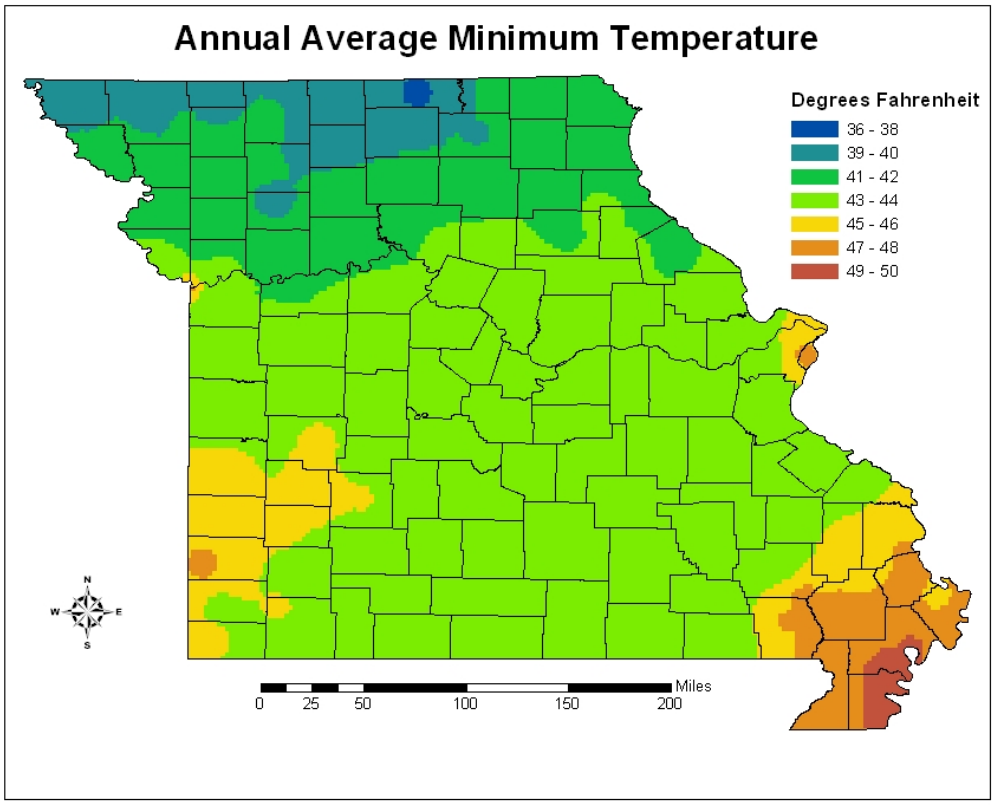

Figure 85: Normal annual minimum temperature.

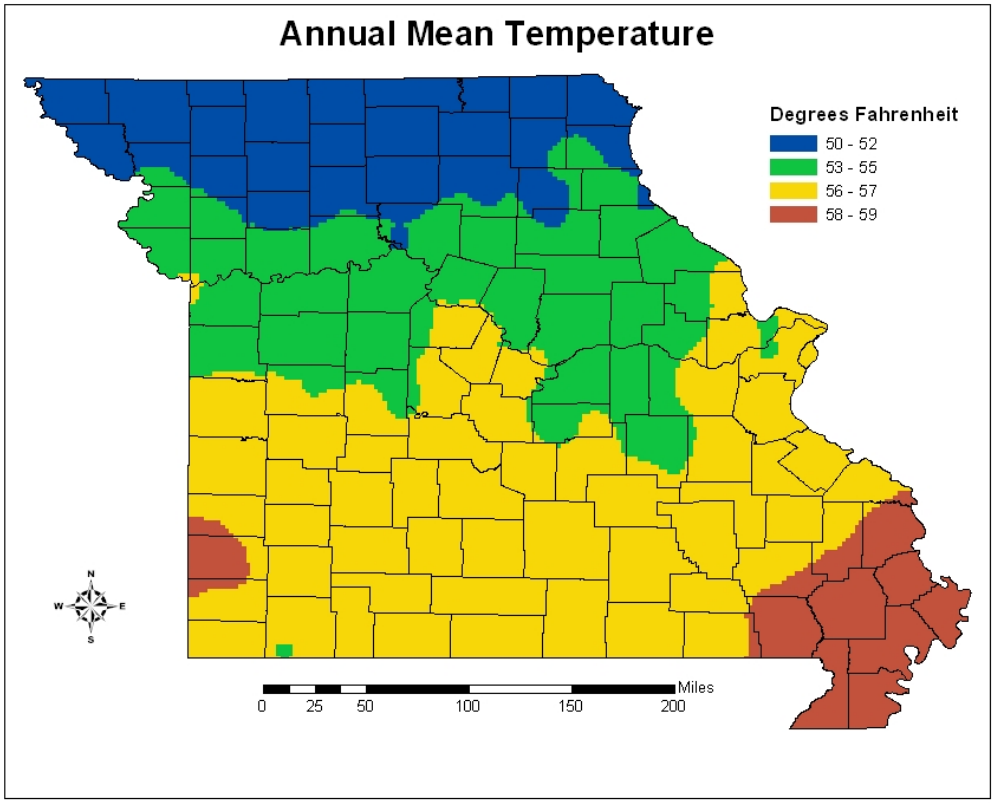

Figure 86: Normal annual mean temperature.

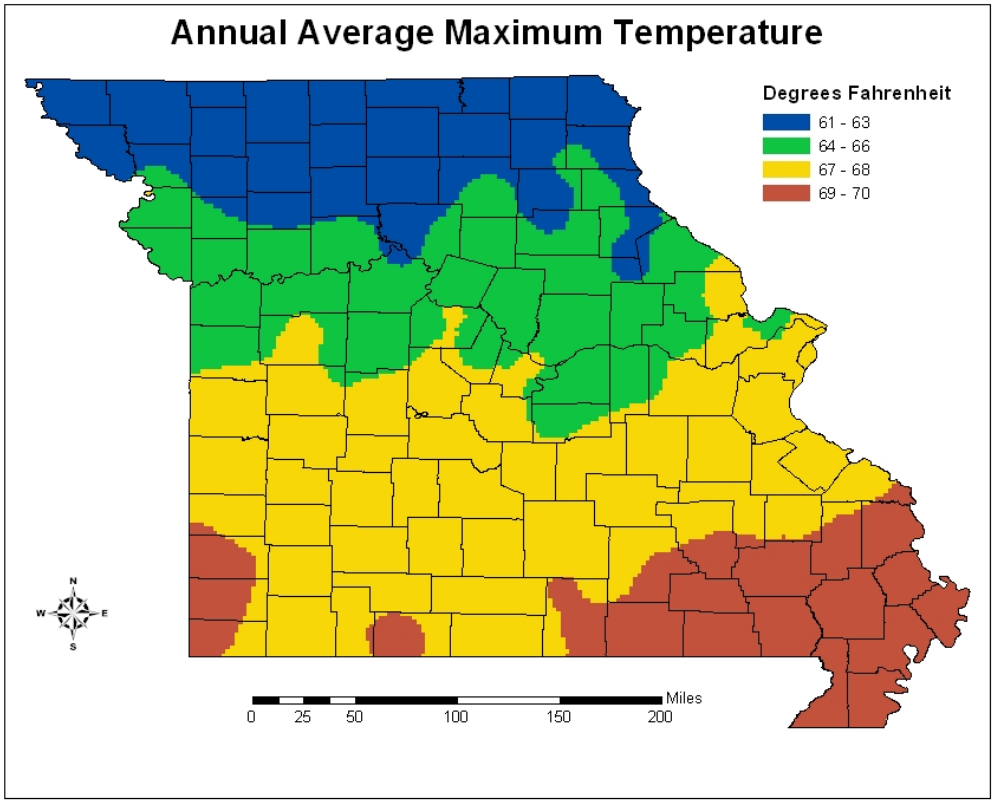

Figure 87: Normal annual maximum temperature.

b) Monthly temperatures

The 30-year norms of minimum, mean, and maximum temperatures for each month are shown in following 36 figures.

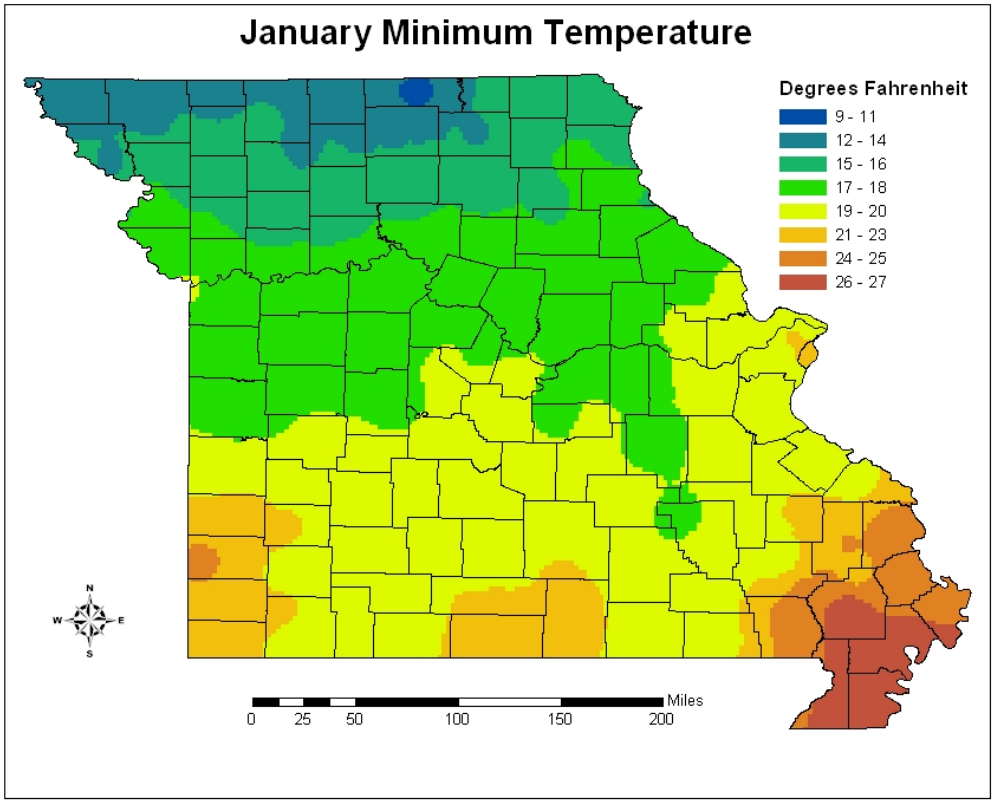

Figure 88: Normal minimum January temperature.

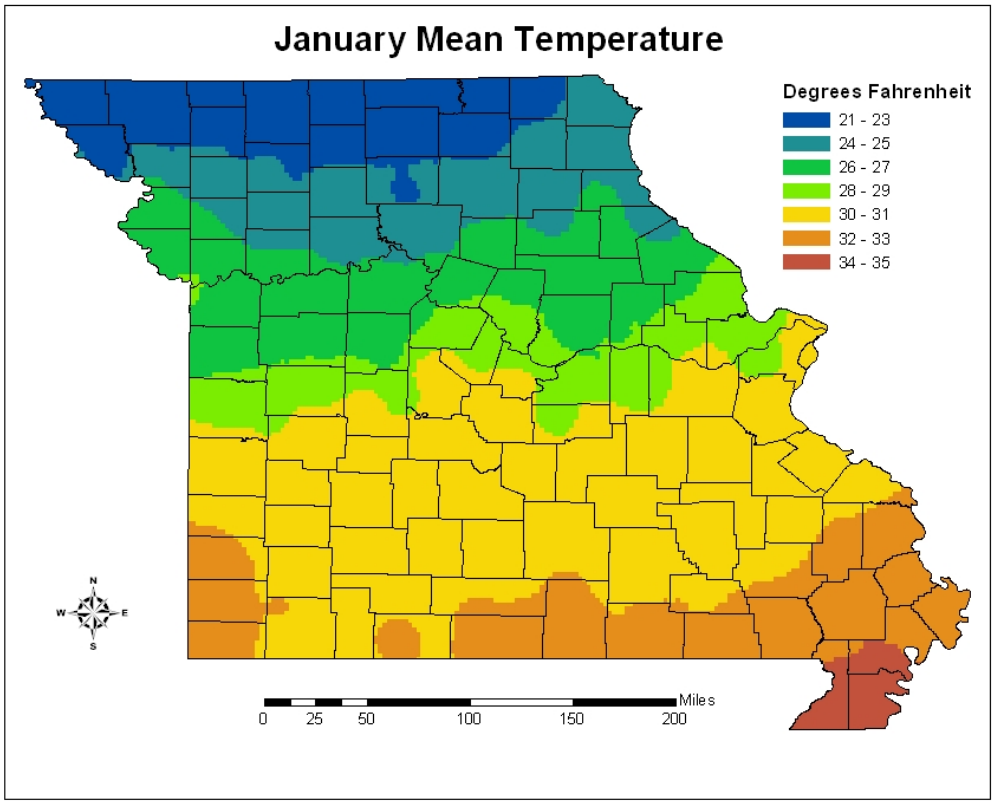

Figure 89: Normal mean January temperature.

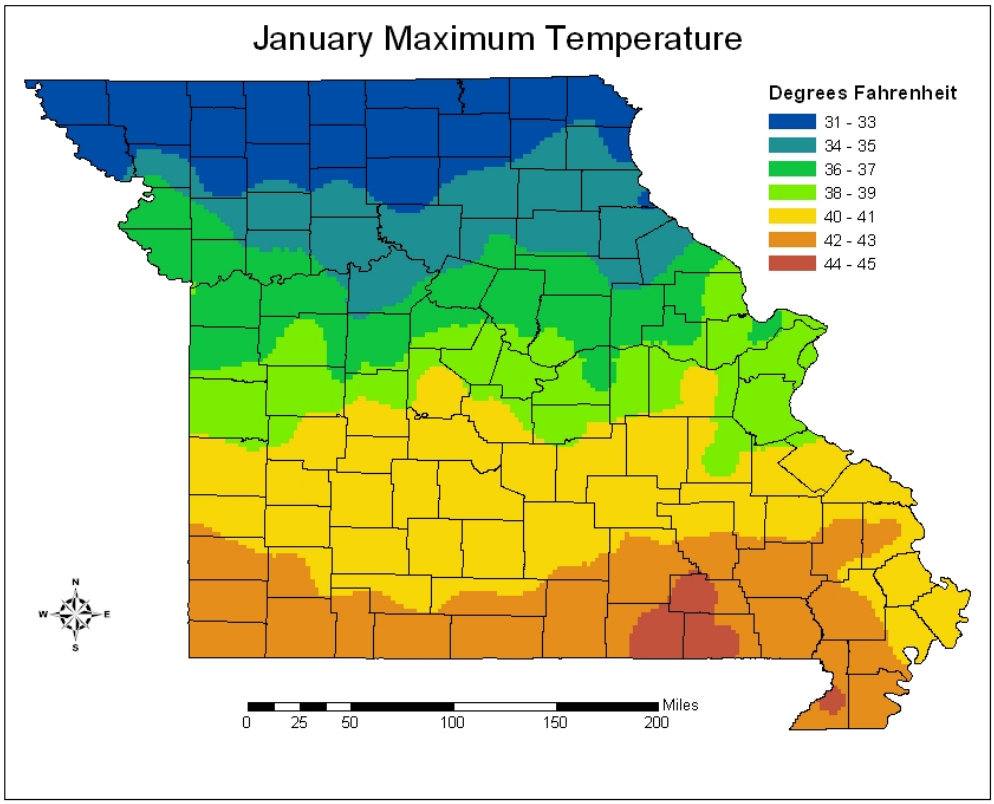

Figure 90: Normal maximum January temperature.

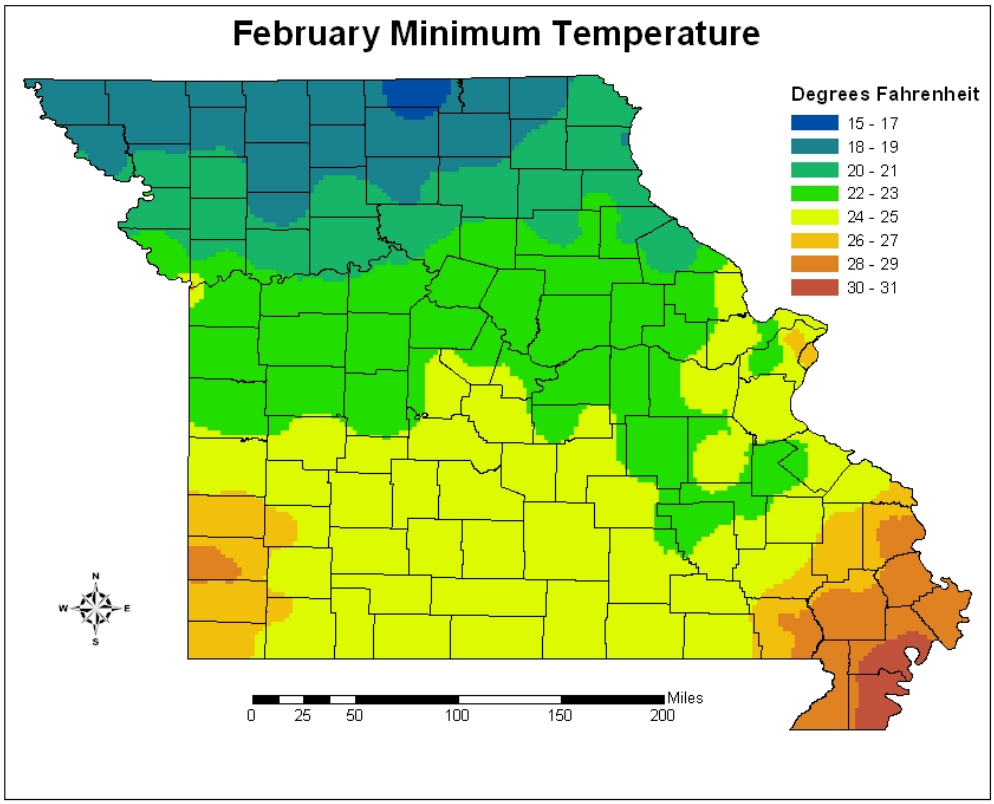

Figure 91: Normal minimum February temperature.

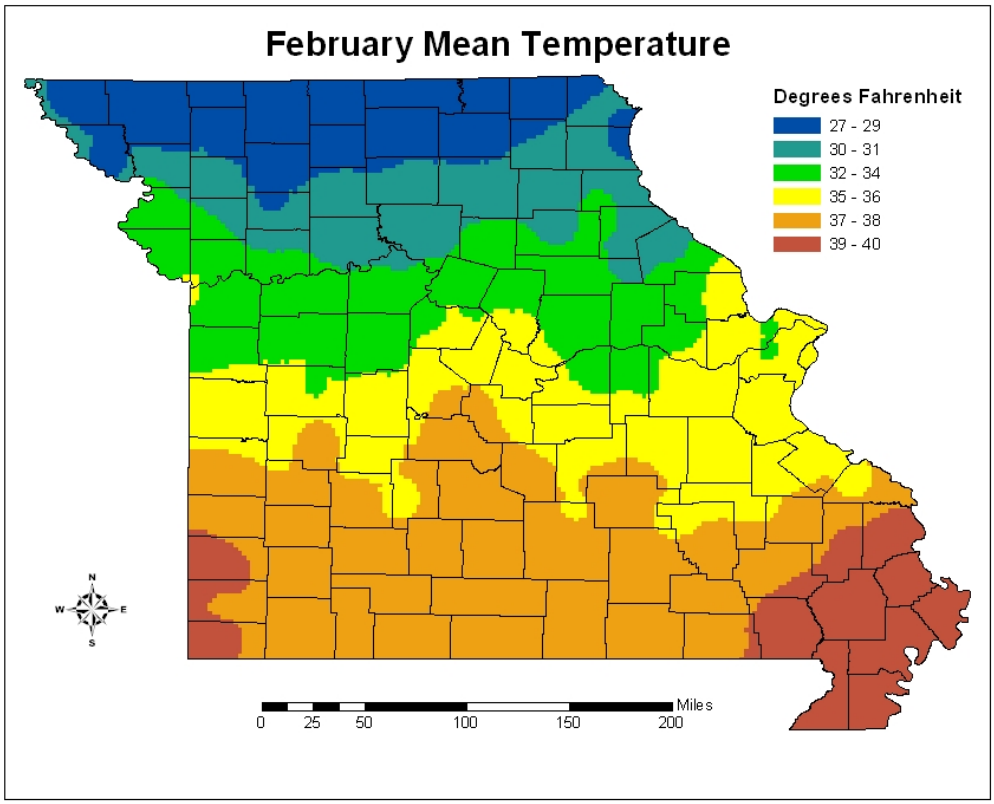

Figure 92: Normal mean February temperature.

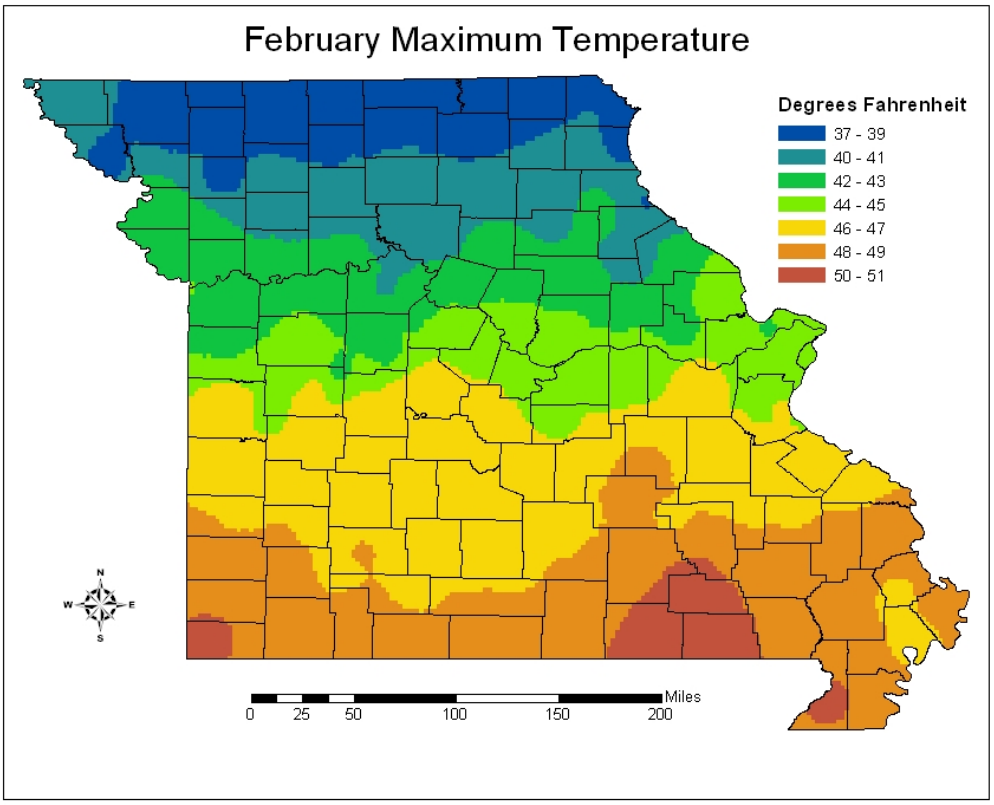

Figure 93: Normal maximum February temperature.

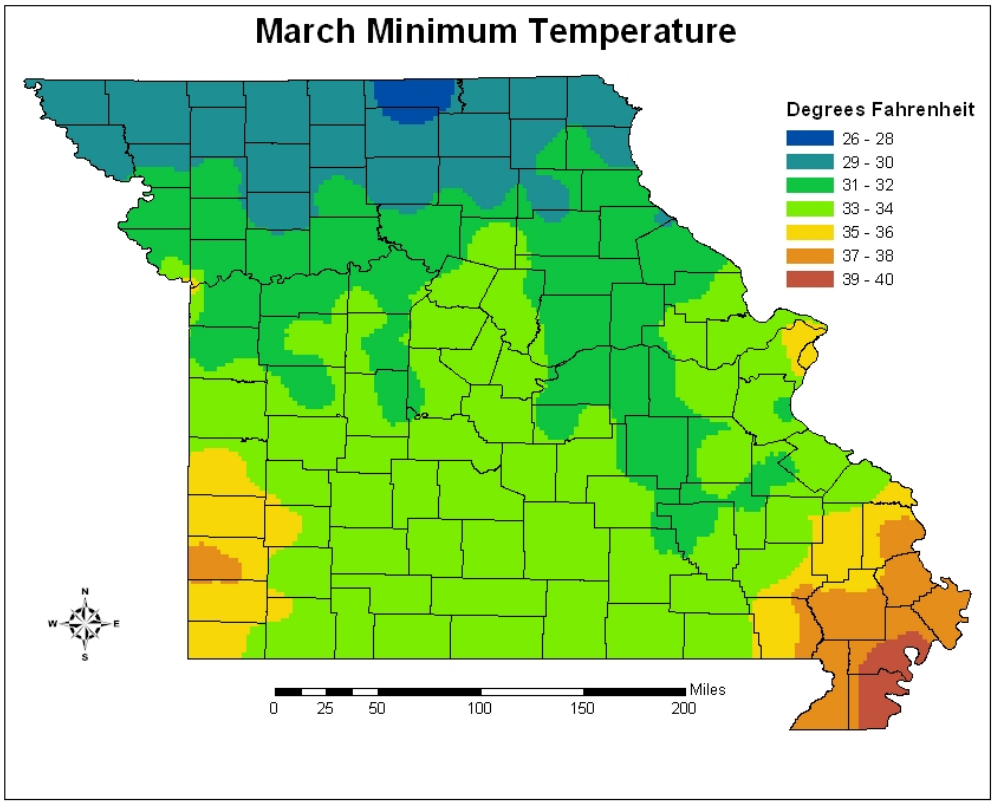

Figure 94: Normal minimum Mach temperature.

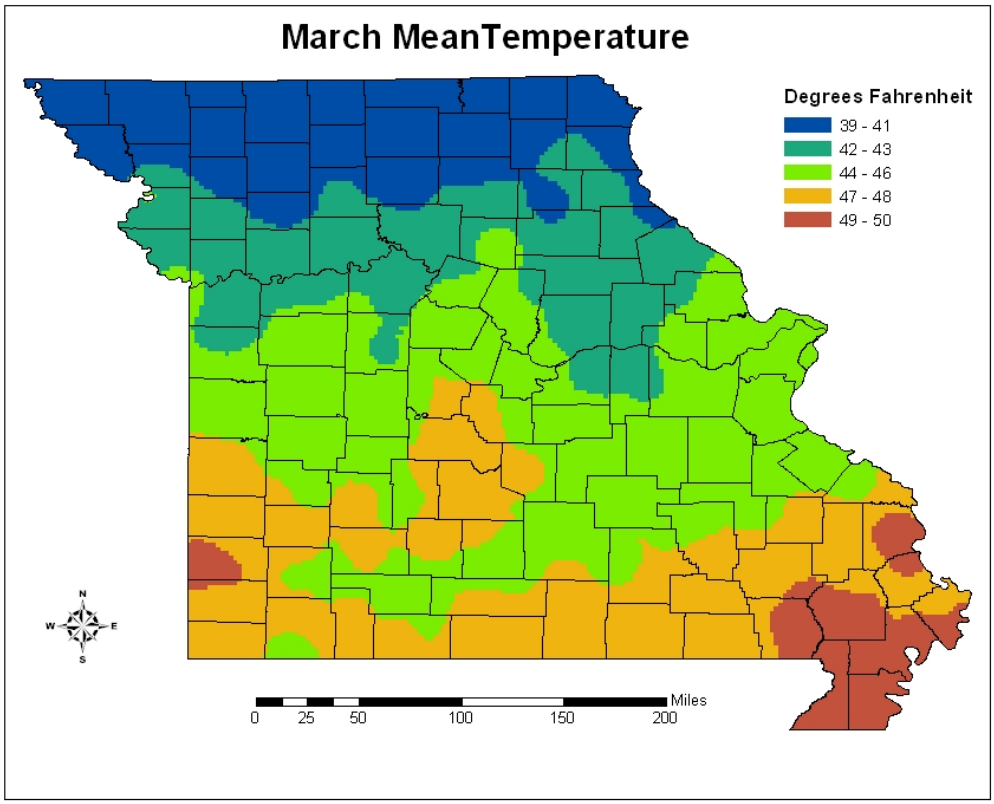

Figure 95: Normal mean March temperature.

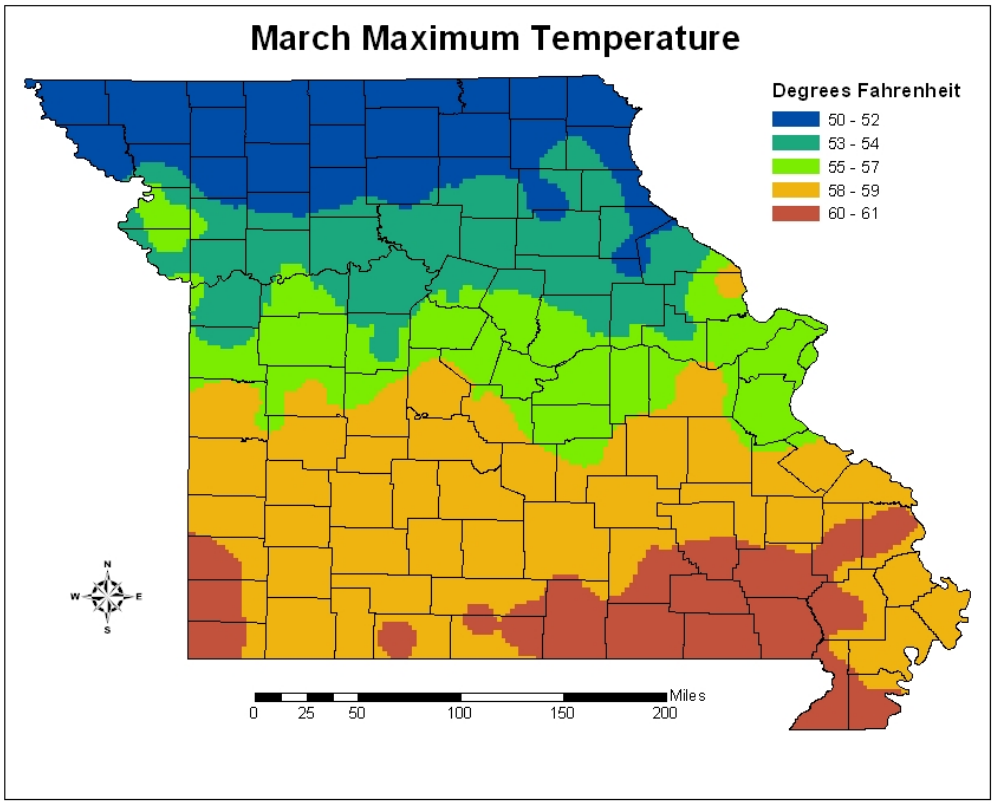

Figure 96: Normal maximum March temperature.

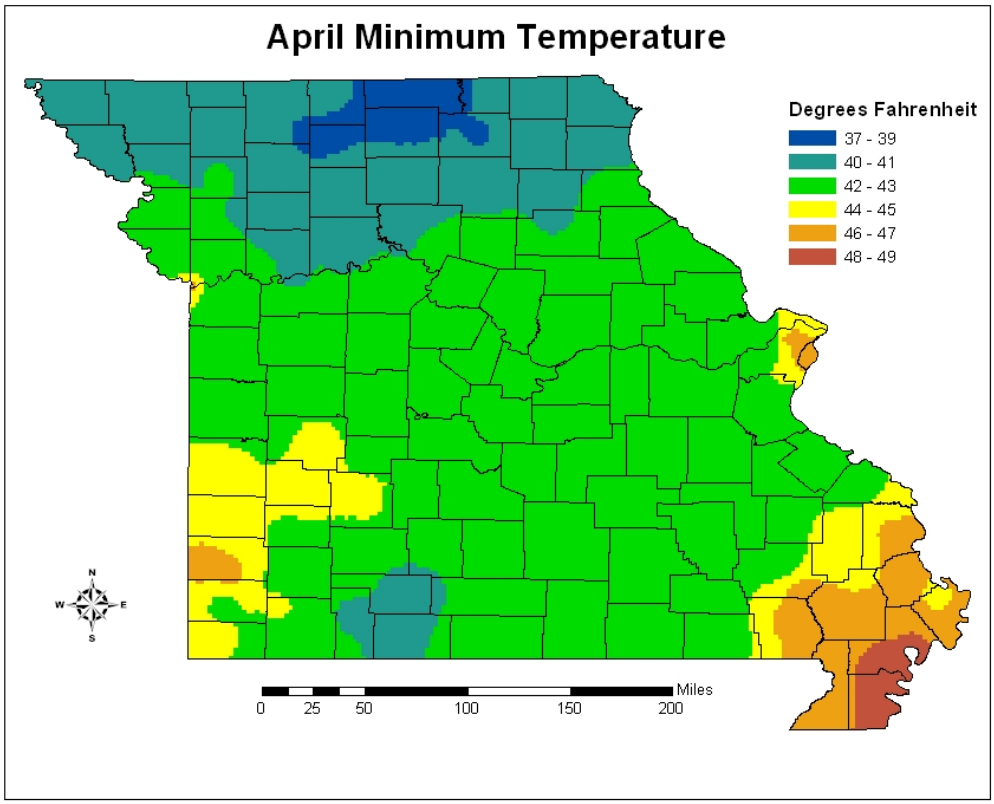

Figure 97: Normal minimum April temperature.

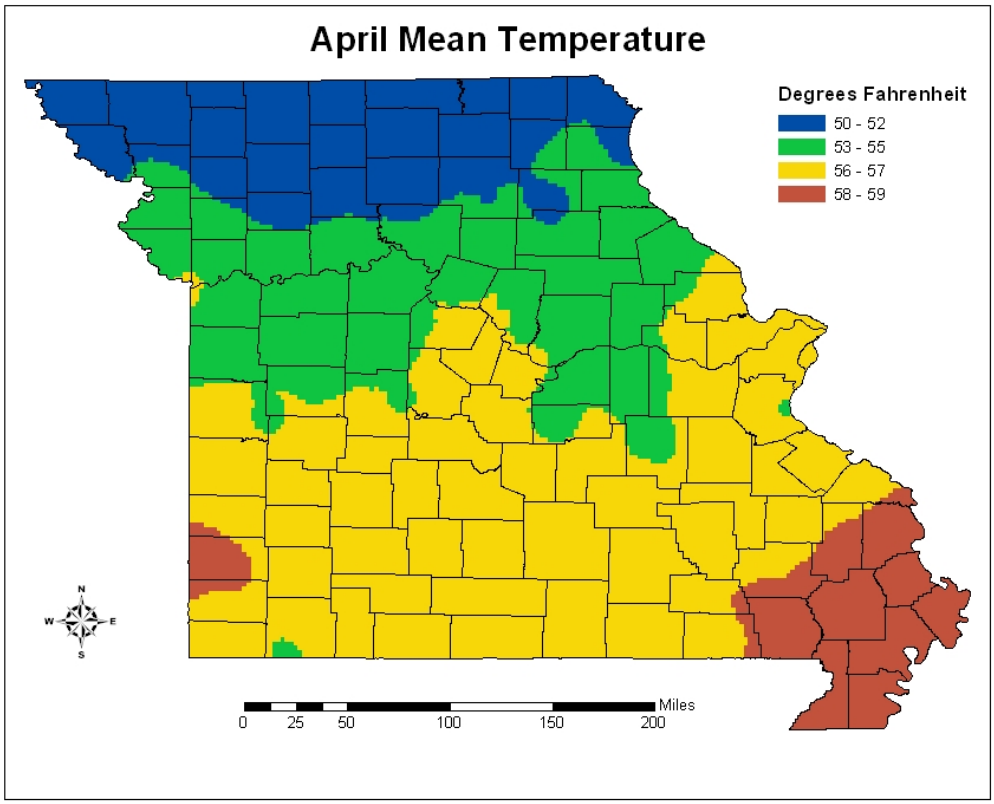

Figure 98: Normal mean April temperature.

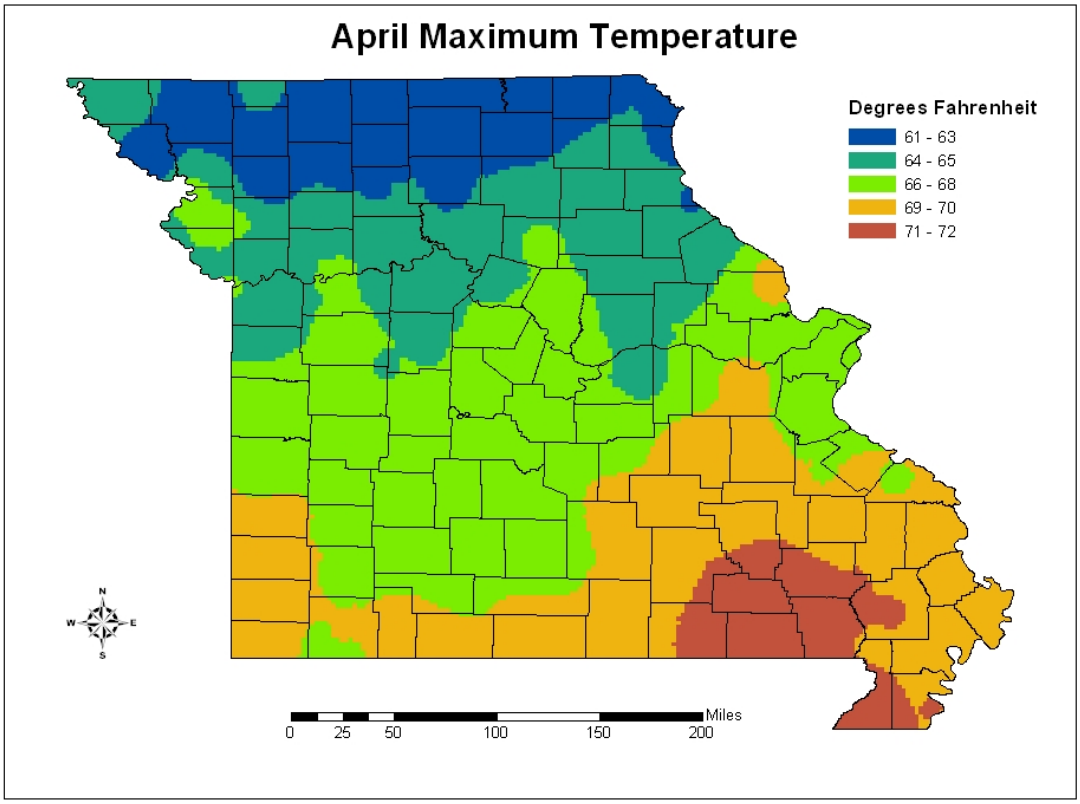

Figure 99: Normal maximum April temperature.

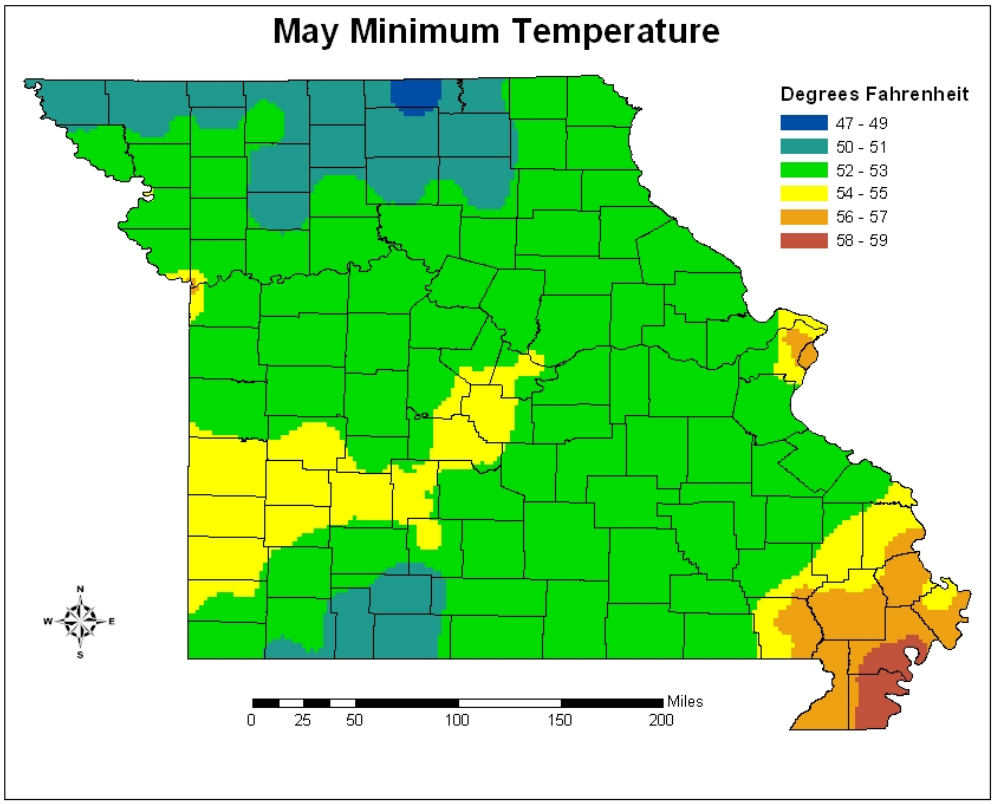

Figure 100: Normal minimum May temperature.

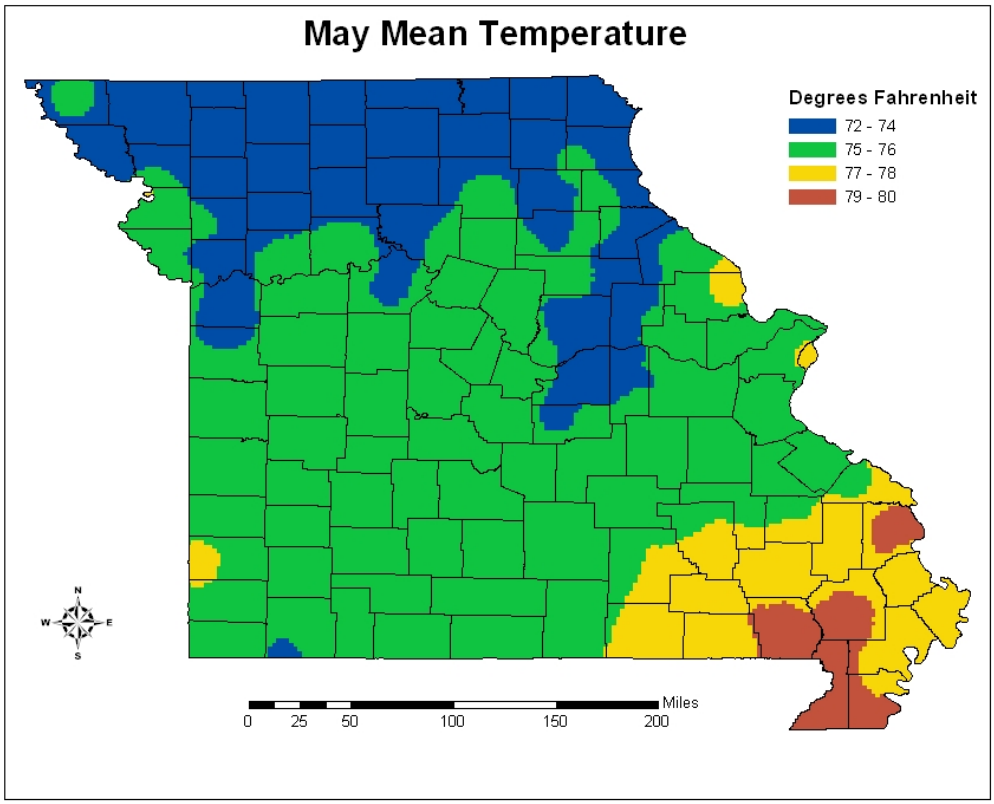

Figure 101: Normal mean May temperature.

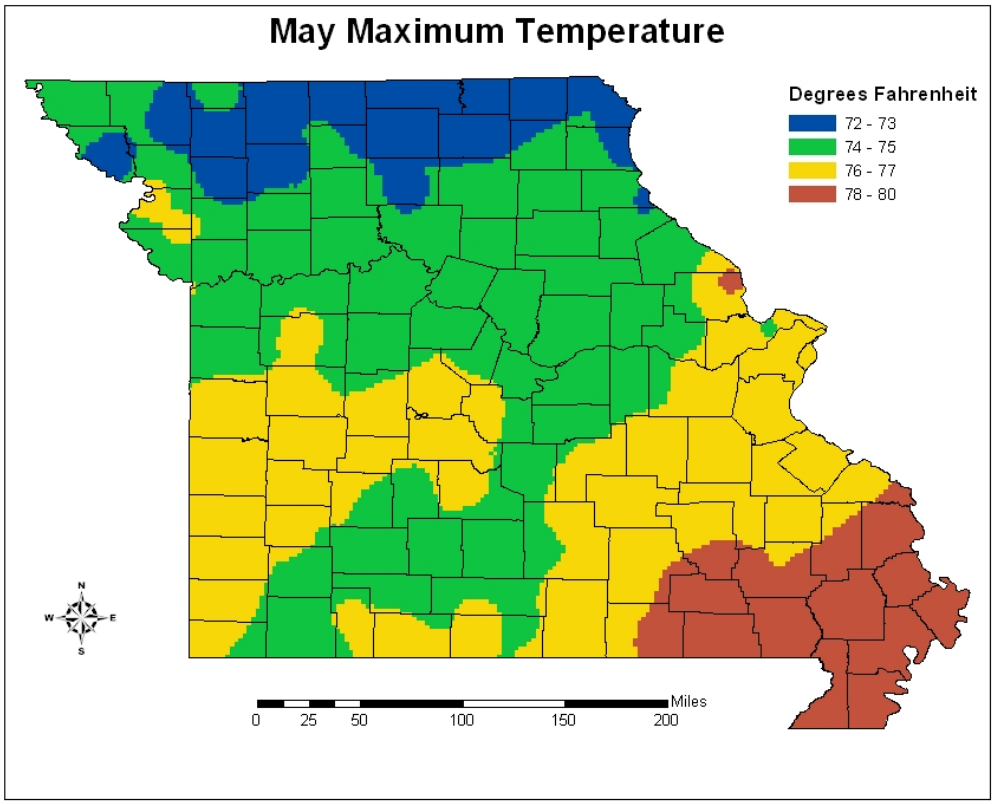

Figure 102: Normal maximum May temperature.

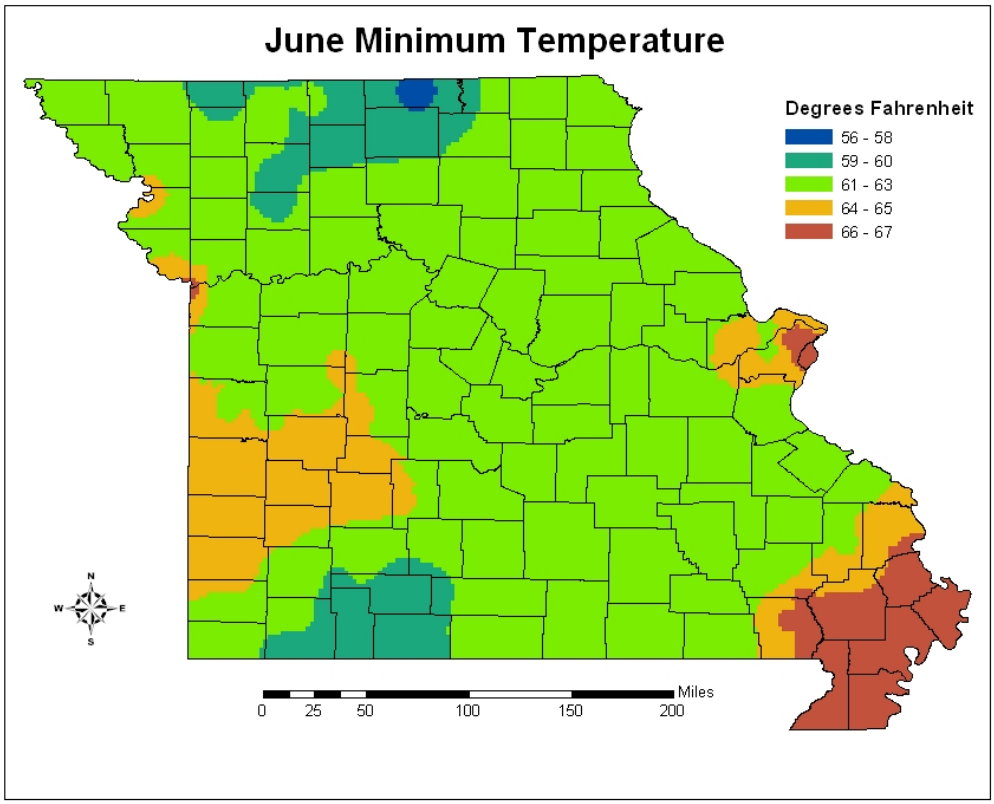

Figure 103: Normal minimum June temperature.

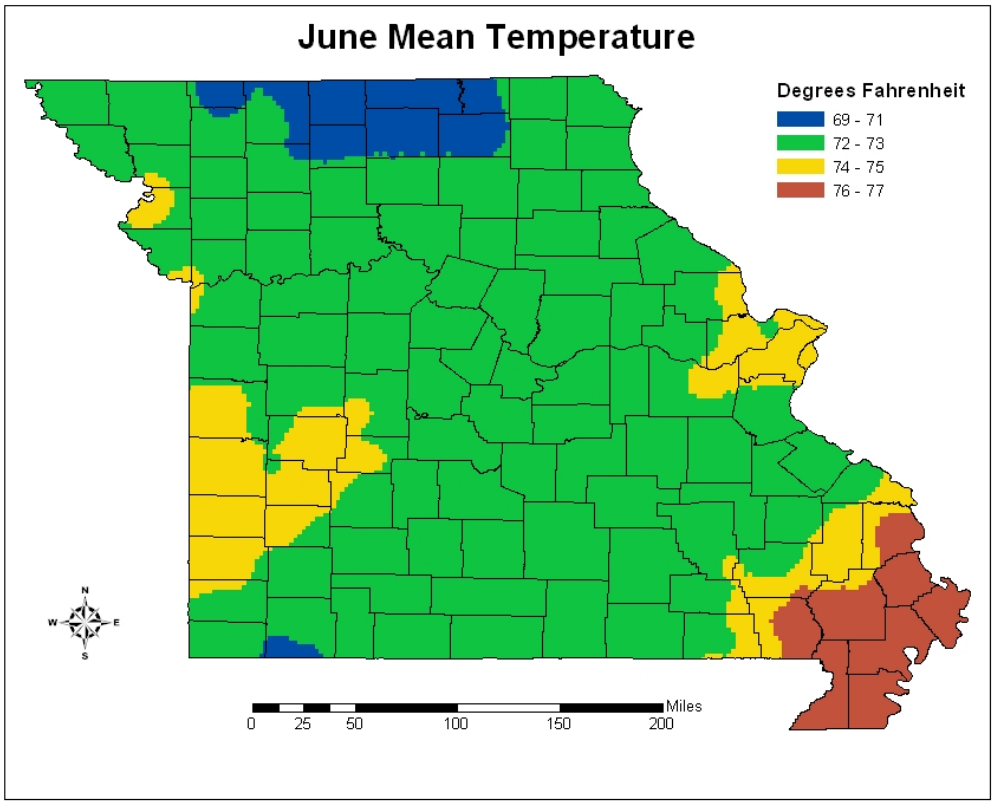

Figure 104: Normal mean June temperature.

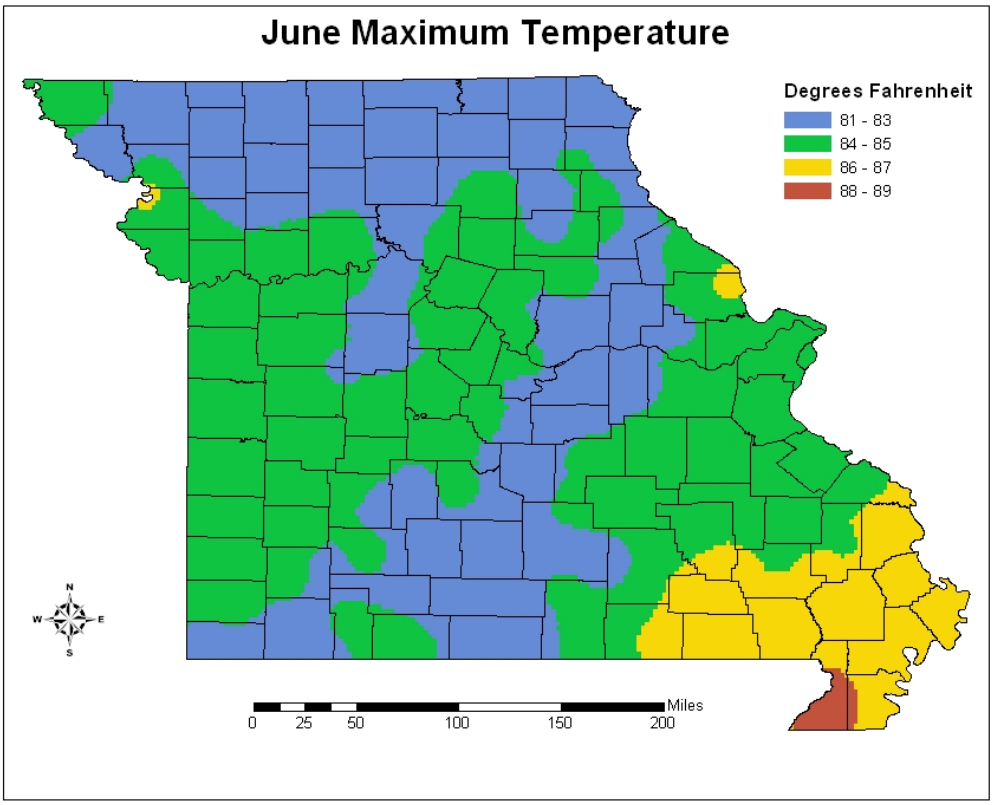

Figure 105: Normal maximum June temperature.

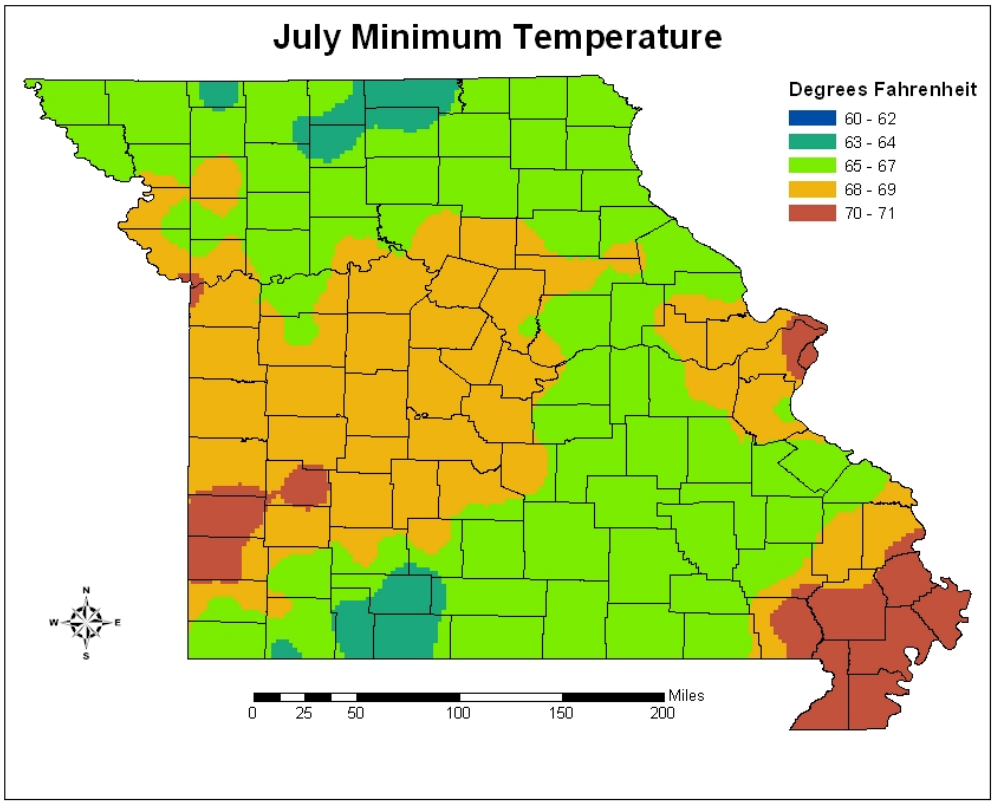

Figure 106: Normal minimum July temperature.

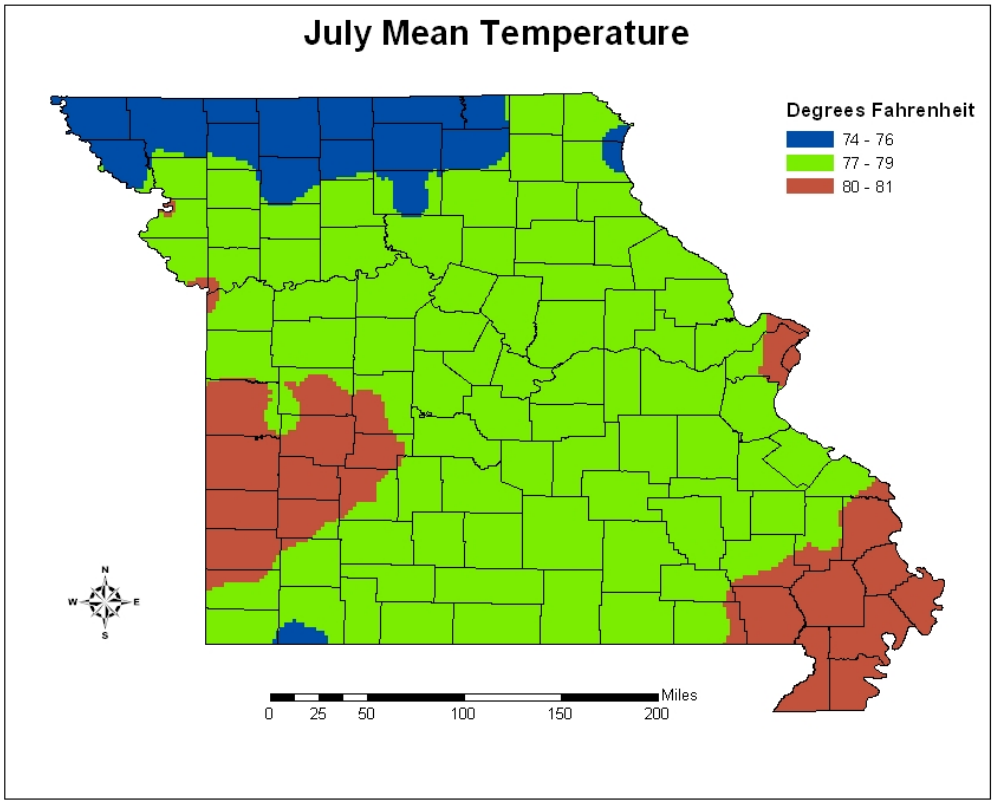

Figure 107: Normal mean July temperature.

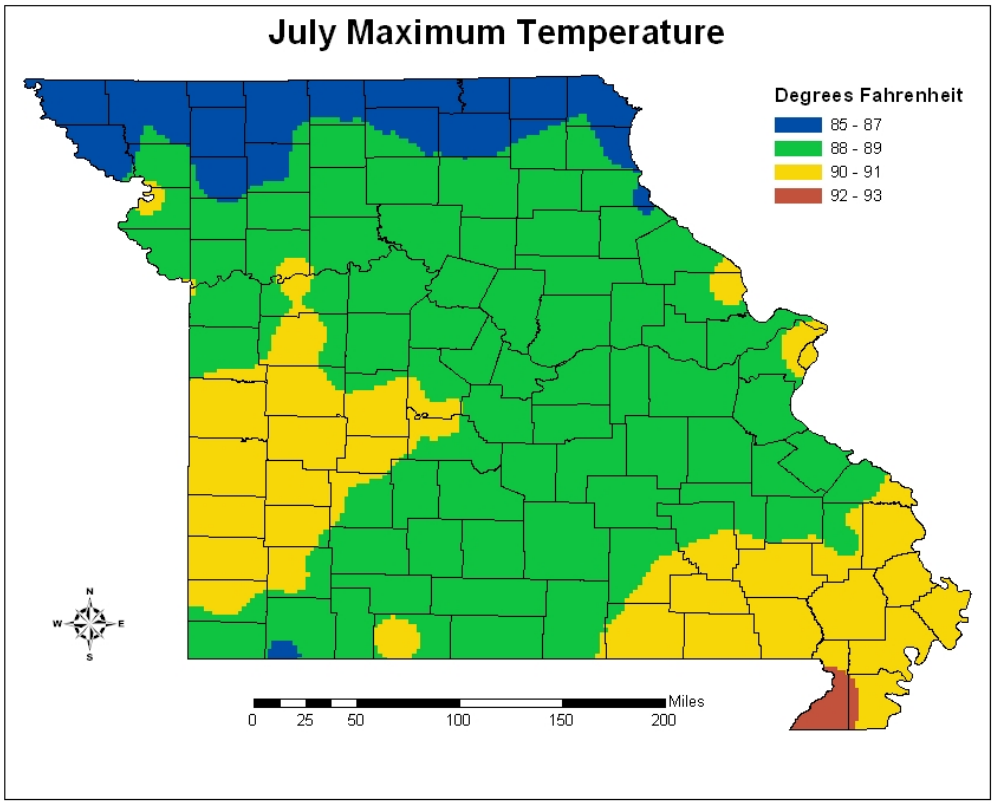

Figure 108: Normal maximum July temperature.

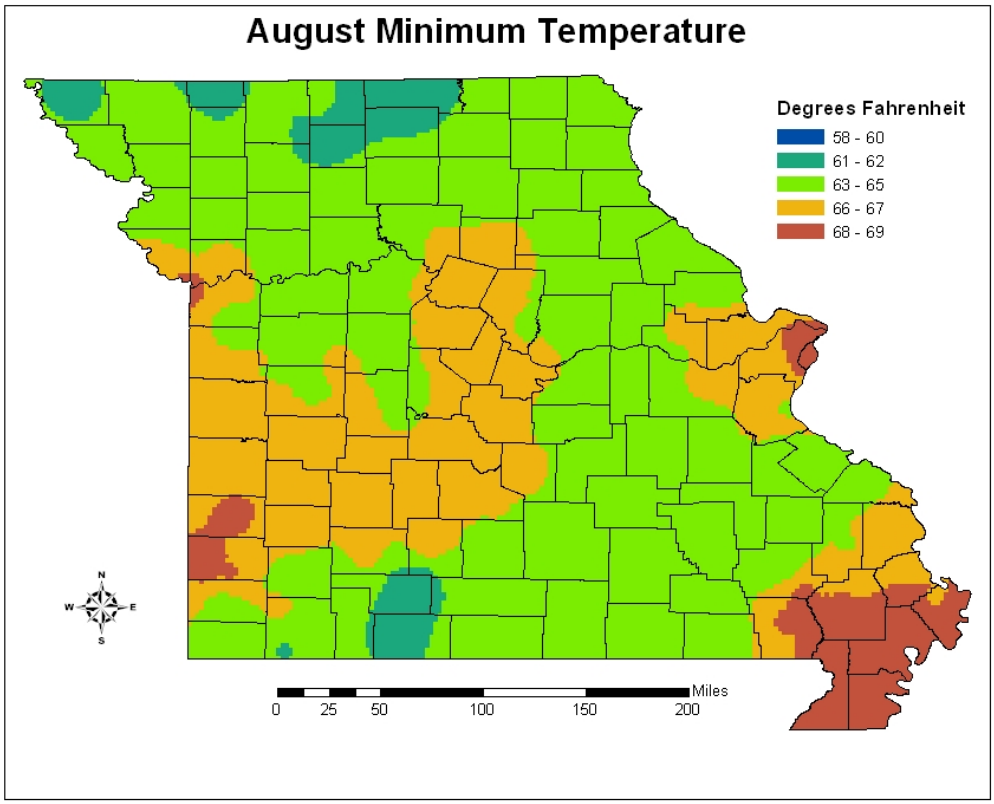

Figure 109: Normal minimum August temperature.

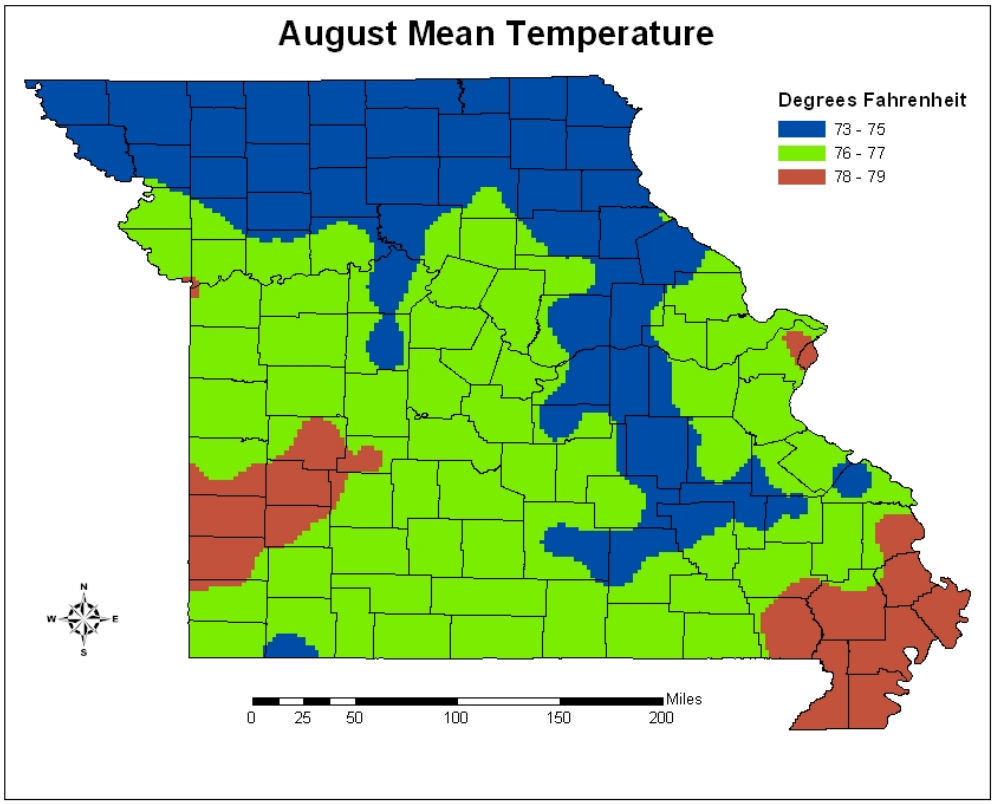

Figure 110: Normal mean August temperature.

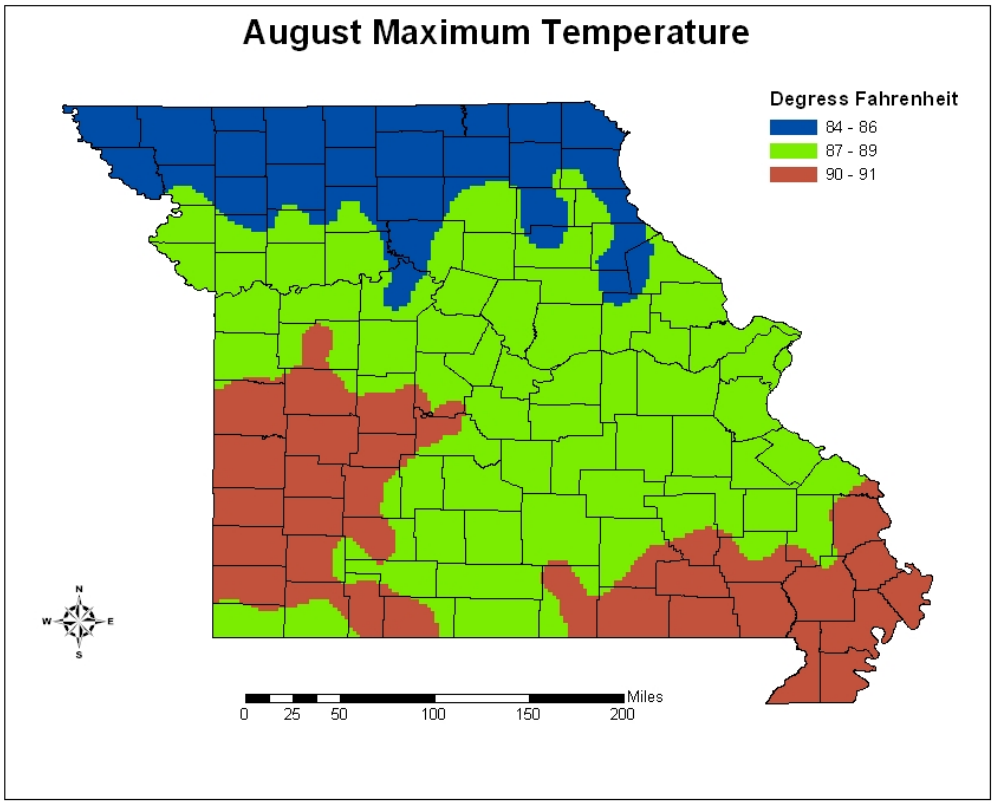

Figure 111: Normal maximum August temperature.

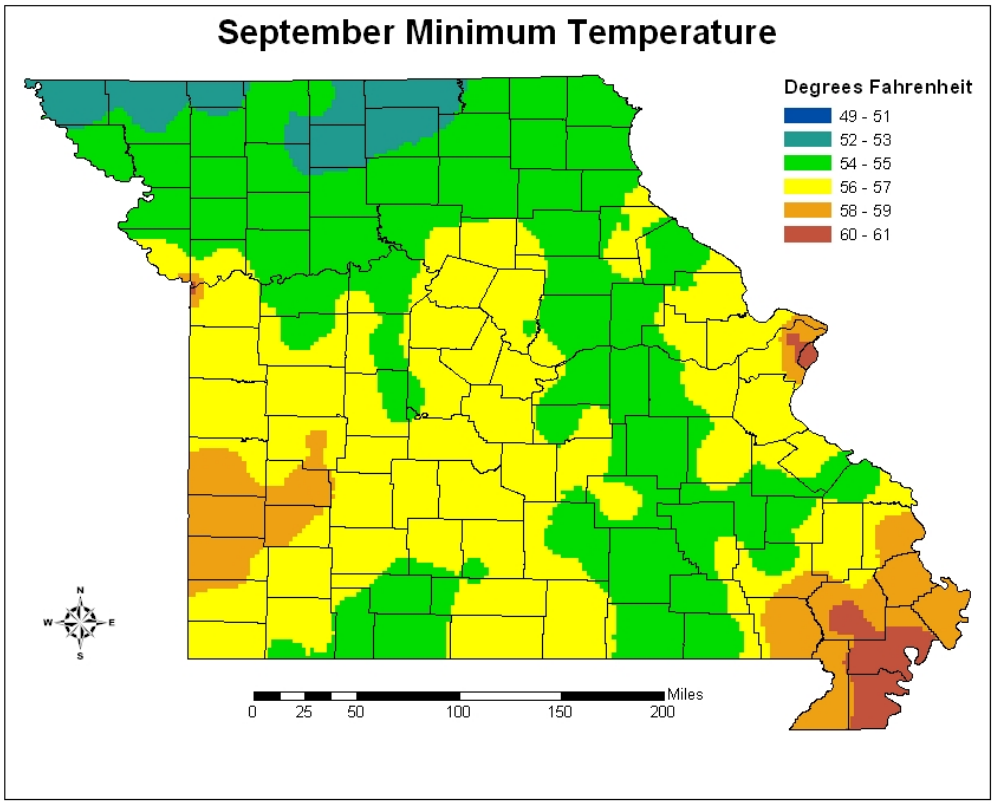

Figure 112: Normal minimum September temperature.

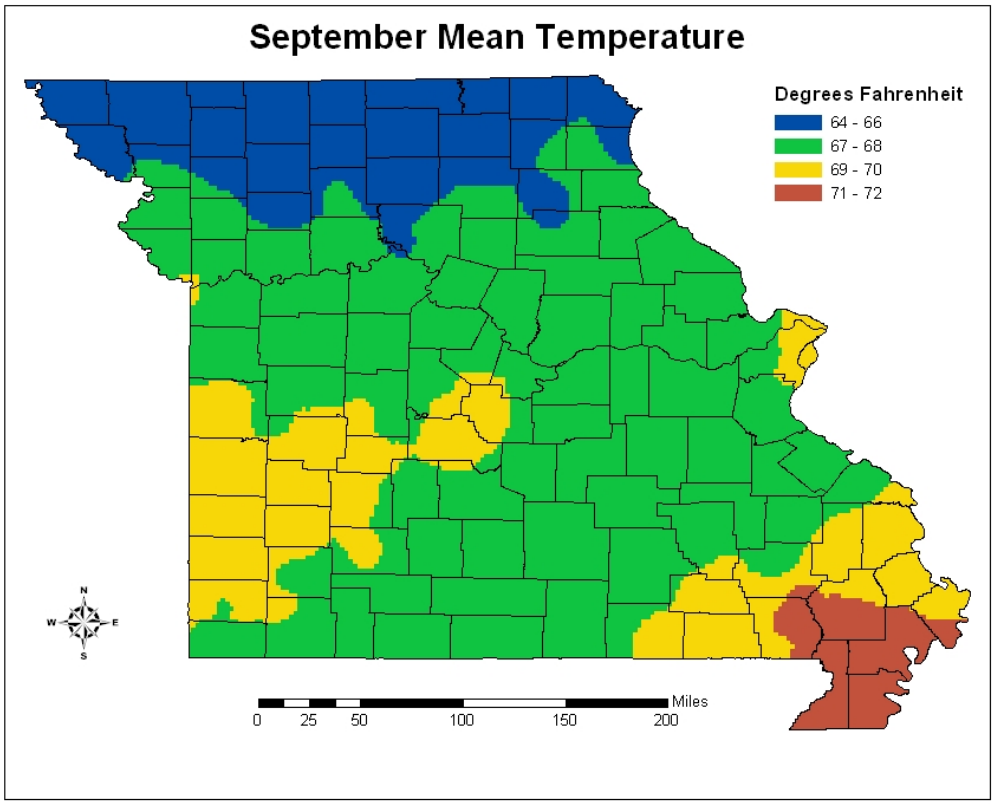

Figure 113: Normal mean September temperature.

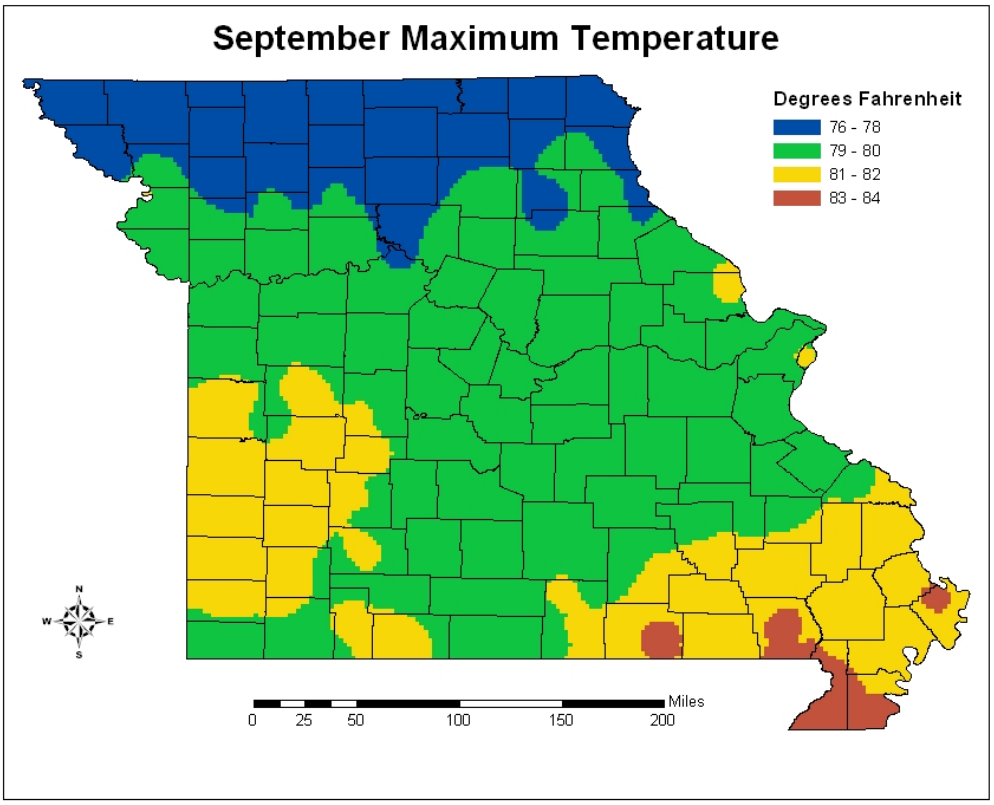

Figure 114: Normal maximum September temperature.

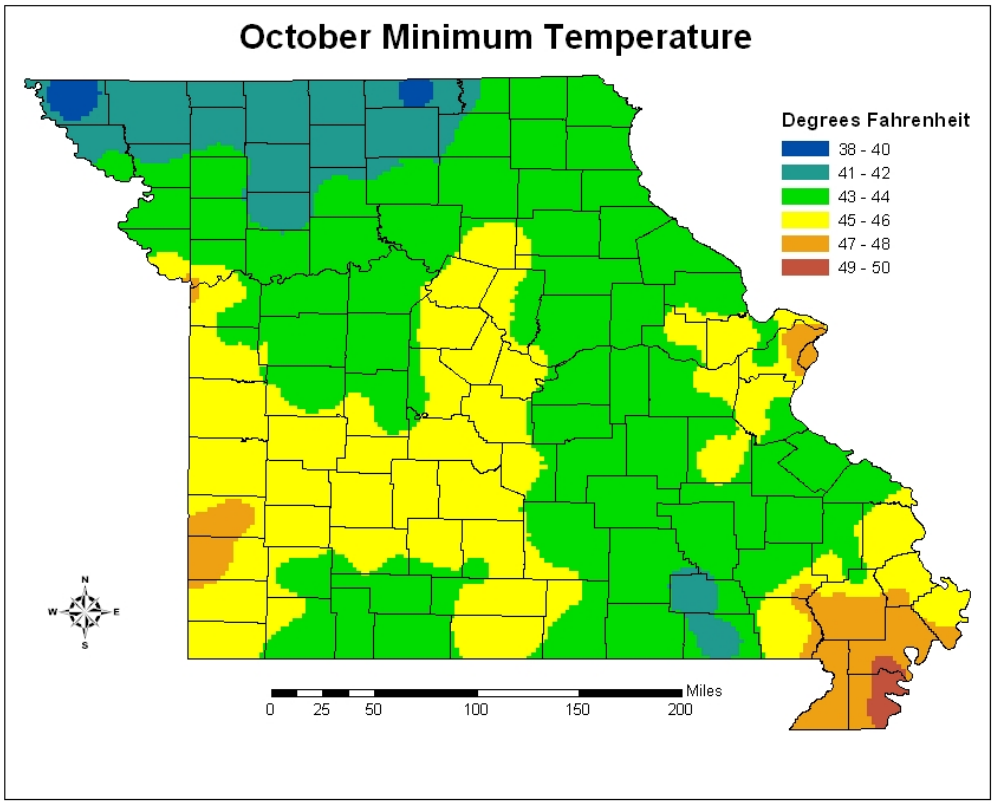

Figure 115: Normal minimum October temperature.

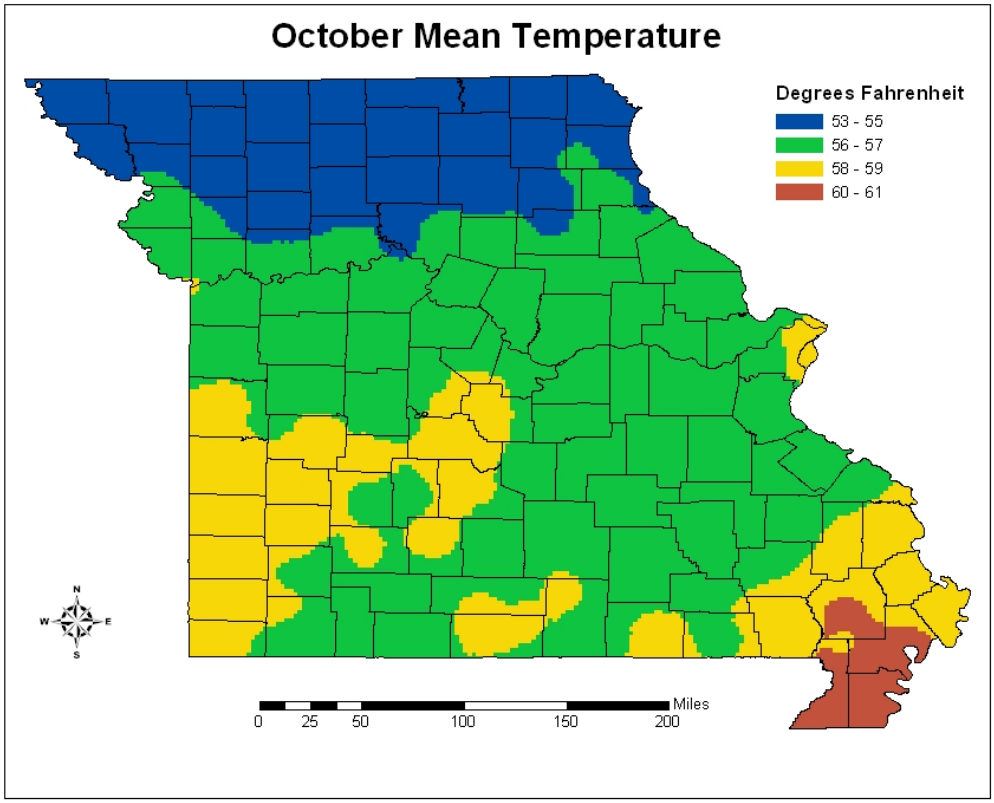

Figure 116: Normal mean October temperature.

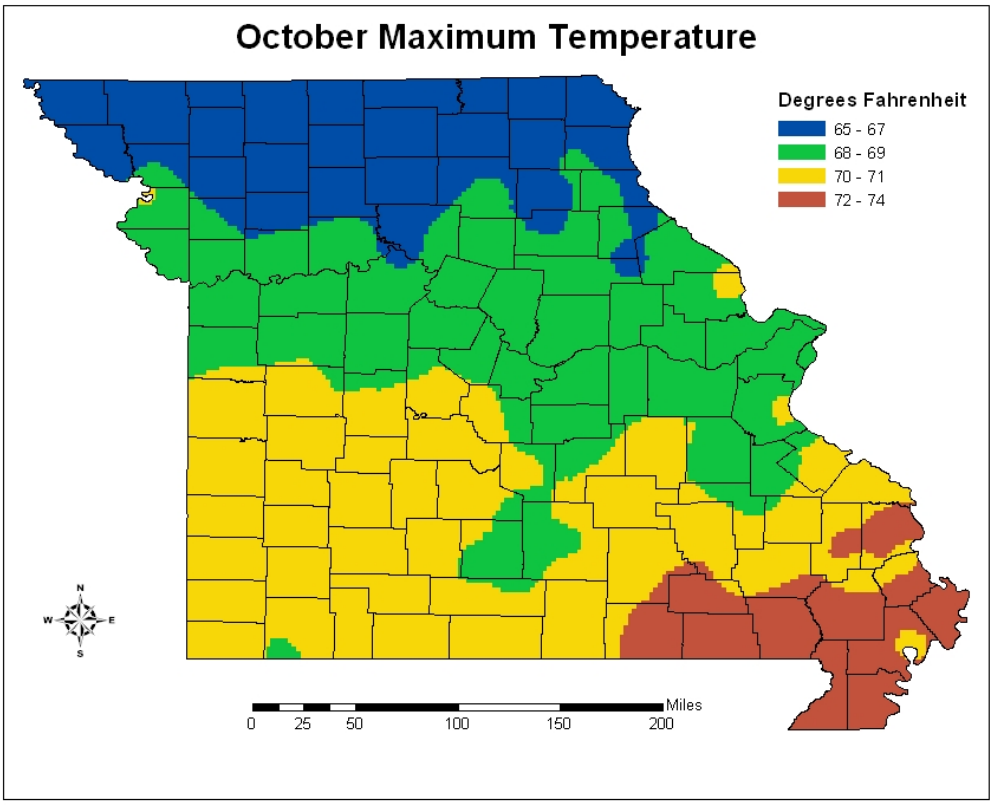

Figure 117: Normal maximum October temperature.

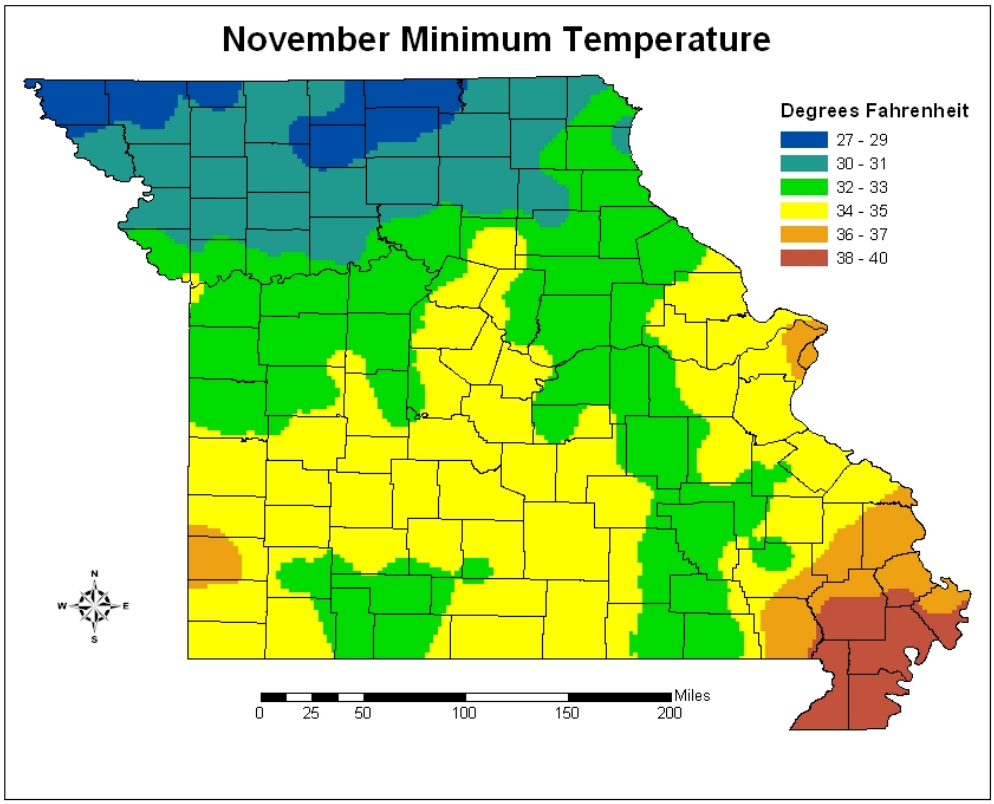

Figure 118: Normal minimum October temperature.

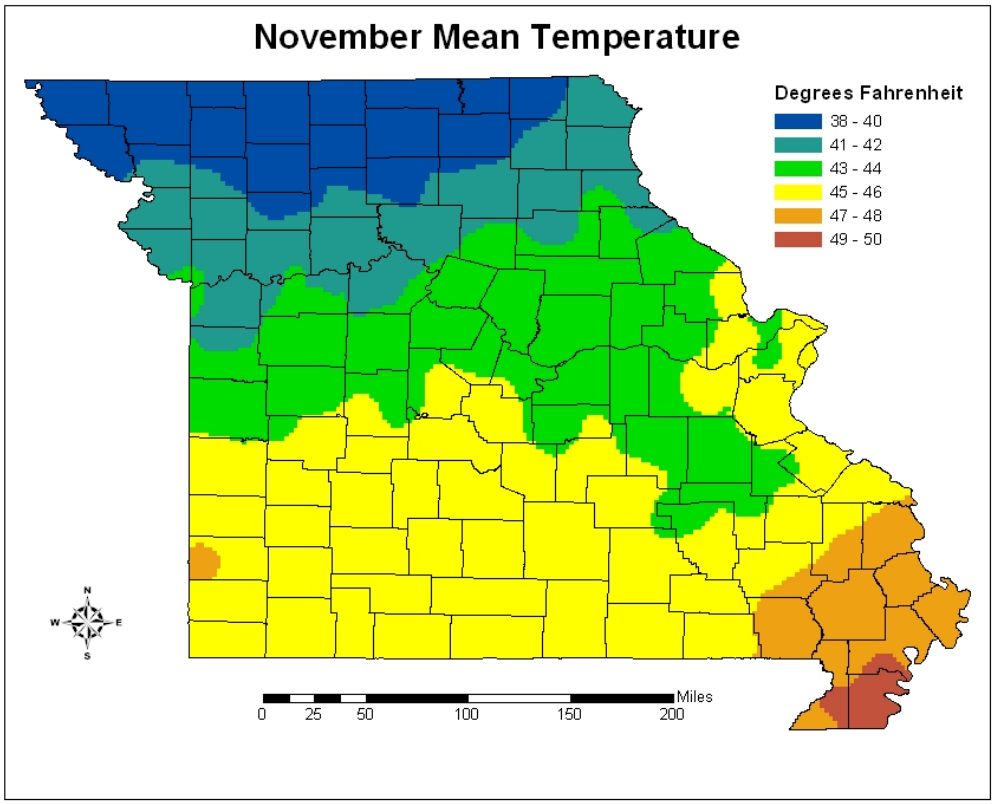

Figure 119: Normal mean November temperature.

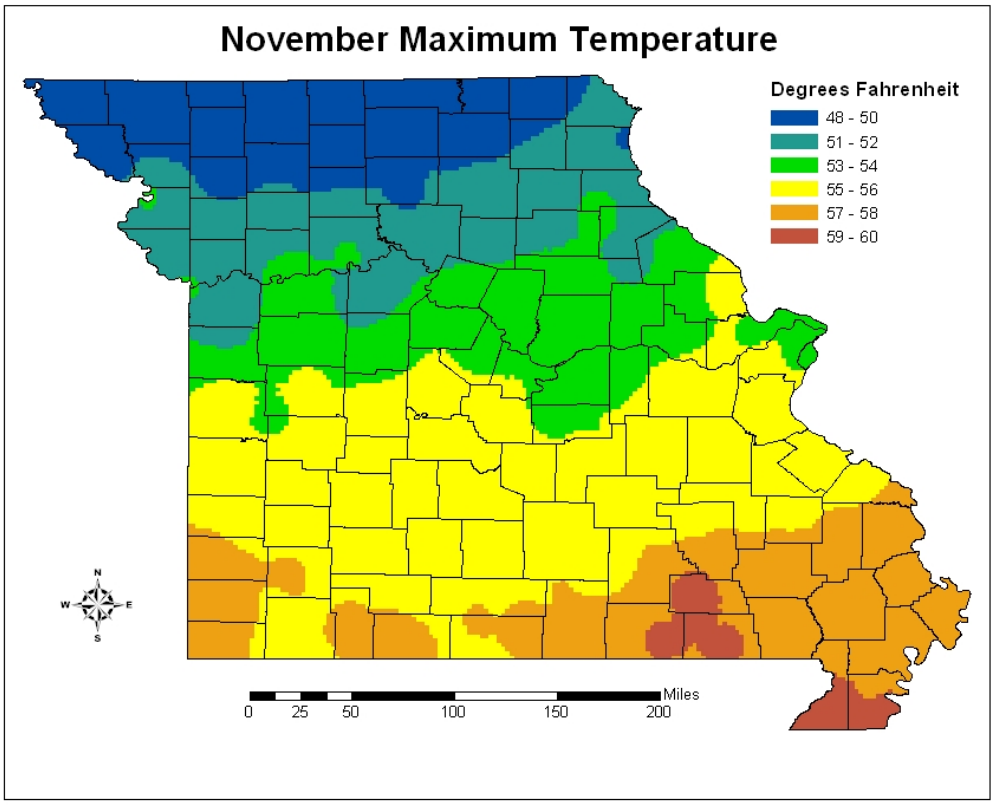

Figure 120: Normal maximum November temperature.

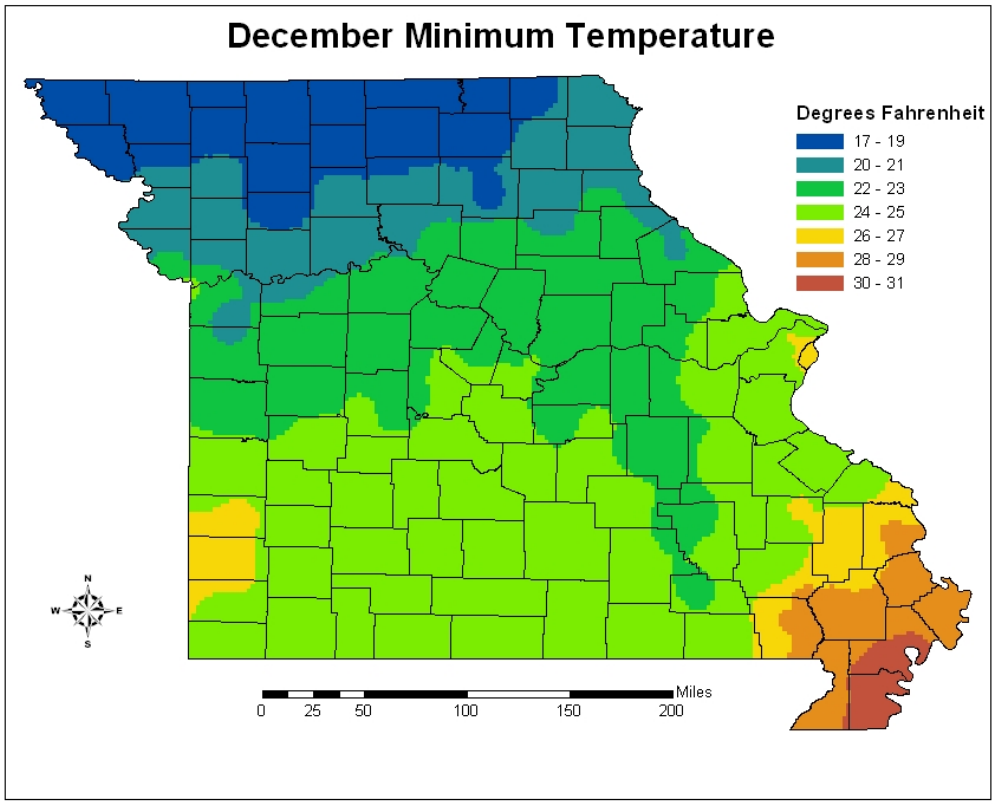

Figure 121: Normal minimum December temperature.

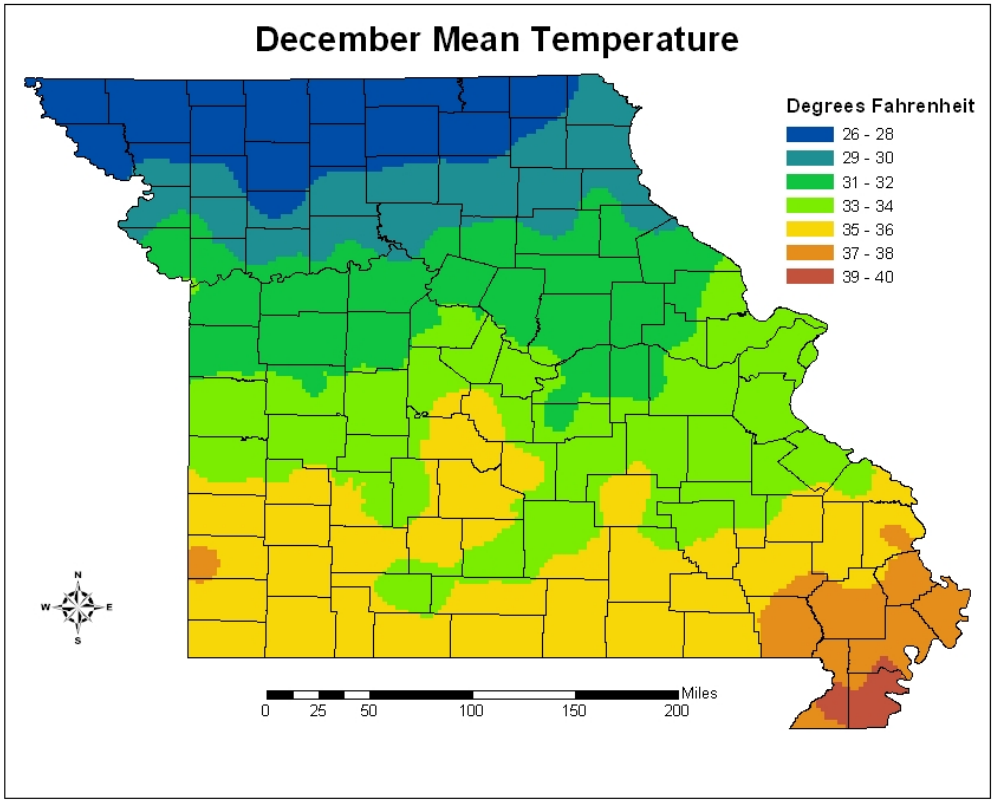

Figure 122: Normal mean December temperature.

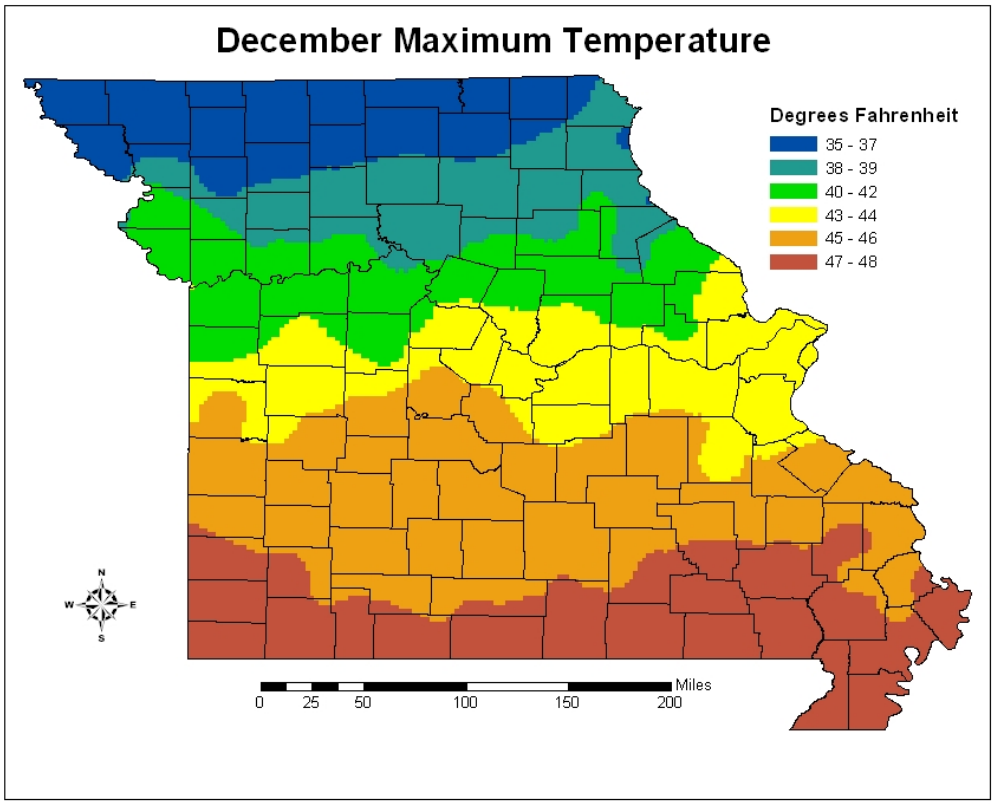

Figure 123: Normal maximum December temperature.

3.2: Cold temperature statistics

Cold temperature refers to subfreezing temperatures, which have direct effects on engineering construction as well as on agricultural crops. Two major parameters measuring the frost-free period in a year, the latest ending and earliest beginning dates of frost-free period during the 30 years are shown in the following two figures. They show that the plateau areas in the south central section of the state have the longest period with possible subfreezing temperatures.

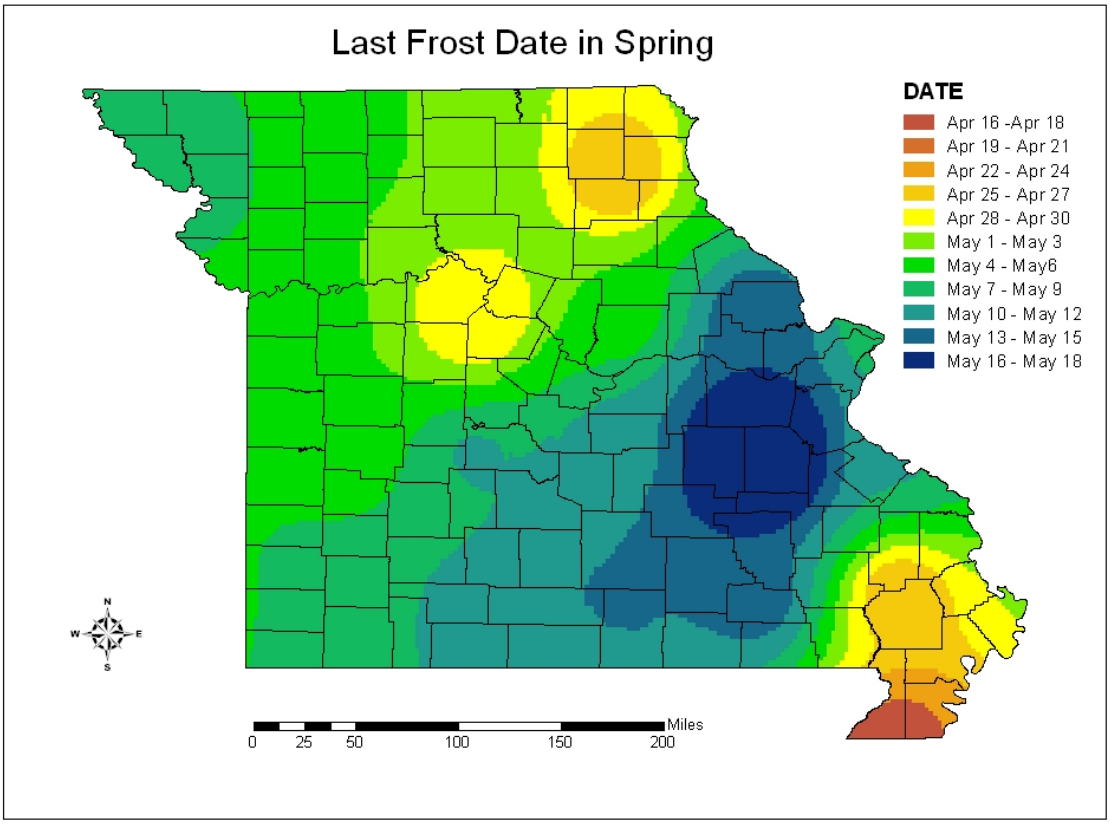

Figure 124: Latest ending dates of frost-free period during 1971-2000.

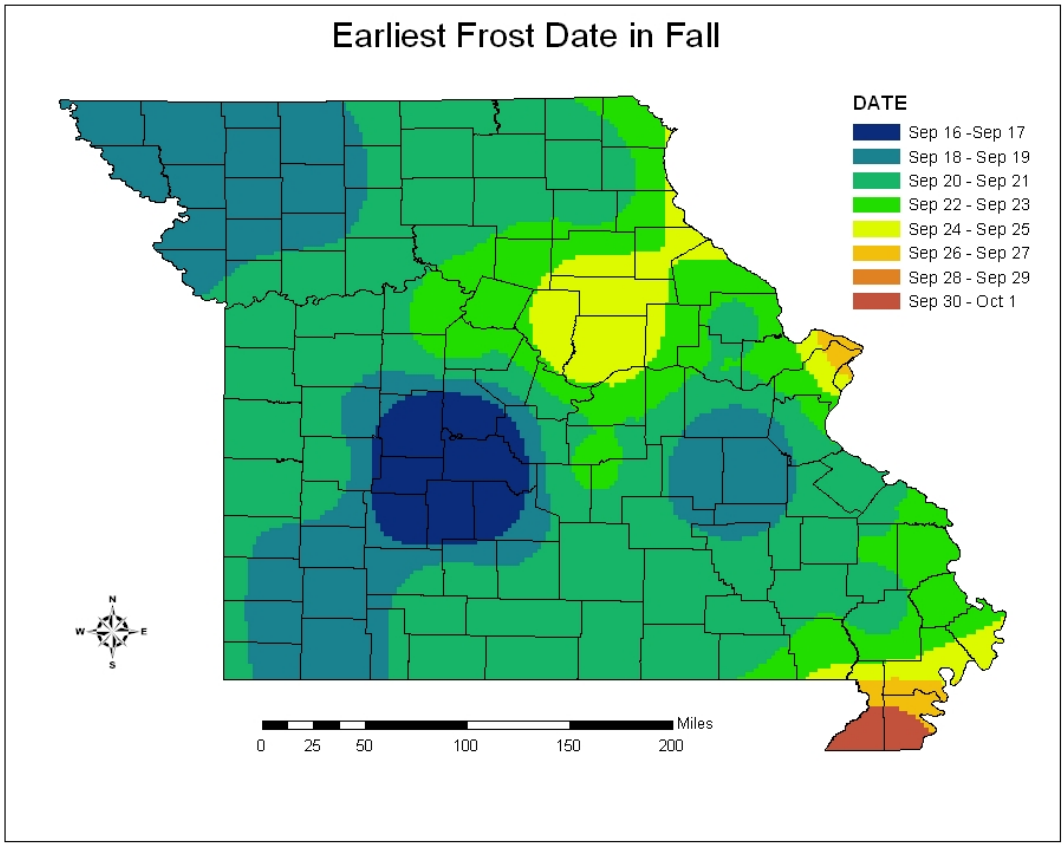

Figure 125: Earliest beginning dates of frost-free period during 1971-2000.

3.3: Probabilities of extremely cold temperatures

Several statistical indicators of frequency and intensity of cold temperatures are shown in the following.

a) Average number of days in a year with minimum temperature at or below 32ºF

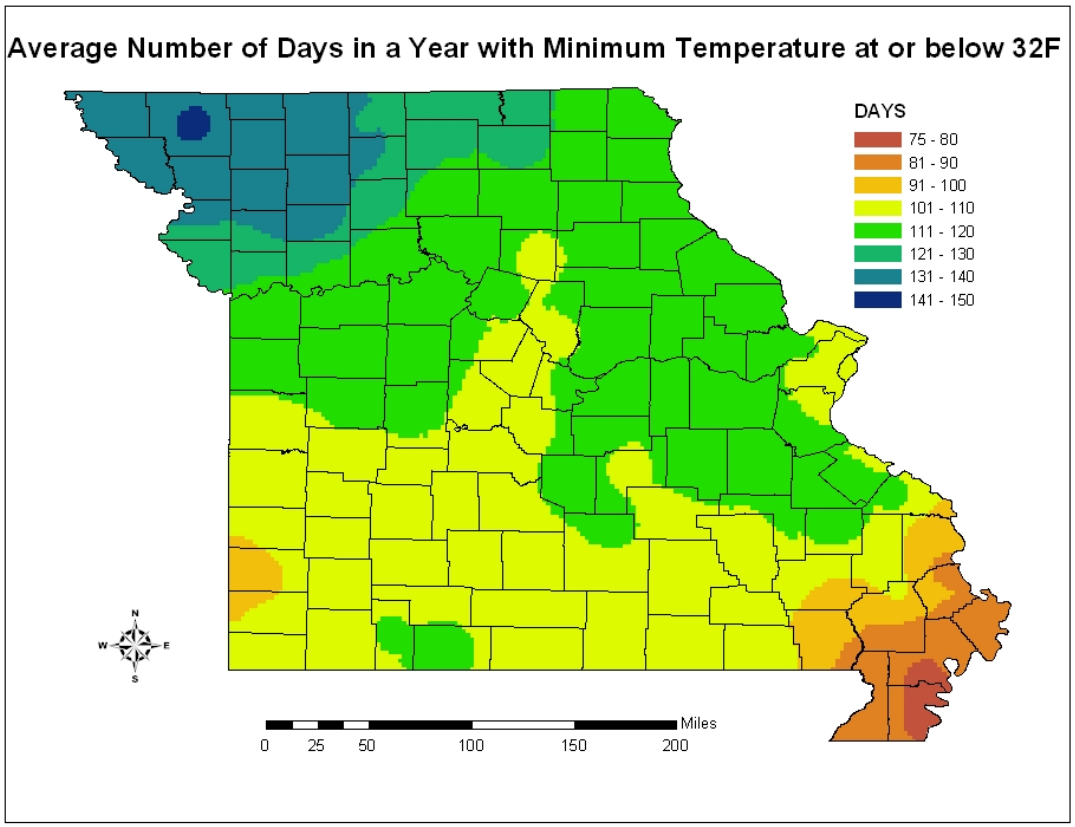

Figure 126: Average number of days in a year with minimum temperature at or below 32ºF.

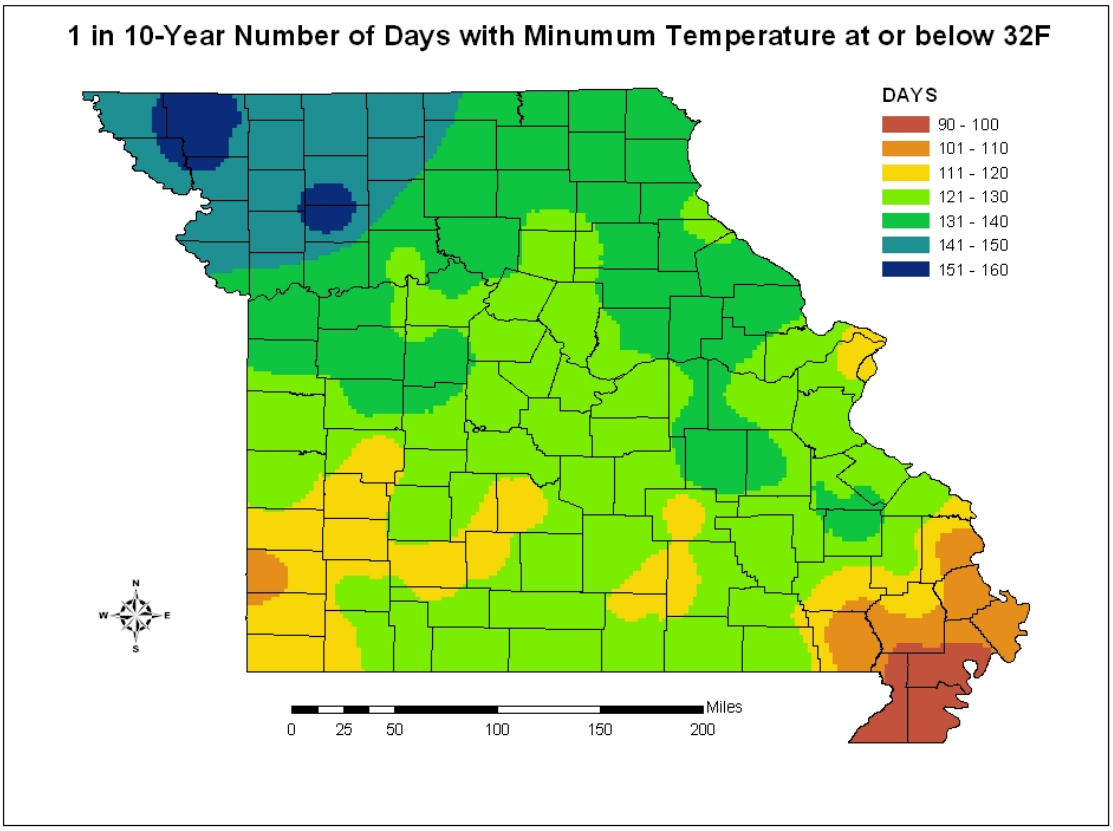

Figure 127: 1 in 10-year number of days in a year with minimum temperature at or below 32ºF.

b) Coldest temperatures in the months of autumn, winter, and spring

Both coldest average temperature and the minimum temperature of the month are shown to describe the probabilities for the monthly average coldness and extremely cold conditions.

i) Coldest monthly average temperatures

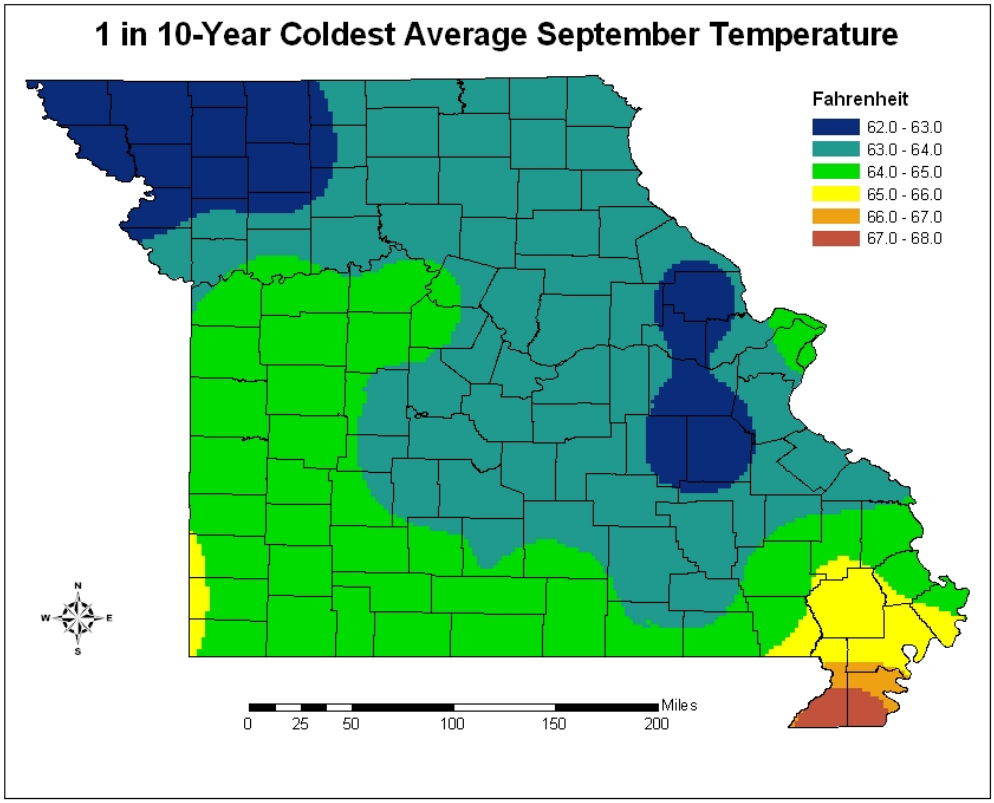

Figure 128: 1 in 10-year coldest September average temperature.

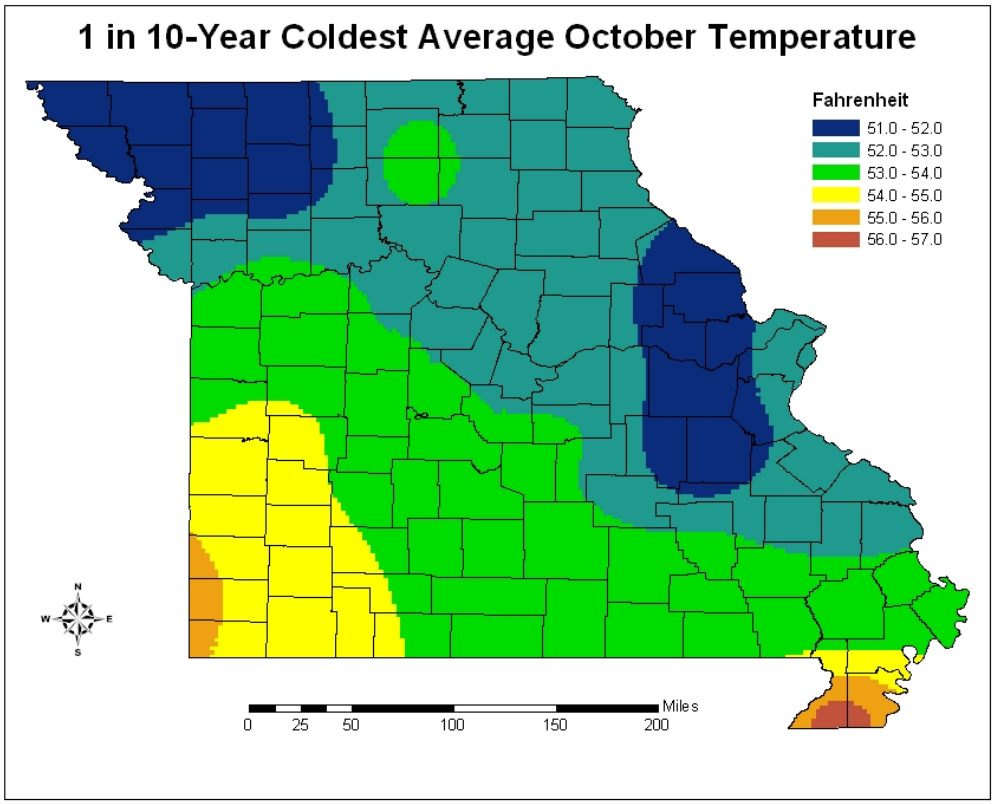

Figure 129: 1 in 10-year coldest October average temperature.

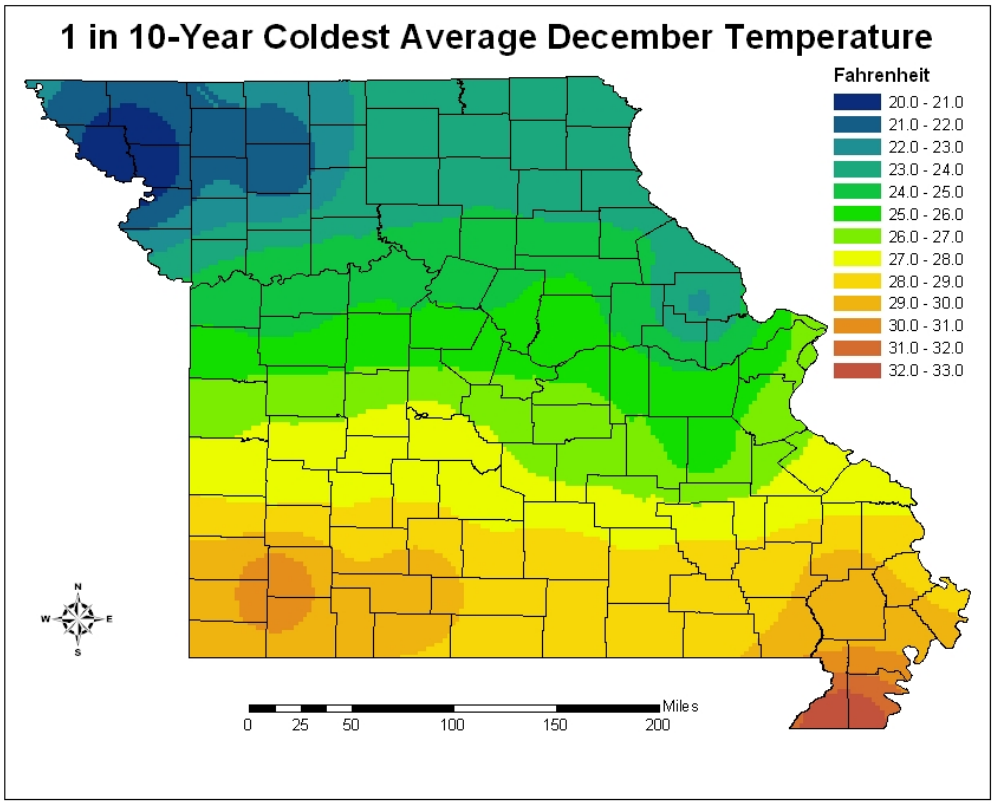

Figure 130: 1 in 10-year coldest December average temperature.

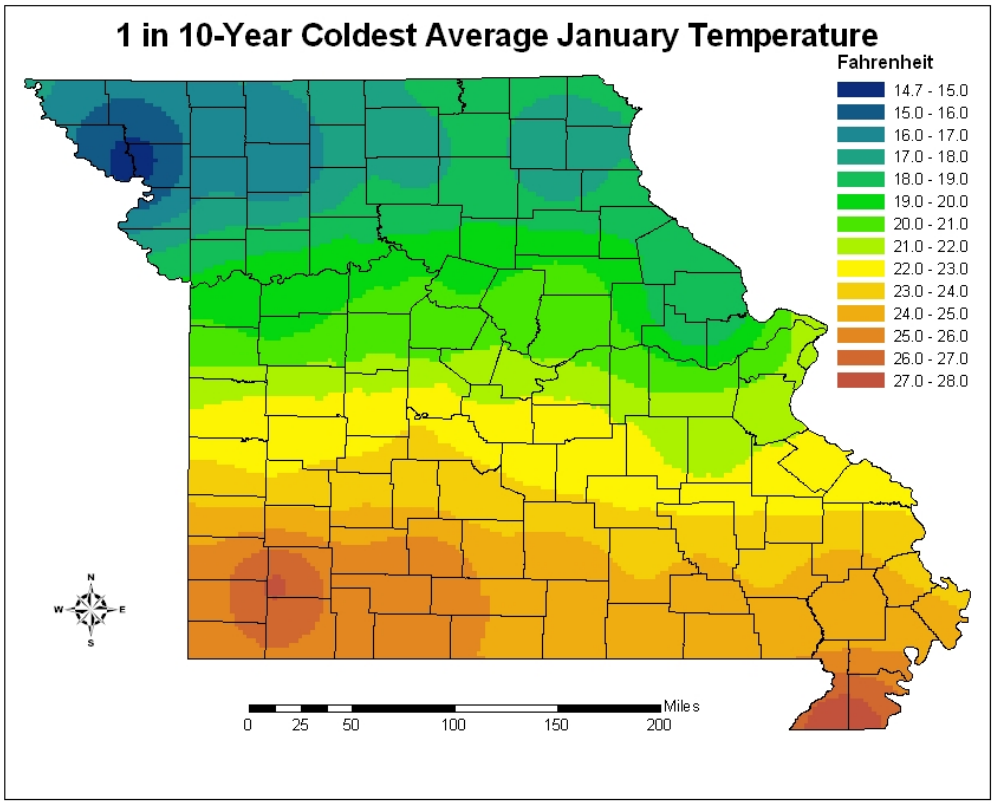

Figure 131: 1 in 10-year coldest January average temperature.

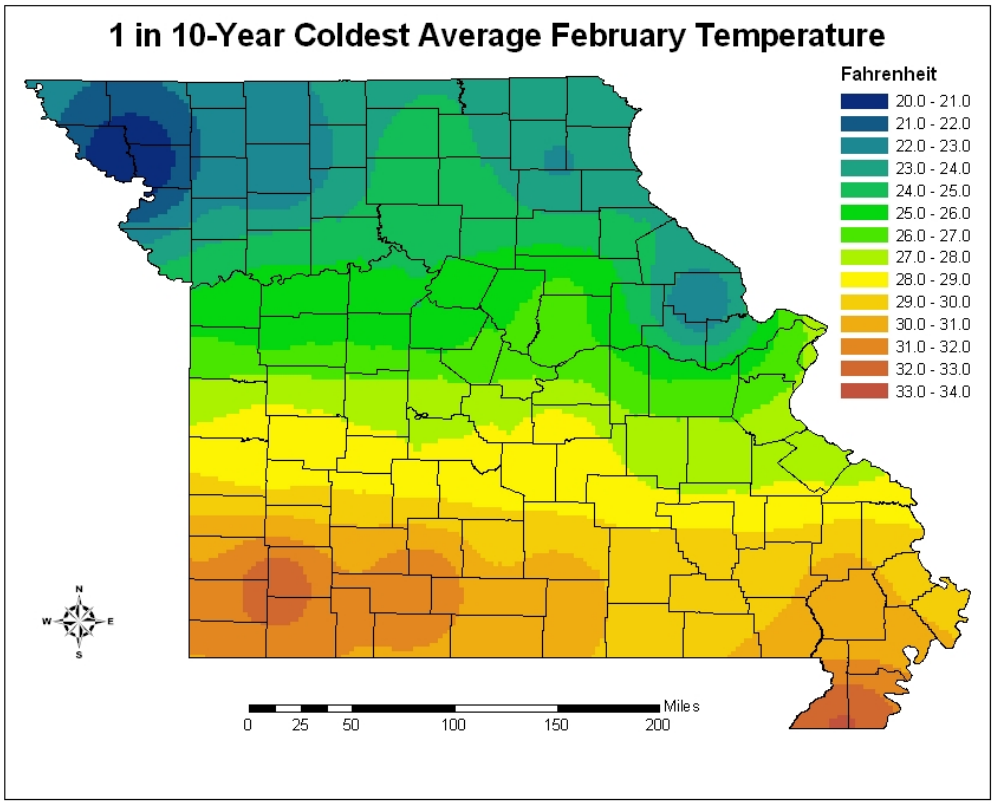

Figure 132: 1 in 10-year coldest February average temperature.

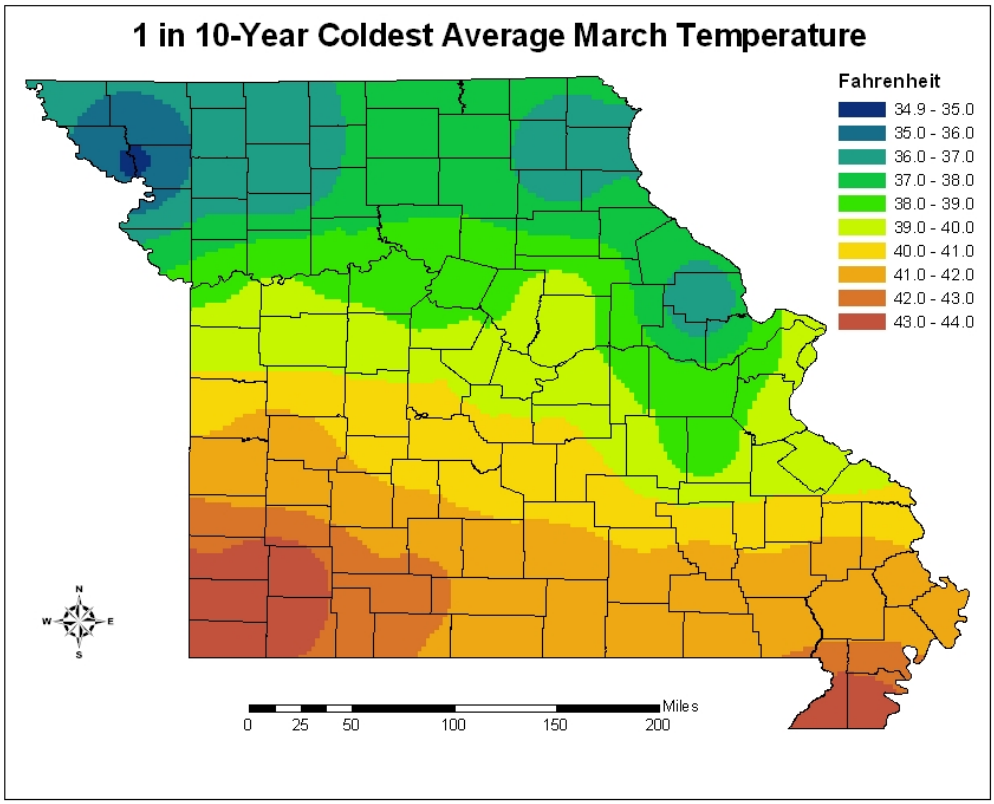

Figure 133: 1 in 10-year coldest March average temperature.

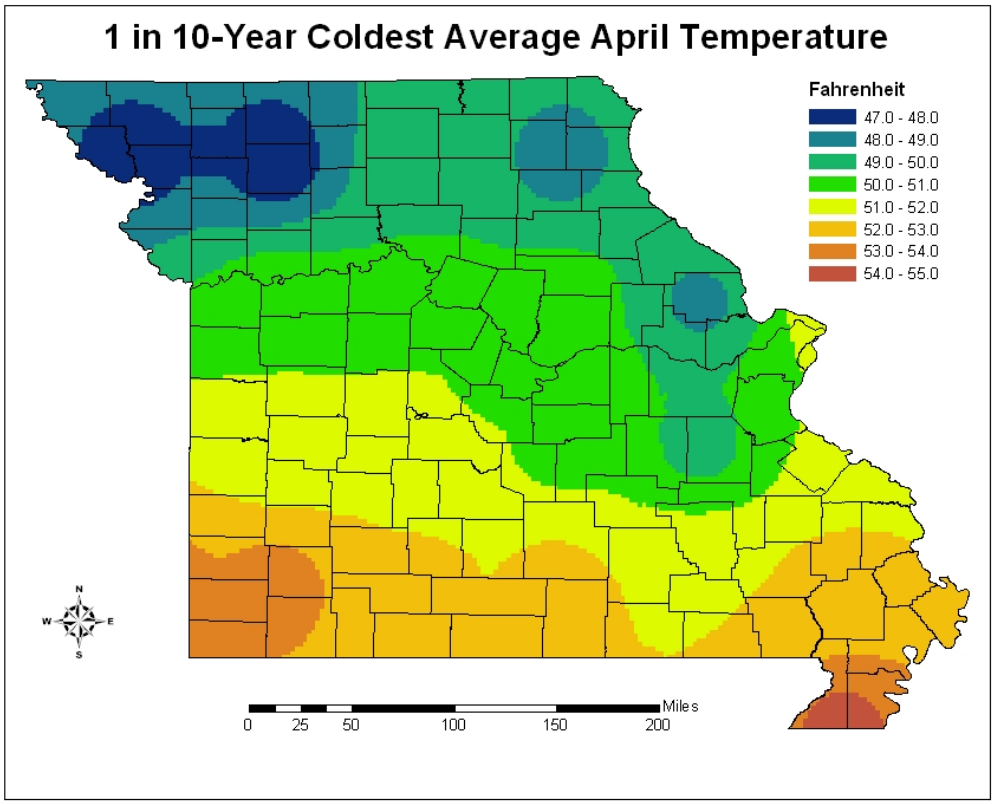

Figure 134: 1 in 10-year coldest April average temperature.

ii) Coldest monthly minimum temperatures

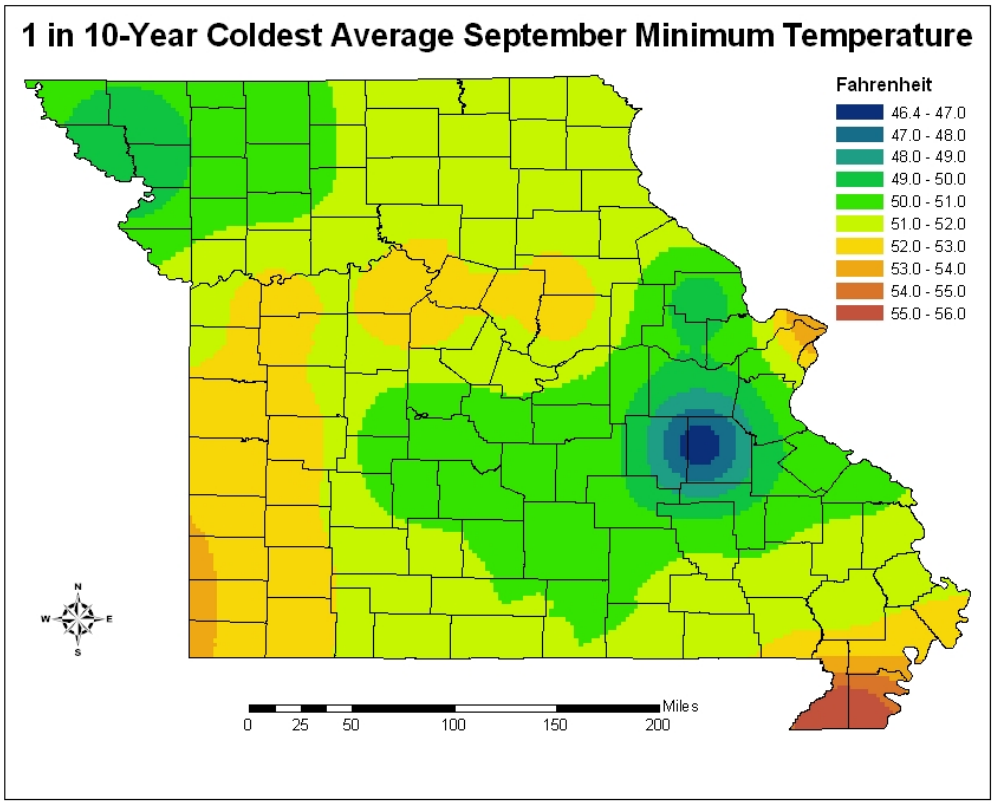

Figure 135: 1 in 10-year coldest minimum September temperature.

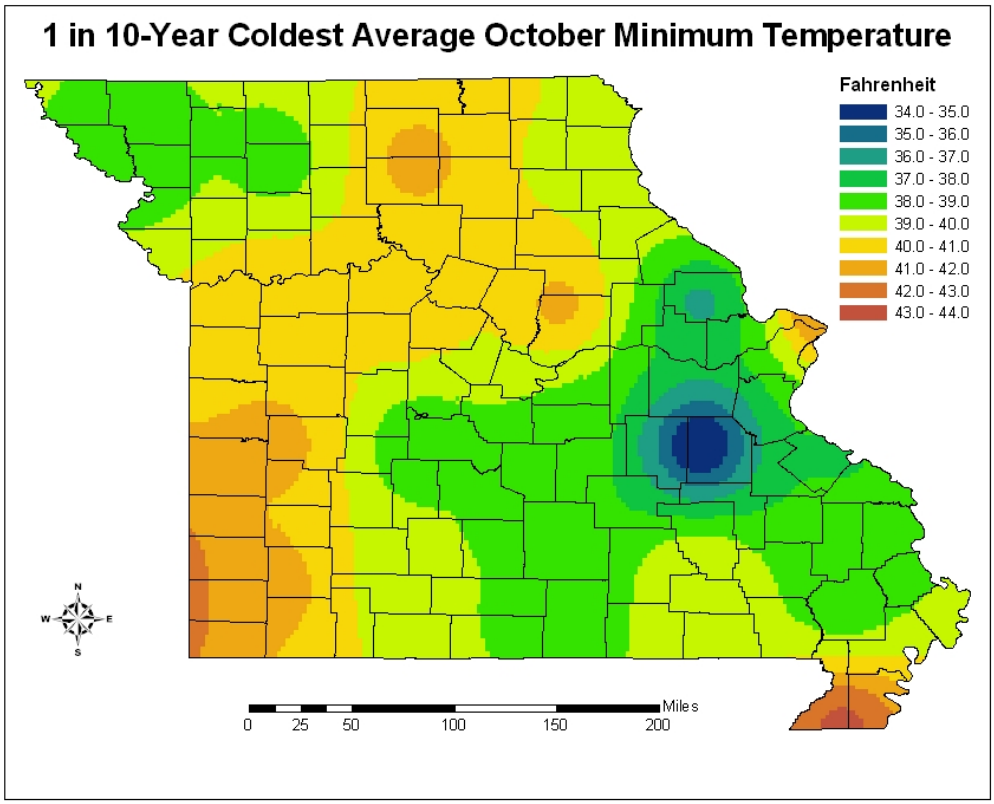

Figure 136: 1 in 10-year coldest minimum October temperature.

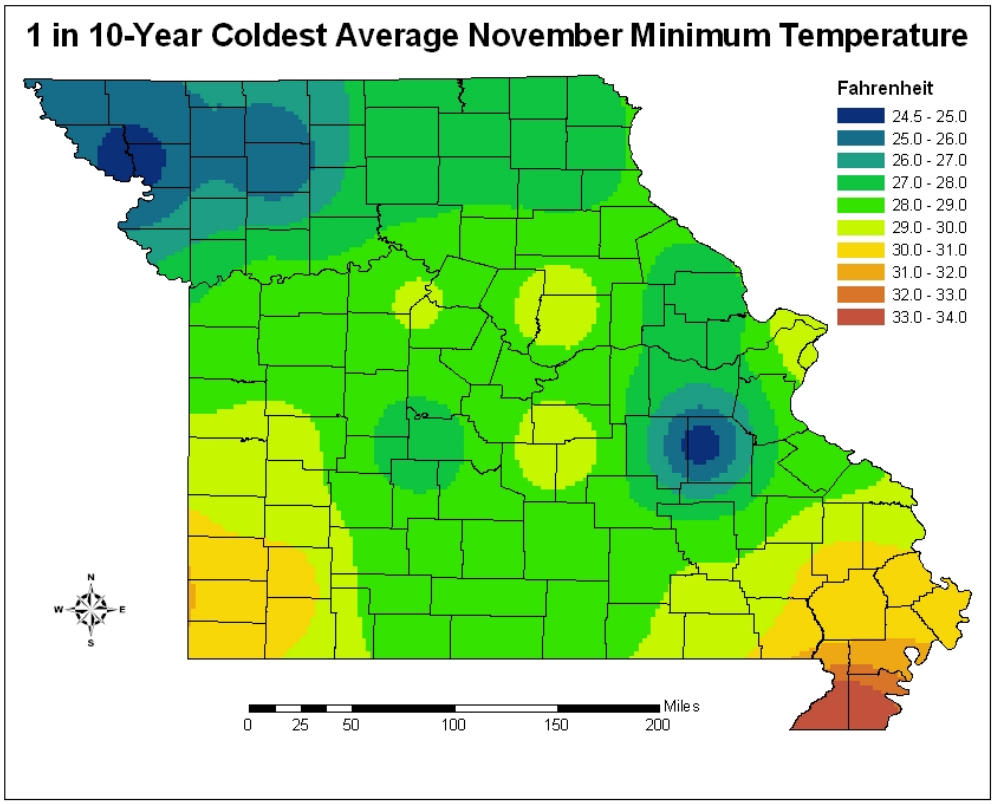

Figure 137: 1 in 10-year coldest minimum November temperature.

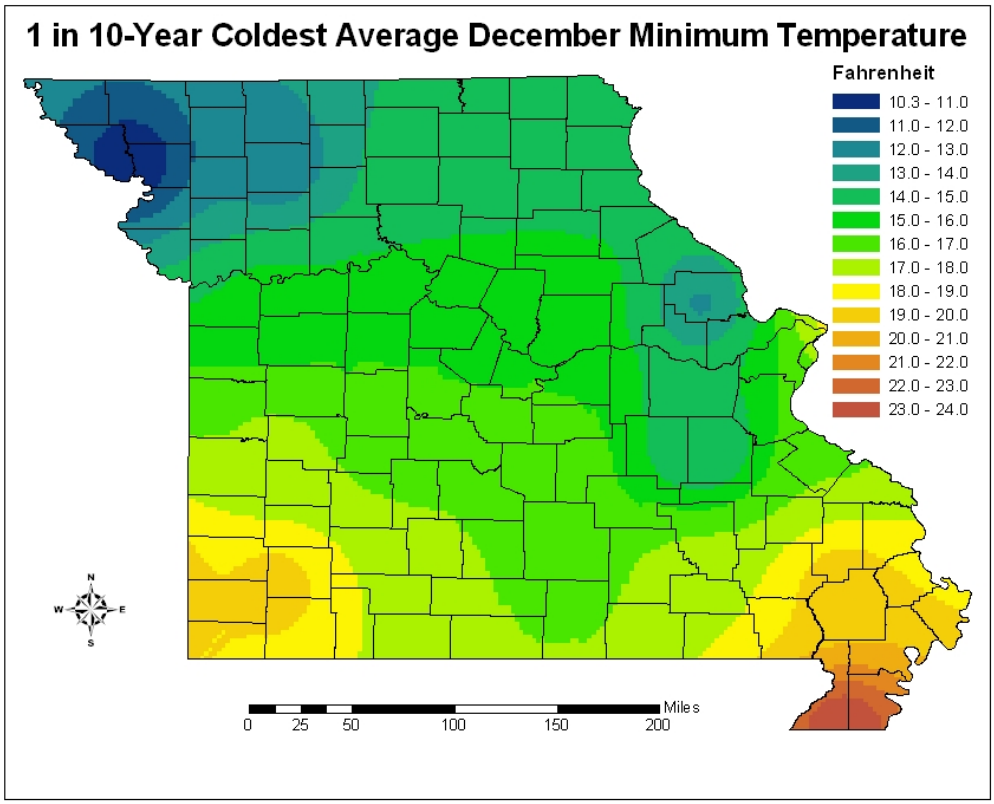

Figure 138: 1 in 10-year coldest minimum December temperature.

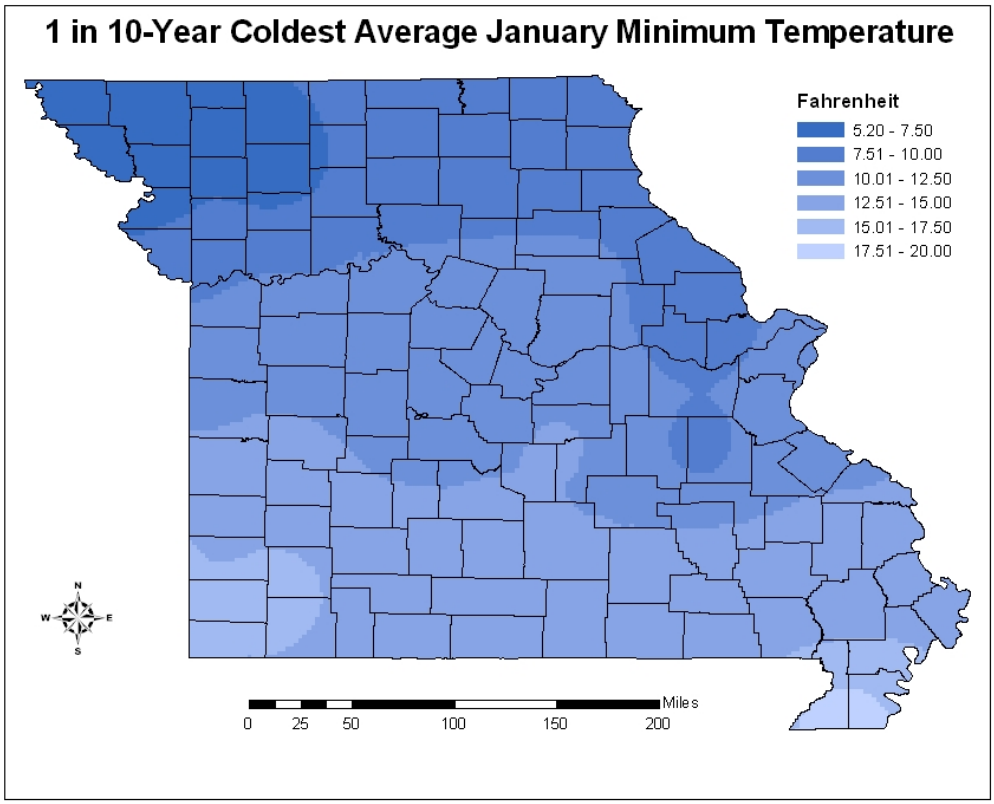

Figure 139: 1 in 10-year coldest minimum January temperature.

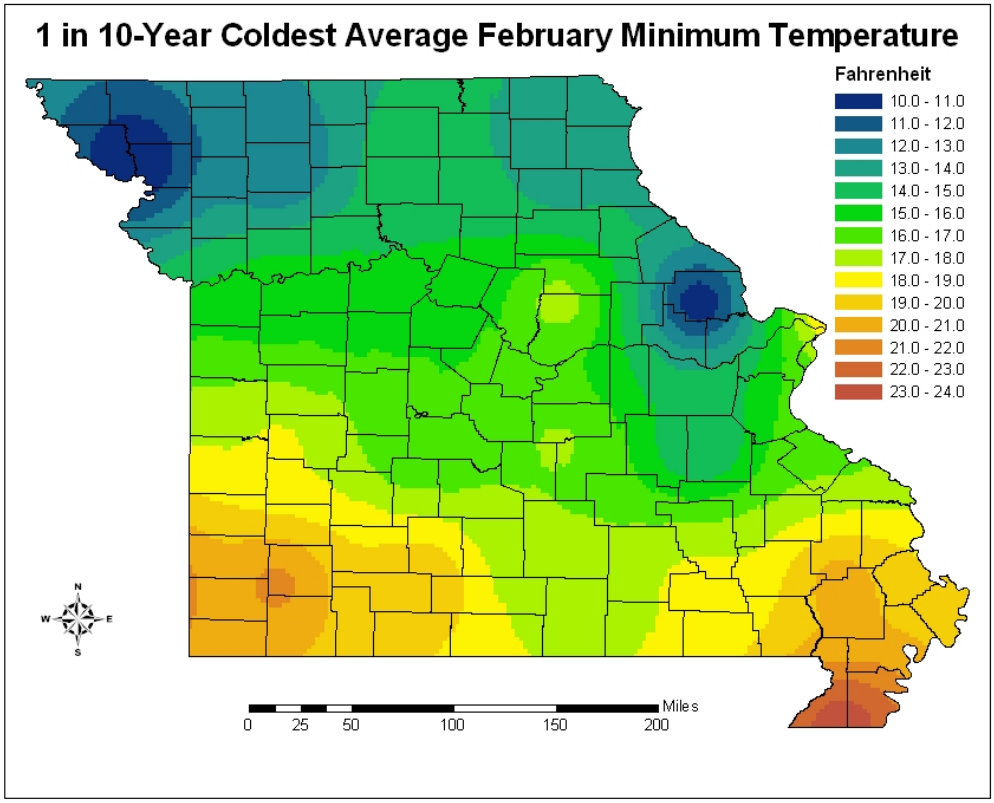

Figure 140: 1 in 10-year coldest minimum February temperature.

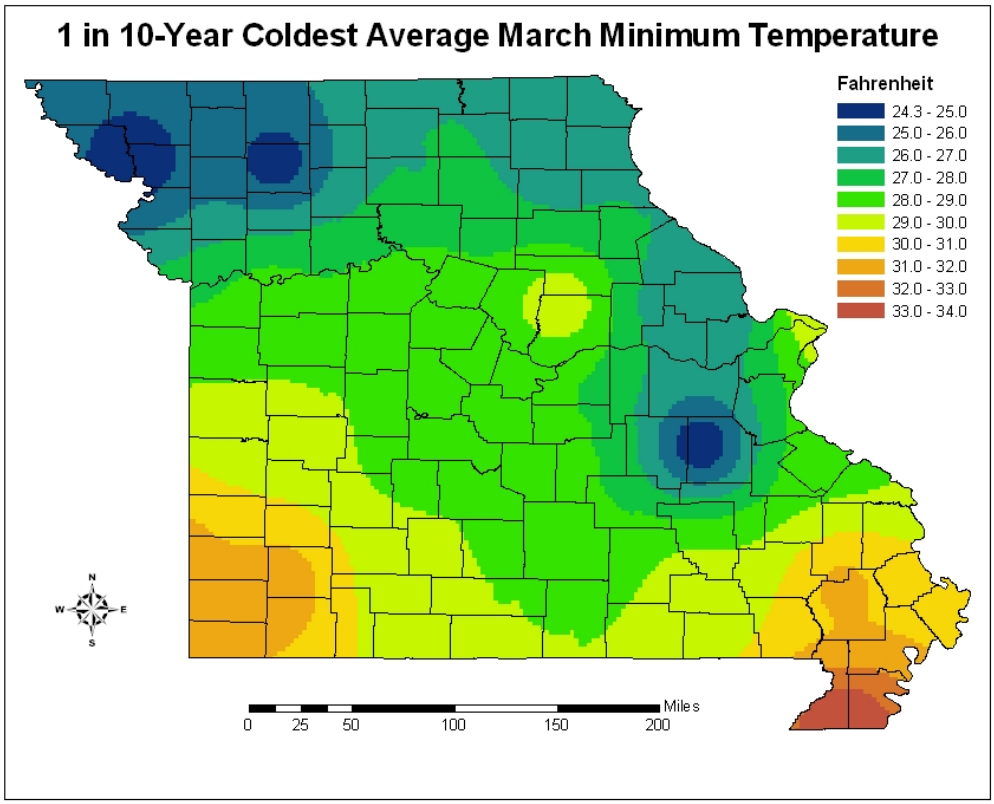

Figure 141: 1 in 10-year coldest minimum March temperature.

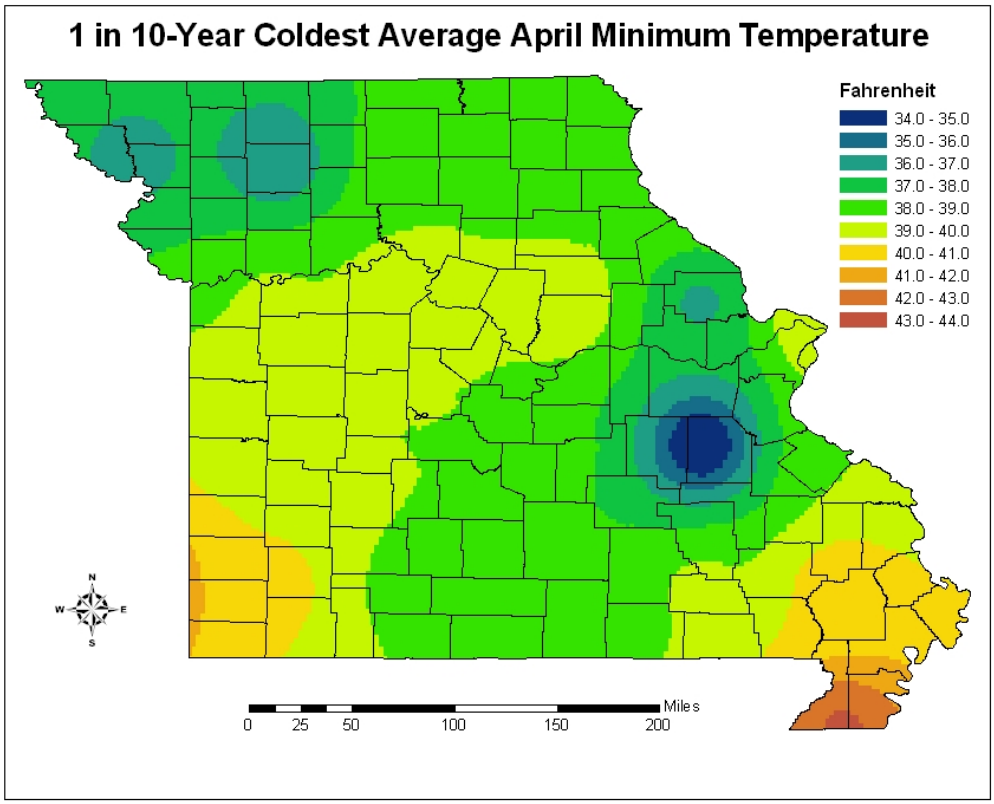

Figure 142: 1 in 10-year coldest minimum April temperature.

4. Surface runoff

Methods used to calculate the annual mean surface runoff and probabilities of minimum and maximum annual surface runoff are detailed in Appendix B section 2. The runoff is presented in Figs. 144 to 151 in terms of percentage of the annual mean surface runoff shown in Fig. 143. Thus, an actual runoff amount at a location can be calculated from multiplying the percentage by the mean annual runoff value at that location.

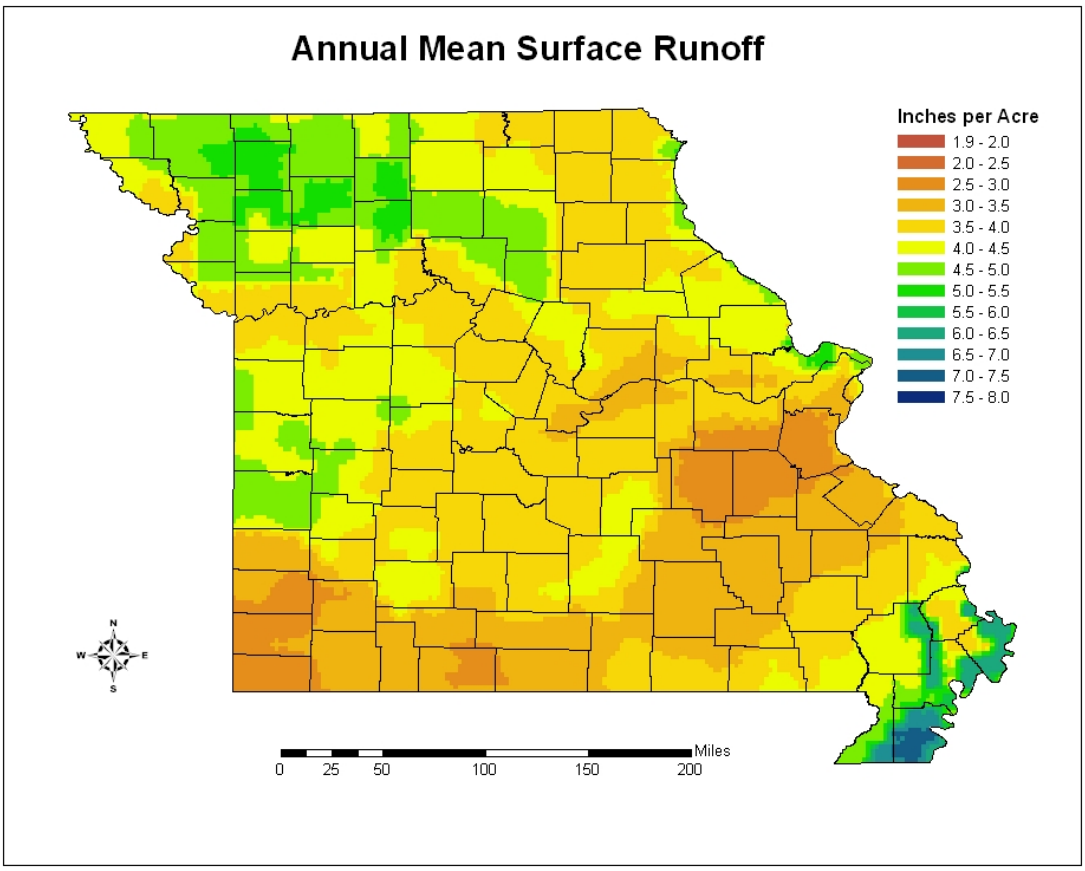

Figure 143: Annual mean surface runoff.

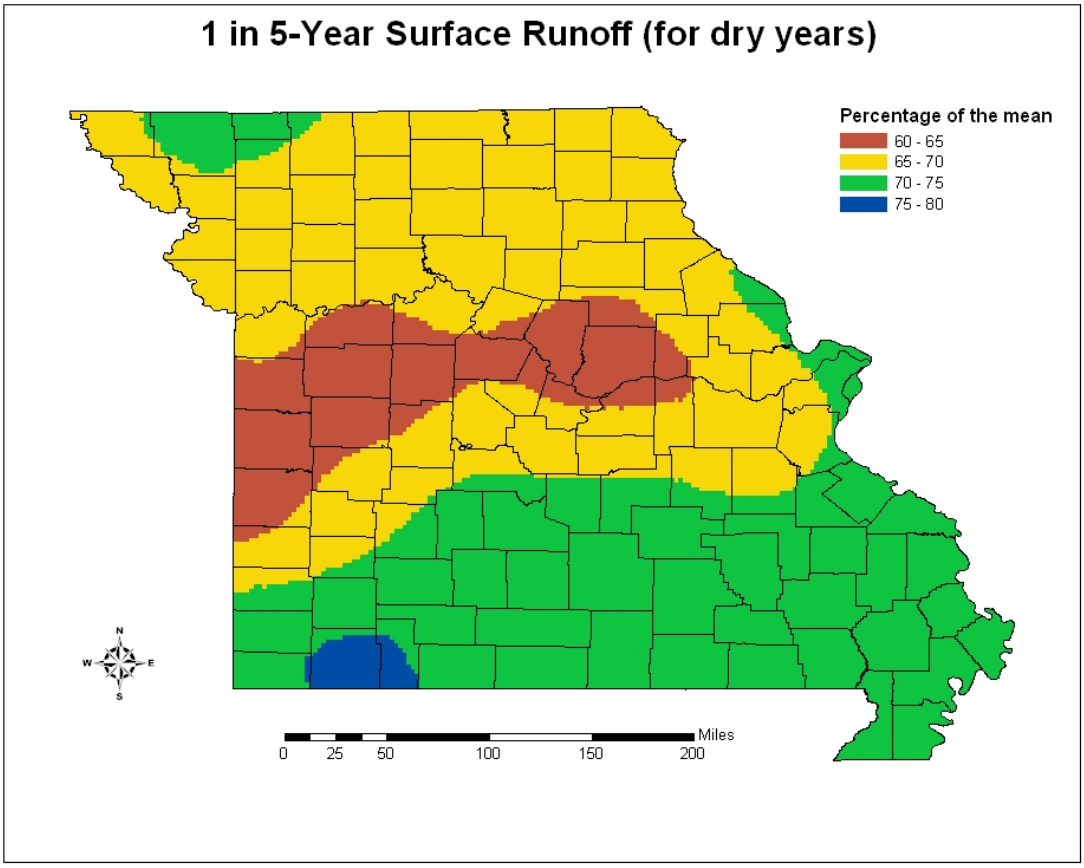

Figure 144: 1 in 5-year surface runoff for dry years.

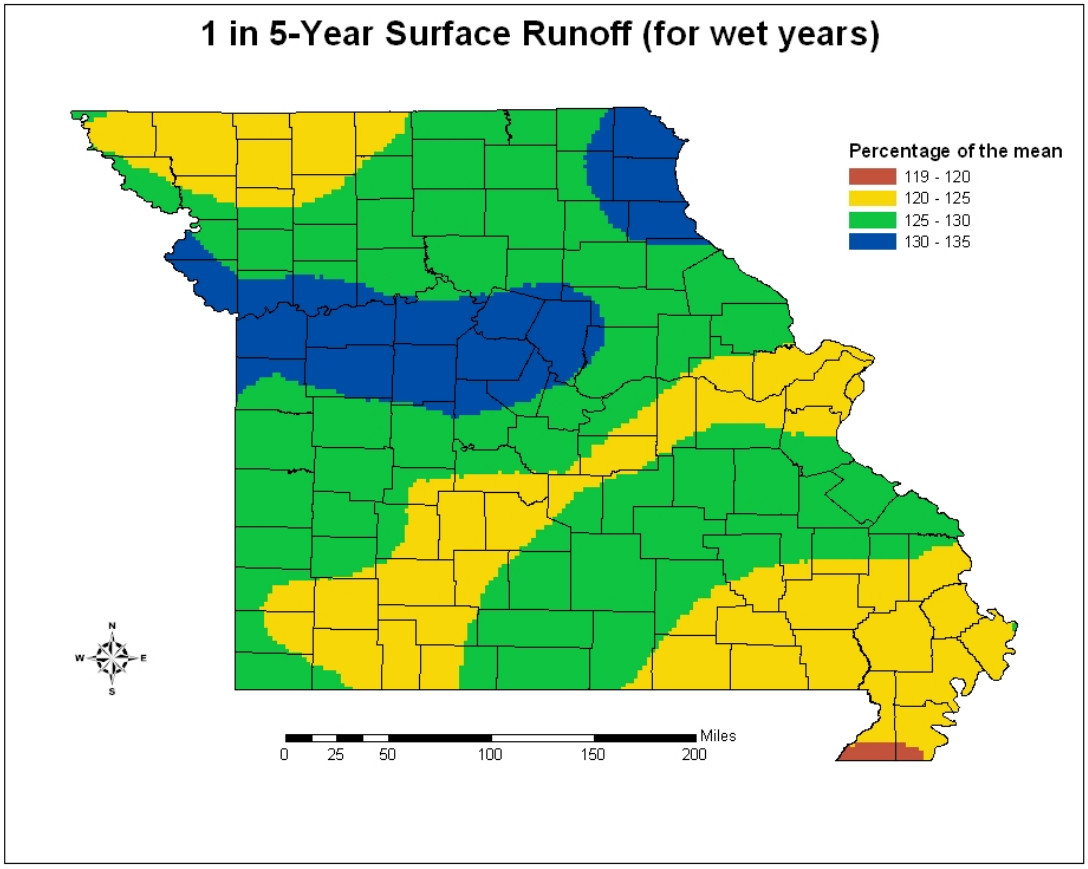

Figure 145: 1 in 5-year surface runoff for wet years.

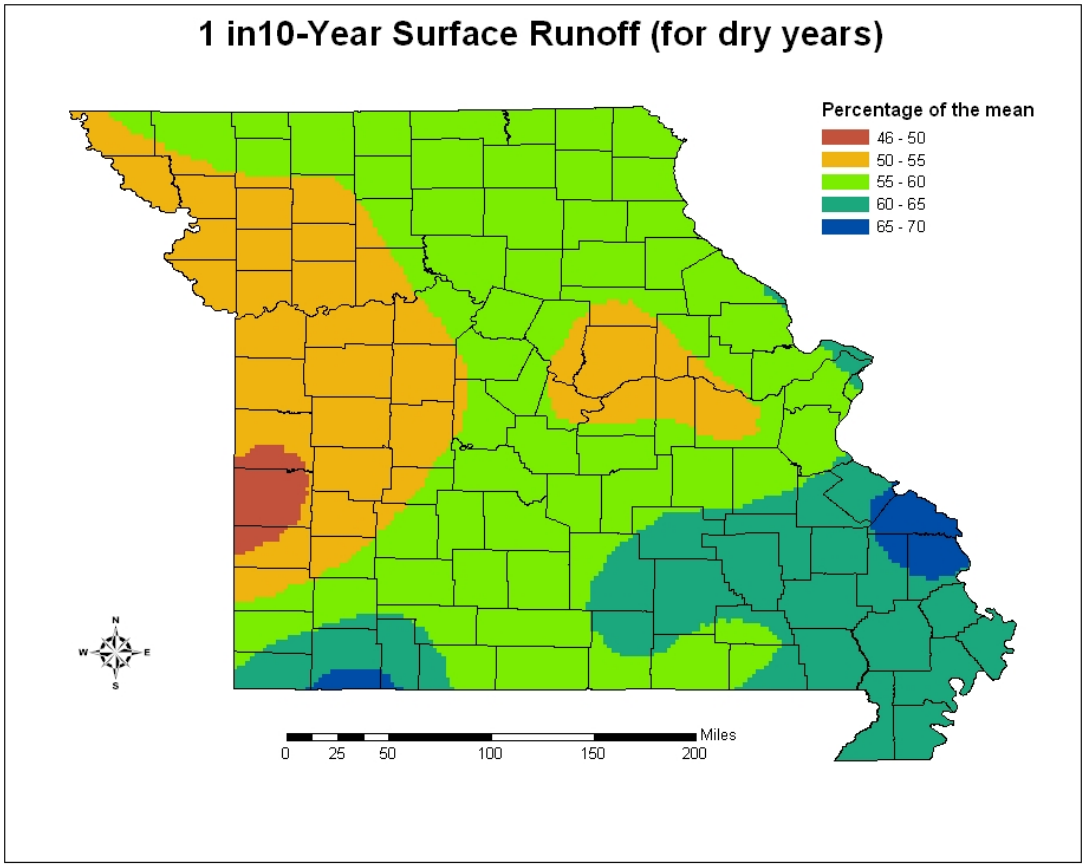

Figure 146: 1 in 10-year surface runoff for dry years.

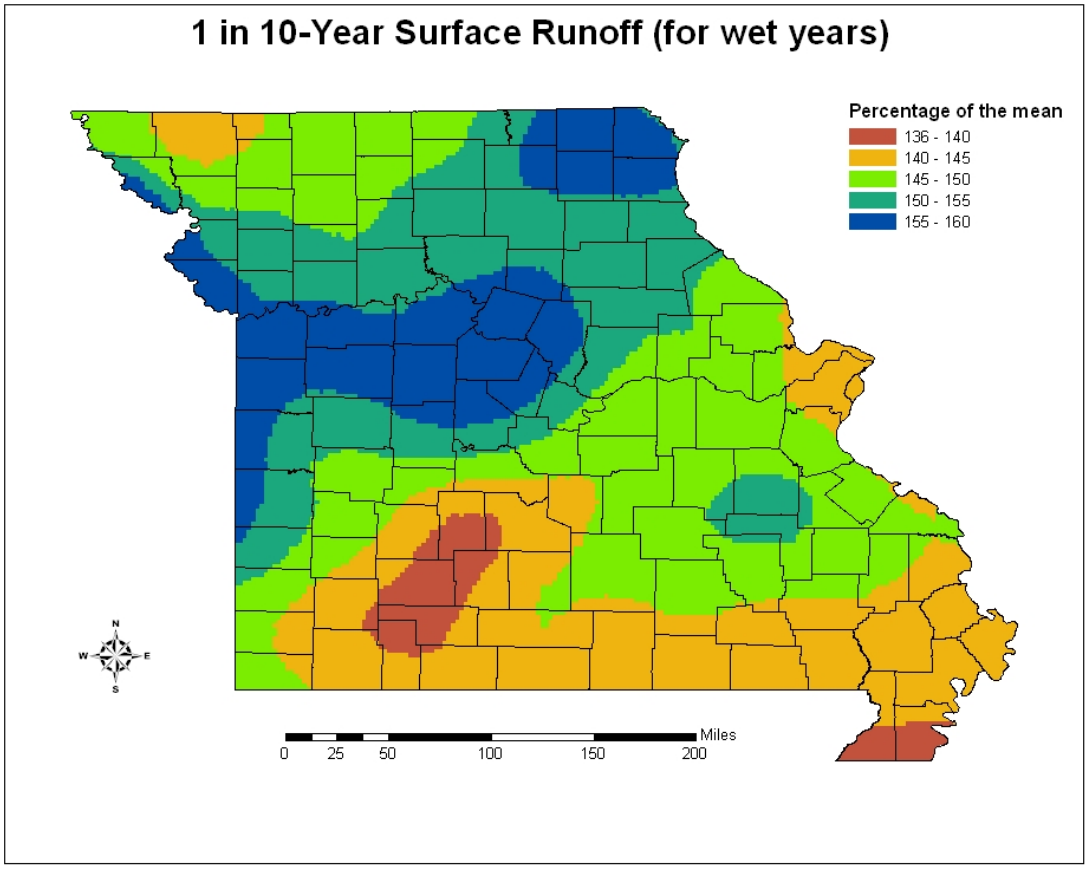

Figure 147: 1 in 10-year surface runoff for wet years.

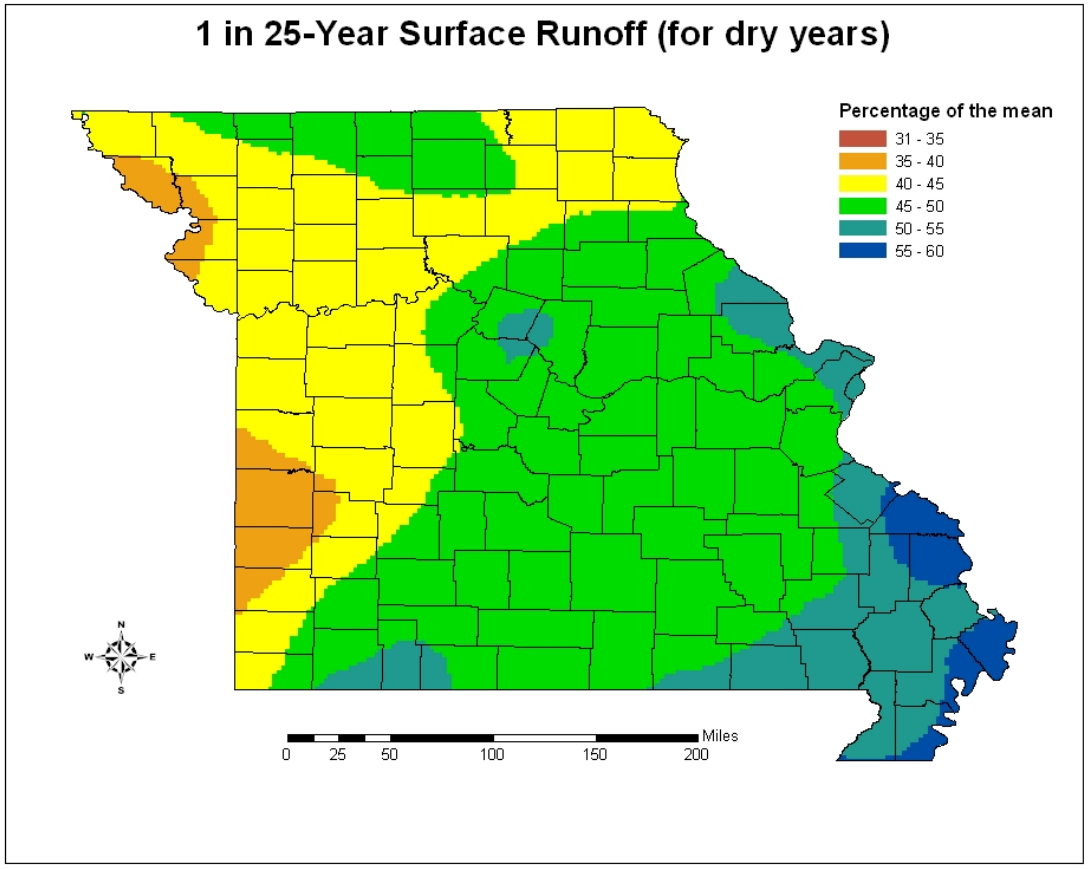

Figure 148: 1 in 25-year surface runoff for dry years.

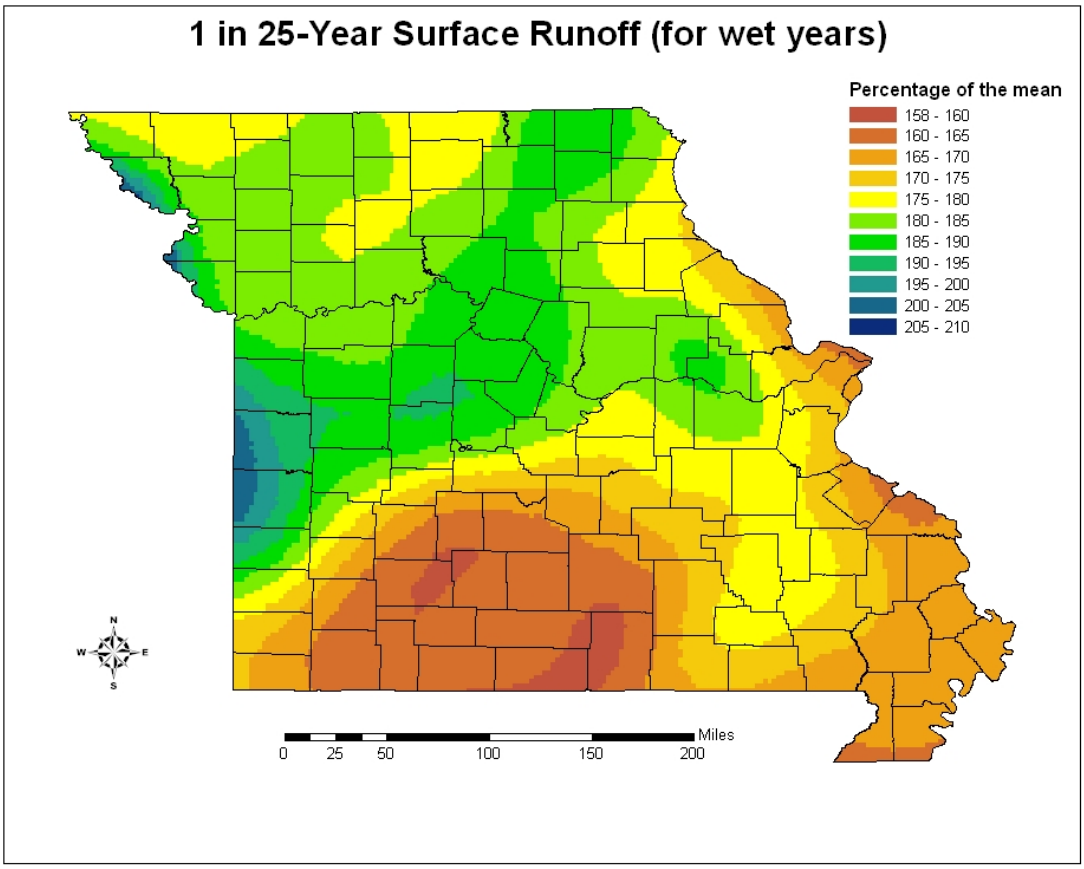

Figure 149: 1 in 25-year surface runoff for wet years.

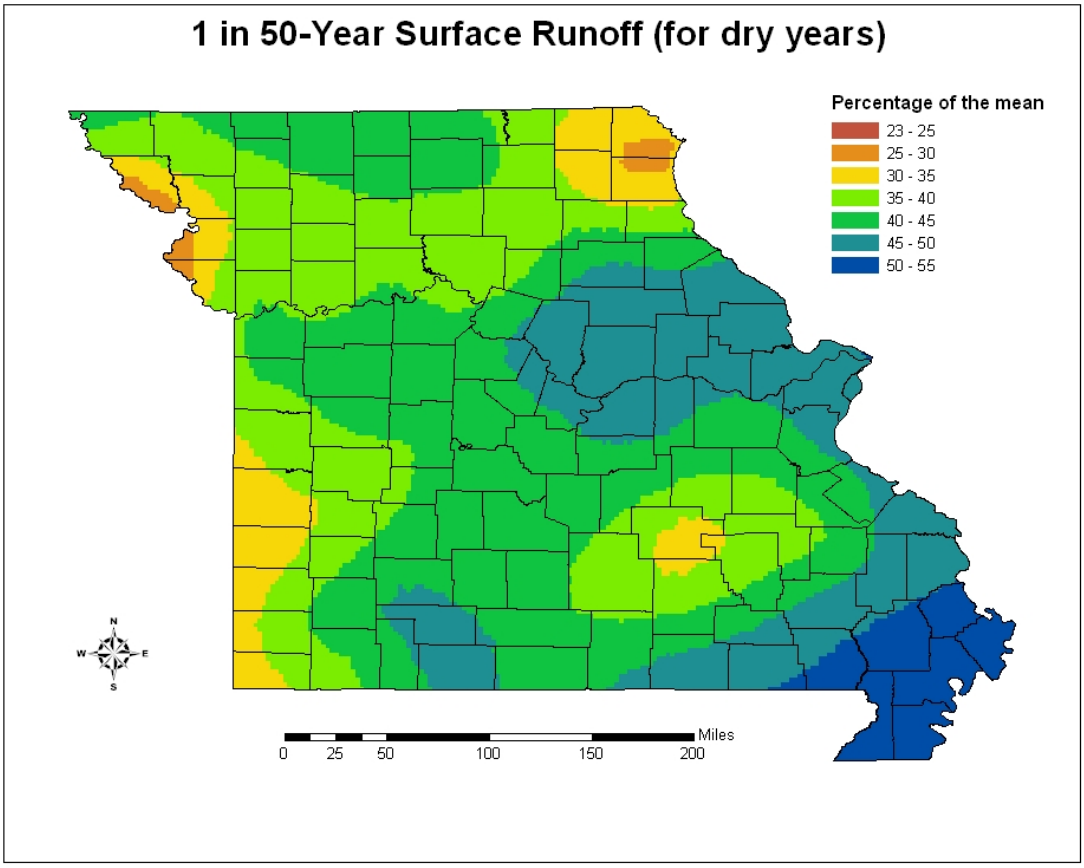

Figure 150: 1 in 50-year surface runoff for dry years.

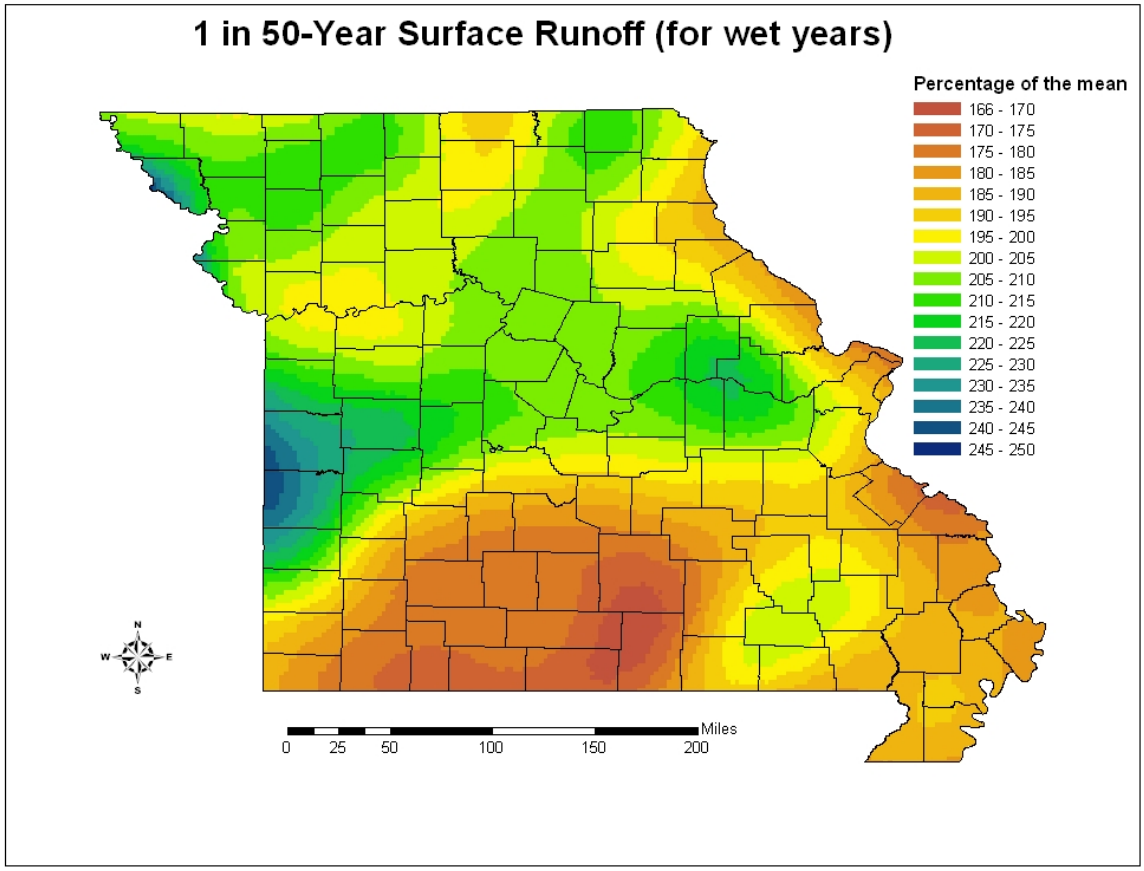

Figure 151: 1 in 50-year surface runoff for wet years.

5. Surface evaporation

There were four National Weather Service stations in Missouri measuring surface pan evaporation in different short periods during the 30 years of 1971-2000. Obviously, those observations are inadequate to describe any features of the surface evaporation across the state. Thus, the evaporation has to be calculated using other climate variables measured or calculated. The calculation methods for evaporation are detailed in Appendix B section 4. The following three figures show the free water surface evaporation and the potential evaporation at open water surface. The latter gives the possible maximum amount of water that can be evaporated from a water body under given environmental conditions.

Figure 154 shows the free water surface evaporation for the warm season, May-October. Cold season total free water surface evaporation can be computed as the difference between the warm season and the annual evaporation in Fig. 152.

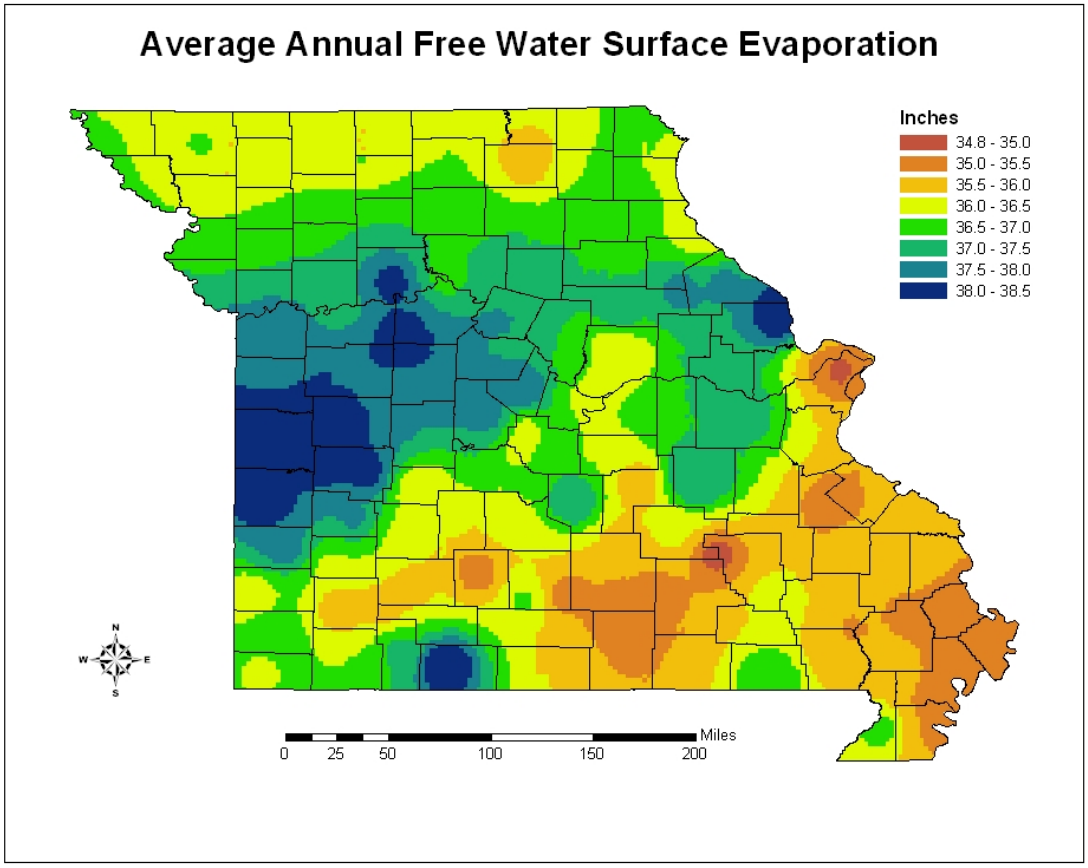

Figure 152: Average annual free water surface evaporation.

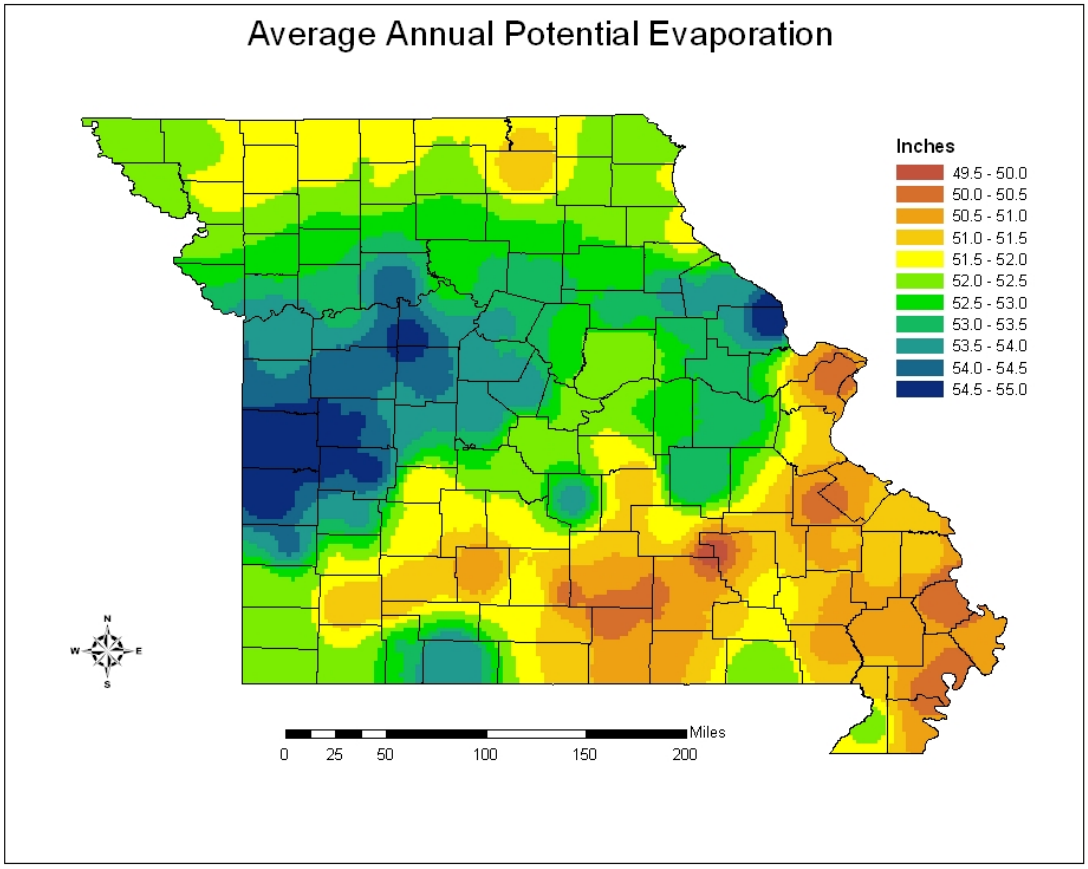

Figure 153: Average annual potential surface evaporation.

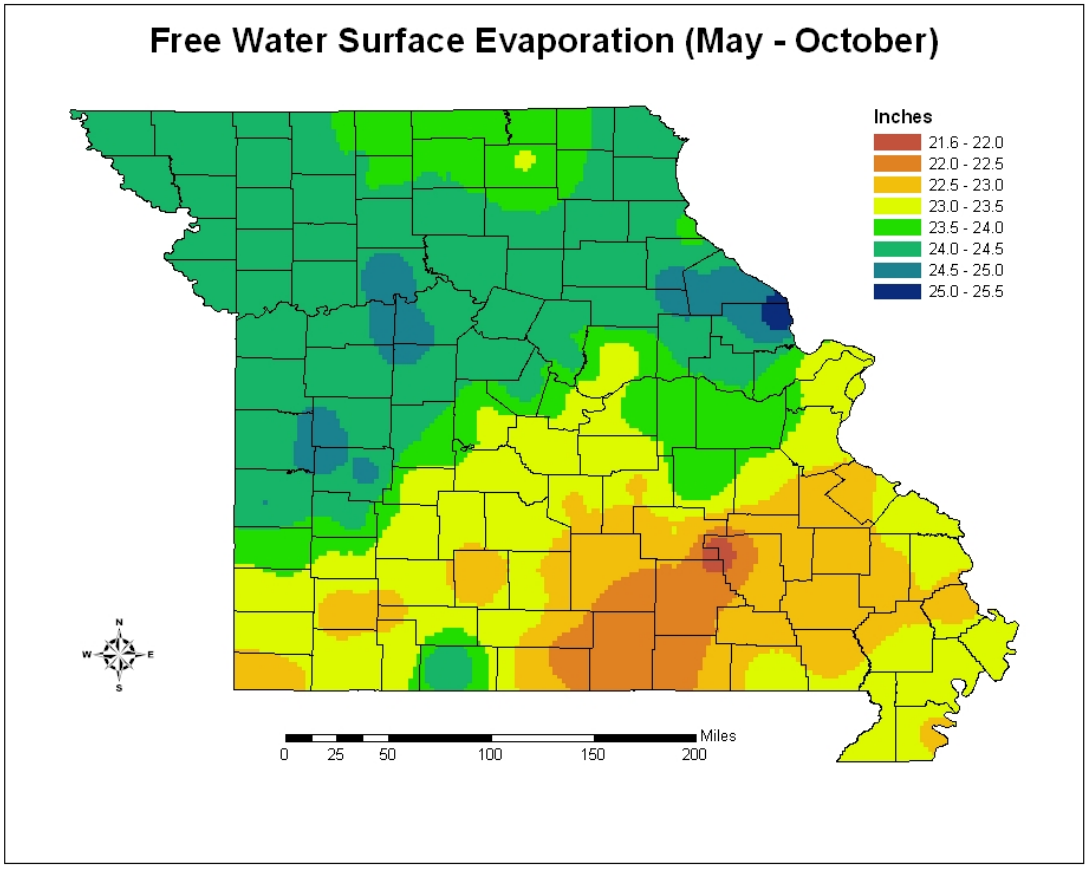

Figure 154: Free water surface evaporation for May-October.

6. Rainfall minus evaporation

Average annual precipitation minus free water surface evaporation is calculated and shown in Fig. 155. Negative values in the figure indicate more evaporation loss of water than water gain from precipitation. Except for some small negative values in the northwest the state on average gains more water from precipitation than loses water via evaporation.

Because of the data limitation, some statistical properties of the rainfall minus evaporation, such as magnitude and probability of largest rainfall minus evaporation in certain time period, 10 years, say, cannot be computed. Some of those values may, however, be estimated using the rainfall and evaporation values presented in sections 1 and 4.

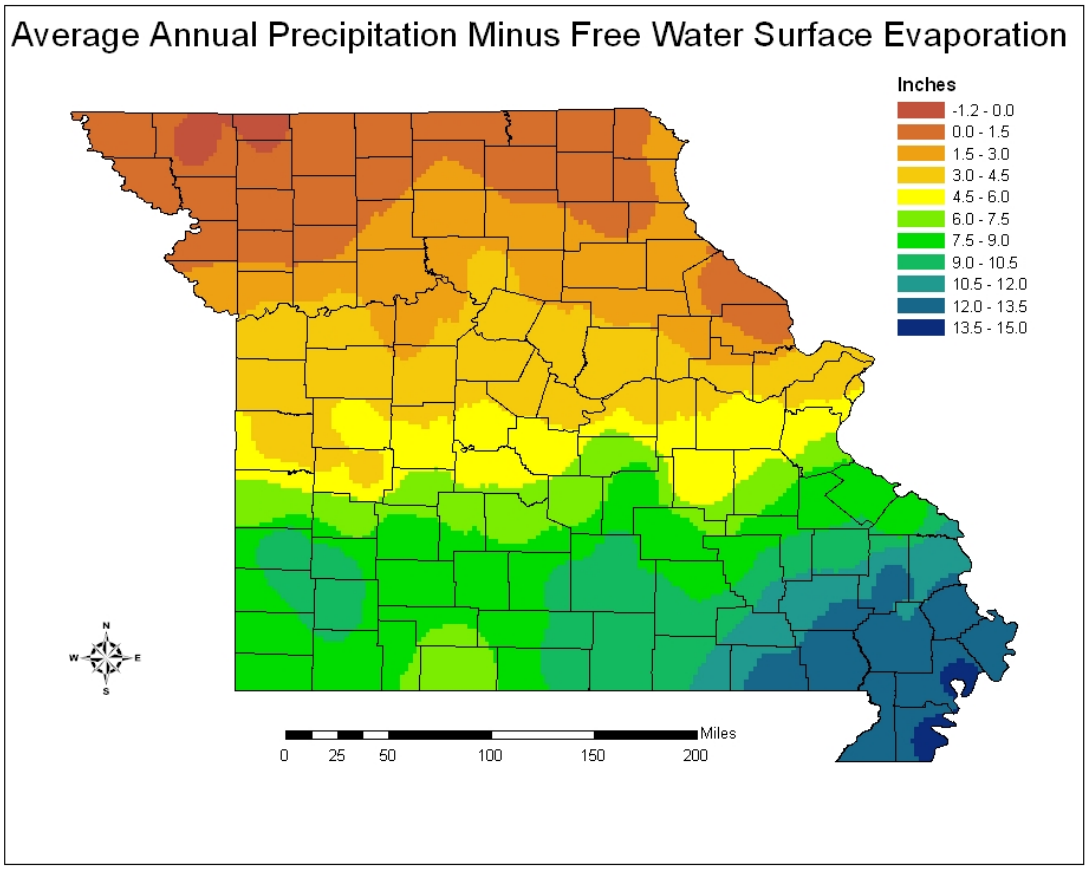

Figure 155: Average annual precipitation minus free water surface evaporation.

7. Soil temperature

Stations measuring soil temperatures at 2 inches below the surface have been implemented over the last 20 years by the School of Natural Resources of the University of Missouri-Columbia. Although some of the stations also measure soil temperatures at 4 inches and deeper layers the number of stations is inadequate for us to develop soil temperature maps for those deeper layers across the state. Thus, only soil temperature climatology at 2 inches is presented.

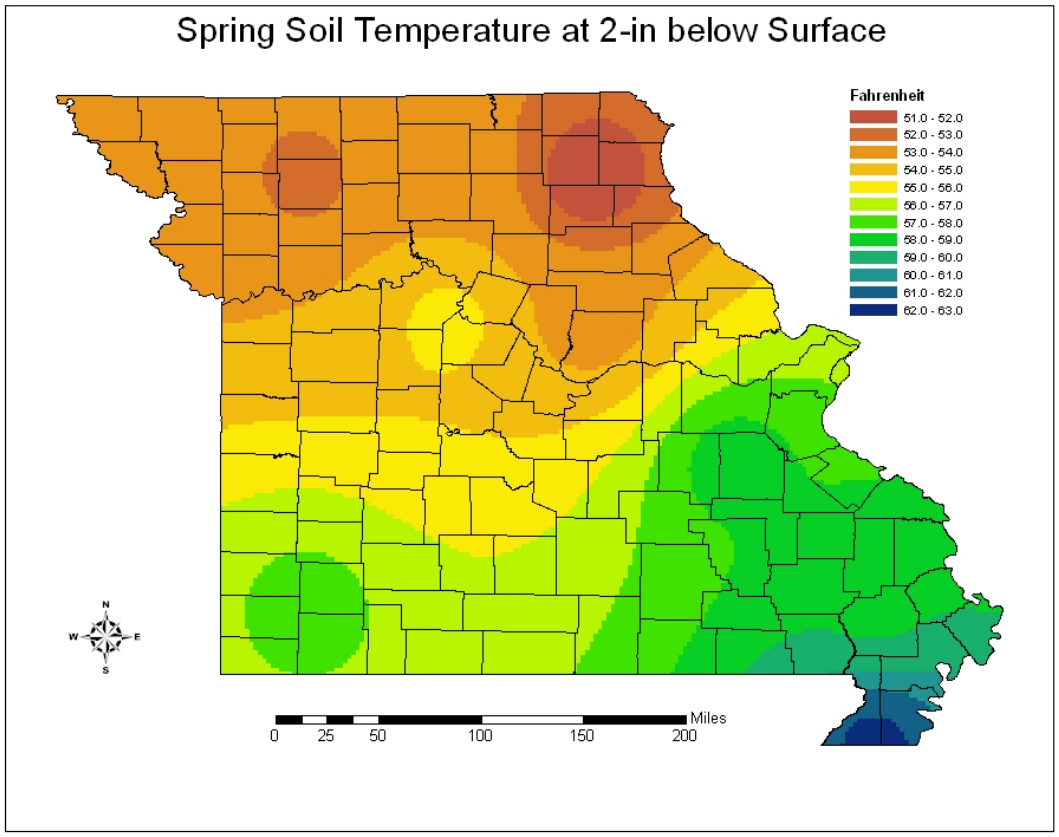

Figure 156: Spring soil temperatures at 2-inch below the surface.

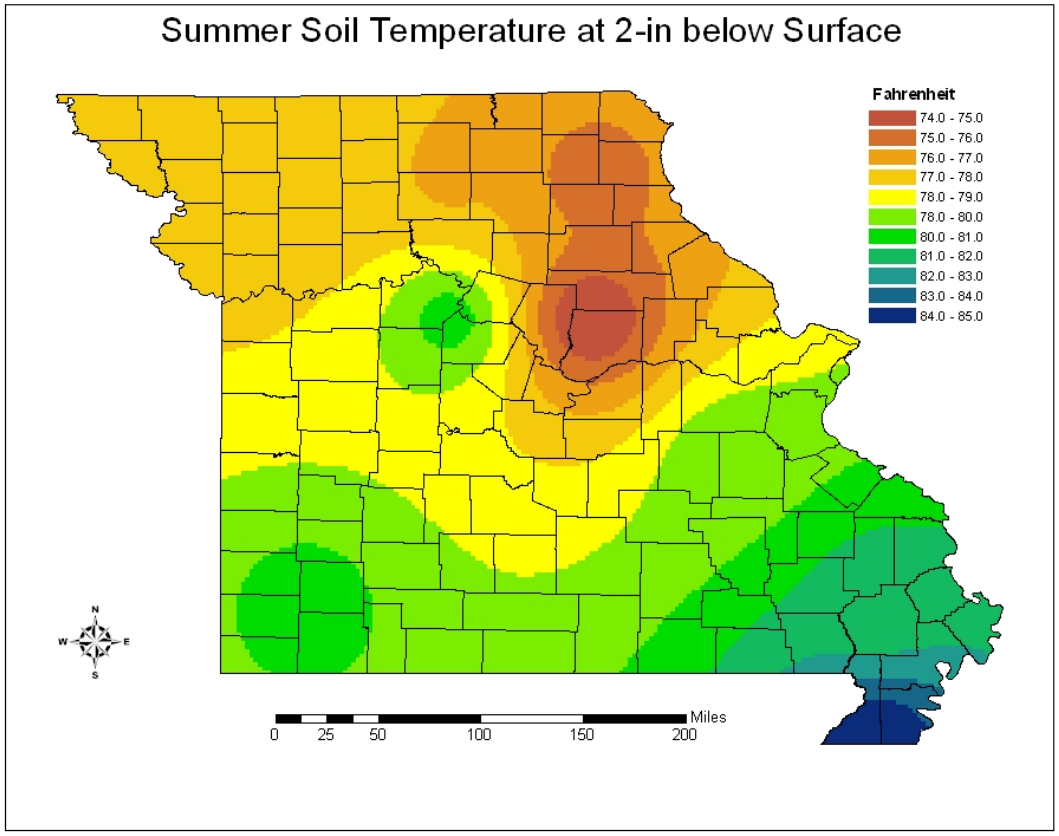

Figure 157: Summer soil temperatures at 2-inch below the surface.

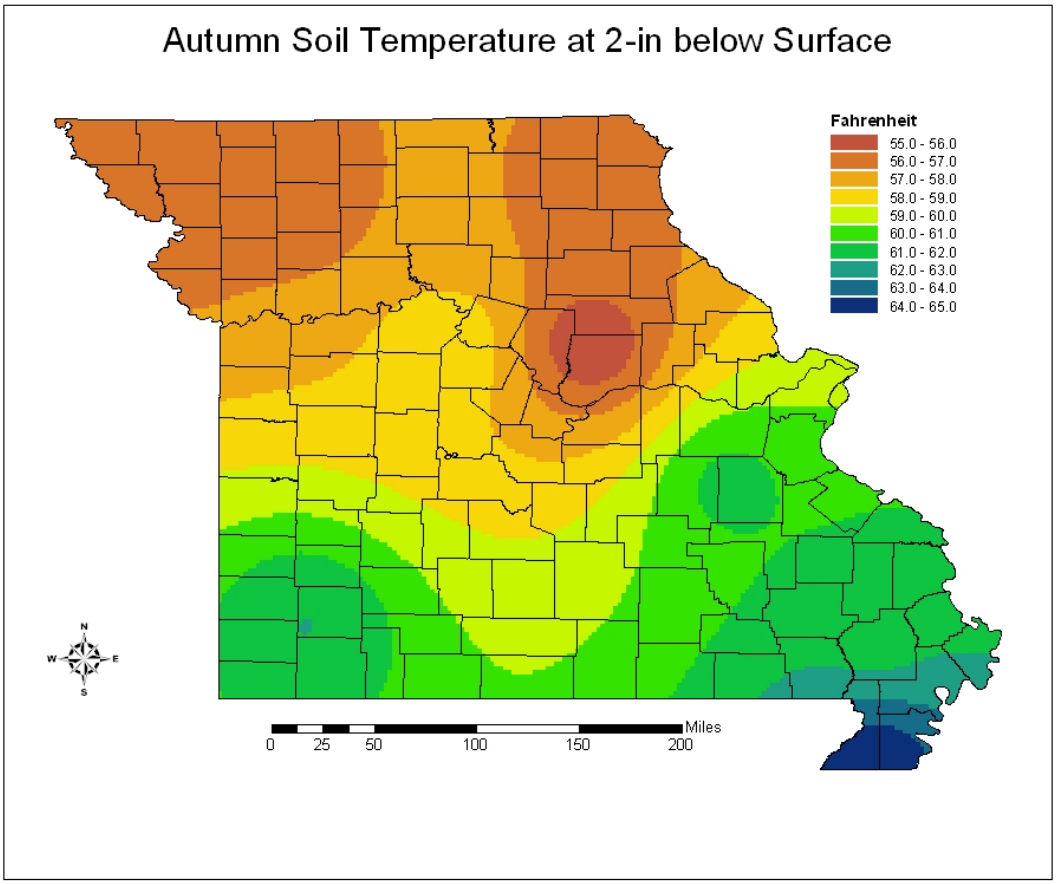

Figure 158: Autumn soil temperatures at 2-inch below the surface.

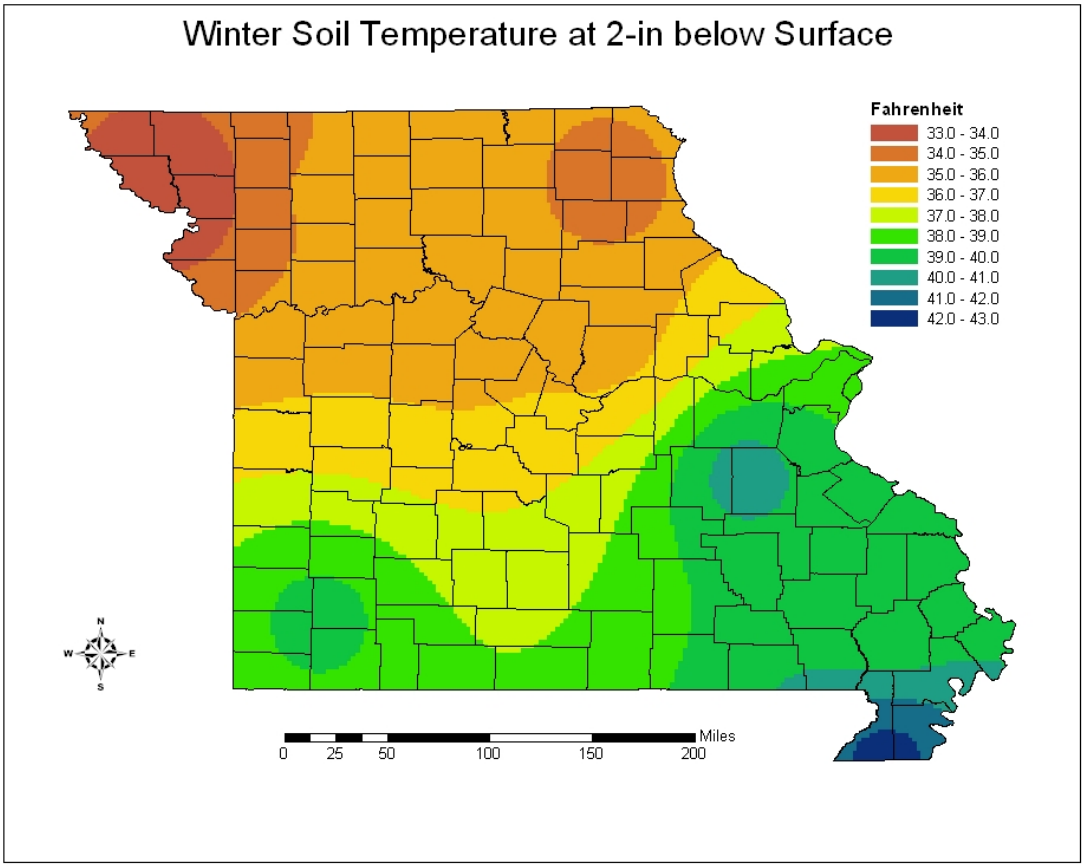

Figure 159: Winter soil temperatures at 2-inch below the surface.

8. Prevailing wind direction and average wind speed for different seasons

Wind speed and direction were measured at 3 meters above the ground from the stations in the Missouri Automated Weather Stations Network. Some data from the first order National Weather Service stations in Missouri also were used in calculating the mean wind speed and prevailing wind directions. Details of the methods are discussed in Appendix B section 7. A general feature of the wind speed is that the wind is stronger in the northern part of the state than in the south, and a weak wind center persisted leeward of the Ozark Plateau in the southeastern Missouri. Prevailing wind direction varies dramatically partly because of local terrain and topographic effects.

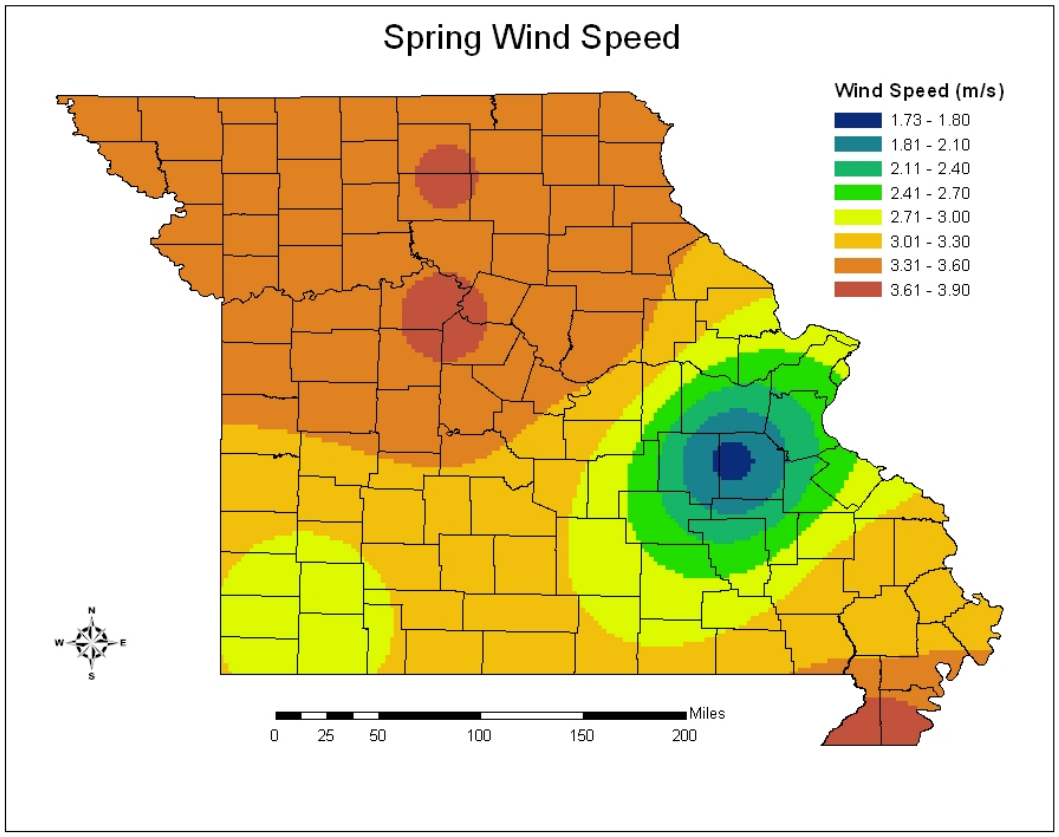

Figure 160: Average wind speed in spring.

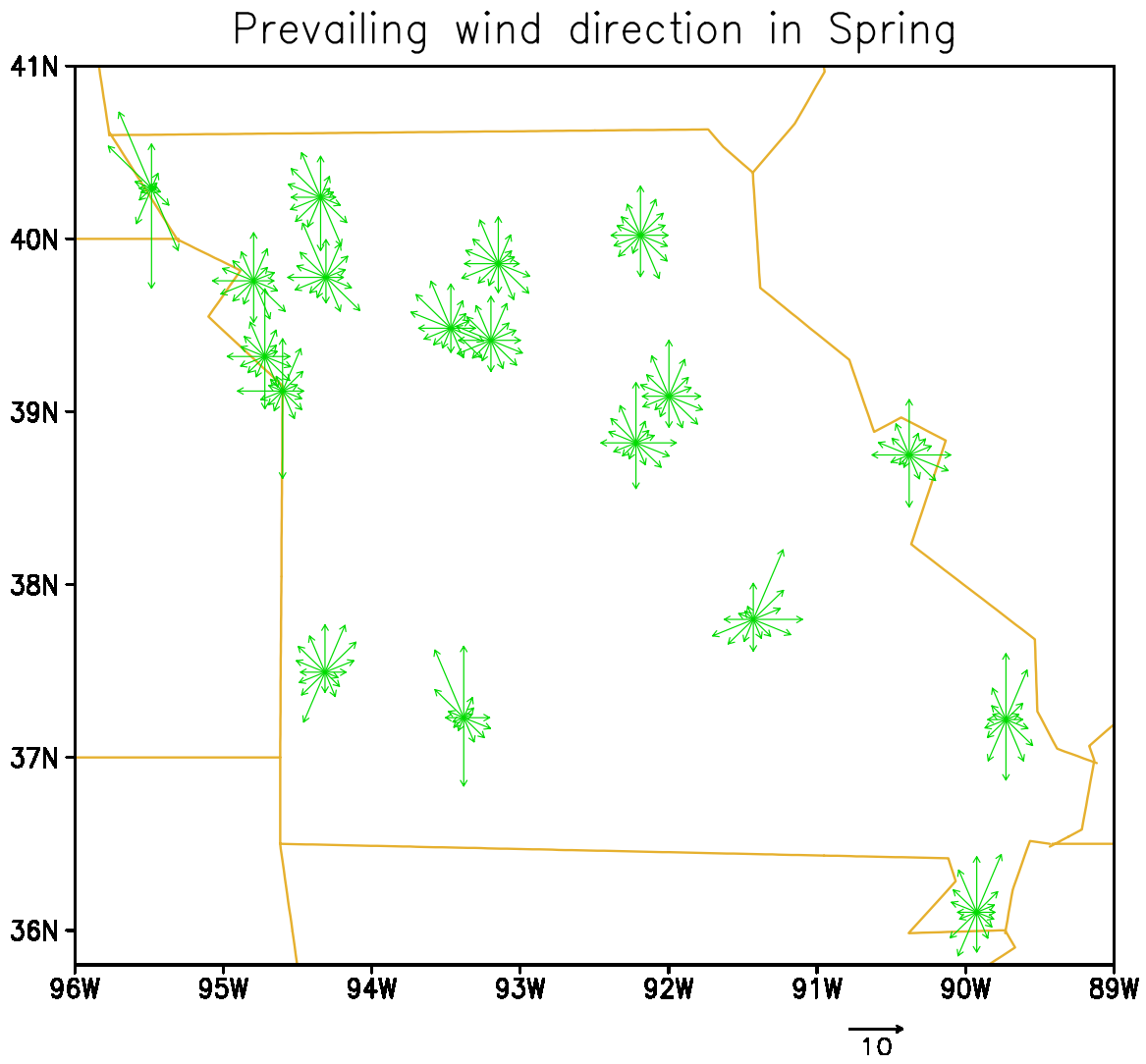

Figure 161: Distribution of wind direction in spring. The arrow shows the percentage of wind falling in the direction (the longer the arrow length is the more frequent the wind blows to the arrow pointed direction, and the 10% arrow is shown below the abscissa).

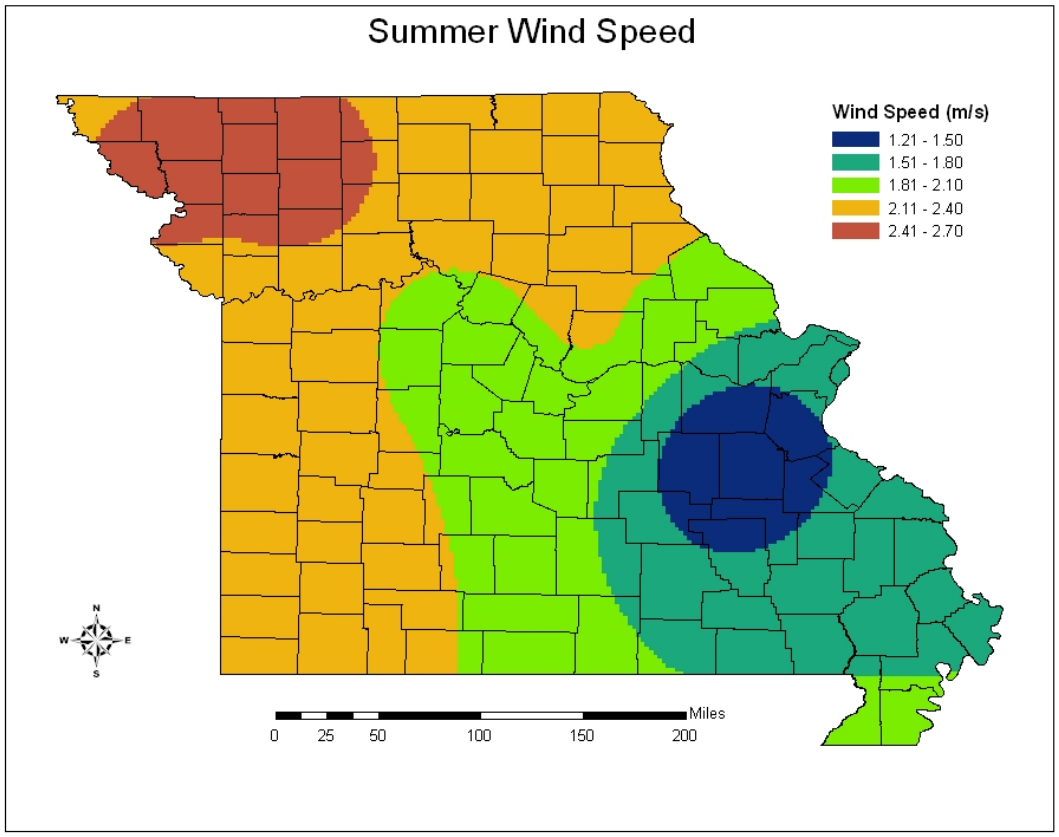

Figure 162: Average wind speed in summer.

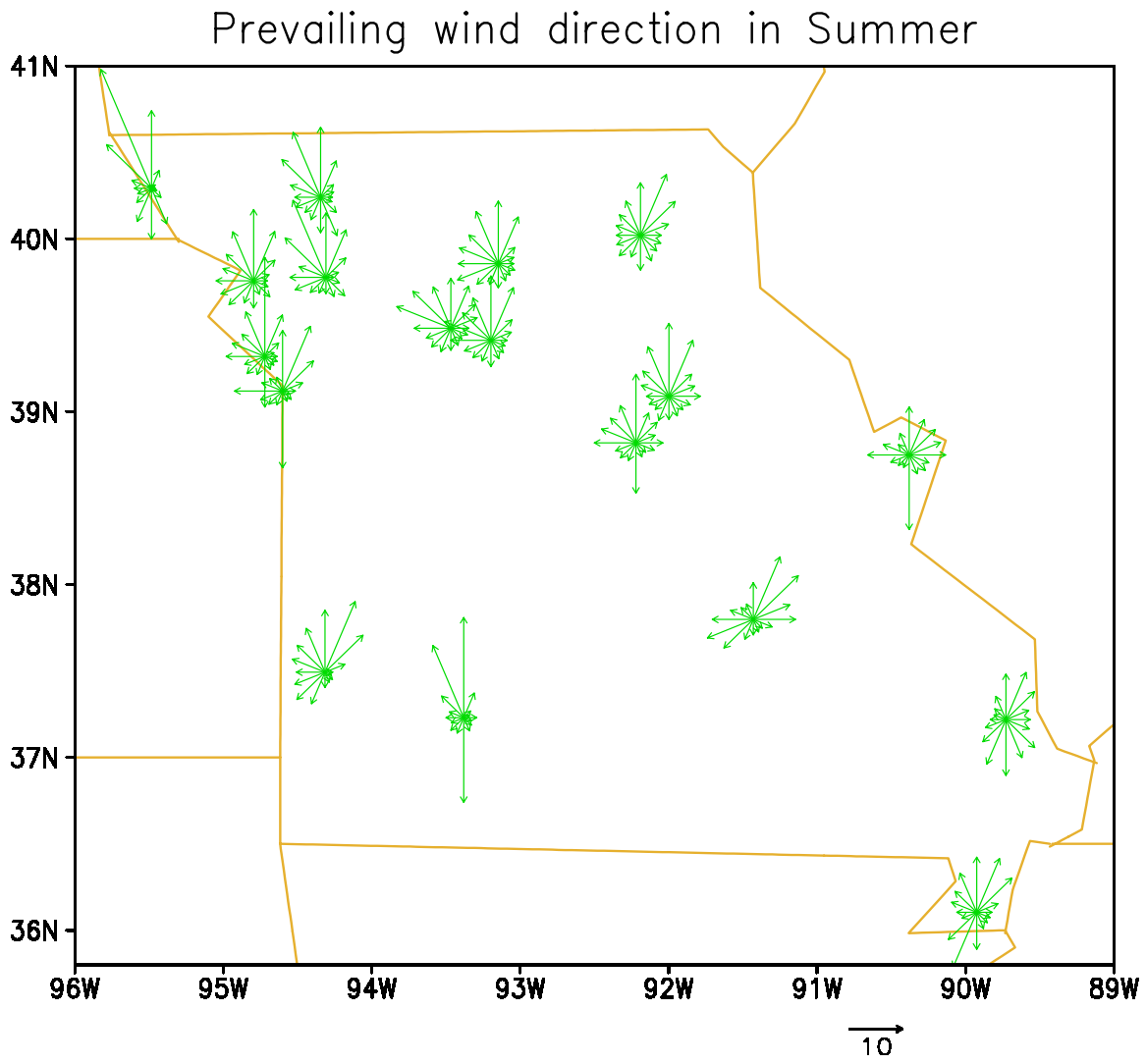

Figure 163: Distribution of wind direction in summer. The arrow shows the percentage of wind falling in the direction (the longer the arrow length is the more frequent the wind blows to the arrow pointed direction, and the 10% arrow is shown below the abscissa).

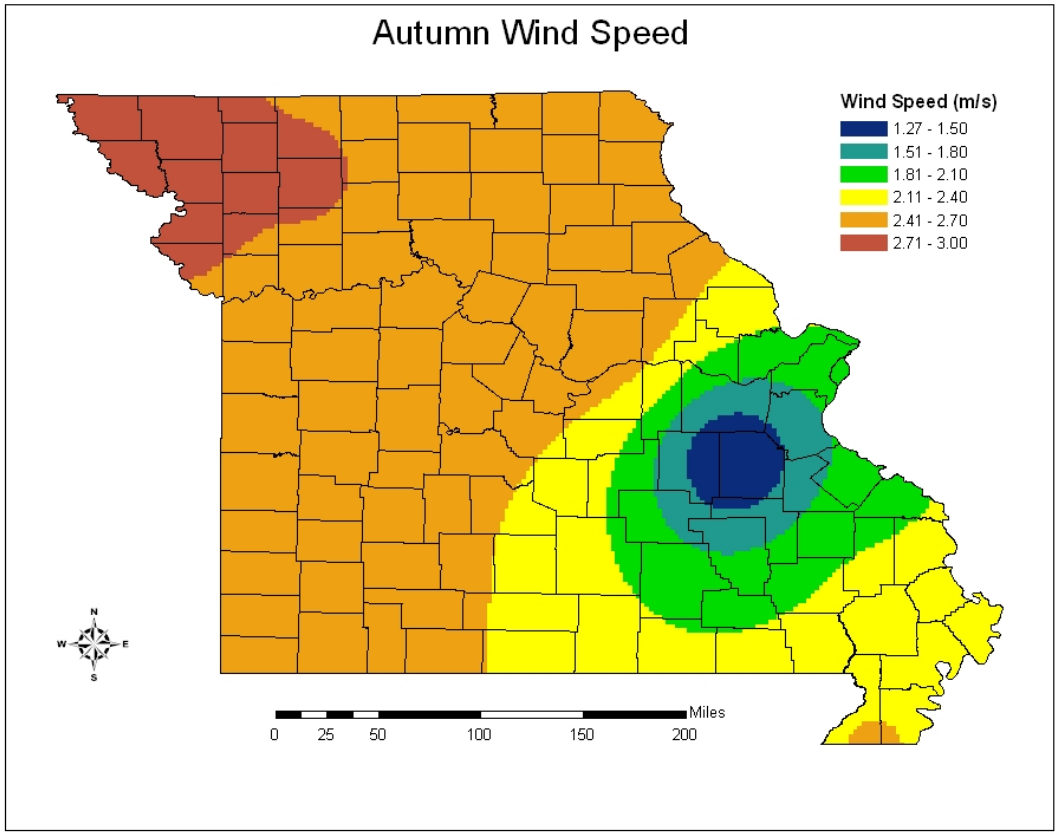

Figure 164: Average wind speed in autumn.

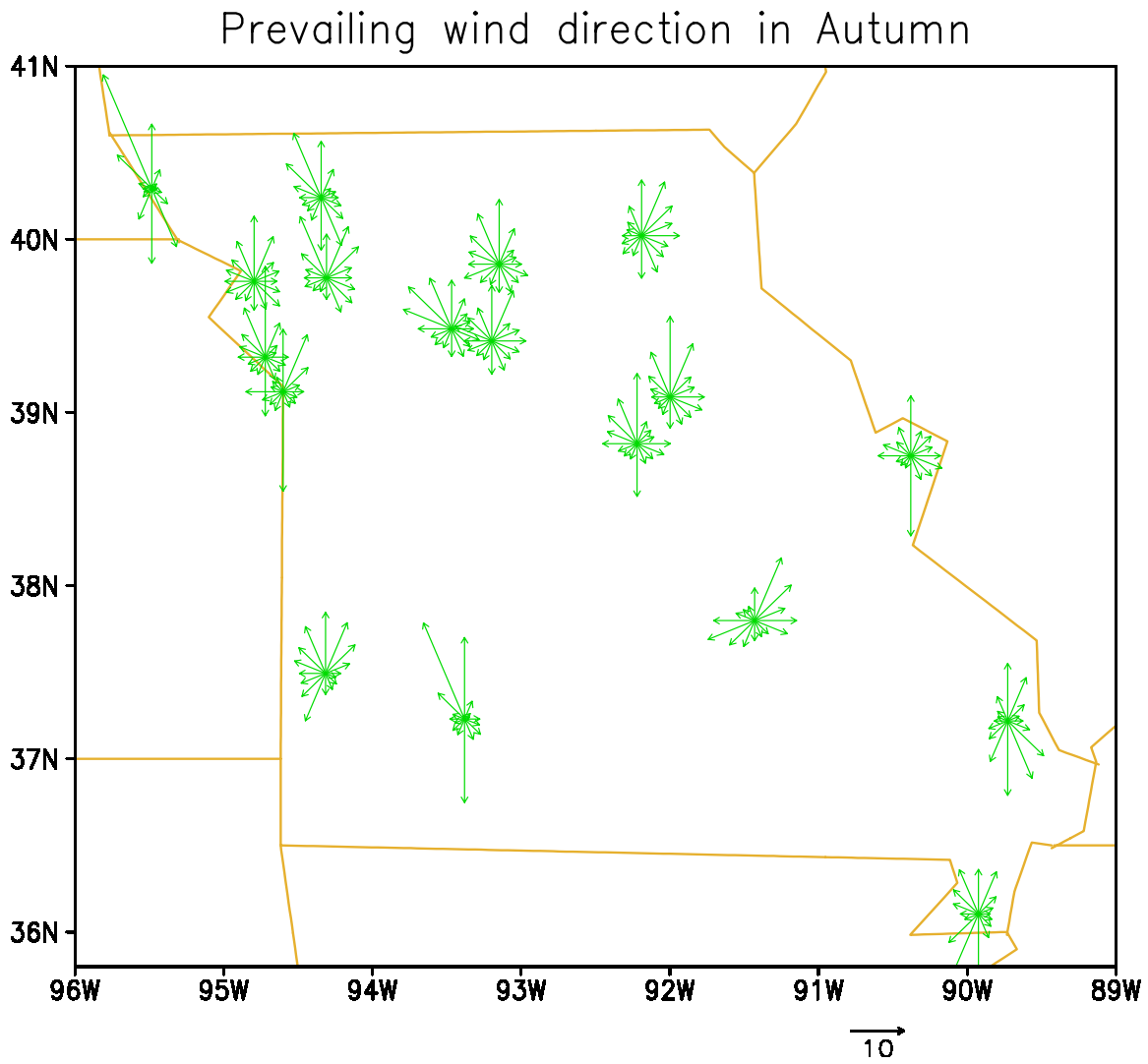

Figure 165: Distribution of wind direction in autumn. The arrow shows the percentage of wind falling in the direction (the longer the arrow length is the more frequent the wind blows to the arrow pointed direction, and the 10% arrow is shown below the abscissa).

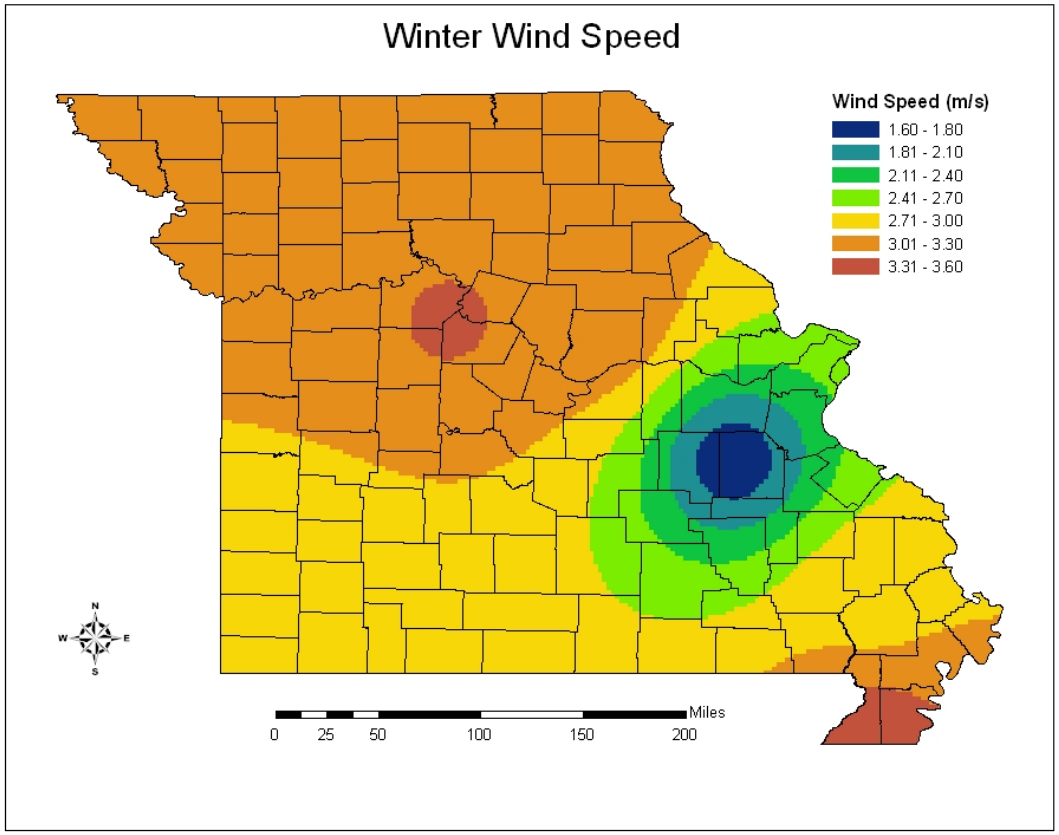

Figure 166: Average wind speed in winter.

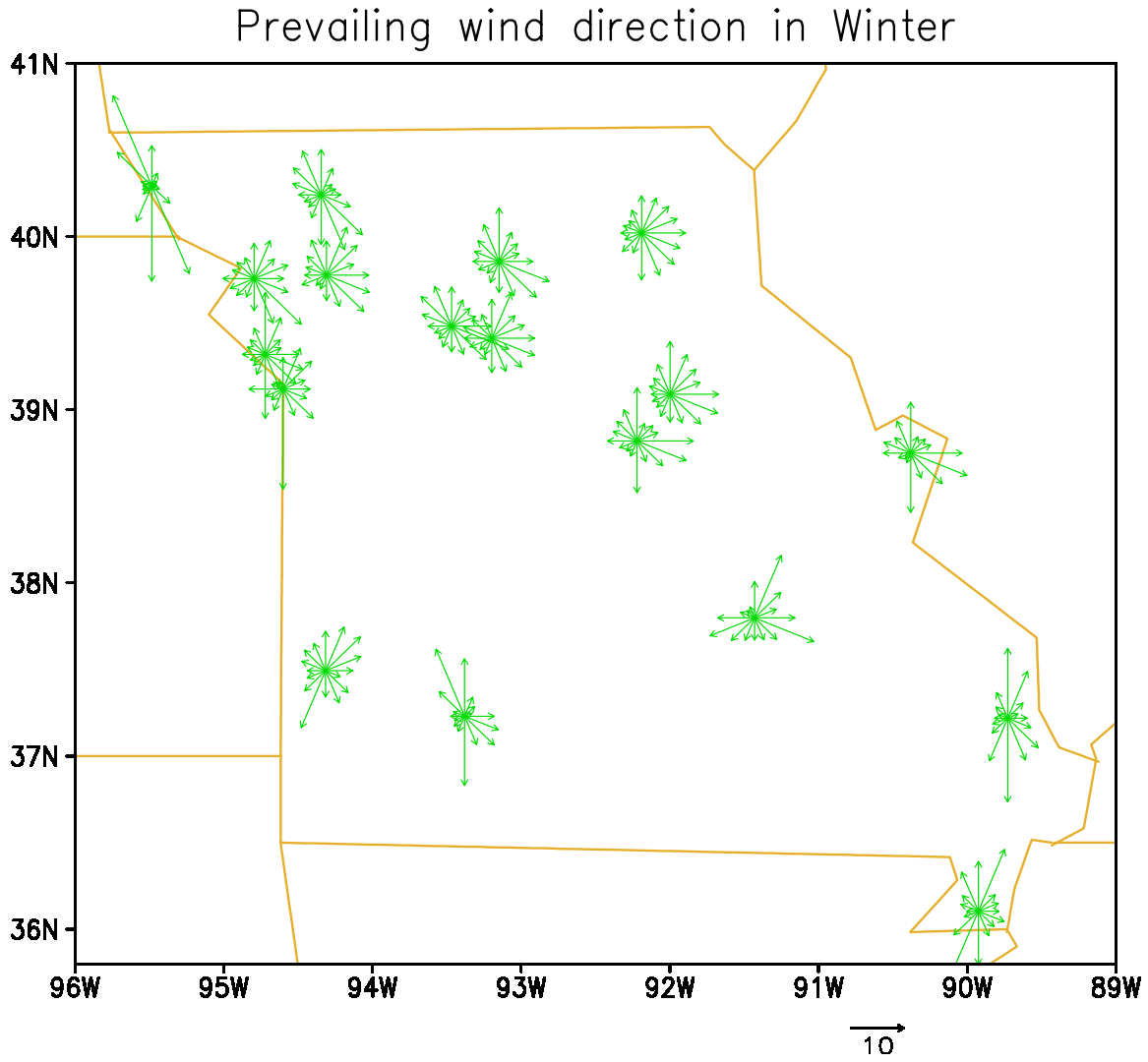

Figure 167: Distribution of wind direction in winter. The arrow shows the percentage of wind falling in the direction (the longer the arrow length is the more frequent the wind blows to the arrow pointed direction, and the 10% arrow is shown below the abscissa).

8. Solar radiation at the surface

Solar radiation at the surface was measured at stations in the Missouri Automated Weather Stations Network. The unit of these values is mega-Joules per meter square per day.

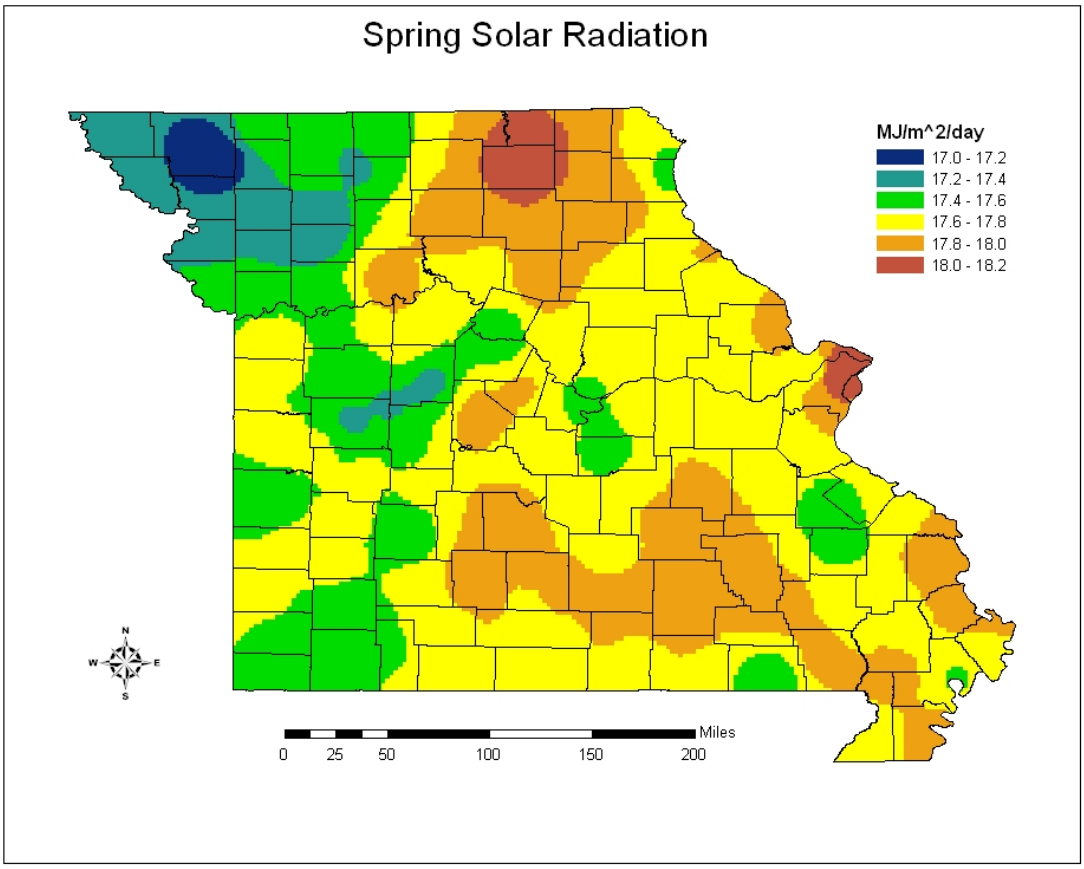

Figure 168: Average solar radiation at the surface in spring.

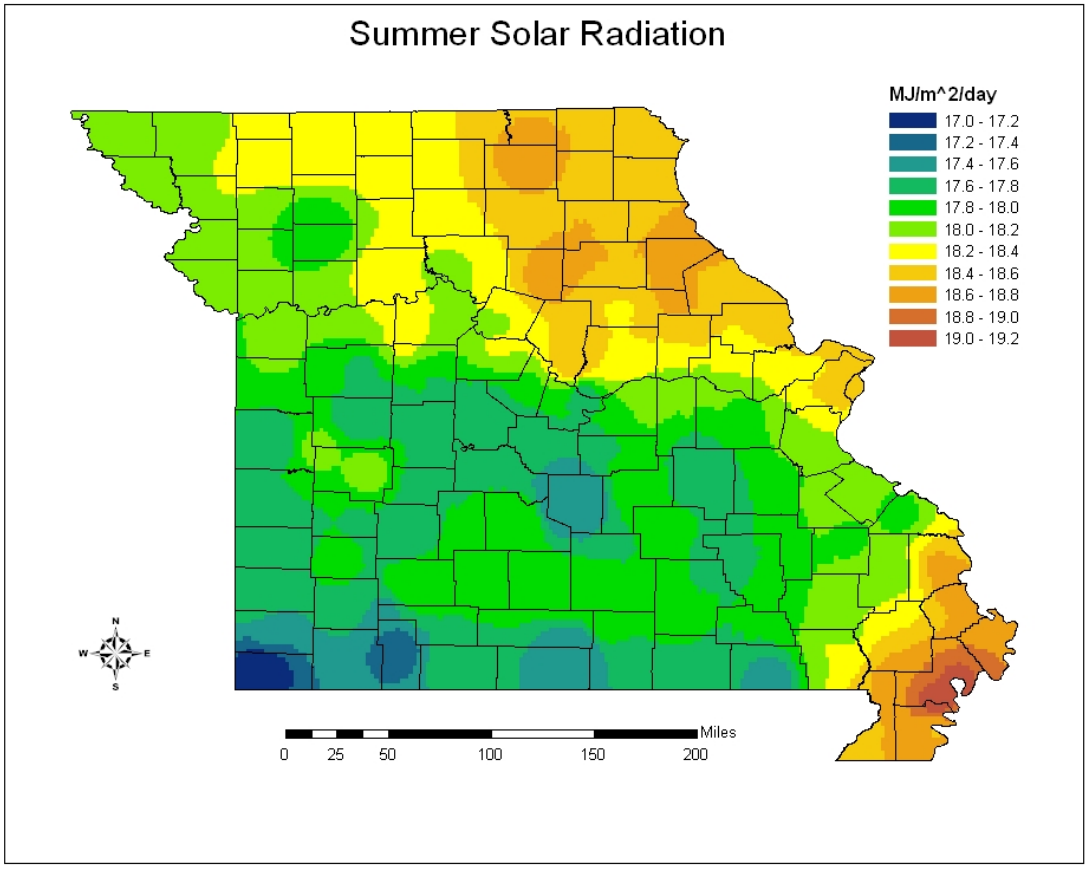

Figure 169: Average solar radiation at the surface in summer.

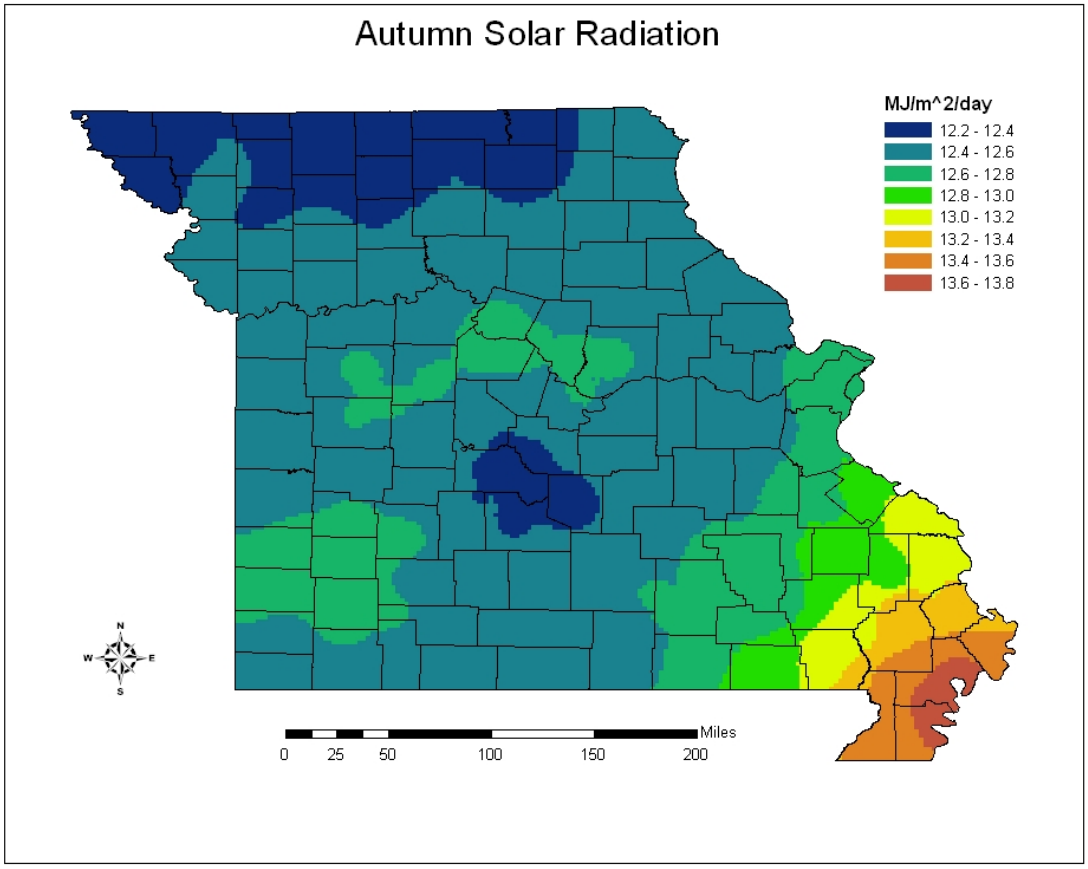

Figure 170: Average solar radiation at the surface in autumn.

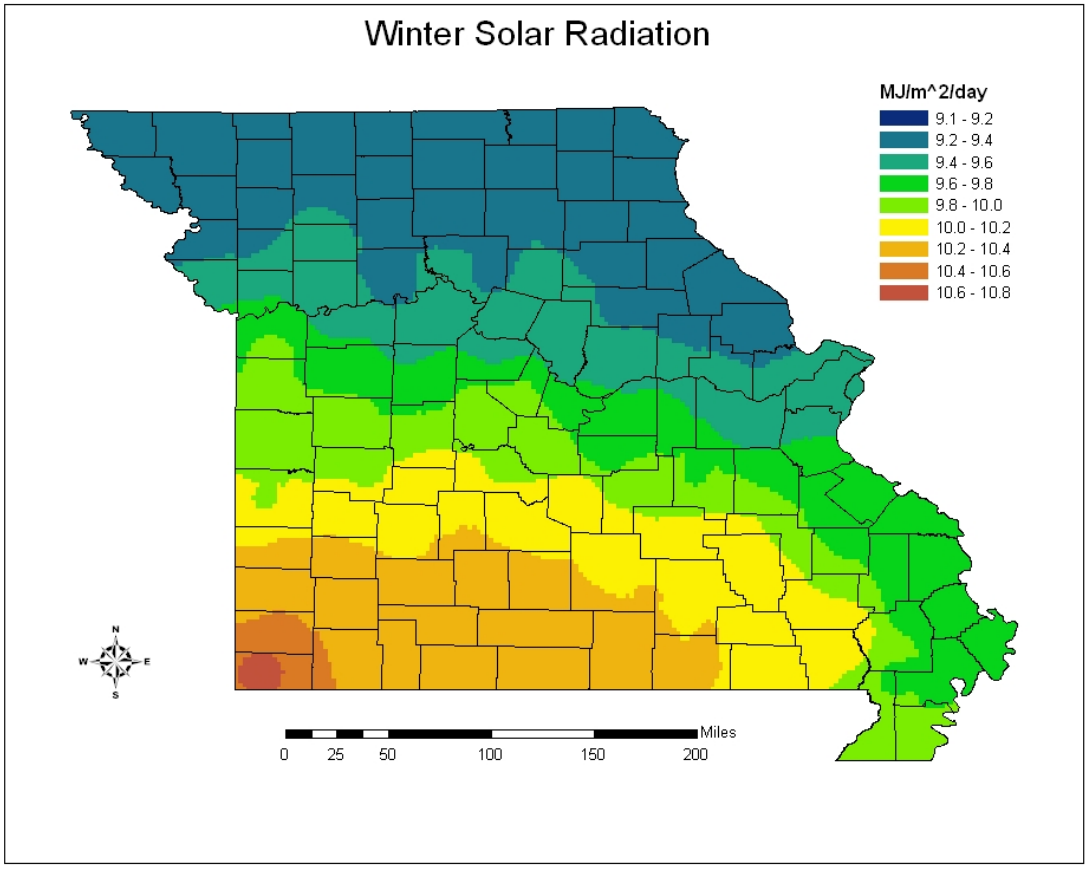

Figure 171: Average solar radiation at the surface in winter.

Appendix A
Climate Data Used in the Atlas

Daily precipitation and maximum (T_{max}) and minimum (T_{min}) air temperature data of 1971-2000 from 91 National Weather Service (NWS) cooperative stations in Missouri were obtained from the U.S. National Climatic Data Center (NCDC). Spatial distribution of these stations is depicted in Fig. A1. Details of each station are given in Table A1. Daily data from these stations have few missing values, less than 1% of the total station data.

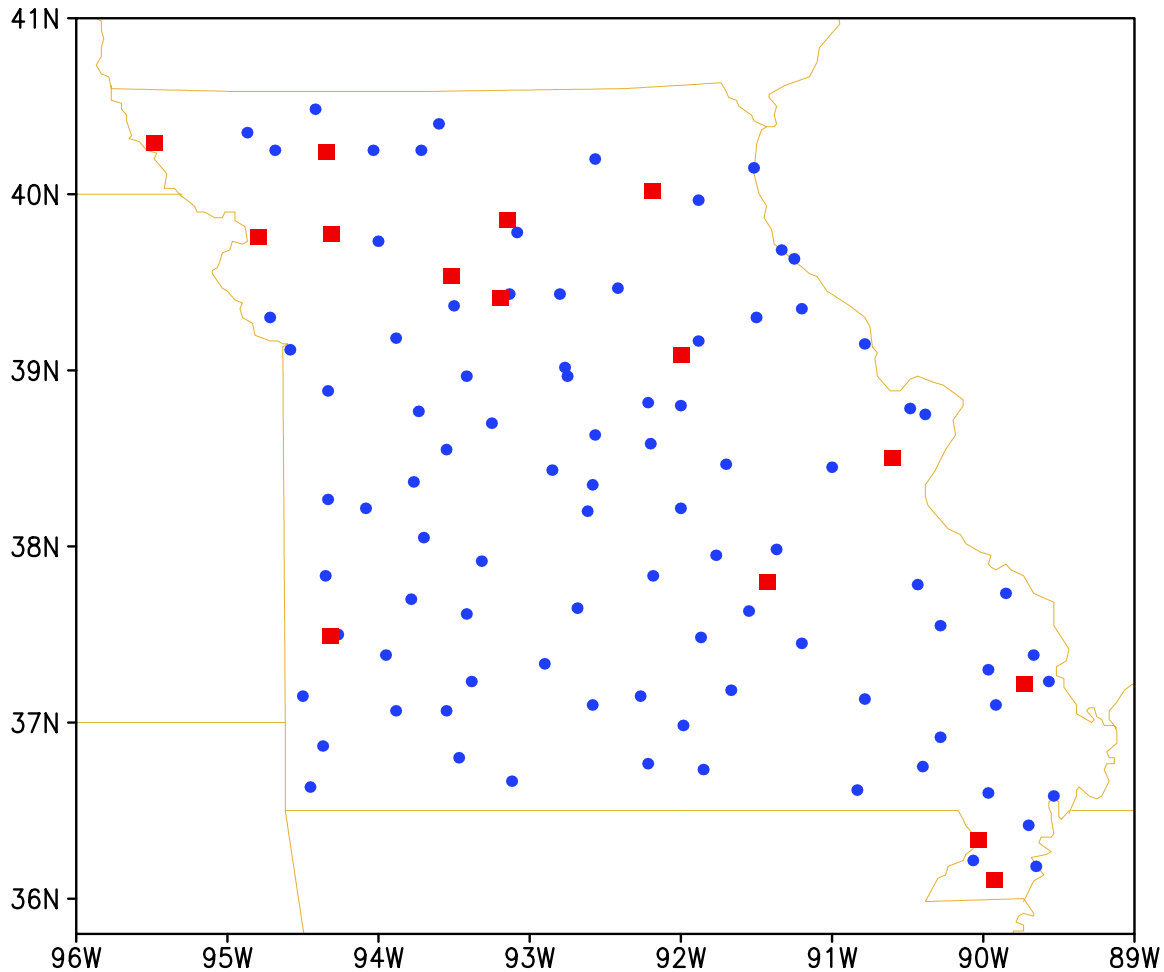

Figure A1: Geographical distribution of the 91 NWS cooperative stations (blue circles). The red squares mark the locations of the 15 stations in the Missouri Automated Weather Stations Network.

Before the stations' daily data were used in analysis they were "quality controlled (QC)," to examine their temporal and spatial consistencies. In the QC procedures, the criteria suggested by Reek et al. (1992) were used to identify erroneous data of air temperature and precipitation. First, erroneous data resulting from typos in reporting and digitizing the data, unit inconsistency, and use of different based values in data conversion (English to metric and vice versa) were

identified and corrected. Then, the daily data were examined for 1) internal inconsistency, such as daily maximum temperature being cooler than daily minimum temperature, 2) excessively large daily temperature range (T_{max} - T_{min}), and 3) data of the same value occurring for at least seven consecutive days (this check was not applied to precipitation data). All the identified erroneous data from these evaluations were flagged. The erroneous data detected by these methods were interpolated using observations in neighboring stations by linear regressions (Hubbard, 2001). The interpolation also was applied to estimate the few missing stations' data to avoid data gaps in stations' data series that could induce temporal and spatial biases in monthly averaged values (Stooksbury et al. 1999).

Table A1: Stations information for 91 cooperative stations.

Station ID	Latitude (N)	Longitude (W)	Elevation (ft)	Station Name
230022	37º06'	89º55'	357.5	ADVANCE 1 S
230164	36º38'	94º27'	1000.4	ANDERSON
230204	38º13'	94º05'	800.3	APPLETON CITY
230608	40º15'	94º02'	911.8	BETHANY
230657	37º04'	93º33'	1361.2	BILLINGS 2 N
230789	37º37'	93º25'	1069.3	BOLIVAR 1 NE
230817	38º58'	92º45'	761.0	BOONVILLE
230856	39º21'	91º12'	902.0	BOWLING GREEN 2 NE
230980	39º47'	93º05'	770.8	BROOKFIELD
231037	39º26'	93º08'	649.4	BRUNSWICK
231101	37º27'	91º12'	1199.8	BUNKER
231145	38º16'	94º20'	859.4	BUTLER
231189	38º38'	92º34'	869.2	CALIFORNIA
231275	40º09'	91º31'	488.7	CANTON L & D 20
231289	37º14'	89º34'	336.9	CAPE GIRARDEAU AP
231340	39º22'	93º30'	751.1	CARROLLTON

231364	36º11’	89º39’	269.0	CARUTHERSVILLE
231674	37º08’	90º47’	639.6	CLEARWATER DAM
231711	38º22’	93º46’	800.3	CLINTON
231791	38º49’	92º13’	892.8	COLUMBIA REGIONL AP
231822	40º15’	94º41’	1111.9	CONCEPTION
232289	36º37’	90º50’	341.1	DONIPHAN
232302	36º46’	92º13’	980.7	DORA
232503	38º21’	92º35’	931.5	ELDON
232591	39º09’	90º47’	449.4	ELSBERRY 1 S
232809	37º47’	90º26’	888.9	FARMINGTON
233038	37º33’	90º17’	719.0	FREDERICKTOWN
233043	38º28’	91º42’	751.1	FREEDOM
233079	38º48’	92º00’	859.4	FULTON 4 SW
233094	36º48’	93º28’	1045.7	GALENA 1 SW
233369	40º29’	94º25’	1131.6	GRANT CITY
233568	39º44’	94º00’	980.7	HAMILTON
233601	39º41’	91º20’	751.1	HANNIBAL WATER WORKS
234226	37º23’	89º40’	459.2	JACKSON
234271	38º35’	92º12’	654.7	JEFFERSON CITY
234315	37º09’	94º30’	987.3	JOPLIN MUNICIPAL AP
234358	39º18’	94º43’	973	Kansas city WSMO AP
234359	39º07’	94º35’	742	Kansas city downtown AP
234417	36º13’	90º04’	269.0	KENNETT RADIO KBOA

234544	40º12’	92º34’	968.6	KIRKSVILLE
234694	38º12’	92º37’	590.4	LAKESIDE
234705	37º30’	94º16’	980.7	LAMAR
234825	37º39’	92º41’	1259.5	LEBANON 2 W
234850	38º53’	94º20’	1000.4	LEES SUMMIT REED WLR
234904	39º11’	93º53’	839.7	LEXINGTON
234919	37º29’	91º52’	1171.0	LICKING 4 N
235027	37º23’	93º57’	1069.3	LOCKWOOD
235207	36º36’	89º58’	301.8	MALDEN MUNICIPAL AP
235227	37º06’	92º35’	1520.0	MANSFIELD
235253	37º18’	89º58’	439.5	MARBLE HILL
235307	37º20’	92º54’	1479.3	MARSHFIELD
235340	40º21’	94º52’	1161.1	MARYVILLE 2 E
235541	39º10’	91º53’	800.3	MEXICO
235671	39º28’	92º25’	859.4	MOBERLY AP
235834	37º09’	92º16’	1459.6	MOUNTAIN GROVE 2 N
235862	37º04’	93º53’	1190.6	MT VERNON MU SW CNTR
235976	36º52’	94º22’	1010.2	NEOSHO
235987	37º50’	94º21’	859.4	NEVADA SEWAGE PLANT
236012	39º01’	92º46’	639.6	NEW FRANKLIN 1 W
236045	36º35’	89º32’	301.8	NEW MADRID
236402	38º03’	93º42’	770.8	OSCEOLA
236460	36º40’	93º07’	701.9	OZARK BEACH

236641	37º44’	89º51’	501.8	PERRYVILLE WATR PLNT
236777	37º55’	93º19’	879.0	POMME DE TERRE DAM
236791	36º45’	90º24’	331.3	POPLAR BLUFF
236804	36º25’	89º42’	278.8	PORTAGEVILLE
236866	40º24’	93º36’	839.7	PRINCETON
237263	37º57’	91º46’	1200.5	ROLLA UNIV OF MO
237397	38º47’	90º29’	521.5	ST CHARLES
237455	38º45’	90º23’	577.3	ST LOUIS LAMBERT AP
237506	37º38’	91º33’	1200.5	SALEM
237514	39º26’	92º48’	721.6	SALISBURY
237578	39º38’	91º15’	469.0	SAVERTON L & D 22
237632	38º42’	93 15’	911.8	SEDALIA
237963	40º15’	93º43’	879.0	SPICKARD 7 W
237976	37º14’	93º23’	1285.8	SPRINGFIELD REG AP
238043	37º59’	91º22’	700.0	STEELVILLE 2 N
238051	39º58’	91º53’	649.4	STEFFENVILLE
238082	37º42’	93º47’	923.6	STOCKTON DAM
238184	37º11’	91º40’	1180.8	SUMMERSVILLE
238223	38º58’	93º25’	701.9	SWEET SPRINGS
238515	38º27’	91º00’	521.5	UNION
238577	39º18’	91º30’	770.8	VANDALIA
238603	38º26’	92º51’	1029.9	VERSAILLES
238620	38º13’	92º00’	769.8	VIENNA 2 WNW

238700	36º55’	90º17’	469.0	WAPPAPELLO DAM
238712	38º46’	93º44’	879.0	WARRENSBURG 4 NW
238777	37º50’	92º11’	800.3	WAYNESVILLE 2 W
238880	36º44’	91º51’	1006.6	WEST PLAINS
238995	36º59’	91º59’	1230.0	WILLOW SPRGS RD KUKU
239032	38º33’	93º33’	951.2	WINDSOR 3 NW

Hourly air temperature, precipitation, wind speed, wind direction, solar radiation, relative humidity, and soil temperature at 5cm below the surface measured at 15 stations in the Missouri Automated Weather Stations Network (Fig. A1) were also used in developing this Atlas. Details of these 15 stations are given in Table A2. Most of the stations were in service since the 1990s and their hourly data are from the middle or late 1990s to the present.

Table A2: Information of the automated weather stations in Missouri.

County	Township	Latitude (N)	Longitude (W)	Record length
Atchison	Corning	40º18’	95º29’	1994-2002
Audrain	Auxvasse	39º05’	91º59’	1995-2002
Barton	Lamar	37º30’	94º19’	1994-2002
South Farms	Columbia	39º32’#	93º31’#	1995-2002
Buchanan	St. Joseph	39º45’	94º48’	1993-2002
Cape Girardeau	Delta	37º13’	89º44’	1997-2002
Chariton	Brunswick	39º25’	93º12’	1997-2002
Crawford	Cook Station	37º48’	91º26’	1997-2002
Dekalb	Cameron	39º47’	94º19’	1999-2002
Gentry	Albany	40º14’	94º21’	1993-2002

Knox	Novelty	40º01’	92º11’	1995-2002
Linn	Linneus	39º51’	93º09’	1997-2002
Pemiscot	Steele	36º06’	89º56’	1996-2002
St Louis	Spirit	38º30’	90º36’	1990-2000[&]
Dunklin	-	36º20’	90º02’	1996-2000[&]

Notes: “#” indicates approximate values because no latitude and longitude information is available, and “&” indicates the data are in daily resolution and no wind direction and soil temperature data are available.

Monthly surface runoff data from 1971 to 2000 for Missouri and its surrounding regions (87.5º-97ºW, 35º-42ºN) were obtained from the Variable Infiltration Capacity (VIC) hydrologic model simulations (Maurer et al. 2002). The spatial resolution of VIC and hence the runoff data is 0.125 latitude × 0.125 longitude. The model was driven by observed precipitation and air temperature and derived solar and longwave radiation and wind. The simulated runoff is shown to match the observations very well over large river basins, such as Missouri and Mississippi River basins. The relative bias between VIC simulated and observed streamflow in the Missouri River basin is about -3.7% (Maurer et al. 2002). This accuracy suggests that VIC mode outputs are adequate for runoff analysis for Missouri.

Appendix B
Methods Used in Developing the Atlas

1. Rainfall

1) Stations' daily precipitation data after quality control were used to calculate the monthly and annual total precipitation for each station. All the stations' precipitation values were then used in spatial objective analyses to derive the monthly and annual precipitation values for a grid system covering the state, and the gridded data were graphed. These objective interpolation and graphics were completed using the Geographical Information Technology (GIS) tools. Using this procedure we produced the monthly and annual precipitation norms for the state and the monthly and annual precipitation for selected years.

2) Probabilities for large annual precipitation and number of precipitation days at 1 in 10-year frequency were computed using the Gamma distribution method. The same method has been used in operation to report monthly and seasonal precipitation events by the U.S. Climate Analysis Center (CAC) (Arkin 1989). Guttman et al. (1993) compared 4 statistical distributions for total precipitation over different time periods, ranging from 1 month to 5 years, and found that the gamma distribution was the best according to the goodness-of-fit test. The gamma distribution usually gives accurate estimations except for the extreme tail quartiles (Guttman et al. 1993) and is an adequate method for our use to calculate the probabilities.

3) Probabilities for extremely heavy 1-day to 2-day precipitation events over time periods from 10- to 25 years were calculated using the "log-log" distribution. This method was described in Angel and Huff (1992), who compared estimates of extreme 1-day precipitation totals for sites in Minnesota and Indiana identified from a "log-log" distribution with those identified from the L-moments and maximum likelihood procedures. Angel and Huff found no meteorological and statistical differences between estimates from those different methods. However, because the log-log distribution method "allows the analyst to incorporate meteorological-climatological knowledge and other pertinent findings" (Angel and Huff, 1992) we used the "log-log" distribution outlined by Huff and Angel (1989) and Huff (1993) in calculation of the heavy precipitation reoccurrence probabilities. Technically, the "log-log" distribution is simply the natural log of the precipitation totals plotted against the natural log of the return period, which generally has a linear trend (Fig. B1):

$$\ln(p) = a + b\ln(T)\,, \qquad \text{(B1)}$$

where p is the precipitation total in inches, T is the return period (in years) corresponding to event p. The parameters a and b are statistically determined. From this relationship, the precipitation total p for a given return period T (e.g., 1 in 25 years) can be computed from:

$$p = \exp[a + b\ln(T)]\,. \qquad \text{(B2)}$$

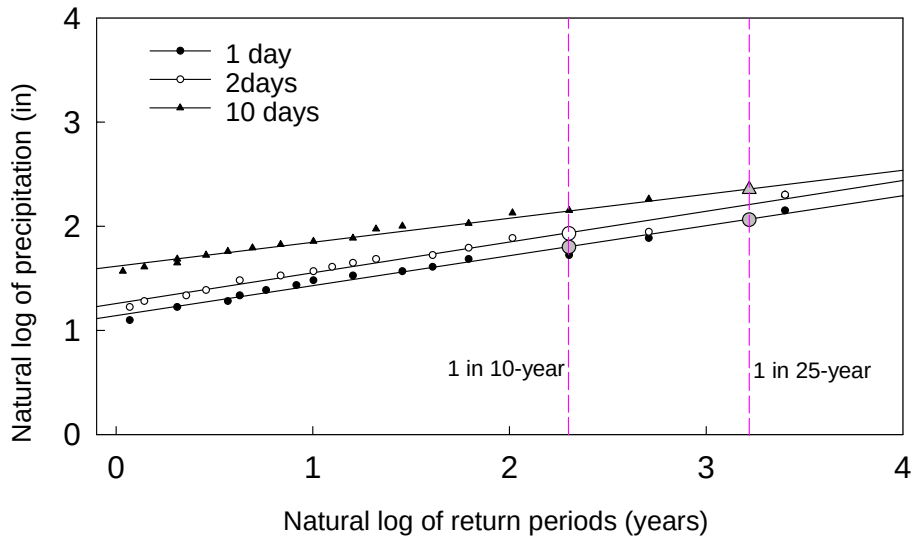

Figure B1: Frequency distributions of precipitation for station Advance 1S (230022).

2. Temperature

1) The average monthly temperature, mean beginning and ending dates of frost-free period, and average number of days in a year with minimum temperature at or below 32ºF were calculated using simple arithmetic calculations and the quality controlled stations' data. The values were plotted using GIS tools.
2) Probabilities of 1 in 10-year coldest average monthly temperature and number of days with minimum temperature at or below 32ºF were computed using Gaussian distribution for temperatures. A similar approach has been used in operation to report monthly and seasonal temperature variations at the CAC (Repeloewski et al. 1985; Arkin 1989).

3. Runoff

There is no generally accepted statistical distribution for surface runoff. To derive a distribution for runoff analysis in Missouri, the regional frequency analysis, the L-moments, described in Hosking and Wallis (1997) was applied. Moments-based methods have long been established in statistics to identify probability distributions in an observed dataset/time series. Conventional moments are not always easily interpreted for information such as the shapes of a distribution, especially skew and kurtosis. The estimates of distribution parameters fitted by the conventional moments are often less accurate than those obtained by other methods, such as maximum likelihood (Hosking 1990). An alternative to the conventional moments is the L-moments. L-moments can be estimated by linear combinations of order statistics (hence the prefix "L"). The main advantage of the L-moments over conventional moments is that the L-

moments suffer less from the effects of sampling variability so they are more robust to outliers in the data (Hosking and Wallis 1997).

Steps for L-moments analysis are outlined in Hosking and Wallis (1997). In L-moments analysis, identifying homogeneous regions is essential. A homogeneous region is defined by a subset of grid points (in a gridded dataset as the VIC dataset used in calculating the surface runoff) with similar frequency distributions (after appropriate scaling). Cluster analyses were used to identify the homogeneous regions and a manual refinement of the regions were often required to assure the regions with homogeneous frequency distributions (Guttman et al. 1993; Hosking and Wallis 1997). In the analysis for this Atlas, because the VIC runoff dataset has very high spatial resolution and VIC input data (such as precipitation and air temperature) at each grid point were the average from several neighboring stations, a 1.25º×1.25º box area (which contains 10 longitude grid points by 10 latitude grid points and is roughly 100km×100km) was chosen as a homogenous region for the L-moments analysis. Specifically, the first homogeneous region was chosen to be encompassed by the 1st to 10th longitude grid points and the 1st to the 10th latitude grid points, and second region was surrounded by the 2nd to 11th longitude points and the 1st to 10th latitude grid points, and so forth. In doing so, each grid point in Missouri was repeatedly used in 100 different regions. The threshold runoff for each grid point and for each quartile, therefore, is computed for 100 times. The final results for each quartile are the average of the 100 times estimations for each grid points.

The annual total runoff for each grid point was scaled as the percentage of 1971-2000 average to make the runoff at each grid point comparable (Hosking and Wallis 1997). Then the goodness-of-fit test was used in each of the 1.25º×1.25º box regions for each of five distributions: generalized logistic, generalized extreme-value (GEV), lognormal, Pearson type III, and generalized Pareto. The percentage of boxes passed the goodness-of-fit test for each distribution is showed in Table B1. None of the single distribution passed the goodness-of-fit test for more than 36% of the computations. We obtained similar results by using smaller 0.675º×0.675º box regions. These results suggested that the above 5 distributions performed poorly in computing Missouri's runoff quartiles.

Table B1: Percentage of box regions passed goodness-of-fit test for different statistical distributions.

Distribution	Percentage
GEN. LOGISTIC	0.210
GEN. EXTREME VALUE	0.356
LOGNORMAL	0.344
PEARSON TYPE III	0.300
GEN. PARETO	0.014

We then assumed the Wakeby distribution as a candidate distribution because it is robust in misspecification of the underlying distribution function for a region (Kotz et al. 1988; Hosking and Wallis 1997). Hosking and Wallis (1997) showed that Wakeby distribution can attain a wide range of distributional shapes with fixed lower bounds that mimic many skewed distributions and is particularly useful for hydrological datasets, such as the runoff. Wakeby distribution also was chosen as default distribution when Gamma distribution failed the goodness-of-fit test to create the U.S. drought atlas (Guttman et al. 1993). The Wakeby distribution is defined as a

probability distribution whose quartiles function or inverse cumulative distribution function, $x(F)$, is

$$x(F) = \xi + (\alpha / \beta)[1-(1-F)^{\beta}] - (\gamma / \delta)[1-(1-F)^{-\delta}]. \qquad \text{(B3)}$$

In (B3), F is the cumulative distribution function, ξ, α, β, γ, δ are real valued parameters.

The Wakeby distribution was used to compute the quartiles 20%(80%), 10%(90%), 4%(96%) and 2%(98%) for each 1.25º×1.25º box region. Since each grid point was used in 100 different box regions, the final quartiles are expressed as the average over the 100 estimations. Because annual total runoff data in each gird point was first scaled by the 1971-2000 climatic mean before L-moments analysis, the runoff thresholds for each quartile was the product of climatic annual total runoff and the averages of the 100 estimations.

The standard deviation (SD) of the 100 estimations for each quartile based on Wakeby distribution was computed. The SD is small (≤ 3%) for quartiles 20%(80%), 10%(90%), and 4%(96%). The SD for the tail quartiles (2% and 98%) is slightly larger. Figure B2 showed the standard deviations for the 2% quartile. In most part of Missouri, the SD is less than 5% except for the Northwestern Missouri, where the annual total runoff was low and the runoff data were highly skewed to tails. The small differences among the 100 estimations suggested that the 1.25º×1.25º box regions are homogenous regions for L-moments analysis.

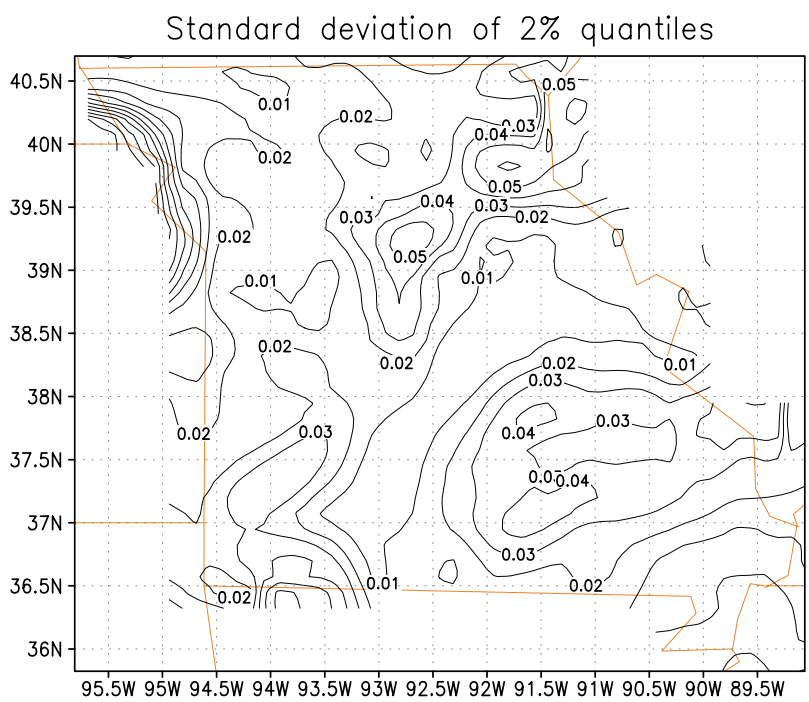

Figure B2: Distribution of the standard deviations for 2% quartile.

The difference between Wakeby distribution with GEV, lognormal, and Pearson type III distributions were small. Figure B3 is an example for 10% quartile. The blank areas indicate those regions failed the goodness-of-fit test for GEV, lognormal, and Person type III distributions. It is evident that in most of the areas, the percentage of runoff estimated by Wakeby distribution has very small difference (≤ 3%) with those estimated by the three major

distributions. This again suggested that the Wakeby distribution is good for describing the runoff.

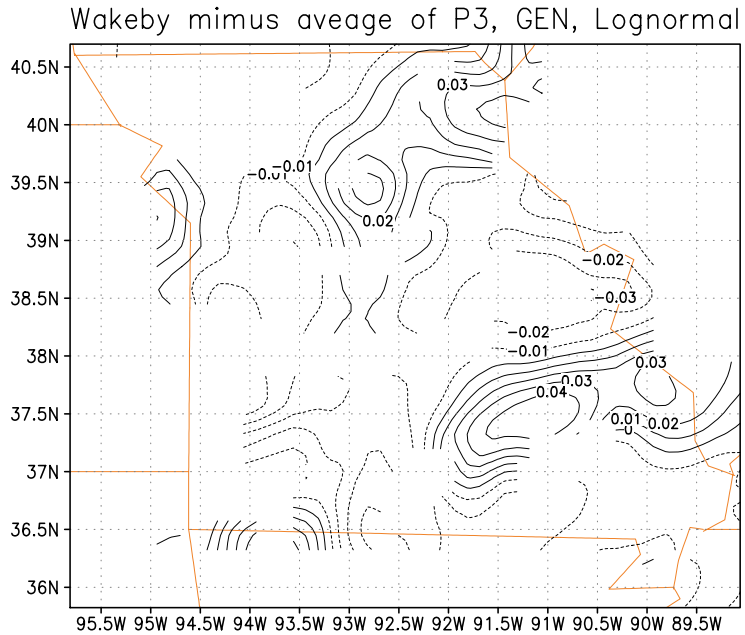

Figure B3: Difference between Wakeby distribution with GEV, lognormal, and Pearson type III distributions.

4. Evaporation

Because the 4 NWS stations' sporadic measurements of surface pan evaporation could not be used to evaluate surface evaporation variations we calculated surface evaporation using the observed and derived parameters.

Potential evaporation (E_p) was computed based on modified Panman combination equation (Jensen et al. 1990):

$$LE_p = \frac{\Delta}{\Delta+\gamma}(R_n - G) + \frac{\gamma}{\Delta+\gamma} 6.43 W_f (e_a - e_d) \qquad \text{(B4)}$$

where, Δ is the slope of the vapor pressure-temperature curve ($kPa{\cdot}^oC^{-1}$), γ is the psychrometric constant ($kPa{\cdot}^oC^{-1}$), R_n is the net radiation ($MJm^{-1}day^{-1}$), G is the soil heat flux to the surface. Because the daily average of G is small, it is assumed to be zero in this calculation. Also in (B4), W_f is wind function, $e_a - e_d$ is mean daily water vapor pressure deficit (kPa), the constant of proportionality 6.43 has the unit $MJm^{-1}day^{-1}kPa^{-1}$, and L is the latent heat of vaporization (MJ kg^{-1}) and is computed from: $L = 2.51 - 2.361\times10^{-3}T$, where T is air temperature in degrees of Celsius.

The input for computing E_p includes air temperature, solar radiation, wind speed, and dew point temperature (or relative humidity). Because the NWS cooperative stations only measure air temperature and precipitation we had to derive the other input values. Allen et al. (1994, 1998) showed several methods to estimate solar radiation, vapor pressure, and wind using daily maximum and minimum air temperatures. In this work, we estimated solar radiation using

the algorithm developed by Weiss et al. (2001) and the details of the algorithm can be found in section 7. The dew point temperature was estimated from (Hubbard et al. 2003):

$$T_d = aT_{\min} + b(T_{\max} - T_{\min}) + c \qquad \text{(B5)}$$

where parameters a, b, and c are regression coefficients, and T_d, T_{min} and T_{max} are daily dew point temperature, minimum, and maximum air temperature, respectively. The location specific coefficients a, b, and c were computed based on observations of 15 automated weather stations in Missouri. The variability of those coefficients was small between different stations, suggesting that the estimations were relatively robust (Hubbard et al. 2003). When ignoring the small differences the following equation resulted for estimating dew point temperature,

$$T_d = 0.98609T_n + 0.16979(T_x - T_n) - 1.41092 \qquad \text{(B6)}$$

Because only 4 first order NWS Coop stations had 30-year wind speed observation in Missouri, we used the daily average wind from the 15 automated weather stations. The winds from 3 automated weather stations closest to a coop station were averaged and the average was used as input to compute E_p for the coop station.

The monthly total E_p calculated using the averaged daily wind speed, estimated solar irradiance, and estimated dew point temperature had very good agreement with that calculated from observed inputs. Figure B4 shows an example for (SUS) SPIRIT_OF_ST_LOUIS station with good agreement between E_p calculated from estimated input parameters (E_{pe}) and E_p calculated from observed parameters. The R^2 between monthly total in E_{pe} and E_p is 0.934, and R^2 for monthly anomalies is 0.488. These comparisons suggest E_{pe} not only reproducing the seasonal variations but also describing the temporal variations of E_p.

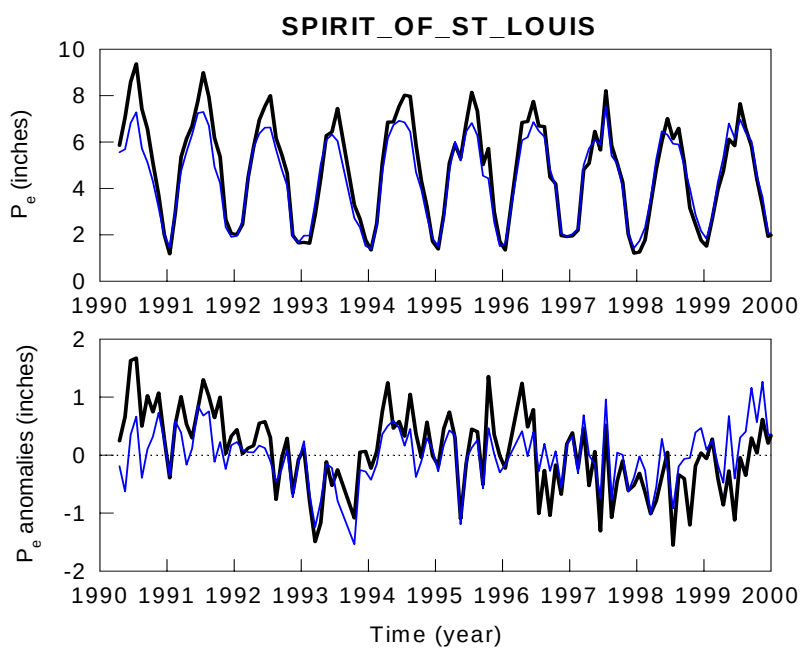

Figure B4: Monthly total (upper panel) and monthly anomalies (lower panel) of E_{pe} (blue line) and E_p (heavy black line).

The free water surface evaporation is calculated by scaling E_p by 0.7 times (Kohler et al. 1955, see their equation 10; Linacre 1994; Roderick and Farquhar 2002).

5. Seasonal soil temperature

Seasonal average soil temperatures at 5cm below the surface were calculated using data from 13 of the 15 stations in the Missouri Automated Weather Stations Network. As previously declared, these stations' data are from the mid-1990s to December 31, 2002.

6. Prevailing wind direction and average wind speed for different seasons

Seasonal average wind speed was computed based on the hourly and daily data from the 15 stations in the Missouri Automated Weather Stations Network for the period from beginning of their measurements to December 31, 2002. Wind observations at the 5 first order NWS Coop stations in Missouri also were used in this computation.

Wind directions data from 13 automated weather stations with hourly data and the 5 first order NWS Coop stations were used to determine the prevailing wind at each of the station location. The prevailing wind direction was determined by counting the frequency of hourly wind directions falling in each of the 16 direction bins. Each bin contains 22.5º and first bin is from -11.25º to 11.25º, the second from 11.25º to 33.75º, and so forth. The direction that has the highest frequency of wind direction is the prevailing wind direction.

7. Solar radiation

Solar radiation is estimated by the following equation which has been recognized as one of the best algorithms in estimating solar radiation in the Northern Great Plains (Weiss et al. 2001).

$$S = 0.75[1 - \exp(-b \times C \times \Delta T^2 / Q_{oi-30})]. \qquad \text{(B7)}$$

In (B7), b is an empirical coefficient, $Q_{oi\text{-}30}$ is the solar radiation at the top of the atmosphere (solar insolation) thirty days prior the time of interest, $\Delta T = T_{\max,i} - (T_{\min,i} + T_{\min,i+1})/2$ is the daily temperature range for day i, and C is the precipitation correction/adjustment factor (Bristow and Campbell 1984) and C=1 if there is no precipitation on the day of interest or if precipitation has occurred for more than two consecutive days including the day of interest (after two days of continuous rainfall it is assumed that there is equilibrium between solar radiation and the ΔT). If there is precipitation on the day of interest (day i) and precipitation has not occurred for more than two consecutive days, C=0.75. If the difference between ΔT on the day prior to precipitation event, day i-1, and the day before (day i-2) is more than 2ºC, ΔT for the day prior to precipitation event is reduced by 25% and C=0.75 for day i-1 (Bristow and Campbell 1984).

Weiss and Hays (2004) showed that the b is highly correlated with ΔT in the U.S. Northern Great Plains. In Missouri, the relationship between the long-term mean annual values of C×ΔT (=$\overline{\Delta T}$) and the location specific b for the 15 automatic weather stations was derived and shown in Fig. B5. A close relationship between b and $\overline{\Delta T}$ is suggested, consistent with the result of Weiss and Hays (2004). This relationship may be described by a nonlinear regression

$$b = -0.0612 + (0.4646\overline{\Delta T} - 2.506)^{-1} \qquad \text{(B8)}$$

The predicted values of b from (B8) for the 15 automated weather stations are also shown by the solid line in Fig. B5. The R^2 of (B8) to the stations' b values is 0.87 and the root

mean square error of the fitting is 0.0179. The F value for (B8) is 26.06 and is significant at 99.97% confident level. From this established (B8), the values of b for each of the 89 NWS stations in Missouri may be calculated to estimate the solar radiation at those locations.

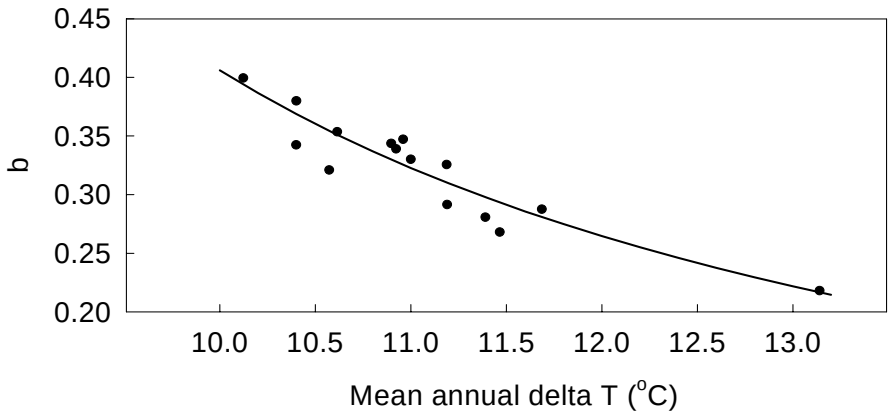

Figure B5: Relationship between local specific coefficient *b* and $\overline{\Delta T}$.

References

Angel, J.R., and F. A. Huff, 1992: Comparing three methods for fitting extreme rainfall distributions: L-moments, maximum likelihood, and graphical fit. *Proc. 12th conf. on Probability and Statistics,* Toronto. Amer. Meteor. Soc., 255-260.

Allen, R.G., M. Smith, A. Peerier, and L.S. Pereira, 1994: An update for the calculation of reference evapotranspiration. *ICID Bulletin* 43:35-92.

Allen, R.G., L.S. Pereira, D. Raes, and M. Smith, 1998: Crop evapotranspiration: guidelines for computing crop water requirements. FAO irrigation and drainage paper no. 56. FAO, Rome.

Arkin, P.A., 1989: The global climate for December 1988-February 1989: Cold episode in the tropical pacific continues. *J. Climate*, 2:737-757.

Bristow, K. L., and G. S. Campbell, 1984: On the relationship between incoming solar radiation and daily maximum and minimum temperature. *Agricul. Forest Meteorol*., 31:159-166.

Guttman, N.B., J.R.M. Hosking, and J.R. Wallis, 1993: Regional precipitation quantile values for the continental U.S. computed from L-moments. *J. Climate*, 6:2326-2340.

Hubbard, K.G., 2001: Multiple station quality control procedures. In *proceedings of Automated weather stations for applications in agriculture and water resources management: current use and future perspectives.* Eds. K.G. Hubbard and M.V.K. Sivakumar, 133-136.

Hubbard, K.G., R. Mahmood, and C. Carlson, 2003: Estimating daily dew point temperature for the Northern Great Plains using Maximum and minimum temperature. *Agron. J.*, 95:323-328.

Huff, F. A. and J. R. Angel, 1989: Frequency distributions and hydroclimatic characteristics of heavy rainstorms in Illinois. *Illinois state water survey bulletins*, 70, 177pp.

Huff, F.A., 1993: 100-year rainstorms in the Midwest: design characteristics. *Illinois state water survey,* Champaign, Circular 176, 20pp.

Hosking, J.R.M., 1990: L-moments: analysis and estimation of distributions using linear combinations of order statistics. *J. Roy. Stat. Soc*., 52B:105-124.

Hosking, J.R.M., and J. R. Wallis, 1997: *Regional frequency analysis: an approach based on L-Moments*. Cambridge University Press, 224pp.

Jensen, M.E., R.D. Burman, and R.G. Allen, 1990: Eavpotranspiration and irrigation water requirements: A manual prepared by the Committee on Irrigation Water Requirements of the Irrigation and Drainage Division of the American Society of Civil Engineers, New York, 332pp.

Kohler, M.A., T. J. Nordenson, and W.E. Fox, 1955: Evaporation from pans and lakes. Weather bureau research papers No. 38. Washington.

Kotz, S., N. L. Johnson, and C. B. Read, eds. 1988: Wakeby distributions, In *Encyclopedia of Statistics*, vol. 9, Wiley, 513-514.

Linacre, E.T., 1994: Estimating U.S. class A pan evaporation from few climate data. *Water International* 19: 5–14.

Maurer, E. P., A. W. Wood, J. C. Adam, and D. P. Lettenmaier, 2002: A long-term hydrologically based dataset of land surface fluxes and states for the conterminous United States. *J. Climate,* 15:3237-3251.

Reek, T., S.R. Doty, and T.W. Owen, 1992: A deterministic approach to the validation of historical daily temperature and precipitation data from the cooperative network. *Bull. Amer. Meteor. Soc*., 73:753-762.

Roderick, M.L. and G.D. Farquhar, 2002: The cause of decreased pan evaporation over the past

50 years. *Science*, 298:1410-1411.
Ropelewski, C. F., J. E. Janowiak, and M.S. Halpert, 1985: The analysis and display of real time surface climate data. *Mon. Wea. Rew*., 113:1101-1106.
Weiss, A., C. J. Hays, Q. Hu, and W. E. Eastering, 2001: Incorporating bias error in calculating solar irradiance: implications for crop yield simulations. *Agron. J*., 93:1321-1326.
Weiss, A. and C. J. Hays, 2004: Simulation of daily solar irradiance. *Agricul. Forest Meteorol*. 123:187-199.